МІНІСТЕРСТВО ОСВІТИ І НАУКИ УКРАЇНИ
Прикарпатський національний університет імені Василя Стефаника
Фізико-хімічний інститут
ННЦ «Напівпровідникове матеріалознавство»
АКАДЕМІЯ НАУК ВИЩОЇ ШКОЛИ УКРАЇНИ

НАЦІОНАЛЬНА АКАДЕМІЯ НАУК УКРАЇНИ
Інститут фізики напівпровідників ім. В.Є. Лашкарьова
Інститут металофізики ім. Г.В. Курдюмова
Українське фізичне товариство
Благодійний фонд" Івано-Франківське математичне товариство"

XIX МІЖНАРОДНА ФРЕЇКІВСЬКА КОНФЕРЕНЦІЯ З ФІЗИКИ І ТЕХНОЛОГІЇ ТОНКИХ ПЛІВОК ТА НАНОСИСТЕМ

Матеріали

Івано-Франківськ, 09-14 жовтня, 2023

Ivano-Frankivsk, October 09-14, 2023

Materials

XIX INTERNATIONAL FREIK CONFERENCE ON PHYSICS AND TECHNOLOGY OF THIN FILMS AND NANOSYSTEMS

MINISTRY OF EDUCATION AND SCIENCE, YOUTH AND SPORT OF UKRAINE

Vasyl Stefanyk Precarpathian National University
Physical-Chemical Institute
Science & Educational Centre of semiconductor material science
ACADEMY OF SCIENCE OF HIGH SCHOOL OF UKRAINE

NATIONAL ACADEMY OF SCIENCE OF UKRAINE
V.E. Lashkarev Institute of Semiconductor Physics
G.V. Kurdyumov Institute of the Physics of Metals
Ukraine Physics Society
CO "Charitable Foundation "Ivano-Frankivsk Mathematical Society"

УДК 539.2

Н 65

XIX Міжнародна Фреїківська конференція з фізики і технології тонких плівок та наносистем. ***Матеріали.*** / За ред. Л.І. Никируя, Р.О. Дзумедзея. Івано-Франківськ : Вид-во Прикарпатського нац. ун-т ім. Василя Стефаника, 2023. 172 с.

Представлено сучасні результати теоретичних і експериментальних досліджень з питань фізики і технології тонких плівок та наносистем (метали, напівпровідники, діелектрики, провідні полімери; методи отримання та дослідження; фізико-хімічні властивості; нанотехнології і наноматеріали, квантово-розмірні структури, наноелектроніка, тощо. Матеріали підготовлено до друку Програмним комітетом конференції і подано в авторській редакції.

Для наукових та інженерних працівників, що займаються проблемами тонкоплівкового матеріалознавства та мікроелектроніки.

Рекомендовано до друку науково-технічною радою Фізико-хімічного інституту Прикарпатського національного університету імені Василя Стефаника

XIX International Freik Conference Physics and Technology of Thin Films and Nanosystems. ***Materials.*** / Ed. by L.I. Nykyruy, R.O. Dzumedzey. Ivano-Frankivsk : Publisher Vasyl Stefanyk Precarpathian National University, 2023. 172 c.

The results of theoretical and experimental researches in directions of the physics and technology of thin films and nanosystems (metals, semiconductors, dielectrics, and polymers; and methods of their investigation; physic-chemical properties of thin films; nanotechnology and nanomaterials, quantum-size structures; thin-film devices of electronics, are presented. The materials preformed for printing by Conference’s Organizational Committee and Editorial Board, are conveyed in authoring edition.

For scientists and reserchers on the field of thin-film material sciences and nanoelectronics.

ORGANIZING COMMITTEE (Ivano-Frankivsk)

Volodymyra Boychuk, *Chair*

Viktor Boryk,; Ivan Budzulyak; Bohdan Dzundza; Roman Dzumedzey; Halyna Hurgula; Roman Ilnytskyi; Iryna Ivanyshyn; Volodymyr Klanichka; Oksana Kostyuk; Galyna Mateik; Ostap Matkivskiy; Myroslav Mazur; Tetiana Mazur; Lyubov Mezhylovska; Bohdanna Naidych; Zhanna Oleksyn; Volodymyr Potyak; Bohdan Rachiy; Yaroslav Saliy; Taras Semko; Liliia Turovska; Ivanna Vakalyuk; Halyna Voytkiv; Ivan Yaremiy; Lyubov Yablon; Rostyslav Yavorskyi; Svyatoslav Yavorskyi

SCIENTIFIC COMMITTEE

Lyubomyr Nykyruy, *Chair;* PNU, Ukraine
Ihor Horichok, *Co-Chair*; PNU, Ukraine
Volodymyr Kotsyubynski, *Co-chair*; PNU, Ukraine
Ihor Lishchynskyy, *Co-chair*; PNU, Ukraine
Maksym Striha, *Co-chair*; V.E.Lashkarev Institute of Semiconductor Physics NAS of Ukraine

Toru Aoki, *Shizuoka University*, Japan
Mahammad Babanly, *Institute of Catalysis and Inorganic Chemistry*, Azerbaijan
Petro Fochuk, *Yuri Fedjkovych Chernivtsi National University*, Ukraine
Yuri Gurevich, *Centro de Investigacion y de Estudios Avanzados del Instituto Politécnico Nacional*, Mexico
Orest Ivasishin, *G. V. Kurdyumov Institute for Metal Physics NAS of Ukraine*, Ukraine
Ivan Kaban, *Leibniz-Institut für Festkörper- und Werkstoffforschung Dresden*, Germany
Sandor Kökényesi, *Debreceni Egyetem*, Hungary
Petro Lytvyn, *V.E.Lashkarev Institute of Semiconductor Physics NAS of Ukraine*, Ukraine
Ivan Protsenko, *Sumy State University*, Ukraine
Olena Rogacheva, *National Technical University Kharkiv Polytechnic Institute*, Ukraine
Petro Smertenko, *V.E.Lashkarev Institute of Semiconductor Physics NAS of Ukraine*, Ukraine
Tomasz Story, *Institute of Physics of the Polish Academy of Sciences*, Poland
Zbigniew Swiatek, *Instytut Metalurgii i Inzynierii Materialowej Polskiej Akademii Nauk*, Poland
Ion Tiginyanu, *Technical University of Moldova*, Moldova

Grzegorz Wisz, *University of Rzeszów*, Poland
Krzysztof Wojciechowski, *AGH University of Science and Technology*, Poland
Rasit Ahiska, *Gazi University*, Turkey
Lukian Anatychyk, *Yuri Fedjkovych Chernivtsi National University, Institute of Thermoelectricity NAS and MES of Ukraine*, Ukraine
Oleksandr Belyaev, *V.E.Lashkarev Institute of Semiconductor Physics NAS of Ukraine*, Ukraine
Ivan Blonskiy, *Institute of Physics NAS of Ukraine*, Ukraine
Anatoliy Druzhynin, *Lviv Polytechnic National University*, Ukraine
Sergiy Fedosov, *Lesya Ukrainka Volynj National University*, Ukraine
Ihor Fodchuk, *Yuri Fedjkovych Chernivtsi National University*, Ukraine
Marian Galushchak, *Ivano-Frankivsk National technical University of Oil and Gas*, Ukraine
Ivan Gasyuk, *PNU*, Ukraine
Petro Gorbyk, Chuiko Institute of Surface Chemistry NAS of Ukraine, Ukraine
Mykola Kharchenko, *B. Verkin Institute for Low Temperature Physics & Engineering of the NAS of Ukraine*, Ukraine
Dmytro Korbutyak , *V.E.Lashkarev Institute of Semiconductor Physics NAS of Ukraine*, Ukraine
Oleksandr Kovalenko, *O. Honchar Dnipro national University*, Ukraine
Bohdan Kyyak, *NAS of Ukraine*, Ukraine
Yaroslav Lepikh, *I. Mechnikov Odesa National University*, Ukraine
Lyudmyla Matveeva, *V.E.Lashkarev Institute of Semiconductor Physics NAS of Ukraine*, Ukraine
Ivan Myronyuk, *PNU*, Ukraine
Mykola Moiseenko, *Ivano-Frankivsk National Medical University*, Ukraine
Yaroslav Ogorodnik, *Radiation Monitoring Devices, inc.*, USA
Bohdan Ostafiychuk, *PNU*, Ukraine
Taras Parashchuk, *AGH University of Science and Technology*, Poland
Roman Peleshchak, *Lviv Polytechnic National University*, Ukraine
Ihor Prokopenko, *V.E.Lashkarev Institute of Semiconductor Physics NAS of Ukraine*, Ukraine
Volodymyr Prokopiv (J.), *Kyiv City Administration*, Ukraine
Oleksandr Ptashchenko, *I. Mechnikov Odesa National University*, Ukraine
Olena Rogachova, *National Technical University Kharkiv Polytechnic Institute*, Ukraine
Vasyl Rubish, *Institute for Information Recording NAS of Ukraine*, Ukraine
Vasyl Shenderovskiy, *Institute of Physics NAS of Ukraine*, Ukraine
Ihor Stolyarchuk, *Ivan Franko Drohobych State Pedagogical University*, Ukraine
Oleksandr Stronsjkyy, *V.E.Lashkarev Institute of Semiconductor Physics NAS of Ukraine*, Ukraine
Mykola Tkach, *Yuri Fedjkovych Chernivtsi National University*, Ukraine

Valentyn Tatarenko, *G. V. Kurdyumov Institute for Metal Physics NAS of Ukraine*, Ukraine
Vasyl Tomashyk, *V.E.Lashkarev Institute of Semiconductor Physics NAS of Ukraine*, Ukraine
Robert Uhrin, *XLight Corporation,* USA
Ruslan Zapukhlyak, *PNU*, Ukraine
Dmytro Zayachuk, *Lviv Polytechnic National University*, Ukraine
Victor Zinchenko, *A. V. Bogatsky Physico-Chemical Institut*e, Ukraine

ОРГАНІЗАЦІЙНИЙ КОМІТЕТ

Володимира Бойчук, *голова організаційного комітету*

Віктор Борик; Іван Буздуляк; Галина Войтків; Богдан Дзундза; Роман Дзумедзей; Галина Гургула; Ірина Іванишин; Роман Ільницький; Володимир Кланічка; Оксана Костюк; Галина Матеїк; Остап Матківський; Мирослав Мазур; Тетяна Мазур; Любов Межиловська; Богдана Найдич; Жанна Олексин; Володимир Потяк; Богдан Рачій; Ярослав Салій; Тарас Семко; Лілія Туровська; Іванна Вакалюк; Іван Яремій; Любов Яблонь; Ростислав Яворський; Ярослав Яворський

НАУКОВИЙ КОМІТЕТ

Любомир Никируй, *голова наукового комітету, Україна*
Ігор Горічок, *співголова наукового комітету, Україна*
Володимир Коцюбинський, *співголова наукового комітету, Україна*
Ігор Ліщинський, *співголова наукового комітету, Україна*
Максим Стріха, *співголова наукового комітету, Україна*

Т. Аокі, *Турція*; **Р. Ахиска,** *Турція*; **Л. Анатичук**, *Україна*; **М. Бабанли,** Айзебарджан**; О. Беляєв,** *Україна*; **І. Блонський,** *Україна*; **Г. Віш,** *Польща*; **К. Войцеховські,** *Польща*; **М. Галущак,** *Україна*; **І. Гасюк**, *Україна*; **П. Горбик,** *Україна*; **Ю. Гуревич,** *Мексика*; **А. Дружинан,** *Україна*; **Р. Запухляк**, *Україна*; **Д. Заячук,** *Україна*; **В. Зінченко,***Україна*; **О. Івасишин,** *Україна*; **І. Кабан,** *Німеччина*; **Ш. Кокенеші,** *Угорщина***; Д. Корбутяк**, *Україна*; **О. Коваленко,** *Україна*; **Б. Кияк,** *Україна*; **Я. Лепіх,** *Україна*; **П. Литвин,***Україна*; **Л. Матвеєва**, *Україна*; **І. Миронюк,***Україна*; **М. Моісеєнко,** *Україна*; **Я. Огородник,** *США*; **Б. Остафійчук,** *Україна;* **І. Проценко,** *Україна*; **Т. Паращук,** *Польща*; **Р. Пелещак,** *Україна*; **І. Прокопенко,** *Україна*; **В. Прокопів** (мол.), *Україна*; **О. Птащенко,** *Україна*; **О. Рогачова,** *Україна***; В. Рубіш,** *Україна*; **В. Шендеровський,** *Україна*; **З. Свьонтек,** *Польща***; П.Смертенко,** *Україна*; **Т. Стори,** *Польща*; **І. Столярчук,***Україна***; О. Стронський**, *Україна*; **М. Ткач**, *Україна*; **В. Татаренко,** *Україна*; **І. Тигіняну,** *Молдова*; **В. Томашик**, *Україна*; **Р. Угрин,** *США*; **С. Федосов,** *Україна*; **І. Фодчук**, *Україна*; **П. Фочук,** *Україна*; **М. Харченко,** *Україна*

PLENARY SESSIONS

Biomedical Data Science from Physicists for Molecular Medicine

Grau M.

University of Münster and University Hospital Münster; Philipps-Universität Marburg, Münster, Germany
Michael.Grau@uni-muenster.de

Modern measurement technologies for molecular medicine and cancer research, like whole-exome sequencing or gene expression profiling, provide a wealth of high-dimensional data for tumor samples from patients. To extract valuable information like somatic DNA mutations in cancer cells, big analysis pipelines are required that combine multiple methodologies and biological knowledge databases. Moreover, multiple concurrent biological pathways are active in the ensemble of measured cancer cells from a tumor sample. This causes a complex overlapping of data signatures that need to be discovered and dissected to gain biological insights. For this task, a focus will be put on Signal Dissection by Correlation Maximization (SDCM), an unsupervised statistical learning method based on modeling at the intersection of theoretical physics and explainable AI. For example, gene expression signatures discovered with SDCM were able to reveal unexpected and strong survival differences between patients who had the same diagnosis and therapy.

Charge-Carrier Transport in Thin Film Solar Cells: New Formulation

Velazquez-Perez J.E.[1], Titov O.Yu.[2], Gurevich Yu.G.[3]

[1]Departamento de Fisica Aplicada, Universidad de Salamanca, 37008 Salamanca, Spain
[2]Instituto Mexicano del Petróleo, Eje Central Lázaro Cárdenas 152, 07730, México, CDMX, Mexico
[3]Departamento de Fisica, CINVESTAV del I.P.N., Apartado Postal 14-740,07000 Mexico, DF, Mexico

Solar cells rely on photogeneration of charge carriers in p-n junctions and their transport and subsequent recombination in the quasineutral regions. A number of basic issues concerning the physics of the operation of solar cells still remain obscure. This talk discusses some of those unsolved basic problems. In conventional solar cells, recombination of photogenerated charge carriers plays a major limiting role in the cell efficiency. High quality thin-film solar cells may overcome this limit if the minority diffusion lengths become large as compared to the cell dimensions, but, strikingly, the conventional model fails to describe the cell electric behavior under these conditions. A new formulation of the basic equations describing charge carrier transport in the cell along with a set of boundary conditions is presented. An analytical closed-form solution is obtained under a linear approximation. In the new framework given, the calculation of the open-circuit voltage of the solar cell diode does not lead to unphysical results.

Electronic and Chemical Surface Properties of $Bi_2Se_{3-y}S_y$, $Bi_{1.993}Cr_{0.007}Se_3$ and Bi_2MnSe_4 Compounds

Gardonio S.

School of Science, Materials Research Laboratory, University of Nova Gorica, Nova Gorica, Slovenija
sandra.gardonio@ung.si

Bi_2Se_3 and related compounds have been extensively studied for thermoelectric applications in the past, but it was not until the late 2000s that researchers recognized their unconventional electronic properties. The discovery of these novel and fundamentally different electronic surface states in compounds based on heavy elements with strong spin-orbit coupling has increased scientific interest, as has the potential to use these compounds, known as topological insulators, for various fields such as spintronics, optoelectronics, and catalysis.

Ternary variants of Bi_2Se_3 have been studied in recent years because they exhibit superior insulating properties compared to their binary counterparts. Calculations have shown that Bi_2Se_2S in its stoichiometric form is a stable topological insulator, but available experimental results have been inconclusive on this issue. We have studied the Bi_2Se_3-Bi_2S_3 binary system over a wide range of compositions and established a clear link between the phase diagram and the electronic properties of the Bi_2Se_3-Bi_2S_3 system.

Although many studies on topological insulators have been carried out in recent years, there is still a need to understand how topological properties are affected by dilute magnetism and how magnetic dopants can change the electronic structure of synthesized materials. Experimental investigation of such effects is challenging from a materials perspective. Stable isolated random atoms on the surface of TI are difficult to achieve. We succeeded in synthesizing Bi_2Se_3 doped with Cr, a magnetic element that has a low solubility limit in Bi_2Se_3, a condition that makes homogeneously distributed isolated dopants thermodynamically favorable. We demonstrated that the presence of Cr dopants alters the topological surface states of Bi_2Se_3, opens an energy gap, and that this effect is visible at room temperature.

An overview of the efforts to obtain the rhombohedral antiferromagnetic topological insulator Bi_2MnSe_4 is presented, and further insights into the electronic and chemical surface properties of the monoclinic Bi_2MnSe_4 are provided.

Is it Possible to Create a MOSFET with a Subthreshold Swing Lower than 60 mV Per Decade?

Strikha M.V.

Taras Shevchenko National University of Kyiv; V.Lashkariov Institute of Semiconductor Physics, NAS Ukraine. maksym_strikha@hotmail.com

The subthreshold swing S is a fundamental characteristic of MOSFET transistors [1]. It shows how many times the gate voltage V_g must be increased in the subthreshold range in order to achieve an increase in the drain current I_d by an order of magnitude: $S \equiv \ln 10 \frac{dV_g}{d(\ln I_d)}$. At room temperature in a high-quality transistor with a large value of sub-gate capacitance, the threshold value of this parameter is equal to $S \equiv \ln 10 \frac{kT}{e} \approx 60$ mV/decade, where e is the electron charge, k is the Boltzmann constant, and T is the temperature in Kelvins.

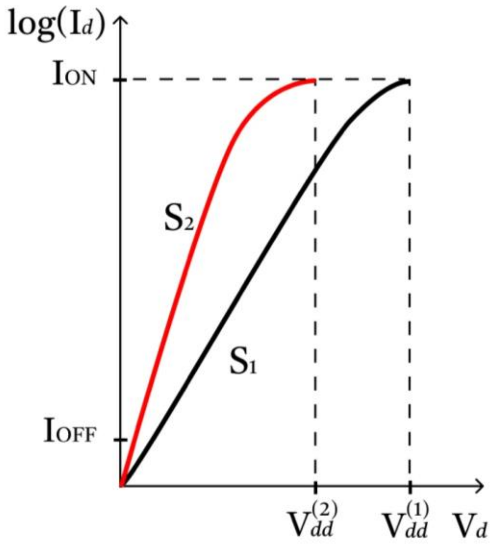

The importance of this parameter lies in the fact that its smallest threshold value determines the minimum possible operating voltage of the transistor supply (on the figure the curve with $S_2 < S_1$ corresponds lower $V_{dd}^{(2)} < V_{dd}^{(1)}$). Therefore, a decrease in S below the fundamental limit would theoretically open up great prospects for further reducing power consumption and scaling transistors.

For this purpose, in particular, it was previously proposed [2-4] to use the effect of negative capacitance in a ferroelectric that forms the gate dielectric layer. However, the futility of such attempts has been proven on the basis of fundamental thermodynamic principles and numerical calculations of real systems in [5].

Therefore, another, much more physical way to overcome the fundamental limit was proposed: to use a cold metal source for electron injection into the MOSFET channel, where, due to the small width of the valence band, the electrons injected into the channel no longer have a "hot" Boltzmann "tail" in their energy distribution. Transistors with a monolayer sub-10-nanometer MoS_2 channel and drain and source on the basis of NbS_2 and TaS_2 with a subthreshold swing below the fundamental limit have already been realized experimentally [6, 7]. However, a visual analytical model that would allow us to estimate the magnitude of the expected effect has not yet been created.

Within the framework of the Landauer-Datta-Lundstrom formalism [8], we have derived an analytical expression for the subthreshold swing S, which implies that S is generally somewhat smaller than the fundamental limit, and the degree of its decrease is determined by the ratio of the energy kT (26 meV at room temperature) to the value of the energy interval between ΔE the top of the valence band of the source material and the value of the surface potential in the transistor channel. Under the limit $\Delta E >> kT$ this expression leads to a standard value S(300 K) = 60 meV/decade. The formula can be used to estimate the magnitude of the effect under study in real state-of-the-art electronics systems.

[1]. S.M. Sze. Physics of Semiconductor Devices. 2nd Edition. John Wiley & Sons: New York, Chichester, Brisbane, Toronto, Singapore (1981).

[2]. R. Landauer. Can capacitance be negative? *Collect. Phenom.*, 2, 167-170 (1976).

[3]. Michael Hoffmann, Stefan Slesazek, Thomas Mikolajick. Progress and future prospects of negative capacitance electronics: A materials perspective. *APL Mater*. 9, 020902 (2021).

[4]. S. Salahuddin, S.Datta. The era of hyper-scaling in electronics. *Nat. Electron*. 1, 442-450 (2018).

[5]. E.A. Eliseev, A.N. Morozovska, L.P. Yurchenko, M.V. Strikha. Could the negative capacitance effect be used in field-effect transistors with a ferroelectric gate? *Physics and Chemistry of Solid State* 23(4), 705–713 (2022)

[6]. Yiheng Yin, Zhaofu Zhang, Chen Shao, John Robertson and Yuzheng Guo. Computational study of transition metal dichalcogenide cold source MOSFETs with sub-60 mV per decade and negative differential resistance effect. *NPJ 2D Materials and Applications* 6, 55 (2022); https://doi.org/10.1038/s41699-022-00332-6

[7]. Kunyi Liu, Fei Lu, Yuan Li. Bias-Independent Subthreshold Swing in Nanoscale Cold-Source Field-Effect Transistors by Drain Density-of-States Engineering. arXiv:2211.02304 (2022).

[8]. Yu.Krugliak, M.Strikha. Landauer – Datta – Lundstrom generalized electron transport model for micro- and nanoelectronics. *2015 IEEE International Conference on Electronics and Nanotechnology (ELNANO). Conference Proceedings*. Kyiv: NTUU "KPI", 70-74 (2015).

Transient Photoconductivity Study of Multilayered Random Networks of 2D Material Flakes Casted from Solution

Urbančič J., Bratina G., Pavlica E.

University of Nova Gorica, Vipavska 13, Nova Gorica SI-5000, Slovenia
egon.pavlica@ung.si

Solution processable two-dimensional materials have great potential in the application of printed electronic elements. Typically their electrical properties like e.g. charge mobility of this randomly oriented network of flakes is significantly lower than in a single flake of the same material. Our recent success was obtained with randomly oriented Ti_3C_2 MXene flakes [1]. The results of time-of-flight photoconductivity measurements[2,3] confirm electron transport with mobilities above 270 cm^2 /Vs, which is substantially higher than previously reported field-effect mobility, which was below 10 cm^2 /Vs. Mobility was increasing with electric field - characteristic to disordered materials. The extrapolated zerofield mobility of 38 ± 15 cm^2 /Vs reaches values measured in single $Ti_3C_2T_x$ MXene flakes (34 cm^2 /Vs). We suggest that this is a consequence of precise MXene exfoliation and efficient deposition process. The exfoliation yielded flakes with the largest dimensions on the order of several microns. The deposition of the layers resulted in up to 6-layer-thick film of interconnected randomly oriented flakes. We demonstrate that the transport through such randomly connected percolation network can be characterized as charge transport through crystalline flakes, perturbed by trapping in the localized states, residing at the interfaces between the flakes. The former process results in high charge mobility, the latter results in a low charge carrier mobility. This duality is likely to be responsible for relatively high values of TOFP-measured charge carrier mobility. These results also suggest that charge trapping at the dielectric interface becomes less important when the charge carriers are transported through several pristine MXene layers above and away from the dielectric interface as in our TOFP experiments. This results in overall higher observed charge carrier mobility. On the other side, the charge carrier mobility exhibits positive dependence on the electric field of the Poole-Frenkel type, which is typical for disordered material. This behavior seems to be pertinent to a multilayered network of randomly distributed flakes with an interfacial electronic structure, which does not suppress the charge transport, but it represents a bypass to improved charge carrier transport.

[1]. J. Urbančič et al., Time-of-Flight Photoconductivity Investigation of High Charge Carrier Mobility in Ti3C2Tx MXenes Thin-Film, Diamond and Related Materials 135, 109879 (2023).

[2]. G. Bratina and E. Pavlica, Characterisation of Charge Carrier Transport in Thin Organic Semiconductor Layers by Time-of-Flight Photocurrent Measurements, Organic Electronics 64, 117 (2019).

[3]. L. Zhang, X. Zhong, E. Pavlica, S. Li, A. Klekachev, G. Bratina, T. W. Ebbesen, E. Orgiu, and P. Samorì, A Nanomesh Scaffold for Supramolecular Nanowire Optoelectronic Devices, Nat Nano 11, 900 (2016).

Session 1

Thin films technology and their research methods

Advanced Nanoindentation in Vanadium Oxide Characterizations

Lytvyn P.M., Dzhagan V.M., Valakh M.Ya., Korchovyi A.A.,
Isaieva O.F., Stadnik O.A., Yukhymchuk V.O., Gudymenko O.Yo.,
Romanyuk B.M., Melnik V.P.

V. Lashkaryov Institute of Semiconductors Physics, NAS of Ukraine,
03028 Kyiv, Ukraine
peter.lytvyn@ccu-semicond.net

In the field of materials science, understanding how synthesis conditions impact the physical properties of functional thin films is critical for optimization. This report delves into the intricate relationship between the structural-morphological characteristics of micro/nanocrystalline vanadium oxide films and their corresponding nanomechanical properties. Utilizing scanning probe microscopy and force spectroscopy techniques, the research elucidates the impact of production modes and post-growth treatments on these properties. An advanced atomic force nanoindentation approach, accounting for both elastic and elastic-plastic deformations as well as film thickness, was developed, showcasing the heightened sensitivity and relevance of nanomechanical tests. The hardness and elastic modulus were quantified with nanoscale spatial resolution and compared with the structural characterization by X-ray diffraction and Raman spectroscopy.

A key finding was that the VO_2-rich films exhibited over 10 times greater hardness compared to the multi-phase (V_2O_5, V_4O_9, V_3O_7, etc.) films. This significant enhancement was attributed to the peculiarities of VO_2 structure with high V-O-V covalency as well as a grain size and crystallinity.

Overall, this work demonstrates that AFM nanoindentation can clearly distinguish differences in nanomechanical properties arising from phase composition in complex functional oxide thin films. It highlights the power of nanoscale mechanical characterization to elucidate structure-property relationships in advanced materials.

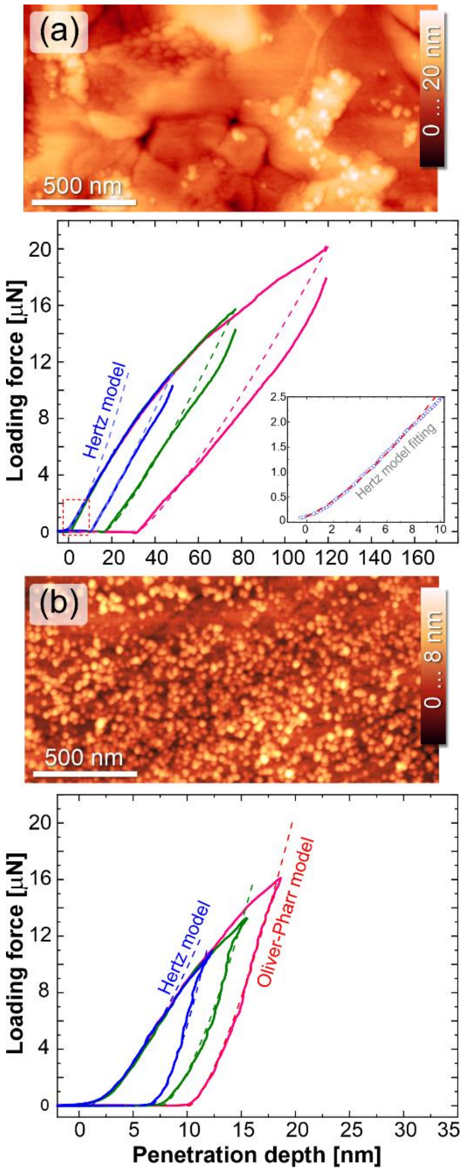

Fig. AFM images and corresponding load-penetration curves for the thin V_xO_y films post-annealed at 400 °C in varied atmospheres: oxygen-enriched (a) and in the Ar inert atmosphere (b). Fits using the Hertz and Oliver-Pharr models are indicated.

CdS Thin Films as Window Layer for Photovoltaic Application

Nykyruy L., Saliy. Ya., Yavorskyi R., Yavorskyi Ya., Matkivskyi O.,
Naidych B., Katanova L.

Vasyl Stefanyk Precarpathian National University, Ivano-Frankivsk, Ukraine,
lilia.katanova@pnu.edu.ua

The main function of thin film solar panel’s window layer is a creation of junction wile transmission of the maximum amount of light through transition area and absorption layer. The correct choice of material and window layer for cadmium telluride photovoltaic elements is important because of its significant influence on light transition into the absorption layer. Cadmium sulphide is actively used as thin n-type window layer in cadmium telluride solar panels [1]. CdS belongs to II-VI semiconductor compounds and is intensively studied because of its stability and wide direct optical band gap (2.42 eV) [2].

CdS thin films were deposited on the amorphous glass substrates using open evaporation in vacuum. Substrate temperature was T_S = 573 K, evaporator temperature of previously prepared Cd-S alloy powder was T_V = 1153 K. Thicknesses of the samples were controlled by deposition time from 60 sec to 150 sec.

Energy dispersive analysis of X-ray diffractogram shows that deposited films has stoichiometric composition independently of film thickness. Morphological properties of the CdS thin films were studied using scanning electron microscopy. The film growth occurs by Stranski-Krastanov mechanism (layer by layer growth).

Transmittance and reflectance coefficients strongly depend on film structure which is defined by obtaining method, film thickness and deposition condition. Correlation between CdS film’s thickness and deposition condition were studied using UV–VIS-NIR spectrometer (PerkinElmer UV WinLab) in the wave range 300-1200 nm. Transmittance and reflectance spectra for CdS thin films were obtained.

This study was supported by the Ministry of Education and Science of Ukraine as the project for young scientists «Hybrid thin film solar cells increased efficiency for energy security and sustainable development (0123U100226)».

[1]. Das N.K., et al. Effect of substrate temperature on the properties of RF sputtered CdS thin films for solar cell applications. *Results in Physics*. 2020. V. 17. P. 103132.

[2]. Khimani A.J., et al. Cadmium sulphide (CdS) thin films deposited by chemical bath deposition (CBD) and dip coating techniques—a comparative study. *Materials Research Express*. 2018. V. 5, № 3. P. 3036406.

Change in Microhardness of Amorphous Metal Alloys based on Aluminium due to Corrosion

Khrushchyk K.[1,2], Kubisztal J.[2], Barylski A. [2], Grzegrzolka M.[2], Karolus M.[2]

[1]Ivan Franko National University of Lviv, Faculty of Chemistry, Department of Physical and Colloid Chemistry, 6 Kyryla i Mefodiya Str., Lviv, 79005, Ukraine

[2]University of Silesia in Katowice, Institute of Materials Engineering, Faculty of Science and Technology, 75 Pulku Piechoty 1A, Chorzow, 41-500, Poland

khrystyna.khrushchyk@us.edu.pl

A fundamental study of the thermodynamics and kinetics of the controlled synthesis of clusters in an amorphous matrix will ensure the optimization of the conditions of their formation with the aim of forming materials with predicted physical and chemical properties. The complex of properties of AMAs during the transition from the amorphous to the nanocrystalline (crystalline) state changes noticeably [1], although the chemical composition, in general, remains unchanged

Amorphous Al – transition metal (TM) – rare earth metal (REM) alloys have high corrosion resistance. The mechanisms of improving the corrosion resistance of metallic glasses are related to the amorphous structure and alloying additions in a supersaturated solid solution [1].

Amorphization is accompanied by the localization of valence electron pairs and thereby increases the electrochemical activity of the alloy surface. Compared to a crystalline alloy of the same composition, the amorphous surface is quickly covered with oxide and hydroxide films (in aqueous solutions) with high protective properties. The complex of properties of AMAs during the transition from the amorphous to the nanocrystalline (crystalline) state changes noticeably [1], although the chemical composition, in general, remains unchanged.

Amorphous metal alloys alloyed with TM and REM have high mechanical properties, which determines their wide use in aircraft construction. Constant expansion of their practical application is facilitated by high corrosion resistance, elasticity under significant mechanical loads.

[1] J.E. Sweitzer, G.J. Shiflet, J.R. Scully. Electrochemica Acta. 48 (2003) 1223-1234.

Conduction Mechanisms in Amorphous SiCN Films

Tkachuk A.I.[1], Tetyorkin V.V., Porada O.K.[2]

V. Lashkaryov Institute of Semiconductor Physics, NAS Ukraine, Kyiv, Ukraine
[1]V. Vynnychenko Central Ukrainian State University, Kropyvnytskyi, Ukraine
[2]Institute for Problems of Materials Sciences NAS of Ukraine, Kyiv, Ukraine
atkachuk08@meta.ua

SiCN ternary compounds are recognized as a promising material for application in modern semiconductor electronics due its excellent high-temperature physical properties, low value of electric permittivity, high chemical, radiation and mechanical stability over a wide temperature range. Amorphous SiCN films were deposited on *p*-Si substrates by plasma-enhanced chemical vapor deposition using hexamethyldisilazane as a main precursor [1; 2]. DC current was measured as a function of bias voltage, temperature, and film thickness. It has been found that the DC conduction in the temperature range 195-353 K and the external electrical field $F \leq 1\cdot10^5$ V/cm is due to the space-charge-limited (SCL) current, caused by unipolar electron injection. Depending on the deposition conditions, shallow and deep donor-like traps are responsible for the SCL conduction. In the case of deep traps, the SCL current is confined within the so-called Lampert triangle [2].

Conduction mechanism was changed at electric fields $F>5\ 10^5$ V/cm. At temperatures $T<250$ K it can be explained by the Pool-Frenkel emission (PF), since the experimental I–V characteristics were linearized in the PF coordinates $\ln(I/F) - F^{1/2}$ and their slope was close to the theoretically calculated value $\beta_{PF}/2kT$, where $\beta_{PF} = (e^3/\pi\varepsilon_0\varepsilon)^{1/2}$ is the PF constant. At higher temperatures, the experimental curves were better approximated in the $\ln I$-F^2 coordinates, which means a change in the conduction mechanism. In strong electric fields ionization of deep centers can occur due to the PF emission, the phonon-assisted tunneling, and the direct tunneling. There are two contradictory approaches to the charge states of deep traps in PF emission [3]. In this study, experimental results are discussed in terms of both conduction mechanisms. Since the characteristic feature of phonon-assisted tunneling is the quadratic dependence of current on voltage, it is most likely that this conduction mechanism is dominant at high temperatures.

[1]. A.V. Sukach, V.V. Tetyorkin, A.I. Tkachuk, O.K. Porada et al. *J. Non-Cryst. Solid*. 2019. V. 523**,** P. 119603.

[2]. A.V.Sukach, V.V.Tetyorkin, A.I.Tkachuk, A.O.Kozak, O.K.Porada, V.I.Ivashchenko**.** *Mat. Sci. Semicond. Proc.* 2022. V.143. P. 106515.

[3]. S.D. Ganichev, E. Ziemann, W. Prettl et al. *Phys. Rev. B.* 2000. V. 61. P. 10361.

Cross Sections of Absorption and Scattering by Metal Truncated Spheres and Segments Located on a Dielectric Substrate

Korotun A.V.[1,2], Rubish V.M.[3]

[1]*National University Zaporizhzhia Politechnic, Zaporizhzhia, Ukraine,*
andko@zp.edu.ua
[2]*G.V. Kurdyumov Institute for Metal Physics of the NAS of Ukraine, Kyiv, Ukraine*
[3]*Institute for Information Recording, NAS of Ukraine, Uzhgorod, Ukraine*

It is known that low metal deposition rates on the substrate favor the formation of island metal films. Selection of the substrate material and parameters, deposition rate, and deposition temperature after annealing makes it possible to obtain metal films with islands of various sizes and shapes, including those in the form of truncated spheres and spherical segments. It should be noted that metal islands are used in solar cells to increase the efficiency of converting solar energy into electrical energy, in the study of fluorescence, and in photodetectors. In this regard, the study of the optical properties of metal islands in the form of truncated spheres and spherical segments is relevant.

As is known, the quantities measured in optical experiments are the absorption and scattering cross sections, which are determined by the expressions

$$\begin{aligned} C_{\mathrm{abs}}^{(\pm)} &= \frac{\omega\sqrt{\text{т}_{\mathrm{m}}}}{c}\,\mathrm{Im}\left(\frac{2}{3}\alpha_{\perp}^{(\pm)}+\frac{1}{3}\alpha_{\parallel}^{(\pm)}\right); \\ C_{\mathrm{sca}}^{(\pm)} &= \frac{\omega^4\text{т}_{\mathrm{m}}^2}{6\pi c^4}\left(\frac{2}{3}\left|\alpha_{\perp}^{(\pm)}\right|^2+\frac{1}{3}\left|\alpha_{\parallel}^{(\pm)}\right|^2\right), \end{aligned} \tag{1}$$

where the "±" signs refer to truncated spheres and spherical segments, respectively; $\alpha_{\perp(\parallel)}^{(\pm)}$ are the diagonal components of the polarizability tensor of islands on the substrate; т_{m} is the permeability of the environment.

Calculations of the frequency dependences of the absorption and scattering cross sections show the presence of two maxima corresponding to transverse and longitudinal surface plasmon resonances (SPR). In this case, the position of the transverse SPR for truncated spheres depends significantly on its geometric parameters (the radius and height of the cut segment), while the position of the maximum corresponding to the longitudinal SPR remains practically unchanged. In the case of a spherical segment, the situation is opposite, and the splitting of resonances is much smaller than for islands in the form of truncated spheres.

It should be noted that the tensor nature of the polarizability testifies to the anisotropy of the optical properties of metal islands of the shapes under consideration, which arises due to a decrease in symmetry from spherical for a spherical nanoparticle to axial for truncated spheres and segments.

Defect Structure and Magnetic Properties of Thin and Thick Yttrium Iron Garnet Epitaxial Systems

Fodchuk I., Hutsuliak I., Dovganyuk V., Kuzmin A., Solodkyi M., Roman Y., Lytvynchyk I., Okolita M.

Yury Fedkovych Chernivtsi National University, Chernivtsi, Ukraine
i.fodchuk@ukr.net

Complex of complementary techniques, including two- and three-crystal X-ray diffractometry, atomic force and magnetic force microscopy and numerical methods of data processing was used to investigate yttrium iron garnet (YIG) epitaxial films of wide thicknesses range from 2.3 μm up to 124 μm. We studied the influence of defect system, created by dislocations of different types and concentrations and film–substrate internal layer, on formation of reciprocal space maps (RSM) and microstructure of magnetic domains.

Characteristic MFM-images of YIG were analyzed. Changes of the magnetic domain structure of films with increasing of thickness were traced. Disordered stripe domains of approximately ~1 μm constant width, accompanied by frequent breaks and bubble domains are presented at small thickness, what appears due to a large influence of film–substrate transition layer. Stripes of thick samples have chaotic heterogeneous structure and thickness, which is typical for the film with well-formed column structure.

Experimental rocking curves and RSMs were obtained for symmetrical (444), (888) and asymmetrical (880) reflections with CuKα-radiation on high-resolution X-ray diffractometer X'Pert PRO MRD.

Simulation of RSM was performed according to Kryvoglaz kinematic theory with Monte Carlo method [1, 2]. Complex of two sets of dislocations of different concentrations, perpendicular to the surface, with Burgers vectors lying in the plane of the transition layer, was selected as the dominant one in the transition layer and film. Sizes of dislocation loops, depending on the sample, are within 2-5 μm, and their concentration is ~10^5-10^8 cm^{-2}. Good correlation between simulated and experimental RSMs was obtained. It was established that the stripe domain structure of garnets dependents a lot on many film parameters, including thickness, and structural perfection of surface and the sample at all.

[1]. Defect structure of high-resistivity CdTe:Cl crystals according to the data of high-resolution X-ray diffractometry / I. Fodchuk, A. Kuzmin, I. Hutsuliak, et all. // Proceedings of SPIE – The International Society for Optical Engineering. – 2020. – 11369(113691H).

[2]. M. A. Krivoglaz, X-Ray and Neutron Diffraction in Nonideal Crystals. Berlin: Springer. 1996.

Developing and Programming the Algorithm for X-ray Diagnostics of the Structure of Near-Surface Layers in Ion-Implanted Monocrystalline Materials

Yaremiy I.P., Yaremii H.I., Vekeryk D.V.

Vasyl Stefanyk Precarpathian University, Ivano-Frankivsk, Ukraine,
yaremiyip@pnu.edu.ua

To analyze the experimental X-ray diffractograms (rocking curve) from ion-implanted surface layers of monocrystals for defining parameters of defects in nonimplanted and implanted monocrystals and films the simulation of diffraction of X-rays in nonperfect crystals was used. To do this, special program has been developed in the C++ Builder, that allowed the modeling of theoretical rocking curves using the given defects parameters of the crystal.

For a comparison of the experimental and theoretical rocking curve, the convolution of the calculated theoretical rocking curve with the function of broadening of the spectrometer is made, and the polarization of the incident X-rays is taken into account.

Two models of the disturbed layer were considered:

– the strain profile (or defect profile) is set up functionally (use in cases, where some functional dependence is physically grounded);

– strain profile (or defect profile) is given in the form of stairs, each of which is characterized by width – sublayer thickness, and height – relative deformation or concentration of defects (use, when the profile is not known beforehand).

For the analysis of experimental rocking curves, a complex of minimization of function is used that characterizes the deviation of the theoretically calculated rocking curves from the experimental ones (in the simplest case, the mean square deviation). In this case, the set of methods of minimization can be applied to several experimental rocking curves at the same time, and allows solving a multi-parameter problem.

Depending on the parameters of the defective subsystem, whose approximation should be carry out, two approaches are used for minimization:

– the first approach – when the approaching parameters are heterogeneous (this situation occurs, when the purposeful change of the values of the parameters of the functionally described strain profiles). This situation suits to the first model of the disturbed layer;

– second approach – when the approaching parameters are homogeneous and can be reduced to two types (this situation suits to the second model of the disturbed layer).

Effect of Chemical Treatment on Electrophysical Characteristics of In/*p*-PbTe/In Structures

Malanych G.P., Tomashyk V.M.

V.Ye. Lashkaryov Institute of Semiconductor Physics, National Academy of Sciences of Ukraine, Kyiv, Ukraine
galya.malanich@gmail.com

Lead telluride is used for the manufacture of injection lasers in the 3-5 μm spectrum, as well as in thermoelectricity. The efficiency of devices based on lead telluride largely depends on the quality of electrical contacts.

In our experiments, the Bridgman-grown no crystallographic oriented single crystals of PbTe have been used. The PbTe characterictics – *p*-type, $[p] = 1.5\times10^{18}$ cm^{-3}, $\mu_p = 650$ cm^2/(V×s), undoped. Technological scheme of PbTe plates processing with etching composition H_2O_2 + HBr + EG is given in [1]. Contacts have been formed on chemically etched surface of *p*-PbTe single crystals by the thermal vacuum deposition method. Pre-deposition surface treatment produced interfaces free from oxide layers. All measurements of the *I–V* characteristics were carried out by the *dc* method in the temperature range 77–295 K on PbTe samples after cutting, chemical-mechanical polishing (CMP) and chemical-dynamic polishing (CDP).

Measurements the *I–V* characteristics of In/*p*-PbTe/In structures were performed at temperatures of 77 K and 292 K. It should be noted the linearity of the corresponding *I–V* characteristics at 292 K. From Fig. 1, it can be seen that at low temperatures, the *I-V* characteristic deviates from linearity.

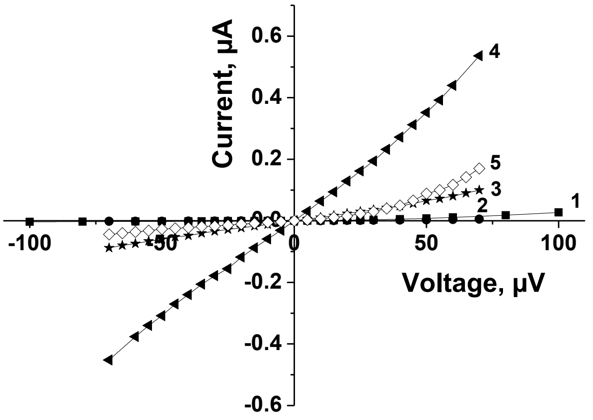

Fig. 1. *I–V* curves for In/*p*-PbTe/In at 77 K after different types of *p*-PbTe samples (7.0×1.2×0.8 mm) after: (**1**) CMP and 2 months in DMF, (**2**) CMP and 1 h in DMF, **(3)** cutting and 2 months in air, **(4)** CDP and 2 months in air, and **(5)** PbTe (1.3×1.3×1.3 mm) CDP and 1 h in DMF.

[1]. Malanych G.P., Stanetska A.S., Stratiychuk I.B., Tomashyk V.M. Technological scheme of mechanical and chemical treatment of PbTe and $Pb_{1-x}Sn_xTe$ solid solutions for obtaining polished surface of single crystal. *Materials Today: Proceedings*. 2021. V. 35, Part 3. P. 558-562.

Effect of substrate bias on the properties of Al-doped ZnO films deposited by magnetron sputtering

Ievtushenko A.I.[1], Karpyna V.A.[1], Bykov O.I.[1], Olifan O.I.[1], Mamykin S.V.[2], Kolomys O.F.[2], Strelchuk V.V.[2], Lytvyn P.M.[2], Korchovyi A.A.[2], Tkach V.M.[3], Starik S.P.[3], Baturin V.A.[4], Karpenko O.Y.[4]

[1]*I. Frantsevich Institute for Problems of Material Science, NASU, Kyiv, Ukraine,*
a.ievtushenko@yahoo.com
[2]*V. Lashkarev Institute of Semiconductor Physics, NASU, Kyiv, Ukraine*
[3]*V.Bakul Institute for Superhard Materials, NASU, Kyiv, Ukraine*
[4]*Institute of Applied Physics, NASU, Sumy, Ukraine*

Transparent conductive oxides are important materials for many applications from industrial to home devices. Nowadays, there is a trend directed to development a cost-effective indium free transparent conductive oxides as world reserve of indium are limited. One of these attractive oxide materials is ZnO doped by III-group elements like Al, Ga or In.

In this work we investigate the influence of voltage bias applied to substrate on structure, optical and electrical properties of ZnO:Al thin films deposited on Si and glass substrates by radio frequency magnetron sputtering. We have realized ZnO:Al thin film growth in layer-by-layer regime of magnetron sputtering. Sample characterization was carried out by X-ray diffraction, EDX spectroscopy, Raman scattering, photoluminescence, IR Fourier transform spectrometry, optical and electrical measurements.

In according to XRD study the lowest full width at half maxima value was observed for ZnO:Al films grown with highest negative voltage bias -30V. Hence, this film demonstrates the best crystalline quality. EDX studies demonstrate that increasing negative voltage on the substrate leads to increase O/Zn ratio from 0.98 to 1.2 that means the concentration of oxygen vacancies was diminished. At the same time Al concentration increases with negative bias voltage improving the incorporation of Al donor impurity into ZnO lattice. It must to be noted that the all deposited ZnO:Al films demonstrate a high transparency over 80 % with an optical band gap in the range 3.34-3.42 eV. AFM studies of ZnO:Al films demonstrate a very smooth surface of the films with a root mean square roughness 4.5-5.5 nm and grain sizes about 20 nm. We have found that applied negative bias voltage to substrate during film growth allow us to increase the conductivity of ZnO:Al films in three times compared to zero biased ZnO:Al films deposited at the same conditions. Results of electrical measurements interpreted by Drude model give us the following parameters: resistivity in the range 1.6-4.1 mOhm·cm and donor concentration in the range 1.06-1.46·1020 cm-3. We believe that developed highly efficient transparent conductive Al-doped ZnO films technology can be efficient and commercialized for solar cell production.

Fast and Slow Components of Ferroelectric Polarization During its Switching in PVDF Films

Fedosov S. N., Sergeeva A. E., Klimenko I. M.

Odesa National University of Technology, Odesa, Ukraine
snfedosov@ukr.net

Polarization switching in polyvinylidene fluoride (PVDF) was studied in a wide range of fields and times. A wide distribution of switching times was found indicating that the P(E) hysteresis loop as well as the coercive field and the remanent polarization depend on epyduration of the voltage application. The phenomenon was analyzed assuming the existence of fast and slow components of the ferroelectric polarization. It was found that switched polarization increases with time due to the compensating action of the charge accumulated at the boundaries between crystalline and amorphous parts.

Experiments were carried out on 12.5 μm-thick biaxially stretched PVDF from Kureha with Al electrodes deposited by vacuum evaporation. Switching experiments were performed utilizing the electrical circuit described elsewhere [1]. After conditioning at 2400 V for 50 s, DC voltage from 0.8 to 2.2 kV was applied in the opposite direction from 10^{-6} to 50 s to perform switching.

Calculation of the switching time gives $\tau_s = 6$ μs. However, only a small part of polarization about 1.5 μC/cm^2 was switched during this time, while the rest was switched at times 6 orders of magnitude larger than the calculated time.

It follows from experimental data that a certain distribution of switching times exists that becomes wider with voltage decreasing. The main conclusion is that fast and slow components of polarization are present during the switching of the ferroelectric polarization. A part of the initially switched polarization flips back, if the field is not applied for a sufficiently long time [2].

To explain experimental data, we used a model similar to that of initial poling [3]. Good agreement of measured and calculated values proved the validity of the approach stipulating the existence of two stages and correspondingly two components of the switched ferroelectric polarization, of which the fast component is essentially field dependent, while the slow one is governed by conductivity. Further development of the switched polarization is possible only if a compensating charge is accumulated at the crystallite boundaries allowing the field in the crystallites to grow again.

[1]. H. von Seggern, S. N. Fedosov, A Novel Displacement Component in PVDF in Ferroelectric Switching, *IEEE Trans. Electr. Insul.* **7** (2000) 543.

[2]. S. N. Fedosov H. von Seggern, Back-switching of ferroelectric polarization in two-component systems, *J. Appl. Phys.*, 96, (2004) 2173.

[3]. H. von Seggern, S. N. Fedosov, Conductivity-induced polarization buildup in PVDF, *Appl. Phys. Lett.*, 81 (2002) 2830.

Investigation of Cadmium Telluride Photovoltaic Absorber Layer

Yavorskyi R.[1], Nykyruy L.[1], Zamurueva O.[2], Naidych B.[1], Semko T.[1], Mateik H.[3]

[1]*Vasyl Stefanyk Precarpathian National University, Ivano-Frankivsk, Ukraine,* r.yavorskyi@pnu.edu.ua
[2]*Volyn National University, Lutsk, Ukraine*
[3]*Ivano-Frankivsk National University of Oil and Gas, Ivano-Frankivsk, Ukraine*

Solar power is the most common and easily available source of energy for all types of social devices and industrial power plants. The variety of semiconductor materials allows to produce devices with optimal efficiency and scientific research of better candidates and construction is still and important task for modern material science. Despite of higher costs and less propagation, cadmium chalcogenides have better strength, chemical stability and suitability for application to a variety of devices[1]. The optical, electrical, and mechanical properties of CdTe thin films can be set up with doping performance.

Thin CdTe films were deposited on glass and (100) silicon substrates by thermal evaporation in vacuum at consistent evaporation and substrate temperatures. The cadmium telluride alloy with indium dopand was evaporated at temperature T_E = 550°C. The deposition temperature was T_S = 200°C. The condensate thickness changes from 540 to 2835 nm predefined by changing of the deposition duration from 30 up to 570 sec.

The glass substrate has a lower heat capacity and has less influence on heat exchange. On the amorphous glass substrate CdTe thin films prevailing main diffraction peak $2\theta = 23.69^{\circ}$ corresponds to the (111) cubic orientation[2]. Crystallites were distributed on the surface (unit area) with $(6.44–17.88)10^9$ cm^{-2} density that decreased with increasing film thickness caused by increasing of the appropriate average grain size and the distance between parallel rows.

The dominant growth mechanism is Stransky-Krastanov with cubic (111) orientation. Thickness of the layer determines surface parameters almost independently on the substrate material. The bigger were crystallites, the lower values of crystal lattice constants were observed.

This study was supported by the Ministry of Education and Science of Ukraine as the project for young scientists “Technology and computer simulation of optimized second generation photovoltaic systems based on compounds II-VI” (0121U108153).

[1]. Romeo A. & Artegiani E. CdTe-Based Thin Film Solar Cells: Past, Present and Future. *Energies*. 2021. V.14. P.1684.

[2]. Yavorskyi R., Saliy Ya., Nykyruy L., Wisz G., Adamiak S., Cieniek B., Naidych B., Yavorskyi Ya. Thermally evaporated CdTe thin films on glass and (100) silicon substrates for solar cells applications. Applied Nanoscience. 2023. P.1

Low-Temperature Technologies of Deposition of Aluminum Nitride Films

Plyatsko S.V.[1], Gromovyi Yu.S.[1], Rashkovetskyi L.V.[1], Liptuga A.I.[1],
Svezhentsova K.V.[1], Petryk I.[2]

[1]*V.E. Lashkaryov Institute of Semiconductor Physics NAS of Ukraine*
[2]*O.O. Chuiko Institute of Surface Chemistry NAS of Ukraine*
rashlv@ukr.net

Aluminum nitride (AlN) films have the following characteristics that make them suitable for a wide range of applications-insulating and buffer layers, photodetectors, LEDs, laser diodes, acoustic devices or designs of opto- and microelectronic devices. Depending on the deposition methods and technological protocols, the structure of AlN films can vary from completely amorphous to monocrystalline, with a tendency to increase the volume fraction of the crystallite sizes. Therefore, the fabrication of AlN-based films requires an understanding of their microstructure as a function of deposition conditions. Compared with other physical fabrication methods, such as vapor deposition, i.e., thermal evaporation, laser deposition is a simple, versatile, rapid, and cost-effective method that can provide precise control of thickness and morphology to fabricate high-quality thin films. That is why the development of thin-film technologies for obtaining aluminum nitrides is relevant and promising and requires a sufficient understanding of their microstructure as a function of deposition conditions. In view of the above, a design was developed and a technological complex was developed for vacuum deposition with the sputtering of aluminum nitride (AlN) target dielectric material by laser IR radiation, taking into account thermal conductivity, dissociation energy, saturated vapor pressure upon reaching the temperature of developed evaporation and the crystal structure of the AlN source. Deposition was carried out in a vacuum of 10-5-10-6 Torr. on "cold" substrates without taking into account surface heating by the erosion flow (it can reach AlN thin films were deposited from a nanocrystalline and recrystallized source by modulated IR laser sputtering. 430K). Based on the results of optical absorption, it was established that depending on the temperature ($300 \leq T \leq 430$ K) of the oriented substrate with a low surface energy value, three crystalline modifications of AlN films are realized. Amorphous on glass with Eg = 4.2 eV, cubic (sphalerite) on (001) KCl and NaF substrates, and hexagonal (wurtzite) on sapphire with corresponding band gaps of 5.8 and 6.2 eV. The refractive index ($0.25 \leq \lambda \leq 1\,\mu$m) of AlN films, determined by the ellipsometry method and from the optical transmission spectra increased from n = 1.72 for the amorphous to n = 2.08 for the hexagonal structure. In the FTIR spectra (950-550 cm^{-1}) a rather extended characteristic band of Reststralen is also observed.

Low-Temperature Charge Transport in Nanosized Gold Films

Apopii V.H. Bihun R.I.

Ivan Franko Lviv National University, Ukraine,
viktor.apopii@lnu.edu.ua

Розвиток методів виготовлення нанорозмірних електросуцільних металевих плівок (з позитивним температурним коефіцієнтом опору, $\beta > 0$) та дослідження властивостей цих плівок є актуальною проблемою обумовленою потребами сучасної прозорої електроніки [1]. Під час росту металевої плівки на діелектричній підкладці коагуляція зародків кристалізації металу призводить до формування шарів з острівцевою будовою. Зменшення впливу процесу коагуляції можна шляхом попереднього нанесення на діелектричну підкладку підшарів змочуючих матеріалів товщиною в декілька атомних шарів. Експериментальні дослідження впливу змочуючи підшарів різної природи на умови формування плівок металів та їх електричні властивості є актуальним, через можливість формування нанорозмірних металевих конденсатів з напер заданими електрофізичними параметрами. Нами проведено досліджено електропровідності нанорозмірних плівок золота товщиною 2-40 нм нанесених на оплавлене поліроване скло та на скло попередньо покрите шаром германію товщинами - 1-3 нм. Плівки германію товщиною в декілька атомних шарів наносили на підкладки безпосередньо перед конденсацією плівки металу в умовах надвисокого вакууму (тиск залишкових газів не перевищував за 10^{-7} Па). Досліджували свіжонанесені шари золота (quenched condensed), вимірювання опору плівок проводили при 78 К та 90 К. Масову товщину плівки оцінювали за зсувом резонансної частоти п'єзокварцового вібратора (чутливість ~ 0,1 нм/Гц).

Оцінка значень питомого опору ρ_∞ та λ_∞ в рамках підходу Фукса-Зондгеймера [1], для плівок золота осаджених при 78 К на чисту скляну підкладку, показала відповідно 10^{-7} Ом·м та $\lambda = 14$ нм, що 4,7 рази більше ρ_0 масивного золота при 78 К. Водночас низькотемпературне ($\Delta T = 78\text{-}90$ К) значення температурного коефіцієнта опору $\beta_\infty = 3{,}1\cdot10^{-4}$ К$^{-1}$, що в 90 раз менше в порівнянні з масивним зразком золота ($\beta_0 = 2{,}8\cdot10^{-2}$ К$^{-1}$, $\Delta T = 60\text{-}80$ К). Зміна знаку β в плівці золота спостерігалась при товщині $d_\Omega = 5{,}5$ нм, водночас у плівках золота осаджених на підшари германію 2 нм та 3 нм, проявлялось зменшення товщини d_Ω, зміни знаку β від від'ємного до позитивного значення від 2,2 нм до 1,4 нм.

[1]. Шпак А.П., Бігун Р.І. , Стасюк З.В., Куницький Ю.А. Структура та електропровідності ультратонких плівок міді, золота та срібла. *Наносистеми, наноматеріали та нанотехнології*. 2010. Т. 8, № 2. С. 339–388.

[2]. Бігун Р. І., Стасюк З. В., Бучковська М. Д., Гаврилюх В.М., Леонов Д.С. Вплив особливостей режиму термостабілізації на структуру та електропровідність нанорозмірних плівок міді,золота та срібла. *Металлофизика и новейшие технологии*. 2020. Т. 42, № 12. Р. 1629–1639.

Modeling of Antireflective Gradient Films based on Porous Si

Politanskyi, R.L.[1], Vistak, M.V.[2], Kogut, I.T.[3], Mykytyuk, Z.M.[4],
Shymchyshyn, O.Y[4], Diskovskyi, I.S[2]

[1]Yuriy Fedkovych Chernivtsi National University, Chernivtsi, Ukraine,
r.politanskyi@chnu.edu.ua
[2]Danylo Halytsky Lviv National University, Pekarska Str., 69, Lviv, Ukraine,
vistak_maria@ukr.net
[3]Vasyl Stefanyk Precarpathian University, Ivano-Frankivsk, Ukraine, ihor.kohut@pnu.edu.ua
[4]National University Lviv Polytechnik, Lviv, Ukraine, zynovii.m.mykytiuk@lpnu.ua

The paper simulates the reflection coefficients of multilayer and gradient dielectric films. On the basis of the matrix method [1], the analysis of the processes of reflection, transmission and absorption of light with different types of polarization, frequency range and angles of incidence to the film surface was carried out. On the basis of the developed mathematical model of light fall processes, the intensity of reflected and absorbed light is calculated for the film intended for the transmission of optical radiation in the infrared range. The performed calculations are the basis for designing an optical filter made on the basis of porous silicon, which is used to select the required wavelength in a photodiode based on IV-IV families of semiconductor materials (Si, Ge, Pb). Porous silicon provides the possibility of manufacturing a material with a variable refractive index (Fig. 1), which depends on the porosity of the material [2].

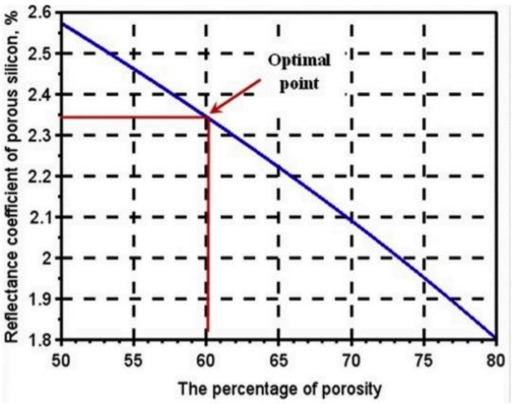

Fig.1. The dependence of the refractive index on the porosity of silicon

As a result of the research, the optimal values of the silicon porosity profile were selected for the successful use of the film on the indium antimonide surface.

[1]. Politanskyi R.L., Vistak M.V., Barylo G.I., Andrushchak A.S. Simulation of anti-reflecting dielectric films by the interference matrix method. *Optical Materials.* 2020. V. 102, No 109782.
[2]. Assadi M.K., Moayedfar M. Various types of anti-reflective coatings (arcs) based on the layer composition and surface topography: a review. *Rev. Adv. Mater. Sci.* 2018. V. 53. P. 187–205.

Obtaining of Carbon Nanomaterials on Thin Films of Ni/Cr and Fe Catalysts by Deposition From a Gaseous Mixture of Carbon Monoxide and Hydrogen

Khovavko A.I.[1], Nebesnyi A.A.[1], Filonenko D.S.[1], Sviatenko A.M.[1],
Barabash M.Yu.[1,2,3].

[1]The Gas Institute of the National Academy of Sciences of Ukraine,39, Dehtyarivska St., 03113, Kyiv, Ukraine, ingaskiev@gmail.com
[2]Technical Center of the National Academy of Sciences of Ukraine,13, Pokrovska St., 04070, Kyiv, Ukraine mbarabash@nasu.kiev.ua
[3]National Technical University of Ukraine "Igor Sikorsky Kyiv Polytechnic Institute", Beresteiskyi Prospect 37, UA-03056, Kyiv, Ukraine

The purpose of this work is to study the formation of carbon nanostructures (tubes, graphene) on substrates with deposited films of Fe and Ni/Cr catalysts. Catalysts for nanotube growth were deposited by thermal evaporation in a vacuum in the form of thin layers of metals on installation VUP-5M (fig.1). Surface layers of Fe and Cr/Ni were deposited on glass-ceramic substrates. Carbon nanomaterials of various morphologies are synthesized from a mixture of carbon monoxide and hydrogen by chemical vapor deposition.

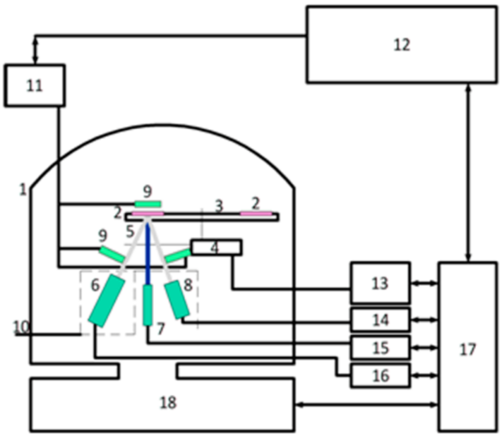

Fig. 1. Scheme of technological unit for producing thin films by vacuum co-deposition.

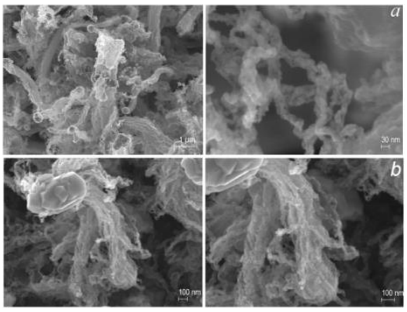

Fig. 2. Surface image (SEM) of carbon nanomaterials: *a* – iron catalyst; *b*–Ni/Cr catalyst.

Optimization of the Poling Field for Obtaining Uniform Polarization in Ferroelectric Polymer Thin Films

Sergeeva A. E., Fedosov S. N., Kichuk S. V.

Odesa National University of Technology, Odesa, Ukraine aeserg@ukr.net

Information on the spatial distribution of polarization in ferroelectric polymer thin films is important both from scientific and practical points of view. Of all suitable methods, the piezoelectrically generated pressure step method (PPS) applied in this study [1] is the most reliable and informative. We studied polyvinylidene fluoride (PVDF) and poly(vinylidene-tetrafluoroethylene) P(VDF-TFE) 20 μm thick films as typical representatives of the ferroelectric polymers. The films have been uniaxially stretched by the supplier.

It appeared that residual polarization was non-uniform after initial poling under the middle field (60 MV/m) with a maximum near the positive electrode [2]. At the same time, homogeneous polarization was formed in high fields (160 MV/m). For optimizing the poling regime, it was interesting to investigate under high-field behavior of the ferroelectric polymer films, originally poled in the middle fields.

Polymer films were polarized in the field of 60 MV/m, and polarization profiles were measured. Then, we increased the voltage to 3.2 kV to make the field grow several times higher than the coercive one (≈ 50 MV/m). However, the increase in the field strength did not lead to the expected improvement of the residual polarization uniformity.

Thus, in order to obtain the high homogeneous residual polarization, it is not enough just to apply the high field. It is also necessary to consider the conditions at which the sample was originally poled. If initial poling was performed in the high field, then the residual polarization would be homogeneous. If initial polling was carried out in a medium or weak field, the non-uniformity of the residual polarization cannot be corrected by subsequent application of the high field.

In this case, for obtaining the uniform profile of the residual polarization, we recommend a complete thermal depolarization of the sample and its annealing in the short-circuited condition at about 160 °C for several hours, so that the trapped charges in the volume will be completely dissipated. After cooling the sample, it is necessary to repole it, but necessarily in the high field.

[1]. Eisenmenger W., Schmidt H., Dehlen B., Space Charge and Dipoles in Polyvinylidene fluoride, *Braz. J. of Physics*, 29, (1999) 295.

[2]. Fedosov S., Sergeeva A. *Formation and relaxation of a polarized state in ferroelectric polymers*, Lambert Academic Publishing, Germany, (2020) 165 p.

Problems of Creation Laser-Induced Thin Films

Trokhimchuck P.P.

Lesya Ukrainka Volyn National University,Lutsk, Ukraine,
trope1650@gmail.com, Trokhimchuck.Petro@vnu.edu.ua

The problem of creation and modelling laser-induced films is connected with problem of phase transformations [1, 2]. During the interaction of laser irradiation with solid bodies, it is necessary to talk more quickly about the phase transformations of the irradiated material, and about the formation of film-like structures that have different physical properties from the irradiated material.

Depending on the conditions of radiation absorption: the nature of the absorbing centers (stable, metastable or unstable) and the intensity of irradiation, we can obtain structures with relatively homogeneous and heterogeneous properties [1, 2]. Structures with more or less uniform elasticity include laser-annealed ion-implanted layers, if irradiation is carried out, which is absorbed in the "defective" and not in the band of its own absorption. In this case, the duration of exposure does not play a significant role, the main thing here is to get the appropriate integral dose of exposure. In this case, the calculation of the radiation dose is quite simple: it is necessary to multiply the concentration of defects by their concentration. This was confirmed for antimonide and indium arsenide. The film thickness is 200 nm.

In the case of irradiation of stable structures (for example, crystals of silicon or indium antimonide), it is necessary to observe the procedures of saturation of the excitation of the corresponding type of chemical bonds. Which lead to the corresponding phase changes [1]. Thus, for silicon, hedgehog-like structures with a set of phases can be formed: diamond - hexagonal - triclinic and monoclinic modifications. Moreover, structures with lower symmetry are formed closer to the surface and on the surface itself. The dimensions of such hedgehogs can reach 50 µm. In this case, it is desirable that the radiation be in the self-absorption range. To change the electrophysical properties of indium antimonide, the sizes of the films are from 0.5 µm to 5 µm.

Laser irradiation of transparent materials leads to the formation of a cascade of optical breakdown [2]. The thickness of the breakdown area is 20-50 microns. This is due to the transformation of focused radiation: diffraction stratification - generation of Cherenkov radiation and interference of the short-wavelength part of this radiation.

Questions about the use of these phenomena in modern optoelectronics are discussed too [1, 2].

[1]. Trokhimchuck P. P. Relaxed Optics: Modelling and Discussions. Saarbruken: Lambert Academic Publishing. 2020. 249 p.

[2]. Trokhimchuck P. P. Relaxed Optics: Modelling and Discussions 2. Cisinau-Saarbruken: Lambert Academic Publishing. 2022. 210 p.

Pulsed Laser Deposition of Thin Films of Chalcogenide Semiconductors for Optoelectronics

Virt I.S.[1], Potera P.[2], Cieniek B.[2]

[1]*Drohobych State Pedagogical University I.Franko Drohobych, Ukraine;*
[2]*University of Rzeszow, Poland.*
isvirt@email.ua

In this report, we have grown and studied the properties of a chalcogenide semiconductor - these are Bi_2S_3 thin films obtained by pulsed laser deposition. It is a chalcogenide semiconductor exhibiting an orthorhombic crystal structure with *Pnma* space group. Materials – 0D Bi_2S_3 nanodots/particles, 1D Bi_2S_3 nanowires/nanotubes, or 3D Bi_2S_3 hierarchical architectures have been extensively exploited for photodetecting applications [1].

The experimental PLD system developed and used to deposit nanocarbon layers has been previously described. The $KGd(WO_4)_2$ laser was used – radiation characteristics: *lamda* = 1067 nm, pulse duration *t* = 20 ns, beam energy density 6–8 J/cm^2, repetition rate 1–5 Hz. The technology module uses the Q-switch to irradiate in modulated goodness factor mode. Thin films were prepared by the laser ablation method by laser deposition of compressed targets. The ablation of the polycrystalline Bi_2S_3 targets was performed in a quartz chamber; the final pressure in the deposition chamber was 10^{-6} Pa. Silicon (111)-Si, Al_2O_3, glass and polymer substrates were used. The deposition temperature (substrate temperature) was about 200 °C. Thin films nanostructures were obtained in substrates with an area of 1x1cm^2.

Under these conditions, the thin films exhibited nanocrystallization, high density, and high microhardness. The crystal structure of all Bi_2S_3 layers was determined by X-ray phase analysis, mainly on silicon substrates. Microstructure studies by X-ray diffraction and SEM showed that the synthesized grains were quite uniform in diameter and formed bundles of 5-20 nm in size. Enhanced (120) peak intensities in the XRD analysis were observed for the nanorod. Electrical properties were considered from optoelectronics application. Optical spectra were obtained using a CARY 5000 spectrophotometer, depending on the wavelength range. For the UV-VIS-NIR range (200-3300 nm), total reflection (both mirror and diffuse) and transmission spectra were determined. We use measurements of transmission values to calculate the absorption spectrum. Transmittance and absorption coefficients with actual density were estimated using the Beer-Lambert law. The width of the band gap E_g=2.2 eV was determined. Measurement of optical characteristics allows us to conclude that absorption is the main mechanism responsible for blocking the transmission of light in the studied materials.

[1]. Chitara B., Kolli B.S.C., Yan F., Near-Infrared photodetectors based on 2D Bi_2S_3. *Chemical Physics Letters.* 2022. V. 804, P. 139876 (1-6).

Shape and Location of Charge Carriers in Linear, Branched and Curved π-Electron Carbon Systems

Pavlenko O.L.[1], Gaponov A.M.[1], Dmytrenko O.P.[1], Kulish M.P.[1],
Naumenko A.P.[1], Kachkovsky A.D.[2]

[1]*Taras Shevchenko National University of Kyiv, 64/13 Volodymyrska Str. Kyiv, Ukraine*
[2]*Institute of Bioorganic Chemistry and Petrochemistry, National Academy of Sciences, 1 Murmanska Str., Kyiv, Ukraine, olpavl57@gmail.com*

We have performed quantum-mechanical study of the charge distribution on the carbon atoms of a series of neutral polyenes, two-dimensional conjugated system of the model graphene ribbon, graphene layer, nanotube and C_{70} fullerene after injection of the charge carriers into the systems. The study shows that charges in the linear, quasi-two dimensional conjugated system of the graphene ribbon , graphene, single wall nanotube and fullerene C_{70} are not localized on separate carbon atoms, but form one-, two- and three-dimensional solitonic charge waves along the sides and surfaces for every structure.

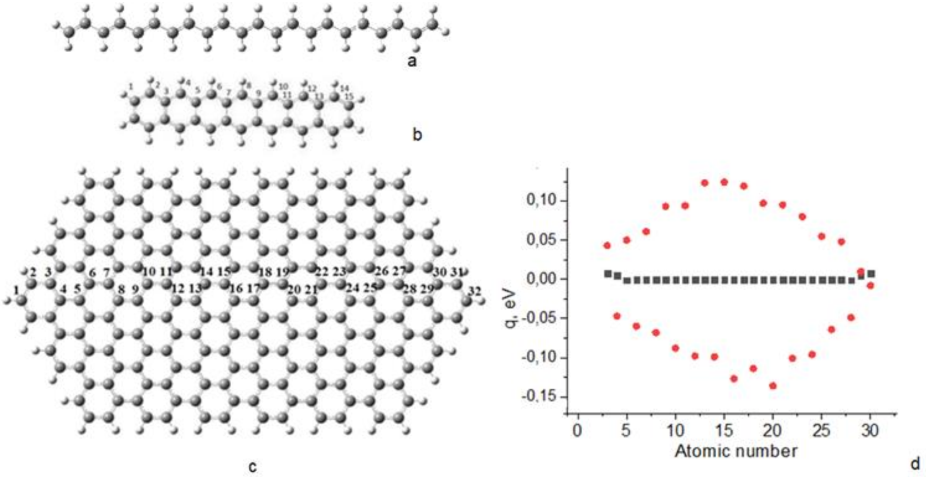

Fig. 1. Linear chain (a), graphene chain (b), graphene layer (c). Charge distribution on the central row of carbon atoms in graphene layer in pure initial state of graphene layer (black squares) and after injection of a charge carrier into graphene layer (red sircles).

Distribution on the central row of carbon atoms in graphene layer, decorated by hydrogen atoms, for it`s pure initial state and after injection of a charge is different. Similar to more simple molecular structures, injection of the charge into the graphene results in a formation of solitonic wave of charge alternation. This wave causes the formation of a bond length alternation wave, known as a geometrical or topological soliton.

[1]. Nychyporenko S.O et al., Shape and location of multiple charge carriers in linear π-electron systems, *Journal of Quantum Chemistry* , 2014. V. 114, No 6. P. 416-428.

Strain Analysis of Diamond Crystals by the Power Fourier Spectrum of Kikuchi Patterns

Borcha M., Fodchuk.I, Solodkyi M., Balovsyak S., Kuzmin A., Hutsuliak I., Tkach O., Unhurian M

[1] *Yuriy Fedkovych Chernivtsi National University, Chernivtsi, Ukraine,*
m.borcha@chnu.edu.ua

Among the methods for calculating crystal strains, methods based on the analysis of backscattered electron diffraction images (Kikuchi patterns) are especially promising due to their high locality and non-destructive nature of research. In particular, the deformations of crystals are determined based on the analysis of the shape of the profiles of the intensity bands and on the basis of the analysis of the energy Fourier spectrum of the Kikuchi patterns [1].

The work presents a modified approach that explains the change of the deformation state in different crystallographic directions for a set of 6 synthetic diamond crystals, obtained by different technological processes, is developed. It is proposed to determine the deformations of local regions of synthetic diamond crystals on the basis of normalized profiles of Kikuchi band intensity (ε_P) and normalized parameters of the energy Fourier spectrum (ε_T) without the use of reference image.

It is established that the normalization of areas S_P and S_{P0} under Kikuchi band intensity profile provides the dependence of S_P and S_{P0} only of the profile shape, and also the possibility of analyzing profiles of different widths for Kukuchi patterns obtained for region of different crystals. It is shown that the normalization of the frequency reduces the effect of noise and the average background of image.

The presented model was successfully used for the quantitative analysis of the deformation characteristics of a series of synthetic diamond crystals. The satisfactory agreement between the values of ε_P and ε_T indicates the correctness of the proposed method for determining strains based on the profiles of the Kikuchi bands and the parameters of their energy Fourier spectra

[1]. Fodchuk I.M., Ivakhnenko S.A., Tkach V.N., Balovsyak S.V., Borcha M.D., Solodkii N.S., Gutsulyak I.I., Kuzmin A.R., Sumaryuk O.V. Local strain distribution in synthetic diamond crystals, determined by the parameters of the energy spectrum of the Kikuchi patterns. Journal of Superhard Materials. 2020. – Vol. 42, №1. – P. 1-8

Structural and Morphological Studies of Films Formed in the Process of Gas-Detonation Deposition of Hydroxyapatite Onto Polymer Substrates

Yukhymchuk V.O., Temchenko V.P., Lozynskyi V.B., Karnaukhov A.V., Isaieva O.F., Dzhagan V.M., Vorona I.P., Valakh M.Ya., Belyaev A.E.

V. Lashkaryov Institute of Semiconductors Physics, National Academy of Sciences of Ukraine, 45 Nauky av., 03028 Kyiv, Ukraine, yukhym@isp.kiev.ua

Nowadays, there is great interest in the development of medical implants, which is due to the huge need for such products in Ukraine and the world as a whole. Implants made based on titanium and its alloys have become the most widespread today. However, despite their relatively good biocompatibility, negative effects are often observed after their implantation in the human body, in particular, the occurrence of inflammatory processes. This problem can be solved by depositing on the surface of implants biocompatible coatings, usually calcium phosphates (CF), which are close in their composition to bones, in particular, it is hydroxylapatite (HAP).

In our work, it is proposed to use polymer implants covered by HAP using the method of gas detonation deposition (GDD). The essence of the latter consists of the acceleration of particles of the original CF powder by a detonation wave, which occurs as a result of the explosion of a propane-butane mixture with oxygen. FC powder particles are introduced into the detonation wave, accelerate to velocities that are 5 times the speed of sound and as a result of their interaction with the surface of the implant, a coating is formed on it. The advantages of the GDD method are high productivity, the ability to apply layers of different thicknesses to substrates of a large area; to widely vary the coating composition; and obtain a coating with high adhesion to the substrate.

The novelty of this work is the deposition of HAP coatings on polymer substrates – polyetheretherketone (PEEK). The latter is a highly effective thermoplastic crystalline polymer with good mechanical properties and is inert to an aggressive chemical environment. Films on PEEK with a thickness of ~200 μm were obtained by GDD. Raman spectroscopy, XRD, SEM, and EPR were used for their characterization. It was established that by varying the distance from the GDD gun to the PEEK substrate, it is possible to obtain the HAP film of good quality without destroying the polymer. The methods of Raman spectroscopy and XRD confirmed the formation of crystalline HAP film. It was established that the formed films have a porous structure. EPR studies demonstrated the absence of paramagnetic defects in the formed film.

The work was carried out within the NFSU project No. 200/0103.

Structural and Phase Transformations in Vanadium Oxide Under the Ultrasound Loading

Tymochko M.D.[1], Melnik V.P.[1], Dubikovskyi O.V.[1], Olikh Ya.M.[1],
Romanyuk B.M.[1], Lepikh Ya.I.[2]

[1]*V.E. Lashkaryov Institute of Semiconductor Physics National Academy of Sciences of Ukraine, Kyiv, Ukraine, tymochko@ukr.net*
[2]*I.I. Mechnikov National University Odessa, Ukraine, ndl_lepikh@onu.edu.ua*

Vanadium dioxide (VO_2) films are promising as a functional material for uncooled microbolometers. The sensitivity of VO_x films (as $x \rightarrow 2$) to infrared radiation is associated with significant (≈ 4 orders of magnitude) changes in their electrical resistance caused by the semiconductor-metal phase transition of the VO_2 phase in VO_x films. The film's structure is a mixture of the phases, but it is the VO_2 phase that has the most optimal transition temperature for use in devices (~ 68 °C). A thin film of VO_2 usually has a polycrystalline structure with a grain size of 30-120 nm that is heavily influenced by the growth conditions. Since the phase transition is related to stresses inside the structure, their change leads to a change in its parameters, in particular, the magnitude of the resistance change ΔR, the width of the transition ΔT, and the temperature of the phase transition. To manage the VO_2 film quality, the temperature of phase transition, the hysteresis of phase transition, and the magnitude of resistance changes it is necessary to apply effective methods of managing the system of defects, in particular ultrasound. A piezotransducer attached to the back side of the substrate was used to excite the acoustic waves, which localized on the substrate surface. The ultrasound loading, longitudinal waves, occurred using a piezoelectric transducer (lithium niobate $LiNbO_3$, cut Y+35°) at a resonance frequency of 6 MHz. The US mode corresponds to the US power $4 \cdot 10^3$ $W \cdot m^{-2}$.

The stoichiometric composition of VO_2 determined the temperature coefficient of resistance of the film. An acoustic-induced increase in the relative vanadium and oxygen contents and a corresponding decrease in carbon and nitrogen (before etching) were revealed on the film surface. At the same time, after etching the surface for 2 min, the contrary effect of an acoustically induced decrease in the relative content of vanadium was observed. The ultrasound causes the acoustically induced redistribution of vanadium atoms between the volume and the surface of the sample (drift of the atoms to the surface and the corresponding depletion of the volume) when applying the film. It was found that the quality of the film structure was improved with the additional use of ultrasound loading to the substrate during the deposition process. Improving the structure of VO_x films under ultrasound loading was confirmed by the results of the SEM image study: for the samples obtained under the conditions of additional ultrasound loading, an arrangement and increase in grain size were observed.

Synthesis and Morphology Characterization of Electrocatalytic Mo-Rich Alloys

Bersirova O.[1,2], Cesiulis H.[1]

[1]Department of Physical Chemistry, Vilnius University, Vilnius, Lithuania
[2]V.I.Vernadsky Institute of General & Inorganic Chemistry NASU, Kyiv, Ukraine
oksana.bersirova@chgf.vu.lt

In recent time, the development of effective cathode materials for hydrogen evolution reaction (HER) is the subject of a lot of publications. It was shown that binary alloys of iron group metals (Ni, Co, Fe) with refractory metals (Mo, W and Re) demonstrate the satisfied electrocatalytic properties for HER. Among these materials the major part of investigations have been focused on the coatings containing a high amount of molybdenum because they are characterized by high thermal, wear and corrosion resistance, exceptional hardness and excellent catalytic properties for HER in alkaline medium.

We are developing high effective production methods that use stable, non-toxic high effective electrolytes for formation of coatings containing a high amount of refractory metal in alloy [1, 2]. As example, at electrodeposition from Mo-rich polyligand highly concentrated ammonium-acetate bath the percentage of Mo has been observed from 92 wt.% at 30 mA cm^{-2} and decreases with increasing the deposition current density. At lower current densities the electrodeposits demonstrate smooth appearance, while at higher values (above 100 mA cm^{-2}) the formation of cracks and pits was noticed, that reduces the catalytic activity of coating for HER [2]. It was shown that Co-Mo and Fe-Mo demonstrate the higher electrocatalytic activity for HER than Ni-Mo (atomic ratio [Mo]:[M]=1:1). A significant improvement of catalytic activity for all tested coatings with increasing of the temperature was founded.

The main regularities of the influence of electrolysis conditions and mechanism of electrochemical synthesis of refractory metals (Mo, W and Re) alloys with iron group metals, on the composition of obtained deposits, as electrode materials promising for electrocatalysis, have been determined.

O. Bersirova thanks for received funding through the MSCA4Ukraine project, which is funded by the European Union (Project No.1233494).

[1]. Vernickaitė E., Tsyntsaru N., Sobczak K., Cesiulis H., Electrodeposited tungsten-rich Ni-W, Co-W and Fe-W cathodes for efficient hydrogen evolution in alkaline medium. *Electrochimica Acta*. V.318. 2019. P.597-606.
[2]. Vernickaitė E., Bersirova O., Cesiulis H., Tsyntsaru N. Design of highly active electrodes for hydrogen evolution reaction based on Mo-rich alloys electrodeposited from ammonium acetate bath. *Coatings*. V.9, №2. 2019. P.85-101.

The Influence of Substrate Type on the Structural and Optical Properties of Solid Solutions $CdTe_{1-x}Se_x$

Vashchynskyi V.M., Ilchuk H.A., Semkiv I.V., Solovyov M.V., Karkulovska M.S.

Lviv Polytechnic National University, 12 S. Bandery Str., Lviv, Ukraine
v.vashchynskyi@gmail.com

Thin film material science is closely associated with the development of modern methods for obtaining functional materials, which currently encompass several dozens of varieties. Recently, particular attention has been drawn to the semiconductor compound cadmium telluride (CdTe), which has found wide application in photovoltaic solar cells and optoelectronic devices. CdTe is unique among AIIBVI compounds since it can exhibit both n-type and p-type conductivity, which is crucial for devices with p-n junctions. It possesses an optimal bandgap width of 1.5 eV for photovoltaics and is characterized by a high optical absorption coefficient. It's worth noting that a deposition parameter such as the substrate type will affect the properties of the obtained films. Glass, silicon, and ITO/glass were used as substrates. To enhance the efficiency of solar cells, modifying the architecture of the solar cell, specifically introducing selenium (Se) into the absorber layer of CdTe to form a solid solution $CdTe_{1-x}Se_x$, can be employed.

For the production of the solid solution $CdTe_{1-x}Se_x$, the method of high-frequency (HF) magnetron sputtering (~13.6 MHz) was utilized on substrates using the VUP-5M vacuum station (Selmi, Ukraine). The substrate size was 5×7 mm. The target–substrate distance was 70 mm. Before the sputtering process, the chamber was evacuated. The gas pressure inside the chamber was 5×10^{-4} Pa.

The sputtering was carried out at a pressure of argon (Ar) in the range of 1.0 - 1.3 Pa. The power of the magnetron was maintained at the level of 50 W and the temperature of the substrate at 489 K. For heating the substrates, a high-temperature tungsten heater with a power of 300 W was used. The temperature was controlled by means of a PID controller for controlling heating and cooling rates, as well as for ensuring the temperature conditions of deposition.

Using the scanning electron microscope-microanalyzer REMMA-102-02, the surface morphology of the samples was investigated. It was determined that the examined layers are polycrystalline and consist of randomly oriented crystals. Individual grains with distinct grain boundaries were observed.

The present work was supported by the National research foundation of Ukraine (project No 2022.01/0163).

The Influence of the Transition Layer of CdTe:Cl/MoO$_x$ Heterostructures on the Electrical and Spectroscopic Properties of Detector Systems

Fodchuk I.M., Kuzmin A.R., Balovsyak S.V., Hutsuliak I.I., Solodkyi M.S.

Chernivtsi National University, Kotsjubynskyi str. 2, Chernivtsi, Ukraine, ifodchuk@ukr.net

Cadmium telluride single crystals are actively used to manufacture the X- and γ-radiation detectors due to their ability to operate at room temperatures, unlike silicon counterparts [1]. The objects of research are CdTe/MoO$_x$ heterostructures obtained by the method of reactive magnetron sputtering.

The fitting of experimental rocking curves of CdTe:Cl/MoO$_x$ heterostructures was carried out using semi-kinematic theory of X-ray scattering, and deformation distribution in the transition layer was calculated (Fig. 1a). The calculated deformation profile (the dependence of Δd/d on the coordinate) in the oxide film/single crystal transition layer demonstrates an exponential decline from 10^{-1} to 10^{-4} (Fig. 1b). This transition layer significantly affects the electrical and spectroscopic properties of the materials.

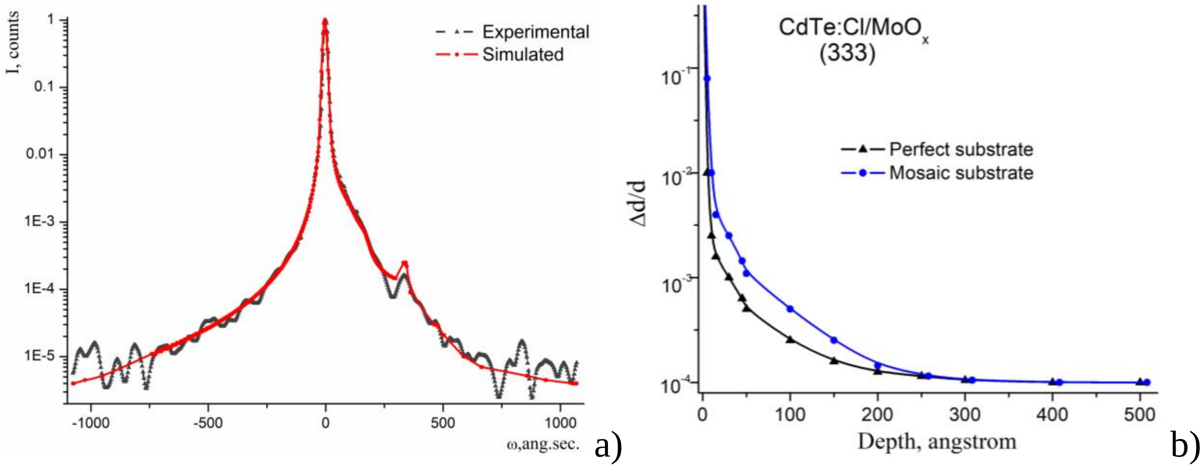

Fig. 1. Experimental and simulated rocking curves for CdTe:Cl/MoO$_x$ heterostructure based on the “perfect” substrate ((333) reflection) (a); deformation distributions in the near-surface layer of CdTe:Cl single crystal for “perfect” and "mosaic" based CdTe:Cl/MoO$_x$ heterostructures (b).

A promising way to minimize deformation is the deposition of graphene layer on crystal surface before deposition of the metal oxide film. The defect structure of the substrates also affects the electrical and spectroscopic characteristics of the X- and γ-radiation detectors.

[1]. Gnatyuk, V.; Maslyanchuk, O.; Solovan, M.; Brus, V.; Aoki, T. CdTe x/γ-ray detectors with different contact materials. *Sensors*. 2021. Vol.21, №10. 3518.

Thin Ag Films as Transparent Conductors

Bihun R.I., Penyukh B.R., Apopii V.H., Koman B.P., Kalivoshka B.M.

Ivan Franko Lviv National University, Ukraine,
roman.bihun@lnu.edu.ua

Metals are favorable candidates for flexible transparent electrodes because they have high electrical conductivity and good ductility. Nano-thin metal films (film thickness < 10 nm) can present low sheet resistance ($R_{\text{sqr}} < 10\text{-}20\ \Omega/\text{m}^2$) and high transmittance (T ≈ 80-90 %) simultaneously. Due to Ostwald ripening many metal films (e.g., Au, Ag, Cu) tend to form in island growth mode, leading to isolated metal islands and non-conducting feature until the films become relatively opaque. We present vacuum deposition of Ge wetting underlayers method that can effectively suppress Ostwald ripening in metal films, which become conducting faster due to shifts percolation threshold at smaller thicknesses. The conducting and transparent metal films are smooth and stable. This work presents versatile strategy to fabricate metal transparent electrodes .

Nano-thin Ag film and underlayers Ge film were deposited by thermal evaporation on glass surface substrate under high vacuum ($P \sim 10^{-7}$torr) condition at room temperature. Mass thicknesses of investigated films have been assessed by the shift of quartz oscillator resonance frequency. Electrical resistance was measured using two-probe method. Transmittance T(λ) and reflectance R(λ) spectra were measured by broadband spectrophotometer Shimadzu UV-3600.

According to percolation approach, percolation thickness d_c was evaluated for impact assessment of Ge wetting layers on Ag films. Thickness dependency of Ag films optical transmittance (T = 500-1700 nm), deposited on clean glass substrate and substrate pre-coated with 1 nm germanium underlayers shows $d_c = 12$ nm and $d_c = 5$ nm respectively. It's indicate, more than 2,4 times reduction of the Ostwald effect on Ag film growth regime. A comparative analysis of the critical percolation parameter γ for the investigated 12 nm Ag films indicates that γ value is between the values of predicted by the Ising models and the 2-D percolation model [1]. While for Ag films with thickness of 5 nm deposited on 1 nm Ge underlayer, this value is greater than the model predictions. The fractal parameter in the case of a 12 nm Ag film is smaller compared to the predictions of the two-dimensional model, which indicates the presence of significant number of empty places on the surface of the substrate. In the case of silver film on a germanium underlayer, the value of the fractal parameter is greater than the value predicted by the two-dimensional percolation model [1].

[1]. Bihun R. I., Buchkovs'ka M.D., Koman B. P., Leonov D. S. Germanium Wetting Layers Dimensional Effect in Structural and Optical Properties of Silver Films. *Nanosystems, nanomaterials and nanotechnologies*. 2022. Vol. 20, № 4. P. 929-939.371.

Session 2

Nanotechnologies and nanomaterials, quantum-size structures

Conductive and Capacitive Properties of InSe<$SmCl_3$> Nanohybrid

Maksymych V.[1], Chabecki P.[2], Shvets R.[3]

[1]*Ivan Franko National University of Lviv, Universytets'ka Str. 1, 79000 Lviv, Ukraine*
[2]*Politechnika Częstochowska, Al. Armii Krajowej 17, 42-20, Czestochowa, Poland*
[3]*Lviv Polytechnic National University, S. Bandera Str. 12, 79013 Lviv, Ukraine*
vitalii.maksymych@lnu.edu.ua

An interesting area of research in the field of non-electrochemical power sources is the effect of spontaneous EMF generation. It was first recorded in the SmS crystal during heating in the absence of external temperature gradients. In some experiments, the EMF value even reached 2.5 V during a 1.3-second pulse and 0.6 V in continuous mode. This phenomenon is due to the uneven distribution of defective Sm^{2+} ions, which, when heated, change the concentration of electrons, thereby forming electron concentration gradients and leading to the emergence of EMF.

In recent work [1], this effect was more successfully realized by the formation of a periodically ordered matrix structure implemented on the basis of a SiO_2 matrix with intercalated SmCl3. Thus, in the synthesized SiO_2<$SmCl_3$> hybrid, an EMF value of 40 V was achieved under a constant temperature field at 290 K. Instead, in [2], the formation of a hybrid 2D structure based on a layered semiconductor single crystal GaSe intercalated with SmCl3 allowed to achieve an EMF of the order of 10 V at room temperature and at temperatures above 315 K.

We continued our research in this direction and formed a 2D structure based on a layered semiconductor single crystal InSe intercalated with SmCl3. It is known that a GaSe single crystal is characterized by p-type conductivity, and an InSe single crystal is, on the contrary, n-type. For the InSe<$SmCl_3$> nanohybrid, the character of the frequency dispersion of the impedance, loss tangent, and dielectric constant under illumination and in a constant magnetic field was determined. The behavior of thermally stimulated discharge currents in the temperature range of 240-360 K was also investigated. Thermogalvanic and memristor effects were observed and their mechanisms were analyzed.

[1]. I. Grygorchak, D. Calus, A. Pidluzhna, F. Ivashchyshyn, O. Hryhorchak, P. Chabecki, R. Shvets. Thermogalvanic and local field effects in SiO2<$SmCl_3$> structure. *Applied Nanoscience.* 2020. Vol. 10(12). P. 4725-4731. doi:10.1007/s13204-020-01447-2;

[2]. F. Ivashchyshyn, A. Pidluzhna, D. Calus, O. Hryhorchak, P. Chabecki, O. Makarchuk. Multivoltaic GaSe<$SmCl_3$> clathrate as new hybrid functional nanostructure. *Bulletin of the Polish Academy of Sciences: Technical Sciences*. 2021. Vol. 69(2). P. e136726-1-5. doi: 10.24425/bpasts.2021.136726.

Controlling by Defects of Switching of ZnO Nanowire Array Surfaces from Hydrophobic to Hydrophilic

Stepanyuk A.N., Balabai R.M.

Kryvyi Rih State Pedagogical University, Kryvyi Rih, Ukraine
alexanderstepanyuk@gmail.com, *balabai@i.ua*

ZnO nanowires possess structural properties, which makes them advantageous for hydrophobic applications [1]. ZnO polar and nonpolar surfaces have different wettabilities. The defects of the oxygen containing surfaces are typically responsible for interchange between hydrophilic and hydrophobic ZnO states. Understanding the atomic-level mechanisms of reversible wettability is essential for developing practical applications of ZnO wires.

We evaluated the energy reliefs of the migration of water molecules along different lateral surfaces of wires without defects and with oxygen and zinc vacancies (Fig. 1). Electric charges around atoms on the path of possible migration of water molecules were calculated using the electron density functional and pseudopotential methods from first principles using our own software code [2].

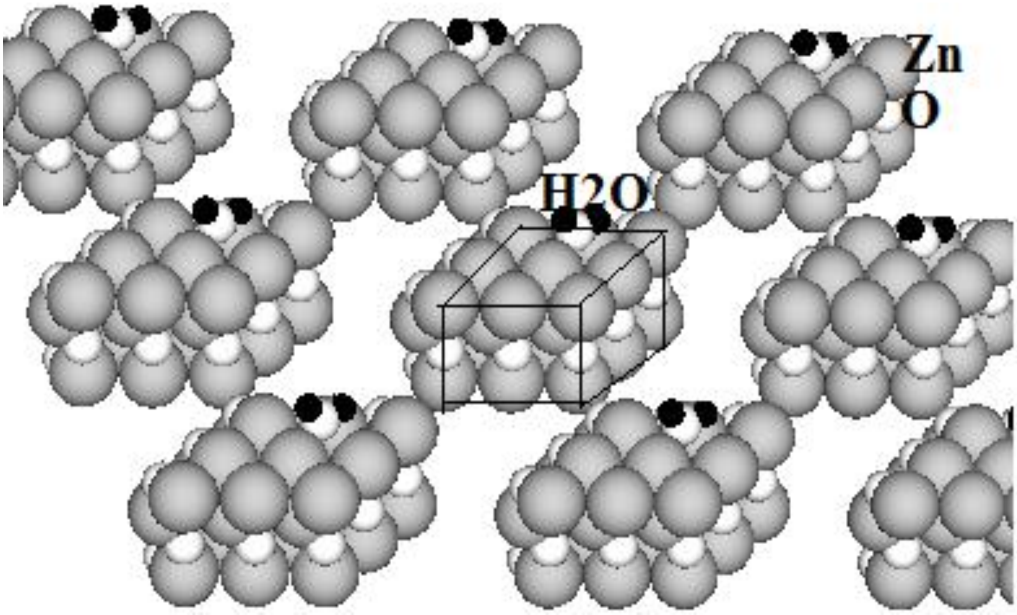

Fig. 1. Fragments of an array of ZnO wires of wurtzite crystal structure grown along the ***c***-axis: layers of Zn/O/Zn/O ions create a sequence in the [0001] direction

[1]. Mardosaitė R., Jurkevičiūtė A., Račkauskas S. Superhydrophobic ZnO Nanowires: Wettability Mechanisms and Functional Applications. Crystal Growth & Design. 2021. Vol. 21, No. 8. P. 4765–4779.

[2]. Naumenko M. V., Balabai R. M. Synergistic properties of β-Ga_2O_3 nanowire arrays. Physics and Chemistry of Solid State. 2023. Vol. 24, No. 1. P. 56–63.

Doping-Induced Phase Separation in (Cd,Cr)Te Magnetic Materials

Popovych V.D.[1,2], Dluzewski P.[3], Morawiec K.[3], Zajkowska W.[3],
Popovych A.V.[1], Stolyarchuk I.D.[1], Hadzaman I.V.[1], Żywczak A.[4], Kuzma M.[5],
Shiojiri M.[6]

[1]*Ivan Franko Drohobych State Pedagogical University, Drohobych, Ukraine,*
vpopovych@dspu.edu.ua
[2]*The John Paul II Catholic University of Lublin, Lublin, Poland*
[3]*Institute of Physics, Polish Academy of Science, Warsaw, Poland*
[4]*AGH University of Science and Technology, Krakow, Poland*
[5]*University of Rzeszow, Rzeszow, Poland*
[6]*Kyoto Institute of Technology, Kyoto, Japan*

Back in 1996 [1], it was predicted that heavy doping of CdTe with Cr should induce strong RT ferromagnetism making the resulting $Cd_{1-x}Cr_xTe$ solid solution a suitable material for spintronic applications. Unfortunately, poor Cr solubility in II-VI leads to the dopant separation and the development of second phases hindering the formation of the homogeneous DMS with ferromagnetism of intrinsic type. On the other hand, dopant precipitation can be used to obtain composites consisting of semiconductor matrix with embedded ferromagnetic nanocrystals, which are currently viewed as prospective spintronic media [2].

In this study, the doping-induced crystallographic phase separation and its effect on the magnetism of vapor-grown single crystals were investigated by a variety of experimental methods. It was revealed by XRD, SIMS and different analytical electron microscopy techniques that upon post-grown cooling of the crystals, monoclinic Cr_3Te_4 precipitates nucleate on the {111} planes of CdTe, and then a dense array of nano-thick lamellas is developed, which are crystallographically oriented with respect to the host lattice.

(Cd,Cr)Te crystals were found to be ferromagnetic from LNT to above RT. Off-axis electron holography experiments proved that their magnetic behaviour is mainly governed by the embedded Cr_3Te_4 particles, although a weak contribution of the $Cd_{1-x}Cr_xTe$ matrix itself to the overall ferromagnetism can be also supposed from the magnetization measurements. Lorentz holography revealed anisotropy of the precipitates, their easy magnetic axis is perpendicular to the [101] crystallographic direction of the zinc-blende structure. The EMR spectra of the crystals consist of multiple lines originating from both Cr atoms dissolved in the CdTe lattice and from Cr-related extrinsic phases. The angle dependences of the lines coming from Cr_3Te_4 lamellas show six-fold symmetry followed from the magnetocrystalline and shape anisotropy of the precipitates.

[1]. Blinowski J. *et al*, Ferromagnetic superexchange in Cr-based diluted magnetic semiconductors, *Phys. Rev. B* 1996. V. 53. 952-9527.
[2]. Dietl T. *et al*, Spinodal nanodecomposition in semiconductors doped with transition metals. Rev. Mod. Phys. 2015. V. 87. P. 1311-1377.

Effect of Electric Field of the Electron and Hole Energy Spectra of Non-Concentric Spherical Core-Shell Quantum Dot

Leshko O.V., Leshko R.Ya.

Department of Physics and Information Systems
Drohobych Ivan Franko State Pedagogical University
St. Stryiska 3, Drohobych, 82100, leshkoroman@gmail.com

Over the past few years, there have been notable strides in nanotechnology, specifically in developing hybrid quantum dots (QDs) composed of various materials. By amalgamating diverse materials, it has become feasible to fabricate multilayer QDs with diverse characteristics. Among the various types of multilayer QDs, the most basic ones are spherical core-shell QDs. The applying of core-shell QDs has primarily stemmed from their capacity to modify the essential optical properties of the core nanocrystals, including their fluorescence wavelength and quantum yield, by growing an epitaxial-type shell composed of a different semiconductor material.

Concentric spherical core-shell QDs are the predominant focus in most theoretical studies. In practical situations, there are no assurances that the core-shell QDs will maintain concentricity. Moreover, the disruption of concentricity can be induced by cation exchange within the layers. However, up to this point, there hasn't been an analytical theory developed for non-concentric spherical core-shell QDs. First analytic model of non-concentric core-shell QD has been presented in our work [1]. We demonstrate that core displacement leads to alterations in both hole and electron energy levels, resulting in the splitting of excited states. The impact of core displacement on electron spectra can be intensified or mitigated depending on the direction and magnitude of the applied electric field, akin to the effects observed in [2] with an electric field and impurity. Furthermore, the external electric field will induce changes in hole energy levels and the effective optical gap.

Consequently, this work's objective is to determine the energy levels of both electrons and holes in non-concentric core-shell quantum dots under the influence of an external electric field, applied in various directions, and to ascertain the combined impact of core position and electric field on the effective optical gap.

[1]. R.Ya. Leshko, I.V. Bilynskyi, O.V. Leshko, M.A. Slusarenko. Electron energy spectrum of the non-concentric spherical core-shell quantum dot. Micro and Nanostructures. 2023. Vol. 181. P. 207615.

[2]. I.V. Bilynskyi, R.Ya. Leshko, H.O. Metsan, M.A. Slusarenko. Effect of electric field and acceptor position on the energy spectrum of GaAs/AlAs quantum dot. Physica B: Condensed Matter. 2022. Vol. 642, P. 414106.

Effect of the Graphene Oxide Doping on the Electrical Properties of Poly(6-Aminoindole)

Horbenko Yu.Yu., Aksimentyeva O.I., Kovalskyi Y .P.

Ivan Franko National University of Lviv, Lviv, Ukraine,
yuliia.horbenko@lnu.edu.ua

The development of new, simpler, and cheaper methods of obtaining composites based on conjugated conductive polymers and the study of their properties is relevant due to the demand for functional materials with better characteristics. The synthesis of conjugated polymers in the presence of doping agents, namely graphene oxide (GO), makes it possible to obtain functional materials with improved or new unpredictable properties that appear because of the fundamental electronic interaction between the highly conjugated structure of GO and delocalized electrons in the chain of conjugated polymers. Polymer composites based on indole and its amino derivatives are promising for use in various fields of science and technology – for the manufacture of electrochromic devices, highly sensitive biosensors, anti-corrosion coating, and chemical electricity sources, as catalysts of organic synthesis, etc. [1-4].

In this work, the influence of the synthesis conditions and the presence of graphene oxide on the electrical properties of poly(6-aminoindole) was established. The temperature dependencies of the specific resistance in the temperature range of 290-373 K were studied. As the temperature increases, a decrease in the specific volume resistance of the polymer (ρ) is observed and, accordingly, an increase in the specific volume conductivity according to the exponential law, which is typical for semiconductors. Determined values of the activation energy of conductivity $E\sigma$ = 0,59–1,23 eV prove the semiconducting nature of the synthesized polymer composites.

[1]. Yang T., et al. Template-free, controllable and scalable synthesis of poly(5-aminoindole) nanoparticles for printable electrochemical immunosensor with ultra-high sensitivity. *RSC*. 2022. Vol.10. P. 78-86.
[2]. Düdükcüa M., Avcı G. Electrochemical synthesis and corrosion inhibition performance of poly-5-aminoindole on stainless steel. *J. Prog. Org. Coat.* 2016. Vol.97. P. 110-114.
[3]. Yue R., et al. Electrosynthesis of a novel polyindole derivative from 5-aminoindole and its use as catalyst support for formic acid electrooxidation. *J. Electrochim. Acta.* 2012. Vol.77. P. 29-38.
[4]. Carbas B.B., Kivrak A., Kavak E. Electrosynthesis of a new indole-based donor-acceptor-donor type polymer and investigation of its electrochromic properties. *Mater. Chem. Phys*. 2017. Vol.188. P. 68-74.

Electrochemical Behavior of the Activated Carbon/$ZnMn_2O_4$ System in an Aqueous Electrolyte

Ivanichok N.Ya[1]., Kolkovskyi P.I.[2], Ivaniv I.I.[1], Rachiy B.I.[1], Borchuk D.S.[1], Kovtonyuk V.A.[1]

[1]*Vasyl Stefanyk Precarpathian National University, Ivano-Frankivsk, Ukraine*
[2]*V. I. Vernadsky Institute of General and Inorganic Chemistry, Kyiv, Ukraine*
natalia.ivanichok@pnu.edu.ua

In this paper, we present a hybrid electrochemical system based on thermally activated carbon (AC) as a cathode and spinel $ZnMn_2O_4$ as an anode. A 33% aqueous solution of potassium hydroxide has been used as an electrolyte. The specific energy-capacity characteristics of the AC/$ZnMn_2O_4$ system have been measured by the method of galvanostatic cycling in a two-electrode cell of the 2525 type.

It was determined that the AC/$ZnMn_2O_4$ electrochemical system exhibits a sloping voltage profile with a maximum value of 1.2 V based on the analysis of the obtained discharge curves (Fig. 1).Moreover, it was calculated for the mass (500 mg) of the material of the electrodes cell (Table 1) based on the obtaining discharge curves which made it possible to determine the specific energy-capacity characteristics of the studied systems.

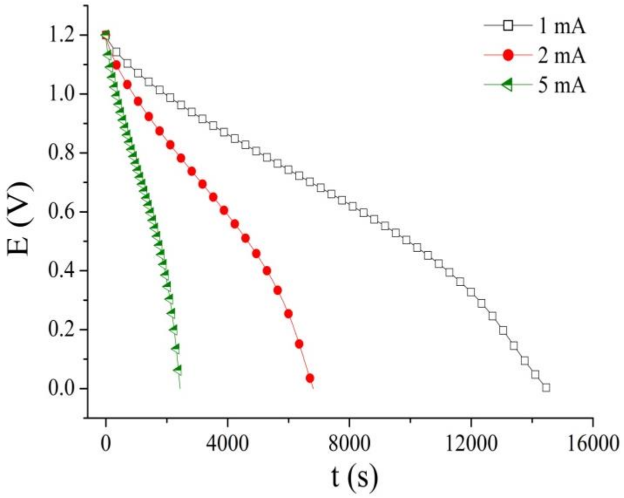

Fig. 1. Discharge curves of the AC/$ZnMn_2O_4$ system

Table 1
Specific energy-capacity characteristics of the AC/$ZnMn_2O_4$ system

$I_{discharge}$, mA	R, Ohm	$C_{specific}$, F/g	$C_{specific}$, mA·h/g	$W_{specific}$, W·h/kg	$P_{specific}$, W/kg
1	2	24	6.7	9.6	2
2	2	23	6.3	9.1	5
5	1.6	20	5.7	8.1	12
10	1.5	19	5.3	7.4	24
20	1.45	18	4.9	6.7	47
30	1.43	17	4.7	6.2	69
40	1.43	16	4.5	5.8	91
50	1.42	16	4.3	5.5	113

Electrochemical Properties of Carbon Biocomposites

Moklyak M.G.[1], Hrubiak A.B.[2], Moklyak V.V.[2], Ostafyichuk B.K.[2]

[1]*Vasyl Stefanyk Precarpathian National University, Ivano-Frankivsk, Ukraine,*
mariamoklyak@gmail.com
[2]*G.V. Kurdyumov Institute for Metal Physics, N.A.S. of Ukraine,*
Kyiv, Ukraine, hrubiak0andrii@gmail.com

In work shows a new approach to improving the peformance of lithium ion power sources (LPS) by using of carbon biocomposites as an active component of the cathode composition. The cathode composition was prepared by homogenizing the amino acids, a conductive additive and a solution of PVDF and the following coating on a commercial graphite foil (TEG) collector.

Discharge profiles of LPS at a specific current of 20 μA/cm^2 shows different electrochemical activity depending on the type of cathode component (Fig. 1). For LPS with a cathode based on a "TEG / Aspartate", the discharge profile has S-shaped with the formation of a potential plateau in the range of 1.8-1.7 V. The final specific capacity at 1.5 V about 1275 Ah/kg in terms of the weight of the organic component. For glycine the discharge profile changes the angle of inclination at a lower voltage than is observed for aspartate. The specific capacity of the discharge based on glycine up to 1.0V are 800 Ah/kg.

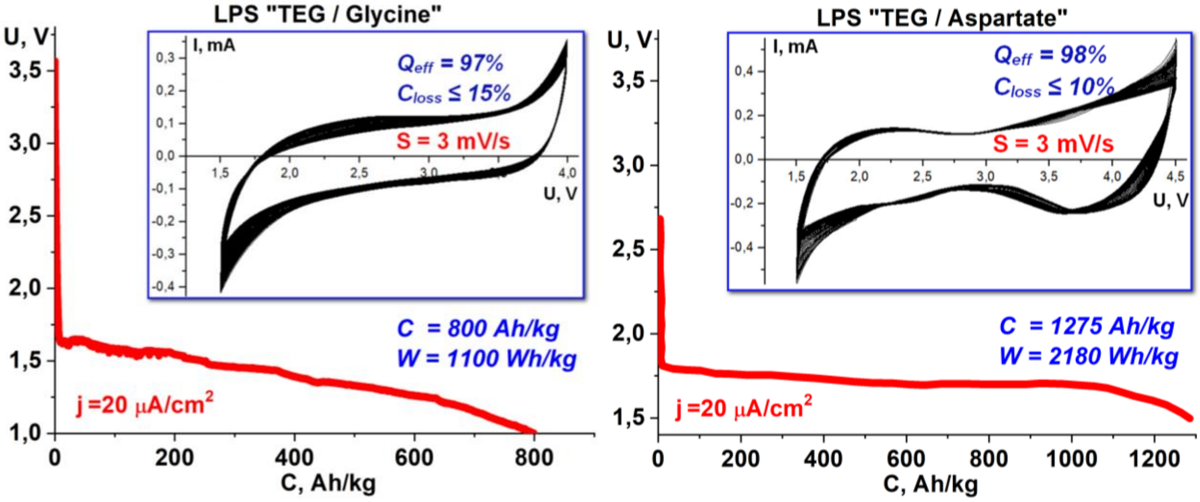

Fig. 1. Discharge profiles and CVA curves for 100 cycles (inset) of LPS with cathodes based on carbon biocomposites.

Cyclic voltammograms (CVA) of LPS shows different appearance, which indicates different mechanisms of current-forming processes at discharge (Fig. 1 - inset). Aspartate is characterized by interaction with lithium ions both through a terminal carboxylic group and by the formation of groups (-COOLi) in the radical (-CH2-COOH), which allows to double the specific discharge capacity compared to glycine, for which characterized by only the course of current-forming interactions at the C terminal bonds. CVA studies of LPS show perfect cycling capacity with Coulomb efficiency for amino acids about Q = 97-98%.

Electrochemical Properties of Nanoporous Carbon Materials Obtained from Waste Coffee Grounds

Rachiy B.I.[1], Ivanichok N.Ya.[1], Kolkovskyi P.I.[2], Soltys A.M.[1], Yablon L.S.[1], Mandzyuk V.I.[1], Khrushch L.Z.[1], Voitkiv H.V.[1]

[1]*Vasyl Stefanyk Precarpathian National University, Ivano-Frankivsk, Ukraine*
[2]*V. I. Vernadsky Institute of General and Inorganic Chemistry, Kyiv, Ukraine*
bogdan.rachiy@pnu.edu.ua

The thermochemical activation temperature is one of the main factors affecting the electrophysical properties of nanoporous carbon materials (NCM). This work explored the effect of activation temperature on the electrophysical properties of NCM, such as conductivity and capacitance. The graphitized content of carbon increases as the temperature increases, leading to a rise in the conductivity of the obtained NCM. Moreover, an increase in porosity results in a decrease electrical conductivity of NCM. Considering these factors, the activation temperature is important for the prospect of using NCM for electrophysical applications, such as supercapacitors, batteries, etc.

The main focus of this work is determination of dependence of the specific electrical capacity of NCM obtained as a result of thermochemical activation of waste coffee grounds with potassium hydroxide. According to the final temperature of thermochemical activation, a series of samples was numbered (S400 ÷ S900), for example, S600 is a NCM obtained at a temperature of 600 ºC.

Electrochemical studies of the NCM/electrolyte system were carried out in three-electrode cells on an Autolab PGSTAT/FRA-2 spectrometer. The frequency range from 10 mHz to 100 kHz and the potential range from -1 V to 0.4 V in steps of 0.2 V were selected for research. Electrodes with a mass of 16.5 mg and a size of 5 mm*5 mm were prepared from the studied materials and placed in a nickel grid.

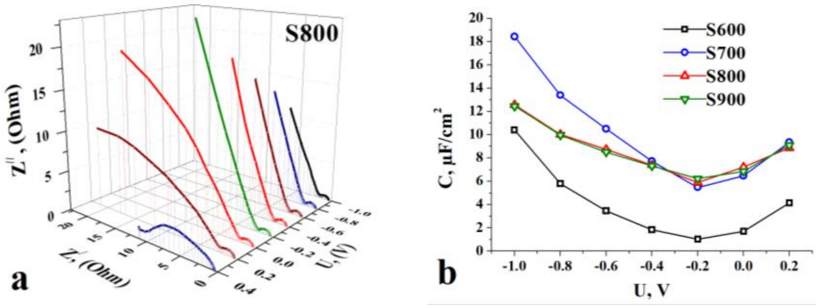

Fig. 1. Nyquist diagrams a) and specific electrical capacity b) of the NCM/electrolyte system.

It is shown that these carbon materials can be used for the manufacture of both positive and negative electrodes of supercapacitors, according to the dependence of the specific capacity of the NCM on the applied voltage (Fig. 1). It was established that the specific capacitance in the negative region is 1.5 times higher than the corresponding value of the capacitance in the positive region.

Electronic Energy Structure of the (100) In_4Se_3 Surfaces by Deferring Preparation and Treatment in UPS Study

Makar T.R.[1], Dzyuba V.I.[1], Nenchuk T.M.[1], Tuziak O.Ya.[2], Galiy P.V.[1]

[1]*Ivan Franko Lviv National University, Electronics and Computer Technology Department,*
[2]*Ivan Franko Lviv National University, Physics Department,*
50 Dragomanov Str., Lviv 79005, Ukraine, pavlo.galiy@lnu.edu.ua

The morphology of indium 0D, 1D nanostructures on A^3B^6 layered templates has been extensively studied in the last years [1,2]. The properties of a growing surface layer are closely related to its quantitative parameters, such as roughness, skewness, kurtosis and electronic energy structure of the surface. The last one also depends on preparation and treatment of (100) In_4Se_3 cleavage surfaces, what has been studied by UPS method.

The UPS studies (Fig. 1) were conducted with application of monochromatic synchrotron irradiation of the sample suited in UHV chamber with $1.5{\cdot}10^{-10}$ Torr residual gases pressure. The last one atmosphere contains mainly CO, H_2O and H_2 and negligible quantity of hydrocarbons that indicated partial pressure less than $\leq 10^{-12}$ Torr. Vacuum ultraviolet photons in the range 10-15 eV were applied and resolution of hemispheric energy analyser and monochromator was 80-100 meV for 50 eV photon energies.

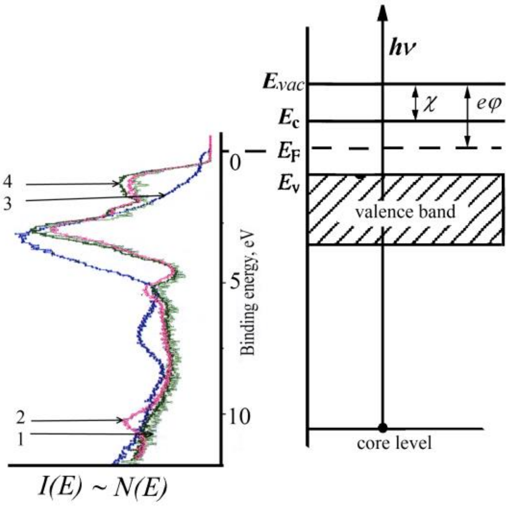

Fig. 1. UPS spectra of (100) In_4Se_3 ($h\nu$=15 eV) after cleavage (curve 1), exposition *in situ* (curve 2 – after night, curve 3 - after 5 hours) and 10 min ionic (Ar^+, E=1.6 keV, I= 10 μA) sputtering (curve 4).

It was concluded, that ion irradiation and non-stoichiometry sputtering of (100) In_4Se_3 surfaces as also further exposition of such surfaces *in situ* changes energetic structure of the surface that is important during obtaining In^0/(100) In_4Se_3 nanosystems - indium quantum nanowires and nanodots.

[1]. Galiy P.V., Nenchuk T.M. et al., InTe surface application as template for indium deposited nanosystem formation. *Mol. Crys. Liq. Crys.* 2021. V. 721, Is.1. P. 1-9.

[2]. Galiy P.V., Mazur P., et al. Self - assembled indium nanostructures formation on InSe (0001) surface. *Appl Nanosci.* 2020. V.10. P. 4629-4635.

Electrophysical Properties of Manganese Dioxide Various Modifications and Composites based on α - MnO_2/C and β - MnO_2/C

Kolkovskyi P.I.[1], Rachiy B.I.[2], Kolkovska H.M.[2], Ivanichok O.M.[2],
Bushkova V.S.[2]

[1]V. I. Vernadsky Institute of General and Inorganic Chemistry, Kyiv, Ukraine
[2]Vasyl Stefanyk Precarpathian National University, Ivano-Frankivsk, Ukraine
PKolkovskyy@gmail.com

Generally, the study of electrophysical properties of transition metals oxides, particularly, MnO_2 of various modifications and composites based on MnO_2 with carbon material is one of the important factors in their application for electrodes of electrochemical supercapacitors. In this work, a comprehensive impedance study of α -MnO_2/C and β - MnO_2/C composites with a percentage of carbon black (CB) of 5, 10, 15, 20 and 25% has been carried out.

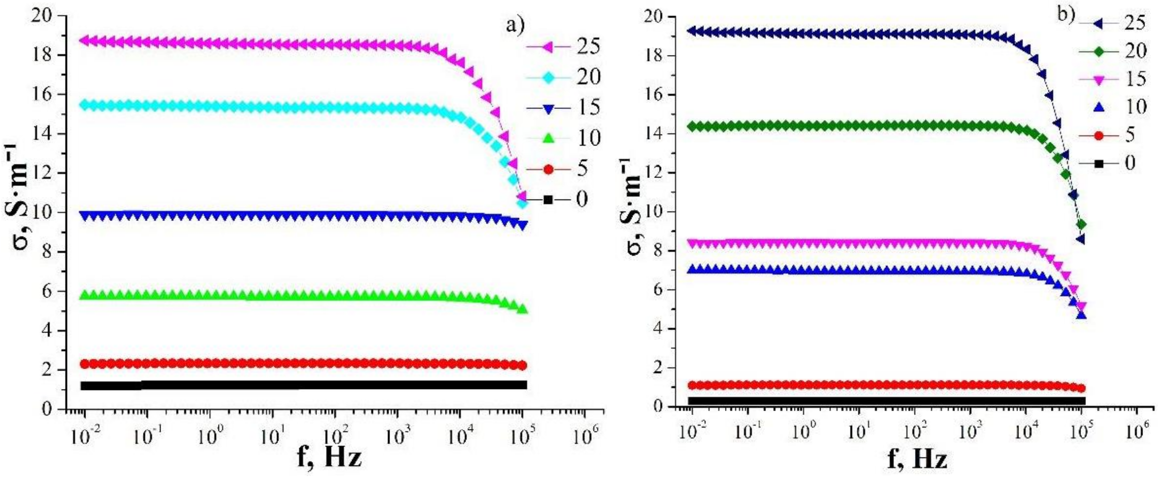

Fig. 1. Frequency dependences of the electrical conductivity of the composite α - MnO_2/C (a) and β - MnO_2/C (b) particles mixed with CB.

Figure 1 a and b shows the experimental spectra of electrical conductivity σ obtained for samples α - MnO_2/C and β - MnO_2/C. Moreover, the σ for pure samples of α - and β - MnO_2 is related to charge jumps mechanism between random embedded semiconductor particles for composites samples α - MnO_2/C 20 and 25% and β - MnO_2/C 10, 15, 20 and 25%, due to the dominance of CB conductivity, a skin effect is manifested at frequencies above 10^4 Hz.

The value of σ for composites with different ratios of CB content to α - and β - MnO_2/C samples have been studied. It is found that electrical conductivity of the α - MnO_2/C composite is increase from 1.31 $S \cdot m^{-1}$ to 18.6 $S \cdot m^{-1}$ and a more rapid increase in electrical conductivity σ for β - MnO_2/C from 0.56 $S \cdot m^{-1}$ to 19.2 $S \cdot m^{-1}$. Therefore, at maximum values of the CB content of 20-25%, the value of electrical conductivity for both samples almost does not change.

Emission Spectroscopy of Porous-Si/c-Si Heterostructures' Surfaces

Galiy P.V.[1], Nenchuk T.M.[1], Tsvetkova O.V.[1], Tuziak O.Ya.[2], Poplavskyy O.P.[3]

[1]*Ivan Franko Lviv National University, Electronics and Computer Technology Department,*
[2]*Ivan Franko Lviv National University, Physics Department, 50 Dragomanov Str., Lviv 79005, Ukraine,* pavlo.galiy@lnu.edu.ua
[3]*Vasyl Stefanyk Precarpathian National University, Ivano-Frankivsk*

The real crystalline (c-Si) and porous (por-Si) surface's elemental and phase compositions are studied by AES and SIMS with mass-spectrometry analysis *in situ*. Por-Si surface contains of almost atomically clean Si or SiH_x and amorphous mixtures of Si oxides and carbon - $Si_yO_xC_{1-x-y}$ coatings [1, 2].

Real surface area of nano- and mesoporous Si (por-Si) is essentially higher than one of continuous initial samples. Dependently on porosity degree and also thickness of porous layer this difference may attain 10^2-10^3 times and, obviously, this promotes high concentration of adsorption centres on the developed surface of por-Si. Thus, the role of the surface evidently is significant for some properties of por-Si, including photo luminescent and other.

The composition of surface contaminants for por-Si etched in HF and rinsed by distilled water and subsequently dried was studied by AES and SIMS methods (LAS-600, RIBER) The analysis was conducted in UHV under surface sputtering rate about 2-3 Å/min. The SIMS spectra of por-Si (see Fig. 1) show the presence of elements and compounds that indicate on samples' oxidation and contamination by hydrocarbons. This is evidenced by O^-, OH^-, $SiOH^-$, SiO_2^- maxima availability along with C^-, C_2^-, CH^-, $C_2H_2^-$ ones. The intensities of all of them diminish almost twice after etching, besides F^-, Cl^- ones.

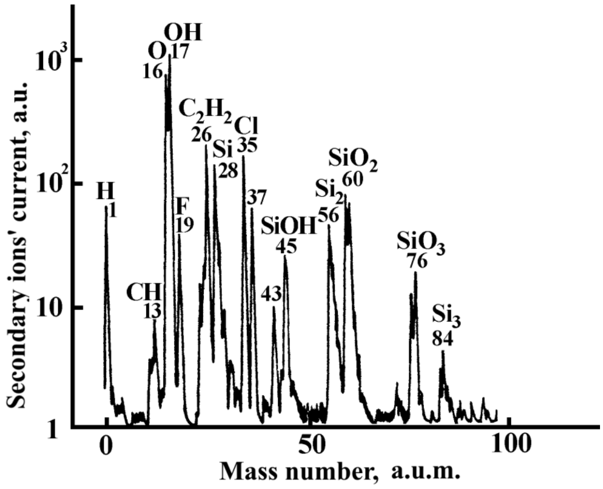

Fig. 1. SIMS spectrum of negative ions from por-Si surfaces etched by HF, rinsed by distilled water and subsequently dried in the air: ion currents of oxide phases and hydrocarbon contaminants from first (initial) monolayers after sputtering of ≅15 Å thickness. (Ar^+, θ=70°, E=1,0 keV, j=10^{13} ion/cm^2 s).

[1]. Galiy P., Nenchuk T. et al., Surface investigations of nanostructured porous silicon. *Thin Solid. Films*. 1998, V. 318, N 2. P. 113-116.

[2]. Galiy P., Nenchuk T. et al., Thermostimulated exoelectron emission studies of porous silicon. *Phys. Status Solidi*. b 1999.V. 212, R7- R8.

Energy Subsystem of Porous Carbon Material After Laser Radiation

Budzuliak I.M., Yablon L.S., Panko I.I., Lyzun Eu.V.

Vasyl Stefanyk Precarpathian National University, Ivano-Frankivsk, Ukraine
igaroshapanko@gmail.com

Carbonization and activation of the material of plant origin in the presence of a pore former (water vapour) leads to structural transformations of the original matrix, resulting in the formation of a porous material with a specific surface area of 800-1000 m^2 and a porosity of 50-70%. Depending on the structural peculiarities of the plant material, fractals in the form of chains, nets and three-dimensional structures are formed in the porous material, which contain C-C bonds of the σ- and π-type.

Under the influence of technological factors, oxidation-reduction processes can be initiated, structural defects can form, and homolytic bond breaks can occur, which collectively cause the formation of unpaired electron localization zones. To detect these effects, we recorded electron paramagnetic resonance (EPR) spectra. Changes in the electronic subsystem of the porous carbon material (PCM) doped with manganese were determined on the ELEXSYS E-500 spectrometer of the BRUKER company with simultaneous control of the frequency in the region of 9800 MHz and the magnetic field strength at room temperature. Superposition of signals is observed in EPR spectra. The content of unpaired electrons is approximately 10^{17} spins per 1 gram of PCM.

EPR spectra taken from PCM doped with manganese indicate the presence of several types of paramagnetic centers, which cause the superposition of the corresponding signals.

Comparing the EPR parameters of different valence forms of manganese, taking into account the shooting conditions and the parameters of the EPR signals of the modified matrix, it was established that only the signal with the parameter g = 1.999 corresponds to Mn^{2+}. The remaining forms are electrons delocalized between matrix fragments of different nature. Since the integral intensity of the line is proportional to the number of unpaired electrons of the corresponding type, the share of unpaired electrons of the electron shell of Mn^{2+} is insignificant and is less than 10%.

During pulsed laser irradiation of PCM doped with manganese, electrons are redistributed between their different states. Part of the electrons goes from the state with g = 3.9 to the state g = 6.0, that is, their mobility increases. Thus, laser irradiation lowers the potential barriers that prevent the transition of electrons from one state to another, that is, it initiates bridges cross-linking. These data correlate with the results of studies of PCM doped with manganese by the method of small-angle X-ray scattering, which indicate structural transformations that occur during the action of laser irradiation.

Ethylene Glycol Functionalized nZVI Nanoparticles

Boychuk V.M.[1], Turovska L.V.[2], Moiseienko M.I.[2],
Kotsyubynska Y.Z.[2], Shurpa M.S.[1]

[1]*Vasyl Stefanyk Precarpathian National University, Ivano-Frankivsk, Ukraine*
[2]*Ivano-Frankivsk National Medical University, Ivano-Frankivsk, Ukraine*

Russian aggression is causing long-term damage to Ukraine's water resources and soil. Heavy metal (HM) ions cause a serious environmental problem due to their persistent, non-biodegradability, and toxicity. The estimated content of HM contamination, which is considered as an indicator of war-made load, for Pb^{2+}, Cr^{3+}, Ni^{2+}, Cd^{3+}, and Cu^{2+} is up to 300, 200, 100, 5, and 250 mg/kg, respectively. Soil and water remediation using nZVI is an emerging technology. Nanoscale zero-valent iron (nZVI) refers to nanoparticles (NPs) consisting of a Fe^0 core and a Fe oxide or hydroxide near-surface layer. Their high reactivity due to their large surface area and redox potential of –0.44 V makes these materials effective reducing agents of HM ions to less toxic forms. Stabilization of nZVI against spontaneous oxidization is the biggest obstacle to its widespread use. Coating the surface of nZVI NPs with surfactants is one of the most advantageous strategies, offering the simultaneous possibility of influencing its size and morphology. In this work, nZVI NPs were synthesized by chemical reduction of $FeCl_3$ in ethylene glycol (EG) solvent using $NaBH_4$ as a reducing agent. EG was used both as a solvent and as a coating agent to ensure air stability of dried nZVI. The obtained materials were characterized by XRD, XRF, Mössbauer spectroscopy and nitrogen porosimetry. According to the XRD data (Fig. 1), the obtained material consists of α-Fe crystallites with an average crystallite size of about 4 nm (estimated by the Scherrer's method), covered with a Fe_3O_4 magnetite shell. The immobilization of HM ions from aqueous solutions was studied using 0.3 mg/L Cu^{2+} ions (obtained by dissolving $CuSO_4{\cdot}5H_2O$) by UV-vis spectroscopy (the volume ratio of solutions of colloidal nZVI to Cu^{2+} ions was 1:100). A 100-fold decrease in free Cu^{2+} ions was observed after 30 min stirring of the mixture at room temperature. Good reducing properties and air stability make EG functionalized nZVI NPs a promising material for environmental remediation.

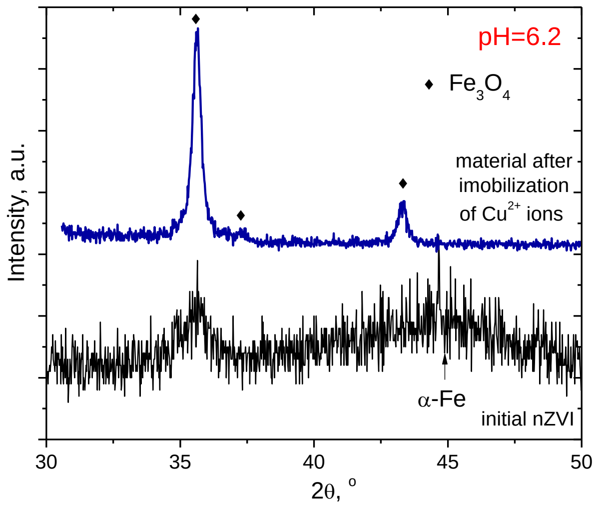

Fig. 1

The work was supported by the project "Preparing the Ground for Reconstruction – Decontaminating Ukraine's Soil, Eco-Entrepreneurs, and Environmental Journalism" of UEA-PNU.

Features of Plasmon Resonance Exciting of Silver Nanoparticles due to Pre-Treatments with Different Duration in Magnetic Field

Redko R.A.[1], Shvalagin V.V.[2], Milenin G.V[3], Redko S.M.[3], Savchuk Y.M.[3]

[1]*V. Lashkaryov Institute of Semiconductor Physics of the National Academy of Sciences of Ukraine, State University of Telecommunications, Kyiv, Ukraine, redko.rom@gmail.com*
[2]*L. Pysarzhevskii Institute of Physical Chemistry of the National Academy of Sciences of Ukraine, Kyiv, Ukraine, vitaliy.shvalagin@gmail.com*
[3]*V. Lashkaryov Institute of Semiconductor Physics of the National Academy of Sciences of Ukraine, Kyiv, Ukraine, milenin.gv@gmail.com, redko.fotya@gmail.com, liza.synelnyk@gmail.com*

The ethanol solutions of the ZnO nanoparticles (NPs) were placed in a constant and homogeneous weak magnetic field (B = 60 mT). Exposure time in the field was: 1 hour, 1 day and 5 days. These solutions were used for photocatalytic formation of ZnO/Ag nanoheterostructures under the action of UV irradiation. The production cycle was repeated during 30 days. During this time, the evolution of the obtained optical absorption spectra of solutions containing ZnO/Ag NPs were measured on a Specord 210 spectrophotometer (relative to a cuvette with pure ethanol), SEM and TEM microscopy data. For reliability of the received results the solution which was not exposed in magnetic field, but stored together with all samples at the same temperature conditions was used as a reference. Under the UV action, photocatalytic reduction of Ag (I) and the formation of a ZnO/Ag colloidal heterostructure occurs, which is characterized by an absorption maximum at 400–460 nm. Moreover, increasing the UV dose leads to a long-wavelength displacement of this peak. These processes are characteristic for all studied samples. But the energy positions of the observed peak at low and maximum doses of weak magnetic field radiation do not match. It was found that within 30 days the final position of the maximum of plasmon absorption of the Ag NPs, which were formed on ZnO solutions, that have been undergone magnetic field treatment, slowly shifts to the position of the latter in the reference sample. The latter circumstance indicates a "memory effect" that lasts for a month. It can be assumed that the observed spectral features upon irradiation of solutions containing ZnO NPs, silver nitrate, and sulfur are due to the photocatalytic reduction of elemental sulfur with ethanol and the formation of colloidal composite ZnO/Ag_2S (core/shell) NPs. The corresponding theoretical calculations, which are in well agreement with experimental results, were performed using “MiePlot 4.6” software (http://www.philiplaven.com/mieplot.htm), which the algorithm was based on Mie’s theory. Obtained information will be value for understanding plasmon resonance-based sensor system natural aging due to presence external actions of magnetic fields.

This work was supported by National research foundation of Ukraine (Project 2022.01/0126).

Ferrite Materials and Their Synthesis by the Sol-Gel Autocombustion Method

Yaremiy I.P.[1], Yaremiy S.I.[2], Bushkova V.S.,
Burdiak V.R.[1], Savchyn V.V.[1], Andriichuk O.P.

[1]*Vasyl Stefanyk Precarpathian University, Ivano-Frankivsk, Ukraine,*
yaremiyip@pnu.edu.ua
[2]*Ivano-Frankivsk National Medical University, Ivano-Frankivsk, Ukraine*

Various types of ferrite materials have been used for many decades. Typically, they were synthesized from the corresponding oxides using standard ceramic technology. Since the active study and use of nanomaterials began, one of the frequently used methods for obtaining nanosized ferrites is the sol-gel autocombustion method. In general, several types of ferrite structures are distinguished, with the most important ones being spinels, garnets, and orthoferrites. These materials of different chemical compositions were synthesized by us using the sol-gel autocombustion method.

To synthesize nanoferrites, metal nitrates, citric acid, and distilled water were used. To ensure a high combustion rate, a molar ratio of metal nitrates to citric acid of 1:1 was employed. The respective quantity of each of the reagents was dissolved in 50 mL of water. With constant stirring, the pH level of the solution was adjusted using a 25% ammonia solution. Then, at a temperature of 130°C, the solution was dried until it transformed into a xerogel. After this, through the autocombustion process of the dry gel, the corresponding powders of nanosized ferrites were obtained.

In many cases, during autocombustion, a single-phase nanomaterial with the crystalline structure we anticipated was formed immediately. However, in the synthesis of ferrites with certain chemical compositions, additional sintering was required to achieve a single-phase material. It is worth noting that, unlike the ceramic synthesis method, the sol-gel autocombustion process for obtaining ferrites proceeds quite rapidly, resulting in nanoscale synthesized powders.

During the synthesis of substituted nickel-iron spinels, lanthanum-containing perovskites, and iron-yttrium garnets, particles with block sizes ranging from 15 to 45 nm were formed, depending on the synthesis method and the chemical composition of the material.

It is worth noting that during the annealing process of the powders synthesized by the sol-gel autocombustion method, the size of their blocks remains almost unchanged up to 600°C, and undergoes only slight changes up to 950°C. Therefore, additional annealing for the purpose of achieving a single-phase material at temperatures up to 950°C often results in the material becoming single-phase with minimal alteration in block sizes.

Fractal Structure of Thermoactivated Nanoporous Carbon Materials

Mandzyuk V.I.[1], Lisovskiy R.P.[2], Rachiy B.I.[1]

[1]*Vasyl Stefanyk Precarpathian University, Ivano-Frankivsk, Ukraine,*
volodymyr.mandzyuk@pnu.edu.ua, bogdan_rachiy@ukr.net
[2]*Ivano-Frankivsk National Medical University, Ivano-Frankivsk, Ukraine,*
lesrom2000@gmail.com

The effect of thermal activation on the fractal structure of nanoporous carbon material (NCM) obtained by hydrothermal carbonization of plant raw material at 750°C (initial material) was investigated. Thermal activation was carried out at temperatures t_{act} 300, 400, 500°C (activation time τ_{act} was 0.5; 1; 1.5; 2; 2.5; 3 hours) and 600°C (τ_{act} was 0.25; 0.5; 0.75; 1 hour).

The fractal dimension of surface D_s (Table 1) was calculated from the analysis of nitrogen adsorption/desorption isotherms according to the equation

$$\ln\left(V/V_{mono}\right) = const + A\left[\ln\left(\ln\left(p_0/p\right)\right)\right],$$

where V is the volume of adsorbed gas, V_{mono} is the volume of adsorbed gas that covers the surface of the sample with a monolayer, A is a degree indicator that depends on D_s, p_0/p is the relative pressure.

Table 1. Parameters of fractal structure of thermoactivated NCM

τ_{act}, hour	t_{act} = 300°C		t_{act} = 400°C		t_{act} = 500°C		t_{act} = 600°C	
	A	D_s	A	D_s	A	D_s	A	D_s
0.25							-0.14	2.58
0.5	-0.26	2.22	-0.09	2.73	-0.16	2.52	-0.13	2.61
0.75							-0.13	2.61
1	-0.21	2.37	-0.11	2.67	-0.18	2.46	-0.12	2.64
1.5	-0.13	2.61	-0.18	2.46	-0.20	2.40		
2	-0.12	2.64	-0.19	2.43	-0.22	2.34		
2.5	-0.12	2.64	-0.22	2.34	-0.24	2.28		
3	-0.11	2.67	-0.26	2.22	-0.26	2.22		

for initial material A = -0.45; D_s = 2.55; absolute error is ± 0,02.

As follows from the Table 1, the fractal dimension of surface increases at a temperature of 300°C due to the formation of a significant number of micropores. Similarly, shorter times of activation of the initial material at a temperature of 600°C almost do not change the dimensions of the surface, although the number of micropores increases sharply to 96%. For activation temperatures of 400 and 500°C, there is a tendency to decrease the fractal dimension of the surface to a value of 2.22, which indicates the formation of an almost smooth surface.

Gadolinium-Decorated Multiwalled Carbon Nanotubes: Synthesis and Characterization

Abaszade R.G.[1], Aliyev E.M.[2], Margitych T.O.[4], Stetsenko M.O.[5,6],
Kotsyubynsky V.O.[3]

[1]Azerbaijan State Oil and Industry University, Baku, Azerbaijan,
[2]University of Birmingham, Edgbaston, United Kingdom,
[3]Vasyl Stefanyk Precarpathian National University, Ivano-Frankivsk, Ukraine,
[4]Kyiv Institute for Nuclear Research, NASU, Kyiv, Ukraine,
[5]College of Physics and Optoelectronic Engineering, Shenzhen University,
Shenzhen, PR China,
[6]Westlake University, School of Engineering, Hangzhou, PR China
abaszada@gmail.com stetsenkomax@gmail.com

Multiwalled carbon nanotubes (MWCNTs) and MWCNT-based composites are trending and promising materials for sensors, bioimaging and industrial applications. Carboxyl-functionalized MWCNTs (CF-MWCNTs) are efficient nanoplatforms for immobilizing multiple molecules via covalent bonds, hydrogen bonds, or π-π stacking interactions. Acid treatment can significantly increase the solubility of MWCNTs by introducing a carboxylic functional group (-COOH) on the side wall and tip of the MWCNTs. Gadolinium and gadolinium oxide (Gd_2O_3) have attracted much attention due to their excellent optical and paramagnetic properties compared to rare earth oxides.

Fig.1

The purpose of this work is to investigate the effect of Gd-decoration of CF-MWCNTs on the structural and PL properties. Decoration of MWCNTs with gadolinium has been carried out by the hydrothermal route. Gd-doped MWCNTs have been studied by Raman spectroscopy, SEM, TEM, XRD, XPS, FTIR, and PL. Hydrothermal doping of MWCNTs with Gd causes the formation of a 3D network architecture (Fig. 1) and sharply increases the content of oxygen surface functionality. The presence of gadolinium in the Gd-MWCNT nanocomposite was confirmed by XPS and FTIR results. The main peaks observed in the XRD patterns of CF-MWCNTs correspond to disordered graphite structures. Doping of CF-MWCNTs with Gd^{3+} leads to the formation of peaks at $2\theta \approx 16°$, 32°, 35°, and 39°, corresponding to the formation of GdOOH, $Gd(OH)_3$, and Gd_2O_3 nanoparticles located on the surface of the nanotubes. TEM images confirmed the tubular morphology of both CF-MWCNTs and Gd-MWCNTs, as well as a nearly smooth and homogeneous surface. The increase in the amplitude of the PL spectra for CNTs doped with 5% Gd may be associated with electron-hole recombination mechanisms and photon-excited electrons. The obtained 5% Gd-doped CF-MWCNTs are promising materials for magnetic-luminescent applications.

Hybridization of Dipole Plasmonic Modes in Metallic Nanoshells of Variable Thickness

Malysh R.O.[1], Korotun A.V.[1,2], Kulykovskyi R.A.[1]

[1]*Zaporizhzhia Politechnic National University, Zaporizhzhia, Ukraine, andko@zp.edu.ua*
[2]*G.V. Kurdyumov Institute for Metal Physics of the NAS of Ukraine, Kyiv, Ukraine*

Plasmonic properties of bilayer metal-dielectric nanoparticles strongly depend on geometry due to the interaction between primitive (dipole) plasmonic modes associated with the interface between the layers and the external surface of the nanoparticle. Alterations in the geometry of nanoparticles (e.g., non-concentricity of spheres or misalignment of cylinders) that reduce symmetry, modify interactions between plasmonic modes, and lead to various shifts in plasmonic characteristics. Ultimately, such nanoparticles could even form the basis for cost-effective optical metamaterials. Therefore, studying the physical picture of plasmonic response shifts can aid in the development of enhanced methods for producing nanoparticles with optimal morphology, and is thus of current relevance.

As is known, expressions for the frequencies of surface plasmon resonance follow from the condition of zeroing the real part of the denominator of the expression for the polarizability of the considered nanostructure. In turn, the expression for dipole polarizability can be obtained from the solution to the electrostatic problem, since the dimensions of the nanostructure are much smaller than the wavelength of light. The resulting value for the frequencies of the surface plasmon resonance coincides with the result obtained using the hybridization scheme of plasmonic modes, in which the frequencies of surface plasmons in the layered spherical particle are calculated by combining already known results for the frequencies of plasmons on surfaces with positive and negative curvatures (sphere and cavity) [1]. Due to the asymmetry of the metallic shell of variable thickness in such a structure, it is possible to excite four dipole plasmonic modes.

In conclusion, it should be noted that in the limiting case, when the distance between the centers of the spheres is equal to zero, the calculation results coincide with the frequencies of the surface plasmon resonance of a concentric metallic shell and, accordingly, instead of four, we will have two surface plasmon resonance frequencies.

[1]. Prodan E., Radloff C., Halas N.J., Nordlander P. A Hybridization Model for the Plasmon Response of Complex Nanostructures. *Science*. 2003. V. 302, No 5644. P. 419-422.

Impact of duration shock-vibration treatment on the structural parameters of nanocompocite SiO_2/Al_2O_3

Yurii Yavorskyi [a], Andrii Hrubiak [b], Myroslav Karpets [a], Olexander Dudka [a]

[a] *Physical Engineering Faculty, National Technical University of Ukraine "Kyiv Polytechnical Institute", Kyiv, Ukraine, yar-yra@ukr.net;*

[b] *G.V. Kurdyumova Institute of Metal Physics of National Academy of Sciences of Ukraine, Kyiv, Ukraine*

It is generally understood that the electrochemical properties of nanosized materials are influenced by structural and morphological characteristics, electronic structure, surface imperfections, and so on. To boost the surface activity of materials, various synthesis and processing processes are applied. Machining, namely shock-vibration treatment (SVT), is one approach for accomplishing this [1]. In this abstract, we little bit describe the effect of the treatment period on the structural and morphological properties of the $0.8SiO_2/0.2Al_2O_3$ mixture.

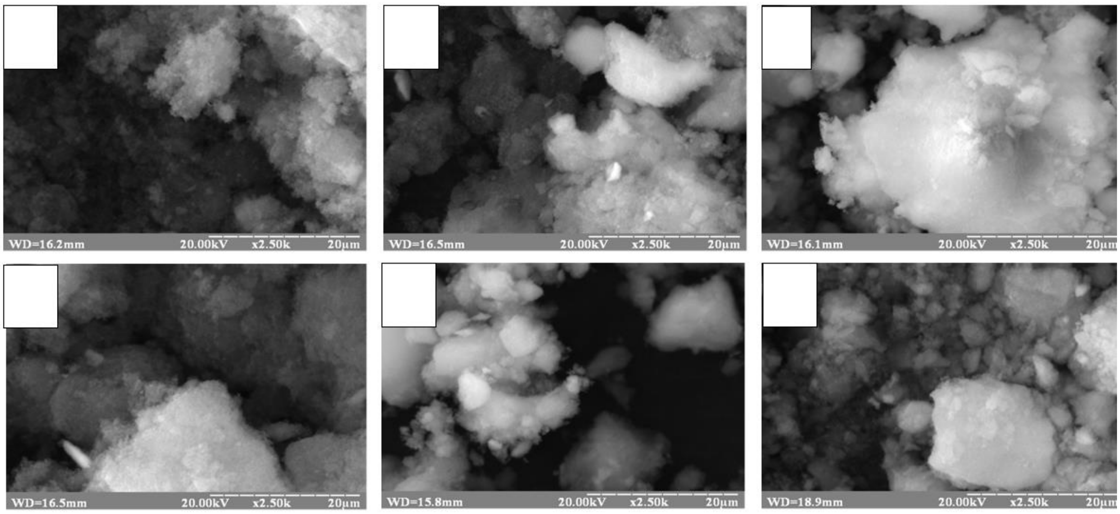

Fig. 1 – SEM of: ***a*** - SA-20; **b** - SA-20-3; ***c*** - SA-20-5; ***d*** - SA-20-10; ***e*** - SA-20-15; ***f*** - SA-20-20, x2500.

From the results of morphological studies using the SEM method, it is found that as a result of MBT nanoparticles are combined into compacted agglomerates and the bulk density of the composite increases. From the results of X-ray diffraction, it is established that as a result of processing, there is an increase in CRS of Al_2O_3, with minor changes only in the parameter "c" of the crystal lattice. The increase in processing time leads to an increase in both bulk density and CRS.

[1]. Influence of machining duration of $0.8SiO_2/0.2Al_2O_3$ nanopowder on electrochemical characteristics of lithium power sources/ Yavorskyi Y.V., Hrubiak A.B., Zaulichnyy Ya.V., Karpets M.V.1, Mokliak V.V., Gunko V.M., Dudka O.I. // Applied Surface Science, Volume 617, 30 April 2023, 156420 https://doi.org/10.1016/j.apsusc.2023.156420.

Interband Absorption of Light in a Spheroidal Quantum Dot with Consideration of Polarization Phonons

Holskiy V.B., Leshko R.Ya., Holska S.V., Karpiy V.R.

Department of Physics and Information Systems, Drohobych Ivan Franko State Pedagogical Univetsity, Drohobych, Ukraine, hol.wit@gmail.com

Experimental and theoretical studies have so far well studied the energy levels of bound states of particles in nanocrystals. However, the influence of phonons in QD requires further research. Due to their unique properties, QDs can be used in night vision devices, solar batteries, field-effect transistors, and light-emitting devices [1]. Research shows that the shape of a QD significantly affects the energy spectrum of a quasiparticle [2]. And experimental work shows its difference from spherical [3-4], which ultimately affects the optical properties of materials. The ellipsoidal shape deserves special attention due to a more realistic comparison with the experimental QD dimensions [3]. The phonon spectrum in spheroidal QDs was studied in works [5-6]. For example, in [5], in the dielectric continuum model, interface optical phonons for QDs in the form of an elongated and flattened spheroid were studied, and it was shown that their spectrum significantly depends on the geometry of the nanocrystal.

In this work, we investigated the spectrum of the interband absorption of spherical *CdS* quantum dots placed in the SiO_2 matrix from the interaction of the electron-hole pair with polarization phonons. The difference between the bulk Freilich model (phonons of a massive crystal) and the interaction of the exciton-phonon system with limited phonons is analyzed. Absorption coefficients due to transitions of charge carriers between the lowest excitonic optically active levels in QDs under the influence of linearly polarized light were calculated.

Such volumes of quantum dots were studied when the energy levels of the electron and the hole are sufficiently far from each other. Therefore, taking into account the possible dispersion of QDs by size in the matrix and taking into account different ratios of semi-axes for QDs in the form of an elongated spheroid, the specified levels can be distinguished when analyzing the frequency dependence of the interband absorption coefficient. Calculations show that both the values of the maxima and the energy of the peaks of the interband absorption coefficient depend not only on the volume and shape of the QD, but also on the choice of the phonon model. Thus, for this heterostructure, we proved the similarity of the absorption spectra when taking into account both phonons of a massive crystal and confined phonons.

[2]. D.V. Korbutyak, et all. Ukr. phys. journ. Reviews 2012. V. 7, № 1 – P. 48-95
[3]. V.I. Boichuk, I.V. Bilynsky, I.O. Shakleina. Ukr. J. Phys. 53, 894 (2008).
[4]. J.H. Blokland, et all. Applied Physics Letters 94, 023107 (2009).
[5]. V. Kladko, M. Slobodian, et all. Phys. Status Solidi A 206, 1748 (2009).
[6]. F. Comas, et all. Physical Review B, Volume 65, (2002) 073303.
[7]. L. Shi, Z.W.Yan. Physica E 41 (2009) 1353–1357.

Manipulating the Band-Gap Value of Phosphorene for Straintronics Application

Solomenko A.G.[1], Sahalianov I.Y.[2], Radchenko T.M.[1], Tatarenko V.A.[1]

[1]*G.V. Kurdyumov Institute for Metal Physics of the N.A.S. of Ukraine, Kyiv, Ukraine,*
sola@imp.kiev.ua, tarad@imp.kiev.ua, tatar@imp.kiev.ua
[2]*Linköping University, Norrköping, Sweden, isagal@ukr.net*

The effects of the uniaxial tensile strain and shear deformation as well as their combinations on the electronic properties of single-layer black phosphorene are theoretically studied [1]. The changes of the strain-dependent band gap are forecasted using the numerical calculations within the tight-binding (TB) approximation (with the bond-length-dependent hopping 'integrals') as well as the first-principles methodology based on the density functional theory (DFT) and compared with previous findings. TB method allows rather easily to carry out calculations for the systems containing millions of atoms (as the real laboratory samples contain), and thus, it is substantially less demanding computationally in comparison with any *ab initio* calculations restricted to periodic supercells or lattice fragments with a relatively small number of atoms due to the computational constraints. The TB-approximation-based findings show that the band gap of the strain-free phosphorene agrees with experimental value and linearly depends on both the stretching and the shearing; it increases (decreases) as the stretching increases (decreases), whereas it decreases gradually with increasing shear. The linear dependence is more or less similar as compared to that obtained from the *ab initio* calculations for the shear strain; however, it disagrees with a non-monotonic behaviour revealed by means of the DFT-based calculations for the single-axis tensile strain. Possible reasons of this discrepancy are discussed. As the parameter defining the bond-length dependence of the hopping 'integrals' within the TB method is enhanced, the linear dependence of the band gap on the uniaxial tensile strain becomes non-monotonic and similar to that obtained from the DFT calculations. Under a combined deformation, when both types of strain (tensile/compression + shear) are loaded simultaneously, their mutual influence extends the realizable band-gap range from zero up to the values intrinsic to the wide-band-gap semiconductors. At the switched-on combined strain, the semi-conducting-to-semi-metallic phase transition in the phosphorene is reachable at a weaker (strictly non-destructive) strain that contributes to fundamental and technological breakthroughs in prospect.

The authors acknowledge the National Academy of Sciences of Ukraine for support within the departmental research for 2022–2026 (state reg. No. 0122U002396) under the budget program КПКВК 6541030.

[1]. Solomenko A.G., Sahalianov I.Y., Radchenko T.M., Tatarenko V.A. Straintronics in phosphorene via tensile vs shear strains and their combinations for manipulating the band gap. *Scientific Reports*. 2023. V. 13. P. 13444; https://doi.org/10.1038/s41598-023-40541-7

Metal Oxide Nanopowders: Synthesis and Applications in Gas Sensors

Venhryn Yu.I., Savka S.S., Bovhyra R.V., Zhyrovetsky V.M.,
Serednytski A.S., Popovych D.I.

[1]*Pidstryhach Institute for applied problems of mechanics and mathematics of National Academy of sciencies of Ukraine, Lviv, Ukraine,*
popovych@iapmm.lviv.ua

Theoretical and experimental research has been conducted to investigate the formation processes of metal oxide (ZnO, Ga_2O_3) nanopowders using pulsed laser ablation in a chemically active environment [1]. The results of ab initio density functional theory studies on the energy spectrum and ground-state parameters of small β-Ga_2O_3 nanoclusters (comprising 5 to 45 atoms) are presented. To assess the stability of β-Ga_2O_3 clusters, the binding energy per one formula unit of Ga_2O_3 was calculated. Analysis of the energy values revealed that for β-Ga_2O_3 nanoclusters composed of one to three formula units, chain-like structures were the most energetically favorable, all exhibiting approximately the same binding energy. As the number of formula units in the systems increased, a transition to ring structures (four to six Ga_2O_3 formula units) and subsequently to compact spherical structures (seven to nine formula units) was observed. Also, conducted a thorough analysis of the mechanisms involved in H_2 gas adsorption on ZnO nanoclusters using the Molecular Dynamics method. To characterize the adsorption phenomena, we utilized key descriptors such as the total system energy, radial distribution functions, and the Centro-symmetry parameter. These metrics provided valuable insights into the intermolecular interactions and spatial organization of adsorbed H_2 molecules on the ZnO nanocluster surface. Experimental investigations were conducted to explore the features of photoluminescence in the obtained nanopowders within various gas environments. Correlation between chemical composition, microstructure and electronic properties of initial, laser-modified and doped metal oxides and their gas sensitivity are established. Significant changes in intensity and shape of luminescence band were observed upon changing the gas environment. These changes were attributed to the redistribution of existing luminescence centers and the emergence of new luminescence absorption centers on the surface of the nanopowders. Chromaticity diagrams of the emitted photoluminescence light were obtained, and it was found that the color coordinates varied depending on the gas environment. These findings suggest that the nanopowders could potentially be used in gas sensors.

[1]. Gafiychuk V.V., Ostafiychuk B.K., Popovych D.I., Popovych I.D., Serednytski A.S. ZnO nanoparticles produced by reactive laser ablation. Applied Surface Science. 2011. V.257, №20. P.8396–8401.

Nanomaterials for Application in Nuclear Forensics

Vasylyeva H.

Uzhhorod National University, Uzhhorod, Ukraine
h.v.vasylyeva@hotmail.com

Nuclear forensics identifies, examines, and controls radioactive devices or compounds that have been found to be out of Regulatory Control. In particular, the tasks of nuclear forensics include the creation of libraries of radioactive compounds and devices; and the creation of guidance on nuclear security issues relating to the prevention and detection of, criminal or intentionally unauthorized nuclear material or other radioactive material [1]. Modern radioactive devices can be referred to as nanomaterials, for example, ^{90}Sr-^{90}Y radioactive sources on ceramic carriers. On the other hand, during the identification and dating of radioactive sources, nanomaterials are used to separate radionuclides in order to accurately determine their amount [2].

The purpose of this work is to summarize the experience (both of foreign scientists and our own experience) of the use of nanomaterials for the needs of nuclear forensics.

The study of zeolites, ceramics, glasses, ion exchange resins, extractants deposited on SiO_2, as well as nanostructured materials based on TiO_2 is relevant to identify and determine the date of production of various unknown radioactive devices (age-dating). At the same time, zeolites, and ceramics are used for the manufacture of radioactive devices, sometimes a radioactive substance is applied to thin metal plates. For accurate analysis of unknown radioactive devices, ion exchange resins, extractants, SiO_2, and nanostructured materials based on TiO_2 are commonly used [3]. It should be noted that this field of research is still developing [1].

The numbers of adsorbents ion exchange resin Dowex HCR s/s, Dowex 1x8, Dowex Mac-3, mesoporous titanium dioxide, and TiO_2 with the chemically modified surface were investigated in our work. In experimental studies, we used XRF and SEM/EDS. Analysis of trace quantities of radioactive isotopes was carried out using ICP-MS and LSC methods. This helped to develop a new method for age-dating of liquid radioactive sources [3]. The next step should be the dating of solid radioactive devices (radionuclides on zeolite, ceramics, or metal substrate carriers).

[1]. Varga Z., Wallenius M., et al. Trends and perspectives in Nuclear Forensic Science. *TrAC Trends in Analytical Chemistry*. 2022, V.146, 116503.

[2]. Vasylyeva, H., Mironyuk, I., Strilchuk, M., et al. Adsorption and possibility of separation of heavy metal cations by strong cation exchange resin. *Chemical Physics Impact*. 2021. 100056.

[3]. Vasylyeva H., Mironyuk I., Strilchuk M., Mayer K., et al. Age dating of liquid ^{90}Sr–^{90}Y sources. *Applied Radiation and Isotopes*. 2023, V. 200, 110906.

$Ni(OH)_2$ Nanoparticles as an Efficient Electrocatalyst for Hydrogen Evolution Under Alkaline Conditions

Solonets D.M., Kotsyubynsky V.O. Boychuk V.M., Klymyuk M.M.

Vasyl Stefanyk Precarpathian National University, Ivano-Frankivsk, Ukraine
dmytro.solonets@pnu.edu.ua

The development of cost-effective and efficient electrocatalysts for hydrogen evolution reaction (HER) in alkaline aqueous electrolytes is crucial for advancing renewable and sustainable energy technologies. In this study, we present a novel hybrid electrocatalyst consisting of ultrafine $Ni(OH)_2$ nanoparticles embedded in a porous carbon matrix (CM). The CM was obtained from plant raw materials through the stages of carbonization and chemical activation with a BET surface area (S_{BET}) of 1055 $m^2 \cdot g^{-1}$; the pore size was in the range of 0.9-6.0 nm with a maximum at 1.0 nm; the ratio between meso- and micropore volumes was 4:6. The preparation of Ni nanoparticles embedded in the CM was carried out using a chemical wetting procedure. Pre-activated by heating to 300°C in a vacuum, the CM was wetted with acetone and added to an aqueous solution of Ni acetate under vigorous stirring. At the next stage, an aqueous solution of $NaBH_4$ was added as a reducing agent. The resulting material was characterized by XRD, XRF, and nitrogen porosimetry. According to XRD data (Fig. 1), the catalyst consists of α-$Ni(OH)_2$ crystallites with an average size of about 4-6 nm. The presence of a core of metallic Ni particle has been estimated. The observed decrease in S_{BET} to 450 m^2/g for the $Ni(OH)_2$/CM material was explained by the filling of CM pores with $Ni(OH)_2$ clusters. The $Ni(OH)_2$/CM catalyst on a Ni foam support exhibits high and stable HER activity with an onset potential of −190 mV (compared to the Ag/AgCl electrode) in 1 M KOH electrolyte with a Tafel slope of 84 mV/dec. For the transparent Ni foam used as the support, the Tafel slope was 113 mV/dec. The results presented here may suggest a new way to create hybrid catalyst for HER synthesis, which has potential large-scale application.

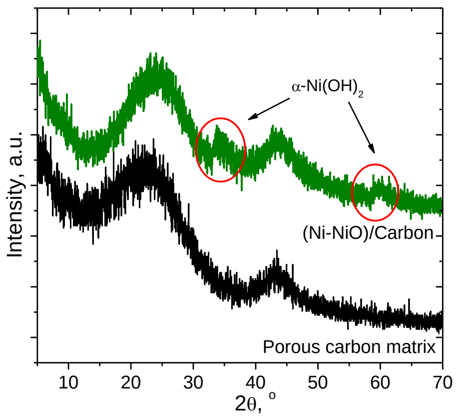

Fig. 1

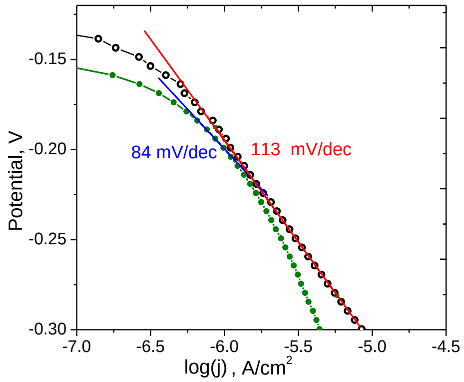

Fig. 2

Periodic Nanostructures Induced by Point Defects in $Pb_{1-x}Sn_xTe$

Horichok I.[1], Saliy Ya.[1], Nykyruy L.[1], Cempura G. [2], Parashchuk T. [2],
Rechkin A.[1], Balan V.[1],

[1]*Vasyl Stefanyk Precarpathian University, Ivano-Frankivsk, Ukraine,*
[2]*AGH University of Science and Technology, Krakow, Poland*

Lead telluride-based compounds are among the best materials for medium-temperature thermoelectric applications. The electronic and thermal transport properties of these materials can well-tuned using the point defects and nano-inclusions. However, a much more interesting effect is the formation of the self-organized nano-inclusions, which may have a significant effect on the physical properties.

In this work, we show the experimental dependences of the component distribution in $Pb_{1-x}Sn_xTe$, which were identified as periodic nanostructures with an amplitude of $\lambda \approx$ 50-500 nm. Materials were synthesized in quartz ampoules evacuated to a residual pressure of 10^{-5} mbar. The obtained ingots were crushed into a fine powder via hand milling in an agate mortar and then densified using the spark plasma sintering technique at 873 K for 20 min in a 10 mm diameter graphite mold under axial compressive stress of 50 MPa in an argon atmosphere. The heating/cooling rate was 50 K/min. For homogenization, all samples were annealed for 20 hours at 873 K in an argon atmosphere. The specimen for TEM investigations was prepared with the FIB technique. For TEM investigations, Titan Cubed G2 60-300 (FEI), a probe Cs-corrected (S)TEM was used.

The observed periodicity is explained by the generation and recombination of point defects due to diffusion processes during the synthesis, sintering, and annealing of samples. A model describing the formation of such inhomogeneities in $Pb_{1-x}Sn_xTe$ ternary alloys during isothermal annealing is proposed.

A proposed model is based on analysis of process of tellurium diffusion which includes two flows (fast interstitial defects and slow substitutions with preservation of lattice nodes) interacting with each other through cationic vacancies. Vacancies may come, for example, from the surface, resulting in the fact, that their local concentration is always consistent with the local composition. For the exponential dependence of the concentration of vacancies on the composition, the homogeneous distribution can become unstable and turn into a certain inhomogeneous structure. With the available data for diffusion coefficients, it was found that the instability forms a layered structure with the concentration of intermodal lead. Due to the presence of acceptor cationic vacancies, this observation can lead to the formation of internal p-n junctions.

[1]. Saliy Ya., Nykyruy L., Cempura G., Soroka O., Parashchuk T., Horichok I. Periodic nanostructures induced by point defects in $Pb_{1-x}Sn_xTe$. *Physics and Chemistry of Solid State.* 2023. V. 24, No 1. P. 70-76.

Photoluminescence Efficiency of the Si – Nanocrystalline CdTe Composite

Trishchuk R.L.[1], Pashchenko G.A.[2], Trishchuk L.I.[2], Tomashyk V.M.[2]

[1]*Igor Sikorsky Kyiv Polytechnic Institute, Kyiv, Ukraine, e-mail: trishchukli@ukr.net*
[2]*V.Ye. Lashkaryov Institute of Semiconductor Physics, NAS of Ukraine, Kyiv, Ukraine*

When CdTe nanocrystalls (NCs) is introduced into Si, the photoluminescence (PL) of Si is enhanced due to the formation of a heterojunction, which ensures the injection of charges into the bulk of Si. We have studied the dependence of the PL intensity of the “porous Si (*p*Si)–CdTe NCs” composite on the *p*Si surface morphology and the conditions for depositing a colloidal solution of CdTe NCs on the porous surface of *n*-type silicon wafers oriented in the (100) direction. *p*Si layers were formed by electrochemical etching to form pores 2.5 μm in diameter, 20-30 μm deep, and 10^6 cm^{-2} in density, or by chemical etching to form smaller, larger diameter pores with lower density and a spongy surface.

The PL spectra were measured at room temperature, radiation was excited by a xenon lamp, and the signal was recorded by a FEU-100. The deposition was carried out in several stages with intermediate washing of the surface.

The measurements showed that during the deposition of CdTe NCs in *p*Si with a small pores diameter (2.5 μm), the radiation efficiency per unit surface area turned out to be lower than for a matrix with larger pores, i.e. NCs penetration occurs more efficiently in pores with a large diameter.

This is probably due to the incomplete filling of pores due to the difficulty of penetration of CdTe NCs into smaller pores due to the presence of an adsorption layer of a stabilizer on the NCs surface, which is used in the colloidal synthesis of NCs to increase the resistance to aggregation and sedimentation.

The cause of incomplete filling of small pores can also be the appearance of an electrostatic field due to the presence of a charge on the surface of CdTe NCs. When applying a colloidal solution of CdTe NCs on a spongy surface, the increase in intensity was not large enough, despite the degree of porosity exceeding the previous cases. This may be due to insufficient exchange of charge carriers between the components of the system. A study is being made of the possibility of removing the stabilizer shell from the surface of CdTe NCs, which will increase the number of NCs embedded in *p*Si pores. Another positive effect of the removal of the shell may be the elimination of the reason for some decrease in the radiation yield from CdTe NCs. To achieve this goal, 5–10% isopropyl alcohol, which dissolves the surface layer of thioglycolic acid, was added to the colloidal solution of CdTe NCs during precipitation. The use of this technique made it possible to increase by a factor of 5 the PL efficiency of the *p*Si–CdTe NCs system, in which the *p*Si layer was formed by electrochemical etching. The authors see the prospects of work in this direction.

Plasmons in a Chain of Spheroidal Metal Nanoparticles Located on a Dielectric Substrate

Maniuk M.S.[1], Korotun A.V.[1,2], Titov I.M.[1]

[1]*Zaporizhzhia Politechnic National University, Zaporizhzhia, Ukraine, andko@zp.edu.ua*
[2]*G.V. Kurdyumov Institute for Metal Physics of the NAS of Ukraine, Kyiv, Ukraine*

Miniaturization of optoelectronic circuits to nanometer sizes is possible when implementing waveguides with lateral mode limitation. Dielectric waveguides do not have this capability, since the minimum beam diameter is determined by the wavelength in the core material. An alternative option is to use a chain of closely spaced metal nanoparticles of various shapes as a waveguide. In this case, signal transmission along the chain is possible due to the strong interaction between plasmons excited on the surfaces of neighboring nanoparticles. It should also be noted that the significant enhancement of local electric fields in the gaps between elongated spheroidal metal nanoparticles, which has wide practical application, is also worth noting. Therefore, the study of the excitation of plasmon resonances in a chain of metal prolate spheroids located on a dielectric substrate is an urgent task.

The initial relationship for consideration will be the expression for the chain polarizability, the zero denominator of which in the non-dissipative approximation allows us to obtain the following expression for the frequency of the transverse chain surface plasmon resonance

$$\omega_{sp}^{\perp\,\mathrm{ch}} = \frac{\omega_p}{\sqrt{\text{т}^{\infty} + \dfrac{1 - \mathrm{L}_{\perp}}{\mathrm{L}_{\perp}}\text{т}_{\mathrm{m}}}}, \tag{1}$$

where ω_p is the plasma frequency; т^{∞} is the contribution of the crystal lattice to the permittivity; т_{m} is the permittivity of the environment; $\mathrm{L}_{\perp}$ is the depolarization factor renormalized due to the interaction of nanoparticles, which is determined by the chain sums associated with the contributions of other spheroidal particles of the chain and image dipoles.

In conclusion, we note that the chain sums are obtained by reducing the lattice (two-dimensional) sums that arise in the problem of determining the optical response of a square lattice of metallic nanospheroids located on a dielectric substrate. Thus, we can conclude that the considered problem is an analogue of the above two-dimensional problem.

Proton-Induced Secondary Electron Emission from ZnO Nanorods Grown on GaN Substrate: Geant4 Modeling

Kindrat V.V., Shlihutka B.T., Ivanyshyn I.P., Goy V.T.

Vasyl Stefanyk Precarpathian National University, Ivano-Frankivsk, Ukraine,
vitalykindrat@gmail.com

Geant4 is an effective software tool for modeling the interaction of high-energy particles with matter. Its advantages are the ability to adequately describe complex multiparameter physical processes and high reliability of predicting the consequences of the particle-solid interaction, including electromagnetic, hadronic, and optical processes. Geant4 package tools allow the creation of multi-component systems with complex geometries, consisting of various materials. A significant advantage of the object-oriented methodologies of Geant4 modeling systems is the flexibility of user-defined physical models. Proton-induced secondary electron emission (SEE) is a powerful tool for studying near-surface solids and can also be used to determine the parameters of low-energy proton beams.

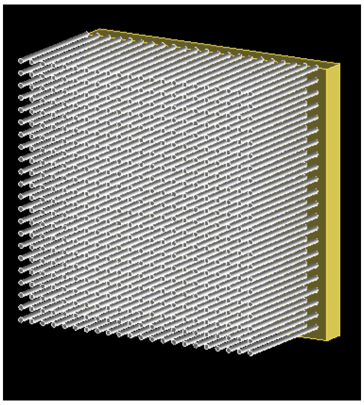
Fig.1

In this work, we present the results of modeling the secondary electron emission from an array of ZnO nanorods located on a gallium nitride substrate. Monte Carlo simulations were performed to study single-event effects in the electronic subsystem of the target. The target was modeled in the form of a 500×500×50 nm^3 parallelepiped of GaN covered with normally oriented ZnO nanorods 100 nm long and 10 nm in diameter (Fig. 1). The target was located 1 cm from the proton source with energies in the range of 1 keV–1000 MeV. The physics lists QGSP_BIC_HP, Geant4-LowEnergy, and Geant4-Penelope, based on dielectric and binary theory formalisms, were used with the low energy model, Geant4-LowEnergy, Geant4-PRECO_HP packages included, which allows for reliable modeling of electrons and photons down to 100 eV. The MicroElec extension (Geant4-MicroElec) has been applied to properly characterize the low-energy ionization models for incident electrons and protons, allowing for improved track simulation. The applied approach makes it possible to simulate the ion strike-induced electron generation, the transport of electrons to the surface, and electron escape through the surface barrier potential. The secondary electron yield, their energies, and angular distribution are calculated. The vertical ZnO nanorod array was found to exhibit a SEE yield that does not depend on the angle of incidence of primary protons. The calculated dependence of the secondary electron yield on the proton energy is similar to the electronic energy loss of the protons.

Raman Spectroscopy Study on Cu_2XSnS_4 (X=Zn,Fe,Co,Ni) Nanocrystals Synthesized by Colloidal Chemistry

Ivakhno-Tsehelnyk O.[1,2], Selyshchev O.V.[1,2], Kotsyubynsky V.O.[3],
Boychuk V.M. [3], Dzhagan V.M. [4], Havryliuk Ye.O. [1,2,4], Mazur N.V. [4],
Kondratenko S.V.[5], Yukhymchuk V.O.[4], Zahn D.R.T.[1,2]

[1]*Semiconductor Physics, Chemnitz University of Technology, D-09107 Chemnitz, Germany,* *zahn@physik.tu-chemnitz.de*
[2]*Center for Materials, Architectures and Integration of Nanomembranes (MAIN), Technical University of Chemnitz, Chemnitz, Germany*
[3]*Vasyl Stefanyk Precarpathian University, Ivano-Frankivsk, Ukraine*
[4]*V. Lashkaryov Institute of Semiconductors Physics, National Academy of Sciences of Ukraine, 45 Nauky av., 03028 Kyiv, Ukraine,* *dzhagan@isp.kiev.ua*
[5]*Physics Department, Taras Shevchenko National University of Kyiv, Kyiv, Ukraine*

$Cu_2ZnSn(S,Se)_4$ (CZTSSe) is among the materials most intensively studied for various potential energy applications [1]. The main advantages are a high absorption coefficient (~ 10^4 cm^{-1}), appropriate bandgaps, nontoxic and affordable constituent elements. Colloidal nanocrystals (NCs) are a promising form for large-area manufacturing of CZTSSe thin-film solar cells (SCs), especially on flexible substrates, compatible with printing technologies [2]. However, there is a high probability of defects and impurity phases (Cu_xS, ZnS, *etc*) in CZTSSe. One of the approaches to stabilize the quaternary phase and eliminate defects is a partial or complete replacement of (one or two) cations. Until now, most works have focused on the substitution of Cu (for Ag) and Sn (for Ge) [1], while the substitution of the group IV element was less studied.

In this work, a series of Cu_2XSnS_4 (X=Zn,Fe,Co,Ni) NCs were synthesized by means of colloidal chemistry in aqueous solutions. The synthesis was performed using two approaches: (i) at about 80 °C and atmospheric pressure or (ii) at 200 °C and 10-12 atm in an autoclave. X-ray diffraction data reveal that Cu_2ZnSnS_4 and Cu_2NiSnS_4 NCs of high structural quality and phase purity were obtained in (ii). In approach (i), all compounds except Cu_2CoSnS_4 were formed. Using vibrational Raman spectroscopy, differences in the spectra obtained at different excitation wavelengths are observed. These can be related to the resonant enhancement of certain vibrational modes due to different strengths of electron-phonon coupling for different modes.

The work was supported by the DFG project ZA 146/59-1 (517869265).

[1]. Kush P. and Deka S. Multifunctional Copper-Based Quaternary Chalcogenide Semiconductors Toward State-of-the-Art Energy Applications. *ChemNanoMat* 2019, V. 5, PP. 373 – 402.

[2]. Stroyuk, O.; Raevskaya, A.; Gaponik, N. Solar Light Harvesting with Multinary Metal Chalcogenide Nanocrystals. *Chem. Soc. Rev.* 2018, V.7, PP. 5354–5422.

Rapid One-Pot Synthesis of Ultrafine $CuFe_2O_4$-rGO Hybrid Nanomaterials

Zapukhlyak R.I., Kotsyubynsky V.O., Boychuk V.M., Homenyuk I.I.,
Trautwein A.A.

Vasyl Stefanyk Precarpathian National University, Ivano-Frankivsk, Ukraine
ruslan.zapukhlyak@pnu.edu.ua

The formation of hybrid nanostructured materials based on spinel ferrite and carbon nanoparticles is gaining increasing interest due to the favorable combination of morphological, magnetic, and electrical characteristics, resulting in their impressive electrochemical and catalytic properties, chemothermal stability and easy functionalization. Reduced graphene oxide (rGO), used as a carbon component, has excellent electrical conductivity and a large surface area combined with chemical stability and easy functionalization. $CuFe_2O_4$-rGO nanocomposites find applications in various fields, including energy storage, gas sensing, environmental remediation, and biomedical devices. Finding the best synergy between the oxide and carbon components by varying the synthesis conditions makes it possible to obtain highly efficient functional nanomaterials with controllable enhanced properties. The key advantages of self-combustion synthesis for spinel-based hybrid materials are its short duration, energy efficiency, fine particle size control, and large scale (compared to the hydrothermal approach). The aim of this work is to report an effective and rapid procedure for the synthesis of $CuFe_2O_4$ and $CuFe_2O_4$-rGO composite. Aqueous solutions of $Cu(NO_3)_2 \cdot 3H_2O$ and $Fe(NO_3)_3 \cdot 9H_2O$, acidified with HNO_3 to pH ≈ 1.0-1.1 (to prevent uncontrolled nucleation of the oxide phase), were mixed with ethylene glycol to suppress agglomeration. The resulting solution was boiled on a hot plate until a gel was formed and a spontaneous burning occurred (total elapsed time was about 20 min). The $CuFe_2O_4$-rGO hybrid material was obtained according to the same protocol, including mixing precursor solutions with colloidal graphene oxide, previously synthesized by the Tour method. The obtained powder materials were characterized by XRD, XRF, Mössbauer spectroscopy and nitrogen porosimetry. It was observed that both $CuFe_2O_4$ and $CuFe_2O_4$-rGO exhibited a single-phase cubic spinel structure with average ferrite nanoparticle sizes of approximately 14 nm and 16 nm, respectively (Fig. 1). A model of $CuFe_2O_4$ phase nucleation in the presence of GO nanosheets and EG molecules has been developed. It has been shown that the oxide phase nucleus grows rapidly due to both a diffusion-controlled process and kinetic restriction caused by the absorption of EG molecules and rapid mixing during boiling, resulting in the formation of $CuFe_2O_4$ nanoparticles on the surface of rGO nanosheets.

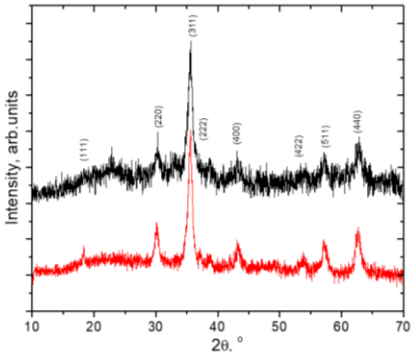

Fig.1

Reflection of Nanowires and Porous Silicon

Onyshchenko V.F.

V. Lashkaryov Institute of Semiconductor Physics NAS of Ukraine, Kyiv, Ukraine,
onyshchenkovf@isp.kiev.ua

Porous silicon and nanowires are used as an absorbing coating of solar cells. The optical properties of nanowires indicate an increase in light absorption by a structured surface [1]. An analytical model of the reflection of nanowires and porous silicon was developed. Silicon with a surface structured by nanowires or pores is considered as a two-layer structure. The porous layer is considered as an effective medium. The expression for finding the reflection of a two-layer structure takes into account the multiple reflection of light from the surfaces of the sample and the absorption of light by the structure. The effective refractive index of the layer of nanowires is complex and depends on the volume fraction of pores. The structured surfaces of the porous silicon layer are Lambert surfaces and scatter light.

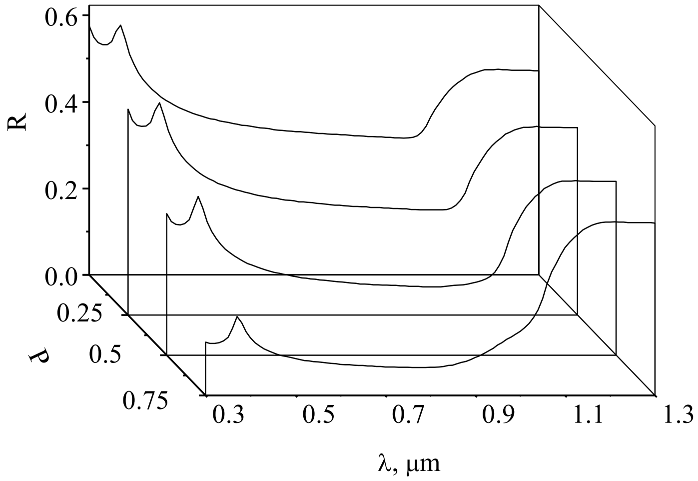

Fig. Reflectance spectrum of nanowires and porous silicon with a volume fraction of pores: 0; 0.25; 0.5; 0.75.

The figure shows the reflection spectrum of nanowires and porous silicon with a thickness of 500 μm at different volume fraction of pores. The pore depth is 100 μm. The reflectance of nanowires and porous silicon decreases as the volume fraction of pores increases. Reflection from the boundary of nanowires with a monocrystalline substrate is observed when the volume fraction of pores is 0.75. The reflection of light with wavelengths from 0.8 μm to 1.3 μm increases. The smallest reflection coefficient of nanowires and macroporous silicon is 0.1, for wavelengths from 0.3 μm to 0.8 μm.

[1]. Gentsar P.O., Stronski A.V., Karachevtseva L.A. and Onyshchenko V.F. Optical Properties of Monocrystalline Silicon Nanowires. *Physics and Chemistry of Solid State*. 2021. Vol. 22, No 3. P. 453–459.

SAXS Study of Reduced Graphene Oxide obtained by Hummers` Method

Bandura Kh.V.[1], Kotsyubynsky V.O.[2], Boychuk V.M.[2], Mazurenko J.S.[1]

[1]Ivano-Frankivsk National Medical University, Ivano-Frankivsk, Ukraine,
banduracristina@gmail.com
[2]Vasyl Stefanyk Precarpathian University, Ivano-Frankivsk, Ukraine

The synthesis of graphene oxide was carried out by Hummers` method followed by chemical reduction under hydrothermal conditions using hydrazine [1]. The synthesized reduced graphene oxide (rGO) was analyzed by XRD and SAXS. It consists of packages formed by 2-3 graphene nanosheets of average thickness about 0.75 nm. The SAXS method was used to clarify information about the parameters of the material structure and morphological features of the material. The X-ray intensity scattering curve as a function of particle size indicates the presence of polydisperse agglomerates (*n*=4) formed by plate-shaped particles (*n*=1.9) in the material. For small values of the *s* scattering vector (low-level Guinier region), the dependence $ln(s) = f(s^{-n})$ with *n*=3.58 was observed. The radius of inertia (R_g) of the scattering centers is calculated using the approximation $lnI = f(s^2)$. The presence of three characteristic sizes of the scattering centers of 2.1, 3, and 25 nm was established. In this way, rGO particles form agglomerates with a fractal dimension of 2.42. The radii of inertia of the primary particles of rGO were obtained using the mid-level Guinier approximation using the dependence $ln(Is) = f(s)$. Under such conditions, the intensity of scattered X-radiation for scattering centers of cylindrical shape with height *L* and radius *R* is described as follows $I(s) = \frac{I(0)}{s} exp\left[-\frac{s^2 R_g^2}{2}\right]$, where $R_g^2 = \frac{R^2}{2}$. For *L*<<*R* the average size of the primary lamellar particles of the material was estimated. The result correlates with the size distribution of scattering centers *F(d)*. It was approximated using two Gaussian functions (Fig. 1), which made it possible to calculate the most probable average sizes of rGO particles are 4.2 and 7.6 nm and their volume ratio between fractions is 45:55.

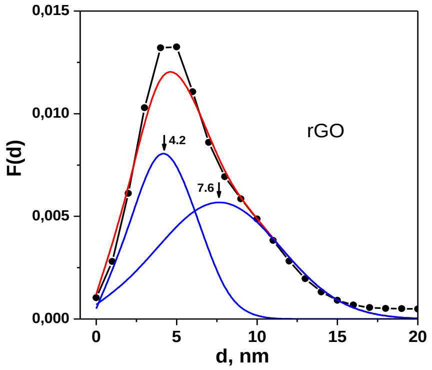

Fig.1. Size distribution functions of rGO particles and distribution curves for two predominant fractions.

[1]. Boychuk V. M., Kotsyubynsky V. O., Bandura K. V., Yaremiy I. P., Fedorchenko S. V. Reduced graphene oxide obtained by hummers and Marcano-Tour methods: comparison of electrical properties. *Journal of Nanoscience and Nanotechnology* 2019, 19 (11), P. 7320-7329.

Selective Laser Sintering of Amorphous Nanoparticles: Molecular Dynamics Simulations

Shtablavyi I., Popilovskyi N., Nykyruy Yu., Mudry S.

Department of Metal Physics, Ivan Franko National University of Lviv, Kyrylo and Mephodii 18, Lviv, Ukraine
ihor.shtablavyi@lnu.edu.ua

In recent years, additive manufacturing technologies have become more and more widespread. The reason for this is the ability to quickly manufacture products of almost any configuration using one device (3D printer). In contrast to 3D printing technologies with polymer materials, printing of metal products has not become so accessible. The reason for this is the significant activity of molten metals in relation to atmospheric oxygen, as well as in many cases unsatisfactory mechanical properties of materials immediately after 3D printing. The mechanical properties are mainly deteriorated by the polycrystalline nature of the materials and defects in the joining of particles in the process of their laser sintering. The solution to this problem can be the use of amorphous metal alloys for 3D printing. The formation of amorphous materials by means of additive technologies will avoid the polycrystalline structure, and will also make it possible to form bulk amorphous alloys of such sizes that cannot be obtained by traditional methods.

However, the main problem in the formation of amorphous materials by this method is their crystallization after laser melting. Crystallization can be avoided in the case of rapid removal of heat from the sintering particles, as well as by choosing optimal thermodynamic sintering conditions. To solve this problem by experimental methods, it is necessary to spend a lot of resources and time. Therefore, computer modeling methods allow optimizing the experimental conditions by obtaining preliminary results on the 3D printing process.

In this work, the method of molecular dynamics simulations was used to model the process of sintering of amorphous iron-based nanoparticles and the conditions of their further amorphization after cooling. The research was carried out at different temperatures and rates of heating and cooling. The results that can be used to optimize the process of 3D printing of amorphous materials by experimental methods have been obtained.

This work was supported by the National Research Foundation of Ukraine (Project No 2022.01/0171).

Structural and Electronic Properties of $LiH_3(SeO_3)_2$ Crystals

Kovalenko M.V., Bovgyra O.V., Onysko M.

Ivan Franko National University of Lviv, Lviv, Ukraine,
mariya.kovalenko@lnu.edu.ua

Significant changes and progress in renewable energy have accompanied recent decades. Solar energy occupies an increasingly important position in using green energy sources. However, achieving higher efficiency of solar panels based on standard semiconductor p-n junctions is limited by the properties of the band structure of the semiconductors themselves. This requires searching for new, efficient, stable materials for converting solar radiation into electrical energy. In this context, one of the research objects is ferroelectric crystals with a domain structure, which provides an additional degree of freedom in the separation and transport of charges, providing effective separation of charge carriers and improved photovoltaic response. In addition, the possibility of changing ferroelectric properties due to compositional modifications and external influences provides opportunities for optimizing the photovoltaic efficiency and stability of such materials. The study of the ferroelectric crystal $LiH_3(SeO_3)_2$, in which the photovoltaic effect is confirmed, is an urgent task.

Based on first-principle calculations within the electron density functional theory, this work investigated the structural and electronic properties of the $LiH_3(SeO_3)_2$ crystal. Structure geometry optimization and band-energy calculations were carried out in the CASTEP software package. Generalized gradient approximation (GGA (PBE, PBEsol) and hybrid functionals (B3LYP, HSE) were used to describe the exchange-correlation potential.

$LiH_3(SeO_3)_2$ is a monoclinic crystal with lattice parameters $a = 6.2534$ Å, $b = 7.883$ Å, $c = 5.4335$ Å, $\beta = 105.18°$ at room temperature. The crystal's unit cell contains two formula units: Li^+ ions are connected by octahedral geometry to six O^{2-} ions (the length of the Li–O bonds varies from 2.15–2.28 Å). Also, structural studies have shown the existence of strong O-H... O hydrogen bonds lie in the crystallographic plane perpendicular to the polar direction [001].

The band gap of 6.0 eV (HSE) was obtained. The properties of the electronic spectrum are described using the partial density of states. The energy states that form the top of the valence band are formed by the *p*-orbitals of O ions hybridized with the *s-p* orbitals of Se, and the states at the bottom of the conduction band are associated with the *p*-orbitals of Se.

The National Research Foundation of Ukraine supported this work within the project 2020.02/0130 "Multifunctional organic-inorganic magnetoelectric, photovoltaic and scintillation materials" (reg. № 0120U104913).

Structuring of (111) PbTe Crystal Surfaces Sputtering with Ar^+ Ions and Self-Organization Processes

Zayachuk D.M.

Lviv Polytechnic National University, Lviv, Ukraine
zayachuk@polynet.lviv.ua

Self-organization phenomena play an important role in the processes of spontaneous emergence of macroscopic ordering in various systems and widely uses for different technical applications. One of the manifestations of this interaction is the formation of ordered patterns on a solid surface undergoing ion sputtering and the appearance of surface figures that form these patterns. In this report, on the example of the PbTe compound, we present the results of the study of the interplay between the crystallographic orientation of the surfaces of high reticular density and easy cleaving of the crystals of cubic symmetry and the shape of surface structures induced by prolonged ion sputtering [1].

We found that ion bombardment of PbTe crystals, which have cubic symmetry, in the presence of protective shields on the sputtering surface forms pseudo-hexagonal pyramidal structures on it. The edges of the pseudo-hexagonal pyramids lie in the planes of the {110} family intersecting along the crystallographic direction [111]. The hexagonal structures covered with protective shields are sharpened with ion beams until the angle at the top of the pyramid reaches a minimum value. We show that in the state of maximum sharpening of the pseudo-hexagonal pyramids their edges are oriented along the crystallographic directions of the families <211> and <122>. When the protective shields are destroyed, the hexagonal structures are transformed into trihedral pyramids. Indistinct edges and terrace-shaped lateral facets characterize the pseudo-hexagonal pyramidal structures, whereas the facets of the trihedral pyramids, into which they are transformed during the ion bombardment, are mirror-smooth. We show that the maximally sharpened pseudo-hexagonal pyramids, ion-induced on PbTe (111) sputtering surfaces, are formed as a result of self-organization of the crystallographic planes of the family $\{0\bar{1}2\}$, the reticular density of which directly follows the reticular density of the plane of the sputtered surface. We also prove that the roughness of the lateral facets of pseudo-hexagonal pyramids, as well as the mirroring of the facets of the trihedral pyramids is due to the impact of crystallographic planes of the {100}family, which are the planes of the greatest reticular density and easiest cleaving for PbTe crystals.

[1]. D.M. Zayachuk, Y.D. Zayachuk, V.E. Slynko, T. Fodor, and A. Csík, J. All. Comp. 924 (2022) 166628, doi.org/10.1016/j.jallcom.2022.166628

Surface Plasmons in Metal-Graphene Cylinders

Karandas, Ya.V.[1,2], Korotun, A.V.[1,3]

[1]*Zaporizhzhia Polytechnic National University, Zaporizhzhia, Ukraine,* andko@zp.edu.ua
[2]*Zaporizhzhia scientific-research expert-criminological center of the MIA of Ukraine, Zaporizhzhia, Ukraine*
[3]*GV Kurdyumov Institute for Metal Physics of the NAS of Ukraine, Kyiv, Ukraine*

It is known that transverse and longitudinal surface plasmon resonance (SPR) can be excited in metal nanocylinders. Longitudinal resonance is particularly sensitive to changing the aspect ratio and can be easily tuned from the visible to the infrared (IR) range, which opens up broad prospects for the use of nanocylinders, in particular, in medicine, chemistry and biology. However, the use of metal nanoparticles to localize the electromagnetic field in the region whose dimensions are smaller than the diffraction limit has limitations in the mid-IR range. One of the approaches to solving this problem can be the use of two-layer nanocylinders "metal - graphene shell", since in graphene it is possible to excite SPR in the IR region of the spectrum. Therefore, the aim of the work is to study the plasmonic properties of metal-graphene nanocylinders.

The plasmonic properties of nanostructures are determined by the frequency dependence of the polarizability, which can be obtained in the quasi-static approximation from the solution of the boundary value problem of electrostatics. Since solutions to this problem exist only for nanoparticles of some shapes, in particular spherical and ellipsoidal, it is appropriate to describe the properties of metal-graphene nanocylinders using ratios for "equivalent" elongated ellipsoids of rotation [1]. These ratios include the dielectric function of the graphene shell, which in the case of a cylindrical graphene shell coincides with the dielectric function of single-layer achiral carbon nanotubes [2]. In this case, the frequencies of the longitudinal and transverse SPR's are determined by the zeros of the real part of the denominators of the expressions for the real components of the polarizability tensor.

Calculations of the frequency dependences of the diagonal components of the polarizability tensor $\alpha^{\perp(\parallel)}$ were performed for metal-graphene nanocylinders of different sizes and with different compositions of the metal core. The presence of a shift in the position of the longitudinal SPR in the IR region (that is, a significant "red" shift from the optical to the IR range in comparison with the metal cylinder) was established.

[1]. Korotun A.V., Karandas Ya.V., Reva V.I. Analytical Theory of Plasmon Effects in Rod-like Metal Nanoparticles. The Equivalent-spheroid Model. *Ukr. J. Phys*. 2022. V. 67, No 12. P. 849-858.

[2]. Korotun A.V., Karandas Ya.V. Infrared Absorption by Achiral Carbon Nanotubes. *Low Temp. Phys*. 2020. V. 46, No 1. P. 76-83.

Synthesis and Characterization of Plasmonic Nanoparticles of Different Shape for Biomedical Applications

Mazur N.V.[1], Kapush O.A.[1], Ivanova I.V. [2], Yukhymchuk V.O.[1],
Sydorenko V.G.[2], Kukla O.L.[1], Demydov P.V.[1], Moroz O.F.[3], Soloviev A.I.[2],
Zholos A.V.[3], Dzhagan V.[1]

[1]V. Lashkaryov Institute of Semiconductors Physics of NAS of Ukraine, 03028 Kyiv, Ukraine,
nazarmazur@isp.kiev.ua
[2]Institute of Pharmacology and Toxicology, National Academy of Medical Science of Ukraine, Kyiv, Ukraine
[3]ESC "Institute of Biology and Medicine", Taras Shevchenko National University of Kyiv, Kyiv, Ukraine

In the past decade, there has been a notable increase in research focusing on the production of silver and gold nanoparticles (Ag NPs and AuNPs). This heightened interest can be attributed to the distinctive blend of their antibacterial, optical, electronic, and catalytic characteristics, which can be used in a wide range of potential applications. One of the tasks addressed by the researchers is tuning the plasmon resonance to a broader spectral range. This allows resonant excitation for broader range of analytes and lasers, avoiding concomitant excitation of analyte fluorescence and other benefits.

In this work, AgNPs of different shape and sizes were synthesized. For synthesis we used sodium citrate, sodium borohydride, ascorbic acid and chitosan. Synthesis was carried out with varying of sodium citrate quantity. For synthesis of AuNPs we also used sodium citrate and tannic acid, by varying the amount of both sodium citrate and tannic acid. In the optical absorption spectra, along with the 480 nm plasmon band for NPs obtained with a low concentration of sodium citrate, with increasing of sodium citrate concentration another band at 560 nm was detected. It may indicate the formation of NPs with a shape other than spherical and allows to use of AgNPs for resonant excitation of SERS in the green band of the spectrum. SEM measurements confirmed formation of AgNPs with triangular and polygon prism shapes with sizes < 50nm. With decreasing amount of sodium citrate (or tannic acid) we observe a red shift of the 525 nm plasmon band in the AuNP absorption spectra to range >600 nm. Those colloidal AgNPs were used as substrates for surface enhanced Raman spectroscopy (SERS) measurements and allowed us to detect standard dye molecule rhodamine 6G (down to 10^{-7}M concentration) and amino acid adenine (down to 10^{-4}M). The SERS measurement was used as a preliminary test of the plasmon activity of the developed NPs, which is a prerequisite of their effect on biosystem, in particular for stimulation of the activity of ion channels.

The work was supported by the Ministry of Education Science of Ukraine (project К-I-105).

Synthesis of Ferromagnetic Nanoparticles for Use as Contrast Agents for Long-Term Magnetic Resonance Molecular Imaging

Kotsyubynsky A.O.[1], Hrytsuliak H.M.[2], Kotsyubynska Y.Z.[3]

[1]*Vasyl Stefanyk Precarpathian University, Ivano-Frankivsk, Ukraine,*
kotsyubynskyao@gmail.com
[2]*Ivano-Frankivsk National Technical University of Oil and Gas, Ivano-Frankivsk, Ukraine,*
gritsulyaka@ukr.net
[3]*Ivano-Frankivsk National Medical University, Ukraine, kotsyubynskayz@gmail.com*

Magnetic resonance imaging (MRI) is the most powerful modern method of non-invasive diagnosis of diseases. Contrast agents are often used to make MRI work more efficient. Correctly designed contrast substances can accumulate in certain areas (the most interesting are cancerous formations) and become a kind of cell markers for detecting and monitoring diseases. The main limitation in the use of contrast agents currently used in clinical practice is their rate of relaxation and time of elimination from the body. To overcome these limitations, ferromagnetic nanoparticles (FNP) of iron with a modified surface can be used, which show a high retention time in organs [1].

We used $FeCl_3$ and $FeCl_2$ salts as initial reagents for the synthesis of nanosized particles, to whose solutions in an aqueous medium (with constant intensive stirring and control of pH and temperature) concentrated NH_4OH was added dropwise. During the reaction, Fe_3O_4 magnetic particles were formed, the size of which depended on the rate of addition of NH_4OH and the intensity of stirring the solution. After the end of the reaction and the growth of the pH value to 10, a specially prepared surfactant ammonium oleate (prepared from oleic acid and concentrated NH_4OH) was added to the suspension.

This makes it possible to counteract the aggregation of FNP and provides space for further modification of their surface. As a result, superparamagnetic hydrophobic FNP with a size of 4-10 nm were obtained. Currently, studies are being conducted on the modification of their surface with polyethylene glycol and their biocompatibility. These research data are quite relevant, because iron-based FNP can become a cheap and effective contrast agent for molecular MRI imaging, with a long-lasting and intense signal.

[1]. Flores-Rojas, G. G., López-Saucedo, F., Vera-Graziano, R., Mendizabal, E., & Bucio, E. Magnetic nanoparticles for medical applications: Updated review. *Macromol*, 2022. 2(3), 374-390.

Synthesis, Structure and Photocatalytic Activity of Mn-Doped Titania

Myroniuk I.F., Kotsyubynsky V.O., Mykytyn I.M., Boychuk V.M., Frolyak V.Y.

Vasyl Stefanyk Precarpathian National University, Ivano-Frankivsk, Ukraine,
volodymyr.kotsuybynsky@pnu.edu.ua

Doping titanium dioxide with transition metals is a well-established approach to creating photocatalysts with improved properties and enhanced photoresponse in the visible light range. Transition metal doped TiO_2 photocatalysts have found wide application in various fields, in particular in environmental remediation and solar energy conversion. Transition metal dopants can serve as electron traps or charge carriers, facilitating the separation of photogenerated electron-hole pairs. This improved charge separation efficiency is crucial for optimizing photocatalytic reactions. The choice of a specific transition metal dopant, its concentration, and synthesis method plays a critical role in tailoring the photocatalytic properties of doped TiO_2 for specific applications.

The synthesis of Mn-doped titania nanoparticles (Mn content of 0, 2.5, 5, and 10 at. %, corresponding to samples labeled as Mn0, Mn2.5, Mn5, and Mn10, respectively) was carried out by a sol-gel chemical route based on the interaction of $[Ti(OH_2)_6]^{3+}\cdot 3Cl^{-}$ as a product of acid hydrolysis of $TiCl_4$ with hydrolyzed $MnCl_2\cdot 5H_2O$. The nucleation of Mn-doped titania, resulting from the oxolation-olation interaction of $[Ti(OH)_h(OH_2)_{6-h}]^{(4-h)+}$ and $[Mn(OH)_h(OH_2)_{6-h}]^{(4-h)+}$ hydrocomplexes, is initiated by a NaOH-induced increase in the pH of the reaction medium to 7.5-8.0, which, according to the partial charge theory, corresponds to the formation of neutral primary species.

The phase composition, morphology, particle size, pore size distribution, and photocatalytic performance of the obtained materials were systematically studied by XRD, FTIR, TEM, low-temperature nitrogen adsorption porosimetry, and UV-Vis spectroscopy. The structural state of all the obtained materials is close to amorphous with a clear manifestation of anatase motifs. An increase in the concentration of the Mn dopant leads to a gradual increase in the specific surface area (from approximately 280 to 385 m^2/g for Mn0 and Mn10, respectively) and an increase in the micropore content while maintaining pore sizes in the range of 3-6 nm. An increase in the content of Mn dopant leads to an exponential decrease in the band gap – 3.20, 3.12, 2.91, and 2.88 eV for Mn0, Mn2.5, Mn5, and Mn10 samples, respectively.

The photocatalytic activity of the synthesized Mn-doped TiO_2 nanoparticles was analyzed by the method of photodegradation of aqueous solutions of methylene blue (MB) dye (15 mg/L) under visible light irradiation (intensity 200 W/m^2). The dye concentration was monitored by UV-Vis spectrometry. The kinetics of MB disappearance is of the first order, which is consistent with the Langmuir-Hinshelwood mechanism. It was found that the Mn10 sample has the highest photocatalytic performance – the rate constant is 0.018-0.019 min^{-1}. For comparison, the rate constant for the Mn0 sample is in the range of 0.006-0.008 min^{-1}.

The Effect of the Mechanical Duration on the Electronic Structure SiO_2/TiO_2 Nanocomposite

Yavorskyi Y., An T., Gou Y., Zaulychny Y.

E.O. Paton institute material science an welding, National Technical University of Ukraine "Kyiv Polytechnical Institute", 35 Politekhnichna Str., Kyiv 03056, Ukraine,
yar-yra@ukr.net.

It is well known that the properties of nanosized materials depend on their structural and morphological features, electronic structure, development and surface defects, and others. Different synthesis and processing methods are used to increase the surface activity of materials. One method that allows achieving this is machining, and in this case mechanical treatment on the microbreaker (MBT) [1,2]. In this work, we conducted a study of the effect of different duration of such treatment on the distribution of valence Op-electrons of the $SiO_2/0.2TiO_2$ nanocomposite, investigated by ultra-soft x-ray emission spectroscopy.

The initial mixture was prepared by conventional stirring for 5 minutes, followed by stirring in a 50 Hz mechanical microbreaker Ardenne with a stainless steel sphere (25 mm in diameter) and ball (10 mm in diameter). Mechanical processing was carried out under the same conditions but for 3, 5, 10, 15, and 20 minutes [2].

From the results of the study of the OKα emission bands of the initial sample and those processed for different durations, it was established that as a result of mechanical processing within 3 minutes, the population of electrons in the 522-526 eV region decreased. Which is most likely the result of the evaporation of sorbed water from the material during processing. During processing for 5 minutes, there is some increase in the population of Op_π-electrons, which presumably corresponds to the formation of π-interaction between the surface atoms of the nanoparticles [1]. However, the shape of the OKα spectra of the samples after 10-20 min of processing corresponds to the shape of the spectra of the sample that is processed for 3 min. This may indicate the breaking of weak bonds that were formed during processing within 5 minutes.

[1]. The dependence between the structural-morphological features mixes SiO_2/TiO_2 and dis-charge capacities of lithium power sources / Yavorsky Yu.V., Zaulichny Ya.V., Gunko V.M., Karpets M.V., Mokliak V.V.// Journal Of Nano-And Electronic Physics – 2019. – Vol. 11 No 6, 060012 (6pp). https://doi.org/10.21272/jnep.10(6).06012

[2]. The Dependence between the structural-morphological features mixes $0.8SiO_2/0.2Al_2O_3$ from the time of mechanical treatment / Yu.V. Yavorsky, Ya.V. Zaulichny, M.V. Karpets, A.I. Dudka, A.B. Hrubiak, V.V. Moklyak // Physics and Chemistry of Solid State, V. 22, No. 3 (2021) pp. 516-521. https://doi.org/10.15330/pcss.22.3.516-521

The Spatial Redistribution of Point Defects and their Self-Organization in the ZnO Semiconductor under the Influence of Pulsed Laser Irradiation

Kuzyk O.V.[1], Dan'kiv O.O.[1], Peleshchak R.M.[1,2], Stolyarchuk I.D.[1],
Kuhivchak V.A.[1], Revutskyi O.O.[1]

[1]*Drohobych Ivan Franko State Pedagogical University, Drohobych, Ukraine*
olehkuzyk74@gmail.com
[2]*Lviv Polytechnic National University, Lviv, Ukraine*

Zinc oxide (ZnO) is a multifunctional inorganic semiconductor material with industrial applications in many fields. The ZnO has a complex system of point defects: interstitial atoms of zinc (Zn_i) and oxygen (O_i), vacancies of zinc and oxygen, as well as antistructural defects. Given that the deformation-diffusion mechanism often plays a decisive role in the self-organization of defects on the surface of semiconductors, an important physical parameter is the deformation potential constant of the conduction band (valence band). This parameter determines the displacement of the edges of the allowed bands under the action of deformation, and for ZnO, the constant of the deformation potential of the conduction zone is quite significant (-2.15 eV).

In this work, the model of the self-consistent deformation-diffusion redistribution of point defects (interstitial atoms and vacancies) in ZnO under the influence of pulsed laser irradiation is developed, which takes into account the diffusion of defects in an nonuniform deformation field created both by the presence of the defects themselves and the temperature gradient, and non-local interaction between defects and matrix atoms.

Within the framework of the developed model, the concentration profiles of interstitial Zn_i and O_i atoms were investigated at different values of their average concentration, substrate temperature, and characteristic distance of the laser beam.

Due to non-uniform heating of the semiconductor, the non-uniform deformation field arises, which creates deformation-diffusion flows of defects. Moreover, defects that are centers of stretching (interstitial atoms) move in the area of relative stretching (toward the surface of the crystal), and defects that are centers of compression (vacancies) move in the opposite direction. It is shown that interstitial atoms accumulate near the irradiated surface of the semiconductor, and vacancies accumulate at a distance of (4 – 10) nm from it. The criteria for the formation of Zn and ZnO nanoparticles depending on the intensity of laser irradiation and the duration of the pulse have been established.

Theory of Superlattices with Two Atoms in the Basis

Bilynskyi I.V.[1], Leshko R.Ya.[2], Bandura H.Ya.[3]

[1]Physics Department, Kryvyi Rih State Pedagogical University, 54 Gagarin Avenue, 50086, Kryvyi Rih, Ukraine, iv.bilynskyi@gmail.com
[2]Physics Department, Drohobych Ivan Franko State Pedagogical University, 3 Stryiska Street, 82100, Drohobych, Ukraine, leshkoroman@gmail.com
[3]Postgraduate , Drohobych Ivan Franko State Pedagogical University, 3 Stryiska Street, 82100, Drohobych, Ukraine, galinka.bandura@gmail.com

The creation of artificial materials with specified physical properties that cannot be found in nature is one of the most important tasks of modern science and technology. Modern technologies of nanomaterials make it possible to create artificial materials from hundreds and even thousands of nano-sized building blocks with an extremely diverse structure. One of the most promising such building blocks is semiconductor quantum dots (QD). And their large number creates a superlattice of quantum dots.

In most theoretical models that are used until now, the QD arrays with identical QD where studied. The review work **Ошибка! Источник ссылки не найден.** describes superlattices of quantum dots and their properties. The authors demonstrated models showing that different layers may have different sizes of QDs. In this connection, there is a need to build a theory that would take into account the presence different QDs in QD arrays. Therefore, in this work, we present theory in the tight binding approaches which describes one dimensional periodically ordered QD array (linear chain) with two different QDs in elementary ceil.

This theory allows you to study different structures. for example, grid elements may vary in type and size. Quantum dots can be moved apart or brought together. The distances between the quantum dots do not necessarily have to be the same, etc. In this way, we can study energy spectra, band widths, and other properties of superlattices.

[1]. Hongbo Lan, Y.H. Ding, Ordering, positioning and uniformity of quantum dot arrays (April 2012) Nano Today 7(2):94–123 DOI:10.1016/j.nantod.2012.02.006

Session 3

Physical-chemical properties of thin films

Catalytic Activity of Amorphous Metallic Electrodes in Redox Processes of Films of Oligomeric Peroxides

Hula T.H.[1], Hertsyk O.M.[1], Kovbuz M.O.[1], Pandiak N.L.[2]

[1] *Ivan Franko National University of Lviv, Kyryla and Mefodiya Str. 6,*
79005 Lviv, Ukraine, djunjer1@gmail.com
[2] *Ukrainian National Forestry University, Gen. Chuprynka Str. 103,*
79057 Lviv, Ukraine, pandyakn@ukr.net

Electrocatalysis of the −O−O− bond dissociation of oligomeric peroxides (OP) in ammonia solutions was investigated based on oligoperoxides: I - vinyl acetate (VA), 3-tert-butylperoxy-3-phenylbutylmethyl methacrylate (TBPM), and maleic anhydride (MA); II - VA-tert-butylperoxy-3-methylbutyl-methacrylate (TBPMM)-MA with a different ratio of VA and MA. Oligoperoxides with an average molecular weight of M ~ 2000 were used for film-forming solutions. From solutions with a concentration of 0.04 mol/l form functional layers on the surface of amorphous alloys capable of turning into protective thin films. To compare the catalytic action, a platinum electrode and amorphous metallic electrodes $Fe_{80}Si_6B_{14}$, $Fe_{78.5}Ni_{1.0}Mo_{0.5}Si_{6.0}B_{14.0}$ were used.

Dissociation kinetics of the oligoperoxide bonds was recorded by the cyclic voltammetry method. The values of the effective rate constants of cathodic (k_c) and anodic (k_a) processes indicate a sufficiently high affinity of oligoperoxides to the surface of amorphous alloys, which initiates the decomposition of −O−O− groups in the surface adsorption layers. Practically, the catalytic activity of the amorphous metallic surface of a multicomponent alloy is not lower than that of the reference catalyst – platinum (Table I).

Table I Rate constants of electrochemical reduction (k_c) and oxidation (k_a) of OP and P(%) - yield of free radicals on Pt and amorphous metallic electrodes.

OP	k	Pt		$Fe_{80}Si_6B_{14}$		$Fe_{78,5}Ni_{1,0}Mo_{0,5}Si_{6,0}B_{14,0}$	
		$k\cdot10^2$, s^{-1}	P	$k\cdot10^2$, s^{-1}	P	$k\cdot10^2$, s^{-1}	P
I 40:20:40	k_c	6,61	4,5	1,60	12,0	6,36	15,6
	k_a	6,31		1,44		6,37	
I 45:10:45	k_c	7,33	10,9	2,06	14,2	6,87	19,2
	k_a	8,23		1,90		7,10	
II 40:20:40	k_c	6,68	4,5	2,13	9,61	7,91	16,1
	k_a	7,00		2,21		7,90	
II 45:10:45	k_c	7,39	11,9	1,98	8,70	8,56	17,8
	k_a	8,40		1,02		7,98	

Dispersion Properties of $(La_{0.06}Ga_{0.94})_2O_3$:Eu Thin Films

Bordun O.M., Bordun B.O., Kukharskyy I.Yo., Medvid I.I.,.Kofliuk I.M, Maksymchuk D.M.

Ivan Franko National University of L'viv, Ukraine,79005, Lviv, Dragomanova str. 50.
bordun@electronics.lnu.edu.ua

Pure and doped films based on β- Ga_2O_3 are used as transparent conductive coatings, and phosphors, which exhibit photoluminescence, cathodoluminescence, and electroluminescence, depending on the preparation method and dopant. Considering that the optical and electrical characteristics of β- Ga_2O_3 thin films can be purposefully changed by the introduction of impurities, we studied $(La_{0.06}Ga_{0.94})_2O_3$:Eu thin films in which some Ga^{3+} ions were replaced by La^{3+} ions and the Eu^{3+} activator was introduced.

Thin films of $(La_{0.06}Ga_{0.94})_2O_3$:Eu with a thickness of 0.3-1.0 μm were obtained by radio-frequency (RF) ion-plasma sputtering on amorphous fused quartz υ-SiO_2 substrates. After the films were sputtered, they were heat treated in argon at 1000-1100°C. The analysis of X-ray diffractograms shows that the structure of the obtained films corresponds to the monoclinic crystal structure of β- Ga_2O_3. The percentage of components was calculated using an OXFORD INCA Energy 350 energy dispersive spectrometer. The analysis of AFM images obtained using the TS-150 NTEGRA atomic force microscope shows that after heat treatment in an argon atmosphere, the size of the nanocrystalline grains that form the film increases in thin films and the average square surface roughness increases. In particular, for the freshly deposited films, the average grain diameter was 47.6 nm and the root mean square roughness was 0.5 nm. After heat treatment, these values were 67.4 nm and 6.1 nm, respectively.

Using a spectrophotometric technique based on the effect of interference in the transmission spectrum of thin films, the film thicknesses and the spectral dependence of the refractive index *n* were determined. It was found that for $(La_{0.06}Ga_{0.94})_2O_3$:Eu films, as well as for β- Ga_2O_3 and $(Y_{0.06}Ga_{0.94})_2O_3$ films annealed in an argon atmosphere, a normal dispersion is observed. An abnormal dispersion is observed for freshly deposited $(La_{0.06}Ga_{0.94})_2O_3$:Eu films. A single-oscillator approximation model was used for the studied films with normal dispersion and the approximation parameters, dispersion energy, degree of chemical bond ionicity, coordination number of the first cation coordination sphere, and characteristic energy of the UV absorption wave were determined. It has been shown that the dispersion dependence of the refractive index is determined mainly by transitions from the zone of 2p oxygen states, which form the upper filled level of the valence band to the bottom of the conduction band formed by hybridized 2p oxygen and 4s gallium states.

Doping of CdTe with Li Impurity

Mazur T.M., Mateik G.D.

Ivano-Frankivsk National Technical University of Oil and Gas., Ivano-Frankivsk, Ukraine,
tetiana.mazur@nung.edu.ua

Modern electronics focuses on the development and production of a variety of devices. One of the key materials for their creation is CdTe. Its significant band gap (Eg=1.5 eV at 300 K) makes it an optimal material for converting solar energy into electrical energy [1]. Devices made from CdTe are capable of operating in the near-infrared range and can be used in high-temperature environments.

The base crystals were obtained using the classical Bridgman method. Studies of their electrical properties made it possible to establish n-type conductivity and resistivity ρ~100 Ohm cm. Pads with a standard size of $4\times4\times1$ mm^3 were produced using a sharp mechanical string. Chemical-mechanical processing of the substrates was carried out using well-known classical technology, and the condition of the resulting surfaces was controlled using widely used methods. Doping with Li impurity was carried out by diffusion from the vapor phase in a sealed quartz ampoule at T = 980ºC and a diffusion time of at least 1.5 hours. Moreover, the CdTe substrate and the Li_2CO_3 diffuser were located at opposite edges of the ampoule [1].

In this work, doping with a lithium impurity causes the formation of intense luminescence in the photon energy region. close to edge absorption. Accordingly, in this spectral range, the optical absorption processes of base CdTe crystals and the influence of the Li dopant on them were studied. Based on the results of a study of optical transmission T_ω, a typical spectral distribution of optical radiation intensity was found in the photon energy region of $\hbar\omega = 1.0$-1.55 eV. A rapid decrease in transmission intensity appears at $\hbar\omega \geq 1.5$ eV. The properties of surface doped layers are determined by interband optical transitions and through centers formed as a result of lithium doping.

Doping a CdTe crystal with impurity Li using a diffusion method can increase the edge emission efficiency by up to $\eta = 12\%$. In this case, luminescence in the edge region is formed due to the recombination of free charge carriers between the bands and the dominant recombination, including the formation of centers with the participation of lithium Li_{Cd}. Doping also makes it possible to obtain high-quality CdTe:Li layers without affecting the properties of the base CdTe crystals. Technological doping modes have also been determined that make it possible to obtain an inversion of the conductivity type from n-type to p-type.

[1]. Prokopiv V.V., Dzundza B.S., Sharyn S.V., Mazur T.M., Turovska L.V., Matkivskyi O.M. Electrical Properties of Cadmium Telluride Thin Films Doped with Calcium and Lithium. *Physics and chemistry of solid state*. 2020. Vol. 21, No. 2. P. 232-237. *DOI: 10.15330/pcss.21.2.232-237.*

Effect of B_2O_3 Addition to Magnesium, Zirconium, Hafnium Fluorides on the Parameters of Thin Films Formed from Them

Zinchenko V.F.[1], Mozkova O.V[2], Magunov I.R.[1], Volchak G.V.[1],
Ieriomin O.G.[1], Babenko A.V.[1]

[1]Bogatsky Physico-Chemical Institute NAS of Ukraine, Odesa, Ukraine, vfzinchenko@ukr.net
[2]State Enterprise for Special Instrument Making «Arsenal», Kyiv, Ukraine olgamozk@ukr.net

Metal fluorides are widely used to create thin-film interference coatings and optical elements based on them. Magnesium fluoride, MgF_2, is the most important compound with high transparency in the UV range of the spectrum. Fluorides of Zirconium, ZrF_4, and Hafnium, HfF_4, on the other hand, are characterized by higher transparency in the IR range of the spectrum. A common problem with metal fluorides is the presence of oxide impurities in their composition. Previously, it was proposed to use the addition of boron oxide to bind the oxide impurity in zinc sulfide [1].

In this work, a similar approach is used to bind oxide impurities in Magnesium, Zirconium, and Hafnium fluorides. Thin-film coatings were obtained by thermal evaporation in a vacuum of the corresponding compounds and composites doped with B_2O_3 additive. The parameters of evaporation processes and the properties of obtaining coatings are given in table.

Table

Parameters of thermal evaporation in vacuum and characteristics of coatings

Parameters	I, A	τ, min.	n (λ = 500 nm)	$d_{opt.}$, nm	$f \cdot 10^3$, nm/min·A^2
MgF_2	140	10	1.42	1258	4.52
$MgF_2–B_2O_3$	140-150	16	1.41	1300	2.94-2.56
ZrF_4	140	25	1.53	2000	2.66
$ZrF_4–B_2O_3$	120	30	1.53	2000	3.03
HfF_4	140	20	1.57	2000	3.25
$HfF_4–B_2O_3$	120	20	1.53	2000	4.54

The volatility parameter (f) of the materials was estimated according to the equation:

$$f = d_{opt}/n \cdot I^2 \cdot \tau,$$

where d_{opt} is the optical thickness of the coating, n is the refractive index, I is the current strength, and τ is the duration of the process. As can be seen from the table the specified parameter changes under the influence of B_2O_3 addition. Instead, it has a weak effect on the value of the refractive index. Possible explanations of the observed effect under the action of B_2O_3 are put forward.

[1]. Zinchenko V.F., Magunov I.R., Volchak G.V., Mozkova O.V., Kocherba G.I. Effect of B_2O_3 additive on the properties of ZnS–Ge system and the resulting thin-film coatings. Materials Today: Proceedings, 2022. Vol. 62, Part 9. P. 5767–5770. DOI.org/10.1016/j.matpr.2022.03.477

Electrochemical Impedance Spectroscopy Study of Thin Films with Insulating and Anticorrosion Properties on Cobalt-Based Amorphous Alloys

Lopachak M.M., Boichyshyn L.M., Reshetnyak O.V.

Ivan Franko National University of Lviv, Lviv, Ukraine, mariia.lopachak@lnu.edu.ua

Electrochemical impedance spectroscopy (EIS) is a powerful tool for studying the surfaces of materials, providing quantitative and time-dependent information about electrode processes and complex interfaces. Passive films on the surfaces of amorphous metal alloys (AMAs), which predominantly exhibit semiconductor properties, are an important subject of research using this method [1]. The materials under investigation were AMAs $Co_{75.5}Fe_{4.6}Si_{6.0}B_{16.7}$, $Co_{66.5}Fe_{4.0}Mo_{1.5}Si_{16.0}B_{12.0}$, and $Co_{73.6}Fe_{3.2}Mn_{3.2}Si_{5.0}B_{15.0}$. Surface films were synthesized in a 3% NaCl using the potentiostatic mode at E = -600 mV (Fig.1).

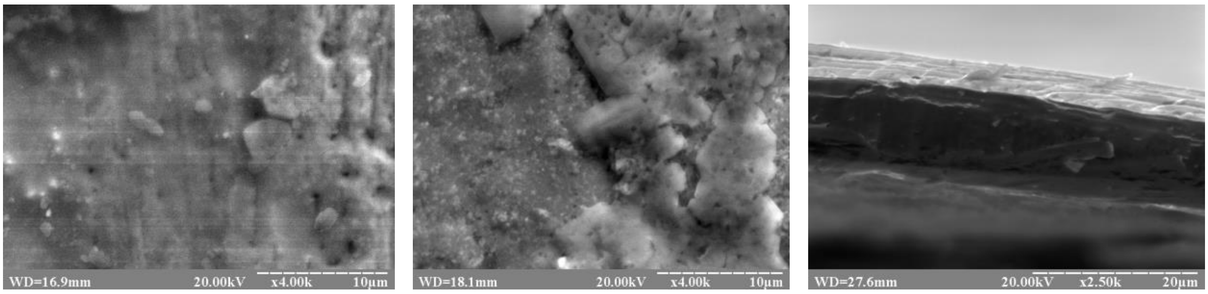

A *B* *C*

Figure 1. Microphotographs of the thin films of $Co_{66.5}Fe_{4.0}Mo_{1.5}Si_{16.0}B_{12.0}$ (*a*) and $Co_{73.6}Fe_{3.2}Mn_{3.2}Si_{5.0}B_{15.0}$ (*b*), and the cross-section (*c*) synthesized in the potentiostatic mode at E = - 600 mV.

From the Nyquist plots, it was determined that the most stable films for $Co_{75.5}Fe_{4.6}Si_{6.0}B_{16.7}$ were formed at potentials between -920 and -780 mV, with a charge transfer resistance across the phase distribution boundary of $\approx 4\times10^3$ Ω and $Z'' \approx 5\text{-}6\times10^3$ Ω. This indicates good insulating properties of the oxide film. Doping AMA with 1.5% Mo led to an increase in the stability of the films, particularly those synthesized at -577 mV, as indicated by the charge transfer resistance of $\approx 2.5\times10^4$ Ω and $Z'' = 1.4\times10^4$ Ω. The addition of Mn showed a tendency to decrease the resistive properties of the oxide coatings, except for the films synthesized at -900 mV, which exhibited the best corrosion resistance among all the samples.

[1]. Cesiulis H., Tsyntsaru N., Ramanavicius A., Ragoisha G. The Study of Thin Films by Electrochemical Impedance Spectroscopy. In: Nanostructures and Thin Films for Multifunctional Applications. NanoScience and Technology. *Springer, Cham.* 2016.

Electron-Stimulated Desorption and Thermodesorption from MgO Film Surfaces

Poplavskyy O.P., Lishchynskyy I.M., Poplavskyy I.O.

Vasyl Stefanyk Precarpathian University, Ivano-Frankivsk, Ukraine,
omelian.poplavskyi@pnu.edu.ua

Materials based on nanopowders are often used in various fields of science and technology. One of their key characteristics is gas adsorption. Therefore, it is essential to determine the qualitative and quantitative composition of gas elements adsorbed on the surface. The most informative methods for studying gas emissions are electron-stimulated desorption (ESD) and thermodesorption (TSD).

As a result of the dissolution of H_2O and CO_2 during the preparation process, as well as the adsorption of components from the air and residual gases in the vacuum system on the surface of magnesium oxide, impurities are formed. These impurities significantly influence the properties of magnesium oxide by leading to the formation of surface structural defects.

Using a radiofrequency mass spectrometer, an analysis of the composition and intensity of TSD from MgO films obtained by electrophoresis was conducted.

Thermal treatment of films in a vacuum at temperature of 570 K results in the TSD of H_2, H_2O, and CO_2 remaining at background levels in the temperature range of 300-620 K, and the emission intensity significantly decreases at temperatures above 620 K. However, CO emissions remain substantial. At temperatures above 620 K, hydrogen and carbon are desorbed from the near-surface region, interact with oxygen. Furthermore, starting from a temperature of 670 K, the decomposition of $Mg(OH)_2$. The repeated thermal treatment at 570 K does not significantly affect the character and intensity of gas emissions, except for H_2O emissions, which decrease.

Investigations of electron-stimulated desorption (ESD) for the MgO surface were carried out in a specialized lamp (where an omega-tron sensor was used as a mass analyzer).

The absence of a significant increase in emission intensity at the initial moment of irradiation indicates the absence of desorption of weakly bound particles from the surface. Under the influence of electron irradiation, processes involving the formation and subsequent desorption of carbon oxide and methane occur in the near-surface region. ESD reaches saturation after 10 minutes of continuous irradiation. Additionally, under the influence of electron irradiation, hydrogen and carbon diffusion take place, resulting in the formation of methane, which is detected using a mass spectrometer. The efficiency of this process stabilizes over time, and further electron irradiation does not lead to an increase in emission intensity.

Features of In Doping on Spectral Properties of CdTe Thin Films

Vakaliuk I.V.[1], Nykyruy L.I.[1], Yavorskyi R.S.[1], Fedosov S.A.[2], Hrytsyak M.D.[1], Ilnytskiy R.V.[1]

[1]*Vasyl Stefanyk Precarpathian National University, Ivano-Frankivsk, Ukraine,*
ivanna.maliarska@pnu.edu.ua
[2]*Lesya Ukrainka Volyn National University, Lutsk, Ukraine*

The use of solar energy is a promising way to solve global energy and environmental problems. Thin-film photoelectric converters based on CdTe are a leading technology among global manufacturers. CdTe solar cells underwent significant improvement which led to increased efficiency to 22.1% [1]. Doping of CdTe thin films makes it possible to change the optical, electrical and photovoltaic properties.

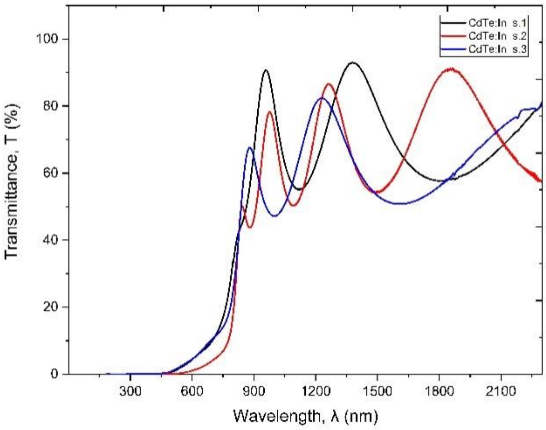

Fig. 1. Transmittance of thin films made of CdTe:In.

In this work, In was chosen as an alloying admixture to increase the electrical conductivity of CdTe thin films. Thin films of CdTe:In were deposited by the method of thermal evaporation in a vacuum. The spectral dependence of optical transmittance (T) of CdTe:In thin films as a function of wavelength (λ) in the range of 300-2200 nm was studied.

Optical constants such as refractive index, absorption coefficient, theoretical film thickness and optical conductivity have been determined by the Swanepoel method.

[1]. Green M. A. et al. Solar cell efficiency tables (version 56). *Progress in Photovoltaics: Research and Applications*. 2020. V.7, No 28. P. 629-638

Influence of the Toxic Vapors on the Electrical Properties and Structure of Polytoluidine Films

Aksimentyeva O.I.[1], Tsizh B.R.[2,3], Horbenko Yu.Yu.[1], Chokhan' M.I.[3],
Stepura A.L.[1], Baluk V.I.[4]

[1]*Ivan Franko National University of Lviv, Lviv, Ukraine, aksimen@ukr.net*
[2]*Kazimierz Wielki University in Bydgoszcz, Bydgoszcz, Poland, tsizhb@ukw.edu.pl*
[3]*Stepan Gzytskyi National University of Veterinary Medicine and Biotechnologies Lviv, Lviv,Ukraine, mariya-choknad@ukr.net*
[4]*National University "Lvivska Polytechnyka", Lviv, Ukraine*

Conducting polymers belonging to organic semiconductors promise to creation sensitive elements for both resistive and optical type of sensors [1]. However, the influence of the vapors of toxic organic and inorganic vapors on the electrical resistance of organic semiconductor films for today is poorly studied. The control of the functional properties of conducting polymers gives the possibility to choose a volatile agent. Among the acidic dopants, the toluenesulfonic acid (TSA) is especially promising. It acts as dopant and as plasticizing agent in polymers providing their high conductivity and processability. We investigated an influence of the vapors of chloroform, tetrahydrofuran (THF), dimethylformamide (DMF), nitrobenzene, toluene and ammonia on the specific resistance and structure of poly-ortho-toluidine (PoT) obtained by oxidative polymerization in TSA medium. The PoT-TSA is characterized by a high level of crystallinity, thermal stability, and sensor sensitivity. The character of influence of toxic vapors on electrical properties of samples depends on the nature of analyte.

After the action of ammonia, the resistivity increases almost 500 times, while the activation energy of conductivity (Ea) also increases from 0.206 to 0.708 eV. As a result of this interaction, the polymer is deprotonated, which causes a significant decrease in the concentration of charge carriers. The action of the polar solvents (DMF, THF) causes an increase in resistance by 1.3-1.4 times, and the values of the Ea decrease, while under the action of chloroform we see an increase Ea of almost 2 times. It is likely that the observed phenomena are due to the peculiarities of polymer-solvent molecular interaction. If the organic solvents, with like PoT chemical structure (nitrobenzene and toluene) act on the sensor element, then we observe a slight decrease in resistance and an insignificant increase in the activation energy of conductivity. Probably, the process of physical adsorption of solvent molecules occurs, which does not affect the electronic properties of the polymer. This phenomenon may be used for selective detection of toxic solvents.

[1]. Wong Y.C., et al. Conducting Polymers as Chemiresistive Gas Sensing Materials: A Review. *J. Electrochem. Soc.* 2020. V.167. 03503.

Investigating Anisotropy Effects in Dislocation Loops Formation in Garnet Structure Materials

Tomyn Y.I.[1], Yaremiy I.P.[1], Yaremiy S.I.[2]

[1]Vasyl Stefanyk Precarpathian University, Ivano-Frankivsk, Ukraine,
tomun1988@gmail.com
[2]Ivano-Frankivsk National Medical University, Ivano-Frankivsk, Ukraine

In modern materials science, it is essential to study how defects in single crystals affect their properties [1]. Of particular interest are defects that form as a result of directed bombardment of materials' surfaces with ions. Due to this influence, vacancies and interstitial atoms are formed along the trajectory of implanted ions, which can later create dislocation loops and clusters. The characteristics of the outer layers of materials will depend on the shape, size, and concentration of these defects.

In the case of dislocation loops, their spatial orientation is very important, and it is essential to consider their orientation when studying the surface layers of single crystals using X-ray diffractometry methods.

Therefore, deriving relationships for calculating parameters of X-ray diagnostics that contain information about the characteristics of existing defects in the crystal (the Debye-Waller static factor and the extinction coefficient), accounting for the mutual spatial orientation of the Burgers vector of the loop and the diffraction vector, is an important task. This includes determining the functional dependence of the extinction coefficient, calculated with consideration for anisotropy effects, on the parameters of dislocation loops, the angular deviation of the incident beam from the exact Bragg position, and the value of the relative deformation of the crystal.

The analysis of X-ray reflection curves, inverse space maps, and the results of X-ray diffraction modeling in ion-implanted monocrystals of gadolinium gallium garnet using statistical dynamic theory [2], taking into account the anisotropy in the orientation of prismatic dislocation loops, has made it possible to establish that the consolidation of radiation-induced point defects into dislocation loops in the surface layer of materials with a garnet structure occurs not in all crystallographic planes but only in the parallel to the surface plane of the sample.

[1]. Dacenko L.I., Molodkin V.B., Osinovskij M.E. Dinamicheskoe rassejanie rentgenovskih luchej real'nymi kristallami. Kyiv: Naukova dumka, 1988. 253 s.

[2]. Olikhovskii S. I., Molodkin V. B., Len E. G., Skakunova E. S., Lizunova S. V. Generalized statistical dynamical theory of x-ray diffraction by imperfect multilayer crystal structures with defects. *Phys. Rev. B.* Vol. 99. Iss. 23.

Investigation of $CdSe_{1-x}S_x$ Solid Solutions Thin Films Obtained by Magnetron Sputtering Method

Karkulovska M.S., Ilchuk H.A., Semkiv I.V., Vashchynskyi V.M., Solovyov M.V.

Lviv Polytechnic National University, Lviv, Ukraine mariana.s.karkulovska@lpnu.ua

Semiconductor compounds based on elements from II and VI groups hold great promise as materials for optoelectronic systems.

These film materials can be used in solar panels, light-emitting diodes (LEDs), photodetectors, and other devices thanks to their properties.

To form thin film materials based on solid solutions $CdSe_{1-x}S_x$, various methods are commonly employed, including chemical vapor deposition, molecular beam epitaxy, closed space sublimation, electrodeposition, and others. Physical deposition methods generally produce superior films compared to chemical vapor deposition. As a result, our choice of deposition method is the high-frequency magnetron sputtering. This method offers advantages over other vapor-phase methods as it allows for the growth of thin films that are difficult to achieve using standard evaporation processes. The technological outcome of that is the possibility of obtaining layers with a homogeneous surface and The technological outcome of that is the possibility of obtaining layers with a homogeneous surface and high-quality structure. Additionally, this method enables control over the structure, composition, and morphology of the obtained films by changing the technological parameters of the deposition process.

The film growth process involved several stages: first, CdSe and CdS films were obtained, and in the subsequent stage, the solid solution $CdSe_{1-x}S_x$ films were formed through the thermal annealing method in an atmosphere of $CdCl_2$.

Film thickness was measured using a Veeco profilometer, model Dektak 8. Phase analysis and refinement of the crystalline structure were conducted using X-ray diffraction (XRD) data obtained with a DRON-2.0M diffractometer. The phase composition and surface analysis of the synthesized compounds were performed using a scanning electron microscope. The spectral dependence of optical transmittance and absorption of the obtained samples was measured using an AvaSpec-ULS2048-UA-50 fiber optic spectrometer (Avantes)

The present work was supported by the National Research Foundation of Ukraine (project No 2022.01/0163).

Ion Intercalation in Two-Dimensional Titania Sheets for Batteries

Prikhozha Yu.O., Balabai R.M.

Kryvyi Rih State Pedagogical University, Kryvyi Rih, Ukraine
prihozhaya.yuliya93@gmail.com, *balabai@i.ua*

Titania nanosheets are attracting considerable interest owing to their characteristic structures with high crystallinity and ultralow thickness and useful applications as electrode materials [1].

We evaluated the energy reliefs of the migration of Li, Na, or K ions into the two-dimensional nanospace between the titania sheets with their pillaring by interlayer different guest molecules. Electric charges around atoms on the path of possible migration of ions were calculated using the electron density functional and pseudopotential methods from first principles using our own software code [2].

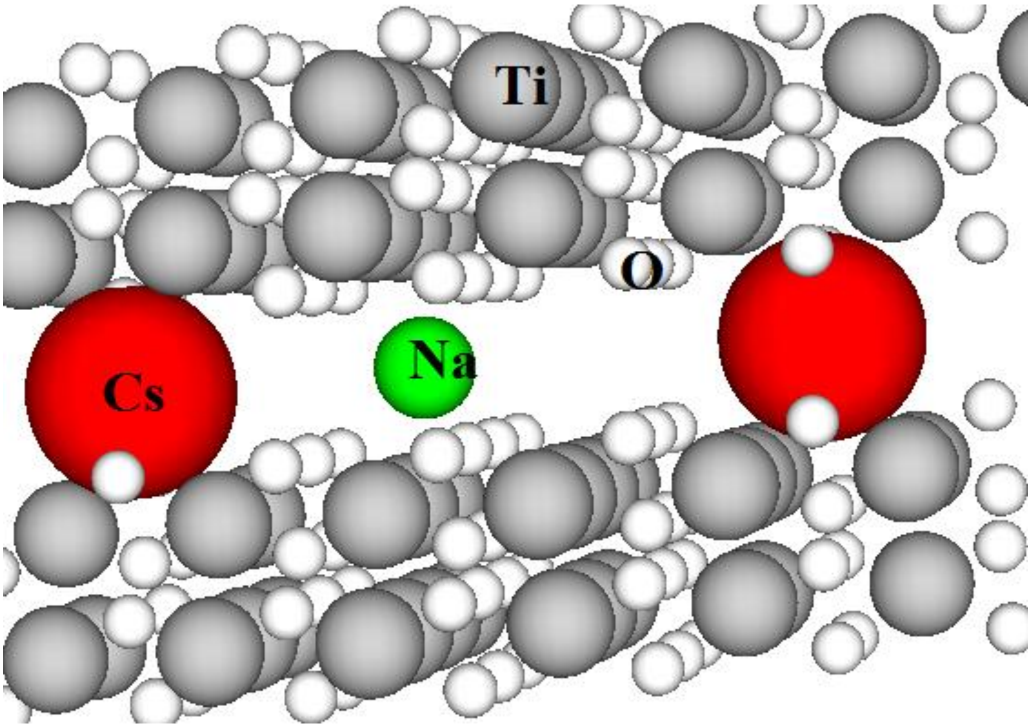

Fig. 1. Li, Na, or K ions intercalation between the titania sheets with their pillaring by interlayer guest molecules

[1]. Jinlin Yang, Xu Xiao, Wenbin Gong, Liang Zhao, Guohui Li, Kun Jiang, Renzhi Ma, Mark H. Rummeli, Feng Li, Takayoshi Sasaki, Fengxia Geng. Size-Independent Fast Ion Intercalation in Two-Dimensional Titania Nanosheets for Alkali-Metal-Ion Batteries // Angew. Chem. Int. Ed. - 2019.- V. 58.- P. 8740 –8745.
[2]. 2. Balabai R., Prikhozha Yu. Li atoms intercalation in the crystals of 2h-$TaSe_2$ gated by a polymer electrolyte $LiClO_4$/PEO: first principles calculation // Physics and chemistry of solid state. 2022. -V. 23, № 1. -P. 165-171.

Light Emitters based on GaN

Slyotov M.M.[1,*], Slyotov O.M.[1,**], Potsiluiko-Hryhoriak G.V.[2]

[1]*Yuriy Fedkovych Chernivtsi National University, Kotsyubynsky Str., 2,*
Chernivtsi, 58002, Ukraine, [*]*m.slyotov@chnu.edu.ua*, [**]*o.slyotov@chnu.edu.ua*
[2]*Chernivtsi Industrial Vocational College, Sadova str., 8, Chernivtsi, 58001, Ukraine*

The creation of radiation sources with high radiation intensity, the possibility of their use in the short-wave range at elevated temperatures is an important issue of solid-state electronics at present. This problem is successfully solved on heterolayers of II-VI compounds [1]. Therefore, nitrides of the III group deserve attention as wide-band gap materials. Among them, GaN is perspective material, since its direct band gap is an important condition for obtaining high radiation efficiency.

The possibility of obtaining efficient light emitters on the basis of GaN that can emit highly efficient radiation in the short-wave region at high temperatures is shown, and their development is carried out. For this, both epitaxial layers and crystals were obtained. At the same time, well-known technological processes of growing materials by the chloride-hydride method were used. The single-crystal structure of the obtained samples is confirmed by X-ray diffraction studies. The main parameters of the band structure and luminescent processes were studied using classical methods and λ-modulation methods. The main energy parameters $E_g = 3.42$ eV, $\Delta_{\mathrm{CR}} \approx 10$ meV, $\Delta_{\mathrm{SO}} \approx 48$ meV, the characteristics and properties of the obtained crystals and GaN layers were determined, and the effect of temperatures up to 450°C on them was investigated. It was established that the intensity of generation-recombination processes differs significantly for the edge ($\hbar\omega \geq E_g$) and visible ($\hbar\omega < E_g$) regions. In undoped GaN, intense emission due to interband transitions of charge carriers covers the ultraviolet (UV) range with a maximum at $\hbar\omega \approx 3.41$ eV. It undergoes almost complete quenching at $T \approx 450$°C.

Intense radiation is obtained on GaN doped with impurities of Mg, Zn, Si, C. The radiation intensity of the material in the corresponding region (3.21eV, 2.89eV, 2.35eV, 2.2eV) increases by 1.5-2.0 orders of magnitude compared to the undoped one. An increase in temperature (up to 380-410°C) slightly reduces the intensity and does not affect the spectral composition. The conducted temperature and time measurements revealed the stability and repeatability of the properties, parameters and characteristics of GaN layers and crystals to the influence of thermal irradiation up to 420°C.

[1]. Slyotov M., Slyotov A The sources of radiation in the short-wave range on the basis of II-VI heterolayers. *Journal IAPGOS*. 2018, V.4. P. 4-7.

Optical Properties of GaN/Al_2O_3 Thin Films Doped with Silicon

Gentsar P.O., Mynaylo A.M., Pekur D.V., Demchyna L.A.,
Stronski A.V., Zayats N.S., Vlasenko O.I.

V.E. Lashkaryov Institute of Semiconductor Physics NAS of Ukraine, 03028, Nauky av. 41, Kyiv, Ukraine, rastneg@isp.kiev.ua

Due to the intensive use of wide-bandgap semiconductors for the production of optoelectronic devices such as LEDs, lasers, and photodetectors in the ultraviolet and visible spectral regions, it is advisable to further study them. Gallium nitride (GaN) has a band gap that is much wider than germanium, silicon, gallium arsenide, gallium phosphide, and silicon carbide. In addition, GaN has high values of the critical (electric) breakdown field, high radiation resistance, mechanical strength, and is a heat-resistant and chemically inert material. It is used to create light-emitting devices for the visible spectrum (GaN-based LEDs emit all colours of the visible range, including white). Strong ionic-covalent bonding and a large band gap with a direct placement of the bands in the quasi-pulse space determine its optical and luminescent properties. One of the ways to control the radiation characteristics of gallium nitride-based devices is to doping thin epitaxial films, so it is important to study the effect of doping on the optical properties of films and the characteristics of doped films.

In this work GaN films doped with silicon (doping level $N_{Si} = 1.5 \cdot 10^{25}$ m^{-3}) grown by gas-phase epitaxy from organometallic compounds on sapphire substrates oriented along the crystallographic c-axis were studied. Optical properties (transmission in the fundamental absorption region, reflection in the visible region, reflection in the spectral range 1.4-25 μm at different angles of incidence of the light, Raman scattering spectra, photoluminescence at temperatures of 77 K and 300 K) were measured. The physical parameters of GaN/Al_2O_3 films were experimentally obtained: electronic transition energy $E_0 = 3.406$ eV, absorption coefficient α at E_0 - $1.8 \cdot 10^6$ m^{-1}, refractive index n value in the spectral wavelength range of 607 nm – 644 nm equals 2.4.

The infrared reflection bands at 534 cm^{-1} and 745 cm^{-1}, the Raman bands at 569 cm^{-1} and 750 cm^{-1} indicate a single crystal structure, namely, the hexagonal structure of wurtzite of symmetry Γ_1. A shift in the frequency position of the A_1 (LO) phonon of GaN in the IR reflection spectra depending on the angle of incidence of light has been found. This effect is explained by the influence of two processes: the presence of mechanical stresses in the film and the heterogeneous silicon doping of the epitaxial GaN film in thickness.

Peculiarities of Obtaining and Interpretation of Multifractal Spectra During Analysis Surfaces of Superthin Semiconductor Layers

Balytska N.O.[1], Moskvin P.P.[1], Skyba G.V.[1], Rashkovetskyi L.V.[2]

[1]*Zhytomyr Polytechnic State University, Zhytomyr, Ukraine,*
skybagalyna26@gmail.com
[2]*Institute of Physics of Semiconductors, National Academy of Science of Ukraine, Kyiv*

One of the directions in solving the problem of mathematical description of the material surface is associated with the use of fractal analysis. The main advantage of such a non-trivial approach in the mathematical modeling of the surface state is its rigorous physical justification, which is based on the principles of self-similarity and fractal symmetries. We have accumulated considerable experience in studying the surface of semiconductor layers [1]. This allows, using the example of image processing of the surfaces of nano layers synthesized by the sol-gel technology in the ZnO-SiO_2 system, to discuss the features of the application of multifractal analysis (MFA) in obtaining quantitative fractal characteristics of their surface. To study the surface morphology of the samples, an FEI Quanta FEG 250 scanning electron microscope was used.

The search for the parameters of the MF spectra was carried out by the method of coarsened partitions according to the standard procedure [2]. Numerical calculations of generalized statistical sums for the area and volumes of spatial nanoforms show the existence of their linear dependences on spatial dimensions, which is the main evidence of the presence of self-similarity and fractal symmetry among the indicated geometric parameters of relief-forming nanoforms. During the implementation of the MFA, technical limitations of experimental process are discussed, it sources are analyzed, and an estimate is made of the magnitude of errors in determining the Renyi's numbers that arise when obtaining images of the layers surface after its synthesis. Peculiarities of using various software for processing photographic images of the layers surface in obtaining data on MF spectra from various geometric parameters of relief-forming nanoforms are considered. This made it possible to develop recommendations for minimizing the errors in calculating the MF parameters of the sample surface. The latter will be a stimulus for further use of the MFA in creating effective and information-intensive quantitative methods for describing the state of complex surfaces and using such data in physical calculations.

[1]. Moskvin P.P., Skyba G.V., Dobriakov V.L, KolodiiM.A., Rashkovetskyi L.V, Kolomys O.F., Rarata S.V. Sol-gel synthesis, surface morphology and spectral properties of ZnO ultrathin films on a silicon single crystal. *Voprosykhimii i khimicheskoitekhnologii*, 2018, vol. 4, pp.36–42. (In Ukr.).

[2]. Feder J. Fractals, Physics of Solids and Liquids, Plenum Press. NewYork, 1988, 183 p. https://doi.org/10.1007/978-1-4899-2124-6

Quantum Size Effects in Thin Films of V_2VI_3 Topological Insulators

Rogacheva E.I.

National Technical University "Kharkiv Polytechnic Institute", Kharkiv, Ukraine,
rogachova.olena@gmail.com

The V_2VI_3 compounds and V_2VI_3 -based solid solutions are currently the best thermoelectric (TE) materials for use in refrigerating devices. Interest in studying the TE properties of V_2VI_3 crystals and thin films has grown sharply after it became known that these materials belong to new objects of quantum physics - topological insulators (TIs) whose unique properties are determined by the presence in them of a metallic surface state protected by time reversal symmetry. Many works have appeared suggesting the possibility of using the properties of TIs in spintronics, quantum computing and thermoelectricity. TI thin-film nanostructures are of particular interest because in them the contribution of surface states to the total conductivity increases. The existence of TI states may affect the manifestation of quantum size effects (QSEs) in thin films, e.g., an oscillatory behavior of the dependences of transport properties on film thickness d. The goal of this work is to summarize and analyze our earlier obtained experimental results on the d-dependences of TE properties in n- and p-Bi_2Te_3, Bi_2Se_3, and $Bi_2(Te_{1-x}Se_x)_3$ polycrystalline thin films prepared by thermal evaporation of crystals in vacuum onto glass substrates (e.g. [1-3]) and to present some our new results. For all films studied, the d-dependences of TE properties exhibit an oscillatory behavior and are well approximated by a sinusoidal function. The obtained results are interpreted within the framework of the model of a rectangular quantum potential well with infinitely high and specularly reflecting walls, considering the peculiar properties of the surface layers of V_2VI_3 films. We believe that a large amplitude, sustained character, and other features of oscillations are associated with the specific boundary conditions in the V_2VI_3 thin films. The results obtained are important for the development of the concepts of solid-state physics and for practical applications of these materials.

[1]. Rogacheva E.I., Budnik A.V., Sipatov A.Yu., Nashchekina O.N., Dresselhaus M.S. Thickness dependent quantum oscillations of transport properties in topological insulator Bi_2Te_3 thin films. *Appl. Phys. Lett.* 2015. V. 106, No 5, P. 053103.

[2]. Rogacheva E.I., Budnik A.V., Sipatov A.Yu., Nashchekina O.N., Fedorov A.G., M.S. Dresselhaus, S. Tang. Thickness oscillations of the transport properties in n-type Bi_2Te_3 topological insulator thin films. *Thin Solid Films.* 2015. V. 594. P. 109–114.

[3]. Rogacheva E.I., Menshikova S.I., Sipatov A.Yu., Nashchekina O.N. Thickness-Dependent Quantum Oscillations of the Transport Properties in Bismuth Selenide Thin Films. *Thin Solid Films.* 2019. V. 684, P.31-35.

Raman Evidence for the Oxidation of Amorphous Arsenic Chalcogenide Film Surface Under Visible Light

Azhniuk Y.M.[1], Lopushansky V.V.[1], Gomonnai A.V.[1,2], Solonenko D. [3], Loya V.Y.[1], Kryshenik V.M.[1], Voynarovych I.M.[1], Zahn D.R.T.[4]

[1]Institute of Electron Physics, Nat. Acad. Sci. Ukr., Uzhhorod, Ukraine,
yu.azhniuk@gmail.com
[2]Uzhhorod National University, Uzhhorod, Ukraine
[3]Silicon Austria Labs GmbH, Microsystem Technologies Research Unit, 9524 Villach, Austria
[4]Semiconductor Physics, Chemnitz University of Technology, D-09107 Chemnitz, Germany

Amorphous arsenic chalcogenides are well-known semiconductor materials interesting due to numerous photoinduced effects which makes them promising for various optical applications. Recently, photooxidation of amorphous As_2S_3 films under illumination by UV light was observed by Raman spectroscopy [1]. Here we present direct Raman evidence for the oxidation of amorphous arsenic selenide-based films under visible laser irradiation.

1.2–1.5 μm thick As–Se–S films were prepared from pre-synthesized $As_2(Se_xS_{1-x})_3$ glasses by thermal evaporation on silicon and silicate glass substrates. AFM studies (Agilent AFM 5420) showed an average surface roughness of about 0.8 nm. Micro-Raman studies were performed at room temperature using a Horiba LabRAM HR800 spectrometer and a 514.7 nm laser.

Micro-Raman spectra of the As–Se–S films measured at a relatively low excitation power density P_{exc}=100 kW/cm^2 are characteristic for amorphous materials with broad maxima near 225 and 340 cm^{-1}, typical for As_2Se_3 and As_2S_3, respectively. However, with increasing P_{exc} above 1 MW/cm^2 (for the ternary As–Se–S films under study) and above 3 MW/cm^2 (for As_2Se_3) new intense narrow peaks near 268, 369, and 560 cm^{-1} rapidly emerge in the spectra. Peaks at such frequencies are known for arsenolite (crystalline As_2O_3).

The photoassisted formation of As_2O_3 on the amorphous arsenic chalcogenide film surface can be explained by the local sample overheating under irradiation followed by partial thermal decomposition of the film material, interaction of As atoms with oxygen from air and vapour growth of As_2O_3 crystallites. Narrower-gap amorphous As_2Se_3 and As_2Se_3-rich ternary As–Se–S films possess higher absorption in the green spectral range which enables the partial thermal decomposition and the formation of As_2O_3. For the broader-gap As_2S_3 the absorption coefficient for the visible light is lower, and the surface photooxidation can be achieved only under intense UV laser irradiation.

[1]. Azhniuk Y., Solonenko D., Loya V., Grytsyshche I., Lopushansky V., Gomonnai A.V., Zahn D.R.T. *Appl. Surf. Sci*. 2019. V. 467–468. P. 119–123.

Raman Study of Thin $TlInS_2$ Films Prepared by Thermal Evaporation

Azhniuk Y.M.[1], Gomonnai A.V.[1,2], Lopushansky V.V.[1], Gomonnai O.O.[2],
Babuka T.[2], Loya V.Y.[1], Voynarovych I.M.[1]

[1] *Institute of Electron Physics, Nat. Acad. Sci. Ukr., Uzhhorod, Ukraine,*
yu.azhniuk@gmail.com
[2] *Uzhhorod National University. Uzhhorod, Ukraine*

Crystalline $TlInS_2$ is a known semiconductor material possessing highly anisotropic layered structure and promising for applications in optoelectronics. The recent years demonstrate a growing research interest to $TlInS_2$ thin films. Here we report on thermally evaporated thin $TlInS_2$ films studied by Raman spectroscopy.

$TlInS_2$ films (thickness d from 10 to 200 nm) were prepared by thermal evaporation on silicon and silicate glass substrates. Raman scattering measurements were carried out at room temperature using an XPloRa Plus spectrometer (Horiba) with a 532 nm solid-state laser and a cooled CCD camera. The instrumental resolution was better than 2.5 cm^{-1}.

Features in the Raman spectra of the films measured at a low excitation power density P_{exc}=4 kW/cm^2 are noticeably broader than for the corresponding single crystal [1] which is an evidence of the amorphous structure of the films. The most intense Raman maximum is observed near 280 cm^{-1}, basically corresponding to the known intense doublet of crystalline $TlInS_2$ [1].

However, with P_{exc} increasing to 40 kW/cm^2 the Raman spectra of the $TlInS_2$ films reveal intense narrow maxima typical for the crystalline $TlInS_2$. The unresolved broader maximum near 280 cm^{-1} splits up and an additional narrow peak near 138 cm^{-1} emerges. This clearly indicates fast crystallization of the film material in the laser spot which most likely results from local heating of the sample by a tightly focused laser beam. For the thinner films (10 and 30 nm) the traces of the "amorphous-like" Raman features are also retained in the spectra, showing that in this case the crystallization effect in the film is partial, which can be explained by a faster heat dissipation for the thinner films due to a lower thermal conductivity of $TlInS_2$ compared to that of the substrate. The partially retained amorphous features in the thin films are observed for the d=10 nm and d=30 nm samples on the silicon substrate and solely for d=10 nm samples on the silicate glass substrate due to the higher thermal conductivity of silicon providing better heat dissipation.

[1]. Gomonnai A.V., Petryshynets I., Azhniuk Yu.M., Gomonnai O.O., Roman I.Yu., Turok I.I., Solomon A.M., Rosul R.R., Zahn D.R.T. Growth and characterisation of sulphur-rich $TlIn(S_{1-x}Se_x)_2$ single crystals. *J. Crystal Growth*. 2013. V. 367. P. 35–41.

Scattering of Charge Carriers in Thin Films PbTe:Bi

Dzumedzey R.O., Boryk V.V., Varvaruk V.M., Oleksyn O.Ya., Sereda I.L.

Vasyl Stefanyk Precarpathian National University, Ivano-Frankivsk, Ukraine

The thin films were obtained by evaporation in an open vacuum of a pre-synthesized compound PbTe:Bi with 1 at.% bismuth. As substrates, we used sital plates, which were subjected to preliminary chemical purification. Evaporation temperature was T_E = 970 K, deposition temperature – T_D = 470 K, and the deposition time was from 3 s to τ = 120 s.

For the calculations of the mobility of carriers in the bulk material, we used a variation method in which, as a rule, a test function is selected in the form of a series of degrees of energy, the coefficients of which are variation parameters and determined by the condition of the best matching of theoretical and experimental results.

For the calculations of the mobility of carriers in the films, then we need to consider additional mechanisms that determine the charge carriers scattering. In particular, this is the influence of the surface and grain boundaries.

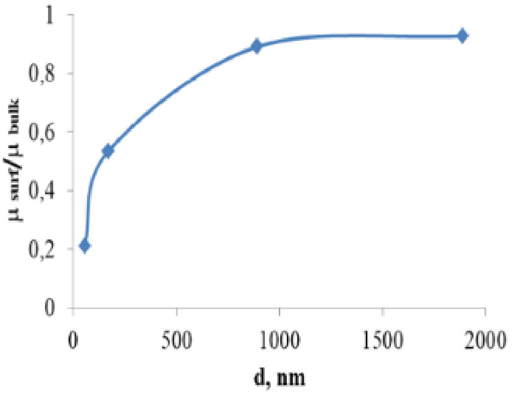

Fig. 1. Ratio of μ_{surf}/μ_{bulk} to the thickness of the samples.

Ratio μ_{surf}/μ_{bulk} from the samples thickness is presented in Fig. 1. The proximity of the ratio μ_{surf}/μ_{bulk} to unity indicates that the total mobility of these scattering mechanisms, which is obtained taking into account the Mattisen rule, is determined mainly by the scattering mechanisms inherent in bulk materials. From Fig. 1 it is noticeable that the contribution of surface scattering disappears in the thin films with thicknesses from 1000 nm and above.

Stripping Voltammetry of Nanoscale Films of Alloys of the Zn-Ni-Cu System

Maizelis A.

National Technical University "Kharkiv Polytechnic Institute", Kharkiv, Ukraine,
a.maizelis@gmail.com

Coatings with double and ternary alloys of the Zn-Ni-Cu system are used as independent coatings, as an underlayer and as base for materials with a highly developed surface. They demonstrate different functional properties depending on the chemical and phase composition of an alloy defining the scope of application. The accuracy of determining the phase composition decreases with decreasing coating thickness, but for each of the methods in its own range of thickness values. The anodic stripping voltammetry (ALSV) method is quite effective in the film thickness range of 10-2000 nm, allowing the identification of oxidation peaks of both phases present in small quantities in the alloy film and X-ray amorphous phases.

The purpose of the study is to evaluate the chemical and phase composition of nanoscale films of binary and ternary alloys of the Zn-Ni-Cu system using anodic stripping voltammetry.

Films of the Zn-Ni-Cu alloy, as well as metals and binary alloys of this system, 10–100 nm thick, and coatings up to 10 μm thick were studied. They were deposited by electrochemical deposition in galvanostatic and potentiostatic modes onto a platinum substrate from weakly alkaline ammonium glycinate polyligand electrolytes having a composition of metal ions corresponding to the deposited films and the same concentration of ligands. The phase and chemical composition of thin films was analyzed by ALSV in a sodium sulfate (SS) solution and in an alkaline ammonia-glycinate (AG) solution. The SS solution was previously used for ALSV of Cu-Zn alloy films, and AG solution was previously used for ALSV of Zn-Ni and Cu-Ni alloys. Therefore, both solutions were used to identify the peaks in the dissolution voltammograms of the ternary alloy films. The phase composition of thick coatings was analyzed by XRD, and their chemical composition was determined by XRF analysis.

The obtained films of both double and ternary alloys are multiphase. The ALSV curves of Cu-Zn alloy films contain oxidation peaks of the γ- and α-phases of the alloy, and with higher polarization, also Zn phase of free; the ALSV curves of Zn-Ni alloy films contain oxidation peaks of the γ- or ε-phases and β-phase of the alloy, and with higher polarization, the α-phase and Ni phase; the ALSV curve of Cu-Ni alloy films contain peaks of dissolution of Ni and solid solutions of Ni in Cu and Cu in Ni. The ALSV curves of the Zn-Ni-Cu alloy revealed oxidation peaks of the α-phase of Cu-Zn, γ- and β-phases of the Zn-Ni, and at high polarization, also solid solutions of Ni in Cu and Cu in Ni.

Structural Properties of Ga-Ge-Te Alloys

Popovych M.V., Stronski A.V., Shportko K.V.

V.Lashkaryov Institute of Semiconductor Physics NAS Ukraine, Kyiv, Ukraine,
niva94@ukr.net

Family of GaGeTe alloys is interesting due to versatile far-IR optics, phase change-type optical memory and sensor applications [1]. The structural features of chalcogenide glasses and films are important for various characteristics and processes, including photoinduced ones. The addition of Ga to GeTe alloys can influence crystallization timings and room temperature stability. Accordingly, better understanding of the structural properties can help in the optimization of the sensitivity and relief formation processes of composite nanomultilayer structures based on chalcogenide glasses, which are promising for the direct recording of optical elements.

In the present report the amorphous Ga-Ge-Te alloys have been studied by X-ray diffraction. Studied bulk Ga-Ge-Te alloys were prepared by the conventional melt quenching technique. Composition was controlled using EDX. X-ray diffraction patterns of samples were recorded with use of the X-ray diffractometer with Bragg–Brentano geometry, using Cu Ka radiation 1.54178 Å and mounted graphite monochromator for a diffracted beam. The diffraction data were collected in the range of scattering vector magnitudes Q between 0.4 and 8 Å, $Q = 4\pi \sin \theta/\lambda$. All samples were examined in transmission geometry. All the X-ray experiments were performed at ambient temperature. The experimental X-ray diffraction patterns were used for calculations of radial distribution functions which have given the positions of the nearest-neighbour bond length r_1 and second-neighbour bond length r_2 (see Table).

Composition	r_1, Å	r_2, Å	Θ, °
$Ga_{7.9}Ge_{11.49}Te_{80.61}$	2.65	4.44	114°
$Ga_{0.1}Ge_{19.14}Te_{80.76}$	2.67	4.31	109°
$Ga_{11.7}Ge_{14.1}Te_{74.2}$ [1]	2.67	4.27	106°

Similar r_1 values were observed for Ga-Ge-Te glasses of other compositions known from reference literature. The values of the r_2 / r_1 ratio are close to 1.63 that is the typical value for a regular tetrahedron structure. The calculated bond angle Θ values are also in good agreement with other published data on GaGeTe alloys. The better understanding of the correlations between structural and macroscopic properties of chalcogenide glasses is needed.

[1]. Popovych M.V., Stronski A.V., Shportko K.V. Structural properties of $Ga_{11.7}Ge_{14.1}Te_{74.2}$ alloys. *Physics and Chemistry of Solid State.* 2022. V. 23, No. 4 pp. 830-835.

Structure and Resistance of Mercury Modified Sb_xSe_{100-x} Amorphous Films

Boryk V.V.[1], Dzumedzey R.O.[1], Durkot M.O.[2], Makar L.I.[2], Pisak R.P.[2],
Pop M.M.[2,3] , Rubish V.M.[2], Solomon A.M.[4]

[1]*Vasyl Stefanyk Precarpathian National University, Ivano-Frankivsk, Ukraine*
[2]*Institute for Information Recording, NAS of Ukraine, Uzhgorod, Ukraine*
[3]*Uzhgorod National University, Uzhgorod, Ukraine*
[4]*Institute of Electron Physics, NAS of Ukraine, Uzhgorod, Ukraine*

In this report the results of investigations of the structure and electrical properties of mercury modified Sb_xSe_{100-x} amorphous films.

Amorphons Sb_xSe_{100-x} (x=0,3,5,7 and 9) films with a thickness 1000 nm were obtained by vacuum evaporation of Sb_xSe_{100-x} glasses from guasi-closed effusion cells. Tne films modification was carried out in special hermetic boxes by keeping them in mercure vapor for 0-120 hours.

The structure of mercury modified films was studied by the X-ray diffractometry and Raman spectroscopy methods. Exposure of films in mercury vapor leads to the formation in the amorphous matrix HgSe crystalline inclusions in the cubic modification, which accompanied by the appearance on the diffractograms of weakly expressed reflexes. As the exposure time increases,the reflexes become pronounced, and their position agrees well with the position of intense reflexes on the diffractograms of crystalline mercury selenide obtained by the hydrochemical method.

Using the samples "graphite probe - Sb_xSe_{100-x} film-graphite probe", the influence of mercury vapor on the electrical resistance (R) of amorphous films of the antimony-selenium system was investigated. It was established that exposure of samples in mercury vapor leads to a decrease in their electrical resistance by 4-7 orders of magnitude. As the temperature increase, the transition time from a high-resistance state to a low-resistance state decreases. When introducing antimony into amorphous selenium and increasing their concentration in the composition of the films, the transition time increases, and the value of the change in resistance decreases. It was established that the change in R is mainly determined by the change in surface conductivity of Sb_xSe_{100-x} films. A decrease in the electrical resistanse of these amorphous films modified with Hg is caused by the formation of mercury crystalline inclusions in their matrix.

The obtained results show the possibility of using amorphous films of antimony-selensum system as sensitive elements of the electric sensors for detecting the mercury vapor.

Study of Structure and Phase Transition in Vanadium Oxide Thin Films by Raman Spectroscopy

Dzhagan V.M., Isaieva O.F., Yukhymchuk V.O., Stadnik O.A., Gule E.G.,
Maksimenko Z.V., Lytvyn P.M., Dubikovskyi O.V., Melnik V.P.,
Romanyuk B.M., Valakh M.Ya.

V. Lashkaryov Institute of Semiconductors Physics, NAS of Ukraine, 03028 Kyiv, Ukraine,
dzhagan@isp.kiev.ua

A reversible semiconductor-metal structural transition (SMT) in crystalline vanadium dioxide VO_2 around 68 °C stimulates numerous studies of this material for improving the parameters of SMT transition. The SMT is connected with a sharp change in electrical resistance (by 4-6 orders of magnitude) and optical transmission in the infrared region, where the relatively high transparency of VO_2 films in the semiconductor state is sharply reduced due to the high reflection coefficient of VO_2 films in the metallic state. Owning to this, VO_2 thin films are very promising fast thermochromic switching in smart windows, thermal sensors, and various other applications.

For practical use, it is desirable to reduce the temperature of the phase transition without affecting other important parameters of the VO_2 film. One of the problems with obtaining the film with desired characteristics is the multivalence of vanadium, which can lead to the formation and coexistence of several other oxides, depending strongly on the technological conditions, such as V_6O_{13}, V_3O_7, V_4O_9, and V_2O_5. The physical mechanism of the SMT remains debatable, and the efect of minor inclusions of other oxides on the SMT transition of the VO_2 phase needs to be studied in more detail. Raman spectroscopy is one of the most frequently used experimental techniques for the investigation of vanadium oxides in general and SMT in VO_2 in particular. However, certain ambiguities in the attribution of Raman bands to different oxides still exists.

In this work, we used magnetron deposition for obtaining thin films of vanadium oxide on silicon or quartz substrates [1,2], with varying the film thickness, from 100 to 200 nm, discharge current in argon plasma, from 0.05 to 0.09 A, temperature of the substrate during grows, 200 to 230 ˚C, as well as temperature and duration of post-growth annealing in inert atmosphere (250 to 450 ˚C and 10 to 30 minutes, respectively). In order to resolve the mentioned ambiguities in the assignment of the Raman peaks to different oxides, a series of reference film samples was obtained by annealing in air.

The work was supported by project No. 4.4/23-P of the program "Support for the development of priority areas of scientific research" for 2023-2024.

[1]. Goltvyanskyi Yu., Khatsevy I., Kuchuk A., Kladko V., Melnik V. et. al. *Thin Solid Films*, 2014, 564, 179-185

[2]. Kladko V.P., Melnik V.P., Liubchenko O., Romanyuk B. et. al. *Semicond. Physics, Quant. Electr. & Optoelectron*. 2021, v.24, N4, 362-371.

Synthesis and Study of Properties of Emulsion Polishes based on Beeswax and Carnauba Wax

Kurta S.A., Aliyeva A.E.

Department of Chemistry, Faculty of Natural Sciences Faculty of Natural Sciences , Vasyl Stefanyk Precarpathian University, Ivano-Frankivsk, Ukraine, sergiykurta@pnu.edu.ua

This work was performed to synthesize and study the properties of water-oil emulsions and polishes based on them. During the work, a number of automotive furniture emulsions ─ polishes based on wax, paraffin and various solvents ─ white alcohol, turpentine, kerosene and solvents №№ 646, 647 were synthesized and their properties were investigated. It is shown that the most successful substances for polishing metal, leather and wood surfaces are polishes based on natural beeswax and carnauba waxes, as well as paraffin and solvents-turpentine gum, white alcohol and kerosene, and or aqueous emulsions based on them, which is confirmed by for measuring the gloss of polished surfaces on a universal glossometer-glossometer WALCOM GM-26

The Department of Chemistry conducted experimental studies to study the ways of obtaining aquatic polymer emulsions and polishes based on the method of microcapsulation. We investigated the physico-chemical properties of aquatic and organic polymer emulsions of bee and Carnauba waxes and ways of preparation of polishes based on them. The shine of surfaces polish polished was experimentally determined, using a new Walcom GM -26 glitter - a new device. As a result, we got the result that the shine of the surface increases with the increase in the content of the polishing base on bee and carnauba waxes in polishes, for different surfaces from 5% to 14%.

In addition, we investigated the polishing speed and polishing time to get the best surface shine and found that on solid surfaces. Namely, on the metals and on the lacquer-colored coatings, the polishing time increases with the increasing content of the polishing base. At the same time, polishing is reduced on porous surfaces (leather, tree) with increasing polishing content. Using a modern glitter -Glosseter Walcom GM -26 - we have succeededTo accurately investigate the shine of surfaces of different properties - paint, metal and glass surfaces - polishes, and polish made on the basis of bee and Carnauba wax.

[1]. ДСТУ 4229:2003 Віск бджолиний пасічний. Технічні умови. *http://online.budstandart.com/ua/catalog/doc-page.html?id_doc=91468*

[2]. https://en.wikipedia.org/wiki/Glossmeter . Блискомір (Glossometer)

[3]. Оригінальний захисний карнаубський віск-паста Gliptone Original Carnauba Paste Wax GT0110 *https://drossel.ua/ua/content/23002-gliptone-original-carnauba-paste-wax-gt0110-vosk-pasta*

The Semiconductor-Dielectric Transition in Ge/$Ge_{(x)}Si_{(1-x)}$ Films

Luniov S.V.[1], Shygorin P.P.[2], Venhryn B.Ya.[3]

[1]*Lutsk National Technical University, Lutsk, Ukraine,*
luniovser@ukr.net
[2]*Lesya Ukrainka Volyn National University, Lutsk, Ukraine,*
shygorin.pavlo@vnu.edu.ua
[3]*Lviv Polytechnic National University, Lviv, Ukraine,*
bohdan.y.venhryn@lpnu.ua

The phenomena of electron transfer in nanostructures are largely determined by dimensional quantization effects, which are not manifested in bulk materials. Semiconductor heterostructures have practical uses in nano- and optoelectronics. Monocrystalline germanium allows obtaining heterostructures of the various compositions and thicknesses on the substrates of Si or $Ge_{(x)}Si_{(1-x)}$ solid solution. The lattice constants of heteropairs can differ quite significantly, which causes for the appearance of significant internal deformation fields. This makes it possible to grow thin films of germanium on the surface of substrates, which are used in constructing the lasers on the quantum wells, electro-optical modulators, MOSFET transistors. The electrical conductivity of such germanium films will be determined by the available quantum-dimensional effects and the deforming reconstruction of their band structure due to internal mechanical strains.

In paper [1], was established that quantum-size effects are effectively manifested in Ge/$Ge_{(x)}Si_{(1-x)}$ thin films with the thickness of $d<7$ nm. In this work, we investigated dependencies of the electron concentration in a germanium nanofilm on its thickness for different content of germanium in the $Ge_{(x)}Si_{(1-x)}$ substrate and doping impurity concentrations with the aim of more detailed studying the influence of internal strains and the degree of doping by the donor impurities on the effects of dimensional quantization in such films. Performed calculations show that semiconductor-dielectric transition for the undoped germanium nanofilms with the thickness of $d<7$ nm and the germanium content in the $Ge_{(x)}Si_{(1-x)}$ substrate of less than 80% with decreasing their thickness at room temperature is observed. An increasing of the concentration of the doping impurity to 10^{13} cm^{-3} leads to the opposite effect the dielectric-semiconductor transition for this films.

Discussed effects will largely determine the electrical properties of considered thin films of germanium and should be taken into account for designing various elements of nano- and optoelectronics based on them.

[1]. Electrical properties of strained germanium nanofilm / S. V. Luniov, P. F. Nazarchuk, O. V. Burban. *Physics and Chemistry of Solid State.* 2021. V. 22(2). P. 313–320.

Session 4

Thin film compounds for electronic devices or nanoelectronics

Deep Levels in Spin-Coated MoS_2 Films

Kondratenko S.V.[1], Datsenko O.I.[1], Kovanzhi P.O.[1], Mykytiuk A.A.[1], Dzhagan V.M.[1,2], Zahn D.R.T.[3]

[1]*Taras Shevchenko National University of Kyiv, 64 Volodymyrs'ka St. 01601, Kyiv, Ukraine,* kondratenko@knu.ua

[2]*V. E. Lashkaryov Institute of Semiconductors Physics, NAS of Ukraine, 41 pr. Nauki, 03028, Kyiv, Ukraine*

[3]*Semiconductor Physics and Research Center for Materials, Architectures and Integration of Nanomembranes (MAIN), Chemnitz University of Technology, D-09107 Chemnitz, Germany*

Two-dimensional transition metal dichalcogenides, particularly MoS_2, are extensively studied due to their exceptional electronic, optical, and transport properties [1-3]. In this work, we use deep-level transient spectroscopy (DLTS) to characterize the electronic structures of deep traps inside the bandgap of MoS_2 prepared as thin films. A heterojunction was formed by spin-coating of solution-exfoliated MoS_2 flakes onto a boron-doped silicon substrate (p-Si) and confirmed by the I–V and C–V measurements. Raman spectra of the studied structures were measured using a Renishaw-1000 system with a micro-scale spatial resolution to characterize the vibrational properties and the uniformity of the thin films. The MoS_2/p-Si junction showed good rectifying I-V characteristics caused by a potential barrier with a height of 0.37 eV.

Electrically active deep levels in the MoS_2/p-Si diodes were probed using a digital DLTS spectrometer FT-1030 with 1 MHz and 100 mV test signals and a Boonton 72B C-meter. The DLTS spectra were obtained by Fourier transform of the capacitance transients recorded as a function of temperature in the range of 80 – 350 K. The DLTS spectra reveal the presence of electron traps below the conduction band of MoS_2 with thermal activation energies of 0.303, 0.440, and 0.633 eV. The defect levels found at 0.303 eV and 0.440 eV below the conduction band minimum are supposed to be related to sulfur vacancies.

This work was supported by the National Research Foundation of Ukraine [2020.02/0134].

[1]. K. Bazaka, I. Levchenko, J.W.M. Lim, O. Baranov, C. Corbella, S. Xu, and M. Keidar, "MoS_2-based nanostructures: synthesis and applications in medicine," J Phys D Appl Phys, 52, N18, pp. 183001 (2019).

[2]. X. Zhang, Z. Lai, C. Tan, and H. Zhang, "Solution-Processed Two-Dimensional MoS_2 Nanosheets: Preparation, Hybridization, and Applications," Angewandte Chemie International Edition, 55, N31, pp. 8816-8838 (2016).

Discoverer of Cold Emission in Island Metal Films (Ukrainian Physicist Petro Borziak. 120th Anniversary)

Kozyrski W.[1], Polevetska O.[2], Schenderovskyj V.[3]

[1]N. Bogolubov Inst. for Theoretical Physics, Ukrainian National Academy of Sciences,
[2]Institute of Physics, Ukrainian National Academy of Sciences
[3]Inst. of Physics, Ukrainian National Academy of Sciences, Leading staff member, Kyiv, Ukraine

The purpose of this investigation is to highlight the scientific activity of Petro Borziak, an expressive representative of Ukrainian intellectual elite whose life was devoted to science, as well as to present memories of a man who left a essential mark in the formation of physical research, put his talent to the development of the first physics institute in Ukraine, and who within his scientific work made the first discovery in Ukraine (Soviet period) [1].

Petro Borziak was born on September 16, 1903 in a Cossack family in Pyshchyky village, Poltava province, now Cherkasy region

In 1925, Petro Borziak became a student of Physics Department at the Institute of Public Education, and after its transformation in 1929 into the Institute of Physics of the Academy of Sciences, he was admitted to the postgraduate course of the Institute.

Petro Borziak's scientific research covers a wide range of problems in vacuum semiconductor and thin-film electronics. He combined deep fundamental works with practical application of scientific ideas and developed completely new principles of creating effective photocathodes. In 1939, the young scientist defended his candidate's thesis, and in 1953 - his doctoral thesis.

In 1961, he was elected a Corresponding Member of the Academy of Sciences of the Ukrainian SSR. Since the same year, he headed the physical electronics department at the Institute of Physics for about 30 years.

In 1965, he and his colleagues Oleh Sarbey and Rostyslav Fedorovych discovered cold electron emission from island films. The work was the first in Ukraine officially registered as a discovery by the State Committee for Inventions and Discoveries of the USSR. Petro Borziak is the author of three monographs. The scientist left behind a large scientific school. In 1986, he became a laureate of the State Prize of Ukraine [2].

Petro Borziak, an outstanding scientist in the field of physical electronics, was a man of high morality, exceptional modesty, and a great patriot of Ukraine.

[1]. Institute of Physics/ Compiled by M. T. Shpak, V. I. Melnyk. Kyiv: Naukova dumka. 1979 118 p.

[2]. KozyrskI W., Len A., Schenderovskyj V. Prolegomenae of Ukrainian physics, or why the Institute of Physics did not turn 80 years old? // Physics (Kyiv). 1999 No. 13 (25).

Effect of MXene Interfacial Layer on the Field-Effect Mobility of a Bottom-Gate Indacenodithiophene–Benzothiadiazole Copolymer Field-Effect Transistor

Urbančič J., Bratina G., Pavlica E.

Laboratory of Organic Matter Physics, University of Nova Gorica, Vipavska 13,
Nova Gorica, 5000, Slovenia
jurij.urbancic@ung.si

Indacenodithiophene-co-benzothiadiazole (IDT-BT) semiconducting polymer exhibits high charge carrier mobility in top-gate organic field-effect transistors (OFETs). In contrast, bottom-gate architecture suffers from a high bias-stressing effect, which conceals its full potential. To better understand the source of bias-stressing, we have introduced an interfacial layer between IDT-BT and dielectric of bottom-gate transistor. The interfacial layer consisted of $Ti_3C_2T_x$ (X is O or OH group termination) MXene flakes deposited on the SiO_2 dielectric of a bottom-gate OFET. Next, an IDT-BT layer was spin-coated on top of MXene layer. The coverage of MXene flakes was 18% and 28%, below the percolation threshold, consequently a non-connected network of MXene flakes was formed at the gate-dielectric/IDT-BT interface. What was found out is that the presence of MXenes has a beneficial effect, boosting the field-effect mobility of more than 100% (shown in Figure 1), reducing the bias-stressing induced hysteresis and also increasing of the current on/off ratio from ~10^4 to ~10^5.

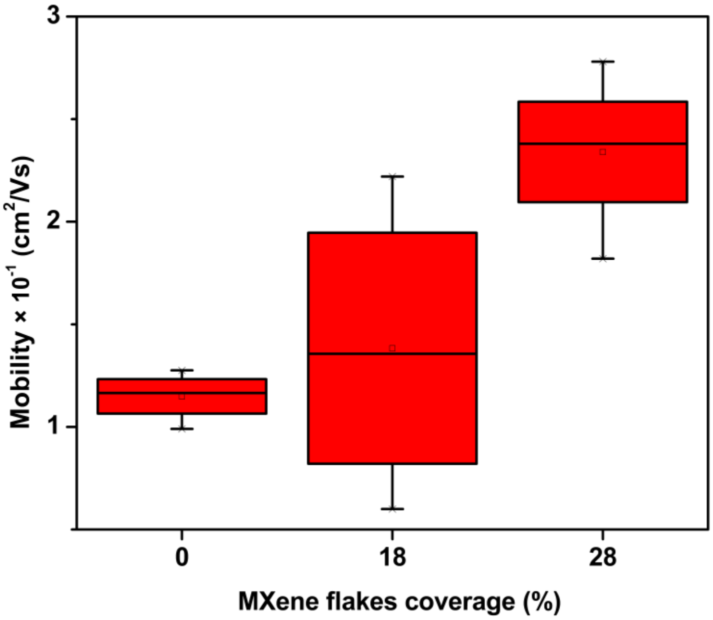

Figure 1. Field-effect mobility of IDT-BT transistors as a function of MXene coverage

Measurement of Blood Oxygen Content and Heart Rate Using the MAX30100 Sensor

Nykyrui R.I., Goyanyuk I.V.

A separate structural unit Kolomyia Polytechnic Vocational College Lviv Polytechnic National University, Kolomyia, Ukraine.

The main task of the device is to read data by direct contact of the phalanx of the finger with the surface of the device and display this information on the screen for monitoring readings in real time.

The MAX30100 sensor allows you to measure the level of blood oxygen saturation (blood oxygen saturation, SpO2) and pulse (heart rate) and transfer this information to the microcontroller via the I2C interface [1].

Light transmission through finger blood is used to detect the amount of oxygen by measuring changes in light absorption in both oxygenated and defatted blood. The graph in Fig.1 shows the difference between HbO2, which is oxygenated hemoglobin, and Hb, which is deoxygenated hemoglobin, at two different wavelengths.

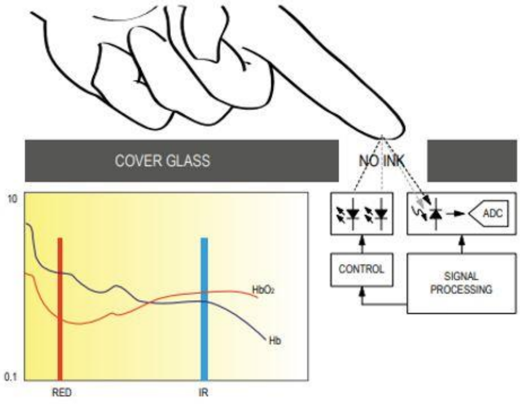

Fig. 1 Block diagram of the MAX30100 system [2]

The ratio of the absorbed wavelengths of IR and red light received by the photodetector gives us the concentration of oxygen in the blood.

Only an IR LED is needed to measure heart rate. This is because oxygenated hemoglobin absorbs more infrared light.

It can be noted that the MAX 30100 model can be used to solve the problems of the patient health monitoring system.

[1]. Web sourse: https://github.com/oxullo/Arduino-MAX30100.

[2]. Web sourse: https://www.alldatasheet.com/datasheet-pdf/pdf/879178/MAXIM/MAX30100.html.

Plasmon-Polariton Photodetectors for Optical Smoke Detectors: Influence of Humidity on Resonance Properties

Mamykin S.V., Indutnyi I.Z., Myn'ko V.I., Romanyuk V.R., Mamontova I.B.,
Redko R.A., Dusheyko M.G., Lyashchuk Yu.M., Savchuk Ye.M.,
Tochkovyi V.O., Shtykalo O.V., Kuznetsova D.A.

V. E. Lashkaryov Institute of Semiconductor Physics, NASU, Kyiv, Ukraine,
mamykin@isp.kiev.ua

Fire alarm systems typically include various types of sensors, which are associated with a wide variety of fire types. Among the sensors are temperature sensors, video cameras, chemical sensors for combustion products, and one of the most important - photoelectric smoke sensors. These sensors have a drawback related to false alarms triggered by aerosol or dust particles unrelated to the occurrence of a fire. Various approaches are applied to address this issue, including additional chemical sensors, the use of multiple wavelengths, angles.

A new type of distinction between fire products and dust particles has recently emerged [1]. Its principle of operation involves exciting the surface plasmon-polariton resonance (SPPR) in a gold film, which is a component of the Plasmon-Polariton Photodetector (PPPD). Gold film contacts with combustion products (CO, CO_2, or smoke particles with sizes ranging from 0.1 to 10 μm), leading to angular or spectral shifts of the SPPR, which are registered by changes in the intensity of the associated photocurrent of the PPPD. This method is insensitive to common dust due to the large particle sizes of it which weakly adheres to the surface of gold film. Therefore they have a weak effect on SPPR. This results in a lower probability of false alarms in dusty environments.

At the same time, increased humidity can lead to the formation of a water film (dew) on the surface of the PPPD, which can shift the resonance and lead to false detector responses. This work investigates the impact of humidity on the resonance properties of PPPD and methods that can prevent the formation of a water film. In particular, maintaining the surface temperature of the PPPD above the dew point is carried out with the help of an electronic connection circuit. This electronic circuit allows one to control and regulate the PPPD temperature and measure its photocurrent. The study also explores the influence of temperature on the resonance, electro-physical, and photoelectric properties of the PPPD.

Authors acknowledges the support from the NRFU grant 2022.01/0126 "Development and implementation of a dust-insensitive smoke detector based on a plasmon-polariton photodetector".

[1]. Shtykalo O.V., Semikina T.V., Mamykin S.V. Smoke Detector Based on a Plasmon-Polariton Photodetector. *Proceedings of the Conference on Semiconductor Physics "Lashkaryov's Readings,"* April 5-7, 2021, Kyiv, Ukraine. P. 31-32. ISBN 978-966-02-9603-9.

Reflection of Macroporous Silicon with Through Pores

Onyshchenko V.F.

V. Lashkaryov Institute of Semiconductor Physics NAS of Ukraine, Kyiv, Ukraine,
onyshchenkovf@isp.kiev.ua

The reflectance spectra of macroporous silicon and nanowires indicate a decrease in reflectance as the volume fraction of pores increases [1]. The reflection of macroporous silicon with through pores is calculated according to the derived formulas. The formulas for calculating the reflection of macroporous silicon with through pores take into account multiple reflections from the inside of the frontal and back surfaces. Macroporous silicon is considered as an effective medium whose surfaces scatter light. Light scattering is taken into account using the effective scattering angle. The reflection of the frontal and back surfaces of macroporous silicon depends on the volume fraction of pores and affects the optical properties of macroporous silicon with through pores.

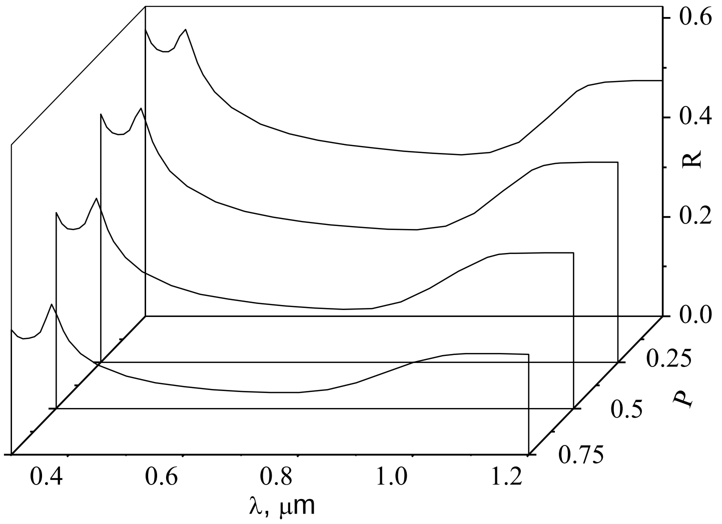

Fig. The reflectance spectrum of macroporous silicon with through-pores with a volume fraction of pores: 0; 0.25; 0.5; 0.75.

The figure shows the reflection spectrum of macroporous silicon with through-pores with different volume fraction of pores. The reflection of the macroporous silicon structure with through-pores decreases with the growth of the volume fraction of the pores, due to the decrease in the difference between the refractive indices of the effective medium and air. The reflection of light with lengths from 0.9 μm to 1.3 μm from macroporous silicon with through-pores is further reduced, due to the decrease in back surface reflection with increasing pore volume fraction.

[1]. Onyshchenko V.F. Reflection of macroporous silicon, nanowires, and a two-layer structure of silicon with an effective medium. *J. Nano- Electron. Phys*. 2023. Vol 15, N 3. P 03026–7.

Solid Electrolyte Membranes Based on Intramolecular Polycomplexes

Kunitskaya L.R., Zheltonozhskaya T.B., Nesin S.D., Klepko V.V.

Institute of Macromolecular Chemistry NAS of Ukraine, Kyiv, Ukraine
larisa_kunitskaya@ukr.net

A solid polymer electrolytes (SPEs) with high ionic conductivity at room temperature has been an importance subject due to their interest in the all solid-state electrochemical devices development. The solid solvent-free polymer electrolytes based on amorphous polymer materials could be the best for these purposes. Nowadays, the mainstream polymer matrix of the SPEs remains poly(ethylene oxide) (PEO) and its derivatives due to good chain flexibility, superior electrochemical stability to lithium metal, low glass transition temperature, and excellent solubility to conductive lithium salts.

However, the high crystallinity of PEO leads to low ion conductivity and inferior Li+ transference numbers (0.2–0.3) at room temperature, which affects the high rate capability of LBs.

In the present work, we investigated diblock- (DBC) and triblock (TBC) copolymers comprising chemically complementary poly(ethylene oxide)/polyacrylamide which form intramolecular polycomplexes (IntraPCs) and due to this allow to reduce PEO crystallization. We also examined DSCs and TBCs partially hydrolyzed derivatives as possible ion-conducting membranes.

Measurement of dielectric characteristics of the studied systems was performed in the frequency range 102-105 Hz using a dielectric spectroscope developed on the basis of the AC bridge P5083 and a three-electrode cell.

It is noticed that ionic conductivity of TBC membranes depends on PEO-block length. Thus, the increase in Mn of PEO-blocks from 6·104 to 3.5·104 kDa led to an increase in ionic conductivity of TBC membranes from 6,2·10-11 to 3,2·10-9 S·cm-1 respectively. The introduction of additional ionic groups -COOH in polyethylene oxide/poly(acrylamide-co-acrylic) acid chains has a positive effect on the conductive characteristics of copolymer membranes for both DBCs and TBCs samples. The ionic conductivity of the investigated membranes filled with LiPF6 increased with increasing salt content. The obtained results made it possible to consider PEO/PAAm block copolymers with interacting blocks as perspective matrices for producing solid electrolyte membranes and their possible application in Li-ion batteries, dye-sensitized solar cells and fuel cells.

Theoretical Modelling of Photoluminescence from Thermally Coupled Levels

Datsenko O.[1], Wang Z.[2], Zhang F.[2], Golovynskyi S.[2],
Wang P.[2], Sun Z.[2], Li B.[2], Wu H.[2]

[1]*Physics Faculty, Taras Shevchenko National University of Kyiv, 01601, Kyiv, Ukraine,*
oleksandr.datsenko@knu.ua
[2]*College of Physics and Optoelectronic Engineering, Shenzhen University, 518060, Shenzhen, P.R. China.*

Temperature (T) dependence of green photoluminescence from thermally coupled levels (TCLs) $^2H_{11/2}$,$^4S_{3/2}$ to $^4I_{15/2}$ of Er^{3+} ions in AlN matrix was studied in terms of using in fluorescence intensity ratio technique of optical thermometry and modelled within a theory based on kinetic equations in a system of three levels (Fig. 1).

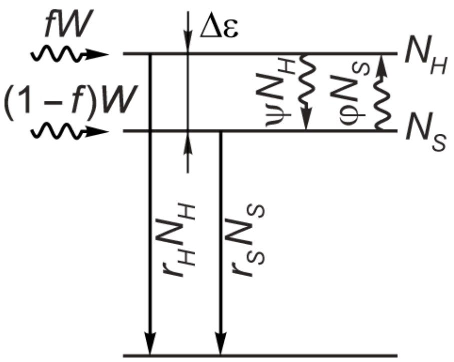

Fig. 1. Transitions and their rates in a system with one ground and two excited levels.

Under below-bandgap of AlN matrics and non-radiative energy transfer of the excitation from the matrix to Er, the concentration dynamics of Er ions on the excited states $^2H_{11/2}$ and $^4S_{3/2}$, respectively, is

$$dN_H/dt = fW - r_H N_H - \psi N_H + \varphi N_s$$

$$dN_S/dt = (1-f)W - r_S N_S - \varphi N_s + \psi N_H,$$

where W is the total rate of excitation of Er^{3+} to both $^4S_{3/2}$ and $^2H_{11/2}$, f is the fraction of the Er^{3+} centers being optically excited onto the level $^2H_{11/2}$, thus fW and $(1-f)W$ are the rates of excitation to the $^2H_{11/2}$ and $^4S_{3/2}$ levels, respectively. Parameters $r_{H,S}$ are the probabilities (reciprocal time constants) of the radiative transitions, ψ and φ are probabilities of the excitation exchange. The effect of temperature on the system manifests through the dependence $\varphi(T) = \varphi_\infty \cdot \exp(-\Delta\varepsilon/kT)$, where Δε is the energy distance between the TCLs and φ_∞ is the value for $T \to \infty$.

In the stationary mode, when $dN_H/dt = dN_S/dt = 0$, the luminescence intensity from the level $^4S_{3/2}$ reveals a usual dependence on temperature, following Mott formula, while that from $^2H_{11/2}$ is predicted to rise with T:

$$I_S = r_S N_S = \frac{r_S}{r_H} \cdot \frac{\psi + r_H[1-f]}{\varphi(T) + r_S[1+\psi/r_H]} W, \quad I_H = r_H N_H = \frac{\varphi(T) + f r_S}{\varphi(T) + r_S[1+\psi/r_H]} W,$$

which was observed in the experiment. The fluorescence intensity ratio (FIR) is

$$FIR = \frac{I_H}{I_S} = \frac{\varphi/r_S + f}{\psi/r_H + 1 - f} = A_0 + A_1 \cdot \exp(-\Delta\varepsilon/k_B T),$$

being reduced to common Boltzmann distribution ($A_0 = 0$) only at $f = 0$, i.e., excitation transfer only to the lower TCL. The value Δε = 76 meV was obtained within the simulation, which is close to that estimated from the spectrum.

Session 5

Functional crystalline materials: growth, physical properties and applications

A Method of Reducing Short-Circuit Currents for Integrated Microsystems

Benko T.G., Kogut I.T., Holota V.I., Gryga V.M.

Vasyl Stefanyk Precarpathian University, Ivano-Frankivsk, Ukraine,
taras.benko@pnu.edu.ua

The current state of development of digital IC is characterized by a constant increase in the degree of integration of elements, as well as the combination of elements in functional blocks and even in whole systems. Increasing the integration of elements and, therefore, reducing their size allows the use of higher clock frequencies. However, the increase in the clock frequency is limited by the permissible power consumption.

In CMOS-inverters, the main part of the power is spent on charging the parasitic capacitance of the gates of the transistors and the load capacitance. Associated with this portion of energy is dynamic power consumption, which consists of two components: transient power consumption and capacitive load. When the logic states of the inverter change in a short period of time, when the PMOS and NMOS transistors are switched simultaneously, a short - circuit current flows. Power losses from short-circuit current are only a small part of the dynamic power consumption.

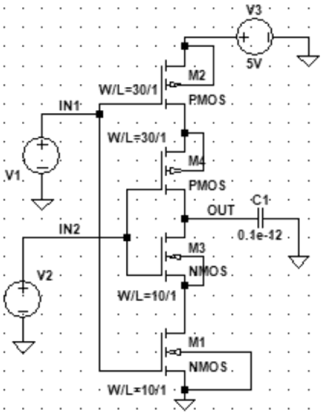

Fig. 1 - Inverter with two clock signals.

During transitions of the logic level, transistors M1, M2 work in the saturation region, while channel resistances and voltage V_{gs} decrease. Accordingly, the voltages Vds of transistors M3, M4 decrease below the voltages V_g, and the transistors begin to function in the deep triode region (line region) as voltage-regulated resistors. The regulating voltage is the voltage of the additional clock signal, which is applied to the gates of transistors M3, M4. Using special forms of the additional clock signal, it is possible to change the voltage V_g, and therefore the resistance of the transistors on the leading and falling edges of the input signal when the short-circuit current flows in the inverter. Thus, the use of transistors M3, M4 as resistors with voltage regulation can limit the short-circuit current and, therefore, reduce the short-circuit power loss.

Atomic-Ordering Kinetics in Layered Fe–Pt Structures

Tatarenko V.A., Radchenko T.M., Koval Yu.M.

G.V. Kurdyumov Institute for Metal Physics of the N.A.S. of Ukraine, Kyiv, Ukraine,
tatar@imp.kiev.ua, tarad@imp.kiev.ua

The challenges dealing with magnetic materials for improving their functionality and fabrication of permanent magnets are well known in recent years. Currently, the basic elements of such strategic products are rare-earth metals (REM), the reserves of which are either restricted in the civilized world or belong to the countries, which are far from the democratic values and possess a monopoly on the REM extraction. In this respect, the ordered magnetic Fe–Pt-alloy phases of the $L1_0$ and $L1_2$ types are promising and act as an alternative, since they do not contain the rare earth elements. Such structural types are attributable to a large number of alloys. However, such layered ordered Fe–Pt-alloy phases possess magnetic properties promising for practical applications: significant magnetocrystalline anisotropy ($\sim 10^6$ J/m^3), high coercive field strength (up to 30 kOe), a wide range of magnetization-saturation values, satisfactory corrosion resistance, *etc*. However, in contrast to the bulk Fe–Pt alloy, which already has an ordered structure at room temperature, in case of nanoscale Fe–Pt films deposited at room temperature, a disordered $A1$-type Fe–Pt phase is formed in the initial state, and, for instance, the diffusional $A1 \rightarrow L1_0$ phase transformation occurs under additional thermal treatment. We study the atomic long-range order (LRO) parameter (η) jump ($\Delta\eta_{eq}$) for the different f.c.c.-Fe–Pt solid-solution phases under the order–disorder phase transformations ($A1 \rightarrow L1_0$ or $A1 \rightarrow L1_2$) in equilibrium conditions and the time evolution of the LRO parameter ($\eta(t)$) during the f.c.c.-Fe–Pt solid-solution ageing. In our simulation technique, we apply the Khachaturyan's microscopic model within the Onsager-type physical kinetics to estimate the time-dependent LRO parameter ($\eta(t)$). The microscopic energy parameters, namely, 'mixing' energies, which determine the LRO kinetics, consist of both paramagnetic ('electrochemical' + strain-induced) and magnetic contributions. Within the scope of both the Krivoglaz's lattice-statics method and the Khachaturyan–Krivoglaz static concentration-fluctuation waves' approach, the energies of strain-induced and magnetic interactions in substitutional–substitutional atomic pairs as well as the 'electrochemical' interatomic-interaction energies are evaluated semi-empirically for the f.c.c.-Fe–Pt solid solutions taking into account both their atomic-crystalline structure discreteness and elastic anisotropy. The heat absorption (or liberation), as important caloric effect, during the above-mentioned order–disorder phase transformations is also considered.

The study is performed within the project 'New Metal-Containing Materials and Innovation Technologies for Priority Branches of Ukrainian Industry' (State Reg. No. 0123U100898) under the budget program КПКВК 6541230.

Calculation of Dissipation Power from Short-Circuit Currents in Integrated Signal Converters on CMOS Transistors

Ilnytskyi R.V., Pavlyuk M.F.

Vasyl Stefanyk Precarpathian University, Ivano-Frankivsk, Ukraine, r.v.ilnitsky@gmail.com.

The problem of reducing power consumption is especially relevant in microprocessors, high-speed IC, mobile devices and devices with powerful output buffers.

Therefore, in digital circuits, reducing the power consumption of CMOS inverters is an urgent problem. The paper considers various methods, approaches and techniques for reducing the switching energy consumption of CMOS inverters.

When switching the inverter, fig. 1a between states of log. 1 and log. 0, the inverter has a transition region of the transmission characteristic $V_{out}=V_{in}=V_m$, and both CMOS transistors are in the saturation region, fig. 1b.

If the conditions $\beta_n \approx \beta_p$, $V_{thn}=|V_{thp}|$, $(W/L)_p/(W/L)_n = \mu_n/\mu_p$, then the middle of the transition region VM = VDD/2 is taken as the switching threshold. In conditional expressions $\beta_n=\mu_n C_{oxn}(W/L)_n$, $\beta_p = \mu_p C_{oxp}(W/L)_p$ – transistor currents

NMOS та PMOS transistors, W/L – width and length of the transistor channel, μ_n, μ_p – mobility of n-type carriers and p-type semiconductor. The middle of the transition region corresponds to the peak value of the short-circuit current Isc from the power source to the ground, fig. 1c.

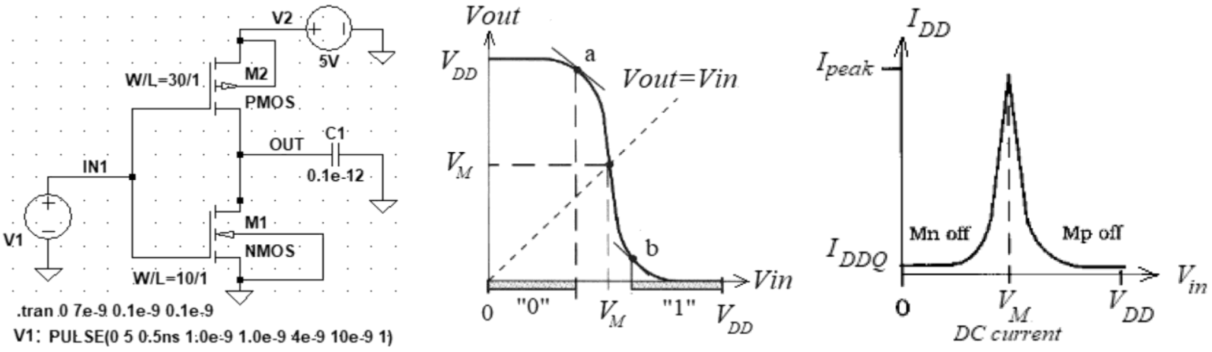

```
.tran 0 7e-9 0.1e-9 0.1e-9
V1: PULSE(0 5 0.5ns 1.0e-9 1.0e-9 4e-9 10e-9 1)
```

a **b** **c**

Fig. 1 Threshold for switching CMOS of the inverter.

To reduce switching energy and power consumption, it is suggested to connect additional PMOS and NMOS transistors with an additional clock signal to the path of the drain current. An additional clock signal will change the state of the additional transistors, and they will function in the triode region as voltage-regulated resistors. It is shown how the timing of additional transistors with signals of different waveforms affects short-circuit currents and power loss.

Conductive Properties of TiO_2 - Ag_2O Composite Materials

Myroniuk, I.F., Mykytyn, I.M., Mandzyuk, V.I.

Vasyl Stefanyk Precarpathian National University, Ivano-Frankivsk, Ukraine,
myrif555@gmail.com, *ihor.mykytyn@pnu.edu.ua*, *volodymyr.mandzyuk@pnu.edu.ua*

The conductive properties of TiO_2 - Ag_2O composite materials obtained by the sol-gel method were investigated using the method of impedance spectroscopy.

Impedance hodographs (Fig. 1) have the form of deformed semicircles, which reflect the processes of electric charge transfer both in the volume of the particle and at the boundary between particles. It is characteristic that an increase in the Ag_2O concentration in the initial TiO_2 is accompanied by a gradual decrease in both the real and the imaginary resistance of the composite, compared to pure oxides. The obtained experimental frequency dependences of total conductivity σ^* on frequency f (Fig. 2) are typical for semiconductors with percolation transport of current carriers (electrons) between localized electronic states. The obtained dependences are characteristic of structurally disordered semiconductor systems at the room temperature. In particular, there is a gradual increase in the value of the specific conductivity in the low-frequency range and a sharp increase in the rate of its growth in the high-frequency part of the spectrum. It is characteristic that for the studied composites, especially in the high frequency range ($f > 10^2$ Hz), a synergistic effect is observed regardless of the Ag_2O concentration, i.e. there is a significant increase in the specific electrical conductivity of the composite compared to the initial oxides.

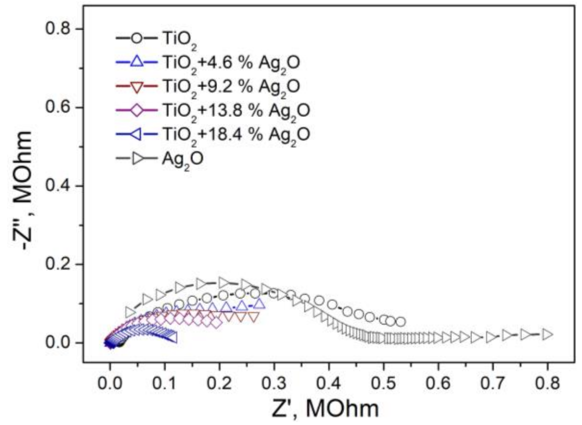

Fig. 1. Impedance spectra.

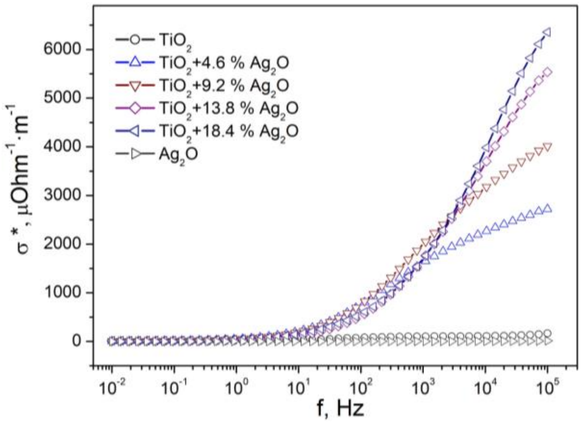

Fig. 2. Dependences $\sigma^*(f)$.

The approximation of the dependences $\sigma^*(f)$ on the basis of Jonscher equation made it possible to determine the constant component σ_{dc} of the specific conductivity of the studied materials. As follows from the calculations, the value of σ_{dc} is 3.23 $\mu Ohm^{-1} \cdot m^{-1}$ for TiO_2, 1.43 $\mu Ohm^{-1} \cdot m^{-1}$ for Ag_2O, and increases from 6.08 to 15.1 $\mu Ohm^{-1} \cdot m^{-1}$ when the Ag_2O content increases from 4.6 to 18.4 %.

Determination of Thermodynamic Properties of Manganese-Bismuth Tellurides Using EMF Method

Orujlu E.N.[1], Babanly M.B.[2]

[1]*Azerbaijan State Oil and Industry University, Baku, Azerbaijan, elnur.oruclu@yahoo.com*
[2]*Institute of Catalysis and Inorganic Chemistry, Baku, Azerbaijan, babanlymb@gmail.com*

Naturally occurring magnetic layers containing tetradymite-type layered phases in the MnTe-Bi_2Te_3 pseudo-binary system are stable compounds and provide an ideal platform to investigate many exotic topological phenomena. The latest version of its phase diagram was reported to host 3 ternary layered compounds [1], while additional study of single crystals grown via directional crystallization shows the existence of another 4 compounds [2].

The phase equilibria and thermodynamic data of corresponding systems can provide more reliable information for synthesizing novel complex phases and the development of modern sample-preparation techniques. An analysis of literature data shows no information on the thermodynamic properties of the manganese-bismuth tellurides has been reported yet.

In the presented work, we report the results of an experimental phase equilibria study of the MnTe-Bi_2Te_3-Te system and the thermodynamic properties of manganese-bismuth tellurides, as well as solids solutions based on Bi_2Te_3 via EMF (electromotive force) method under standard conditions.

Alloys of the studied system were synthesized in evacuated quartz ampules at 1000 K for 5 h followed by quenching in icy water. The resulting ingots were further annealed at 700 K for 45 days to form equilibrium phases.

For EMF measurements, the concentration cell of

(–) MnTe (solid) | liquid electrolyte, Mn^{2+} | (Mn–Bi–Te) (solid) (+)

the type was assembled. According to the constructed phase diagram of the system, all ternary compounds have a tie-line connection with $MnTe_2$. Based on this, partial molar quantities of the manganese can be considered thermodynamic functions of the virtual cell reactions. Using these data and the corresponding thermodynamic functions of MnTe and Bi_2Te_3, the standard thermodynamic functions of formation and standard entropies of the $MnBi_2Te_4$, $MnBi_4Te_7$, $MnBi_6Te_{10}$, and $MnBi_8Te_{13}$ compounds were calculated.

[1]. Aliev Z.S., Amiraslanov I.R., Nasonova D.I., Shevelkov A.V., et al. Novel ternary layered manganese bismuth tellurides of the MnTe-Bi_2Te_3 system: Synthesis and crystal structure. *Journal of Alloys and Compounds*. 2019, V. 798. P. 443-450.

[2]. Amiraslanov I. R., Aliev Z.S., Askerova P.A., et al. Crystal structure and Raman-active lattice vibrations of magnetic topological insulators $MnBi_2Te_{4\cdot n}(Bi_2Te_3)$ (n=0,1,…,6). *Physical Review B*, 2022, V. 106, P. 184108.

Dose Dependences of Phosphorescence and Conduction Current Relaxation in ZnSe Crystals

Bondar M.V.[1] , Degoda V.Ya.[2], Podust G.P.[2], Savchuk V.R.[2], Kozhushko B.V.[1]

[1] *Institute of Physics of the National Academy of Sciences of Ukraine, Kyiv, Ukraine*
[2] *Taras Shevchenko National University of Kyiv, Physics Department, Kyiv, Ukraine*

From dose dependence phosphorescence one can see the amount of light sum accumulation, but it is impossible practically to obtain reliable material parameters. In order to obtain reliable parameters, it is desirable to record a set of phosphorescence and conduction current relaxation dependencies with different intensities of X-ray excitation that are measured simultaneously. Than this set of curves should be compared with corresponding theoretical dependences.

The aim of the work was to determine the dose dependence of phosphorescence and conduction current relaxation using the dependences for long time phosphorescence[1] and conduction current relaxation for a multicenter model of crystal phosphor[2] by usage of the dose dependence of light sum accumulation[3]. Moreover, the obtained theoretical dependences for the intensity of phosphorescence and the magnitude of the conduction current in an analytical form take into account the intermediate acts of localization of charge carriers on shallower traps. Research of the dose dependence of phosphorescence and relaxation of the conduction current at different intensities of X-ray excitation confirmed that the light sum accumulation in ZnSe crystals occurs according to the exponential law, but with different time constants. It is in good agreement with the dose dependence of thermally stimulated luminescence and thermally stimulated conductivity.

An explanation of the experimental fact that the curves of phosphorescence and relaxation of the conduction current at the same irradiation dose, but at different excitation intensities and, accordingly, at different excitation times, cross each other, has been obtained. It has been determined that at least three types of traps (shallow, phosphorescent and deep) participate in the phosphorescence and relaxation of the conduction current at any excitation temperature. It has been defined that the level of filling of various traps depends on both radiation dose and the intensity of excitation. The main parameters of these traps has been obtained.

[1]. V.Ya. Degoda, Y.P. Kogut, I.M. Moroz, F.A. Danevich, Long time phosphorescence in $ZnMoO_4$ crystals. *Journal of Luminescence*. V. 161, January, 2017, P. 269-276.

[2]. Дегода В.Я. Кінетика рекомбінаційної люмінесценції та провідності кристалофосфорів при фото- і рентгенівському збудженні. Київ, Видавництво «Фенікс», 2021, 437 с. *[in Ukrainian]*.

[3]. V.Ya. Degoda, G.P. Podust, and M. Alizadeh, Light Sum Accumulation in ZnSe Crystals at X-Ray Excitation, *Advances in Condensed Matter Physics* Volume 2019, Article ID 8784109, 9 pages.

Effect of Laser Irradiation on the Optical Properties of Thin Near-Surface Layers of p-$Ge_{1-x}Si_x$ Solid Solution in 2-25µm Region

Demchyna L.A., Mynaylo M.A., Pekur D.V., Vuichyk M.V., Gentsar P.O., Stronskyi O.V., Levytskyi S.M.

V.E. Lashkaryov Institute of Semiconductor Physics NAS of Ukraine, 03028, Nauky av. 41, Kyiv, Ukraine, e-mail: rastneg@isp.kiev.ua

Study of electronic phenomena in semiconductor materials due to their use in optoelectronic devices is of great interest. In the present work, the optical reflection spectra in the spectral range 0.2-1.7µm and transmission in the region of the fundamental optical transition E_0 of $Ge_{1-x}Si_X$ solid solutions (x=0.85) were measured. The effect of laser irradiation λ = 532 nm wavelength on the optical properties of thin near-surface layers of p-$Ge_{1-x}Si_X$ solid solution in the spectral region 2-25µm when irradiated in the energy range of 46.6 mJ/cm^2- 163.5 mJ/cm^2. It is shown that, assuming a linear dependence of the energy of the fundamental optical transition E_0 on the solution composition x, the following relations are fulfilled:

$$E_0(Ge_{1-x}Si_x) = E_0(Ge) + k \cdot x\,; E_0(Ge_{1-x}Si_x) = E_0(Si) - k(1-x)\,,$$

where E_0(Ge) = 0.66 eV; E_0(Si) = 1.11 eV.

An increase in the reflectivity of thin near-surface layers of the p-$Ge_{1-x}Si_x$ (x = 0.85) solid solution under laser treatment has been experimentally shown. This integral effect is explained by the differences in the optical characteristics of the near-surface layer and the material volume. The obtained optical reflection spectra of the experimental samples indicate that laser-stimulated interaction of impurities and defects occurs during irradiation, which leads to the formation of neutral complexes and a decrease in the intensity of impurity scattering processes. It has been established that the main mechanism of influence of pulsed laser irradiation on the optical properties of thin surface layers of the studied crystals is structural heterogeneity, i.e. absorption due to the presence of semiconductor sites with defective structure and the ability to actively to absorb point defects and to bind impurities in thin surface layers of solid solution p-$Ge_{1-x}Si_X$. In silicon, the role of a heterogeneous layer is played by SiO_x, SiO_2, Si_3N_4, $SiO_{2-x}P$, SiC, and others; in germanium, the role of a heterogeneous layer is played by GeO_2, GeO, and others. From the quantitative analysis of the optical reflection spectra, the numerical value of the energy corresponding to the optical transition $E_1(\Lambda_1^c - \Lambda_3^v)$ of $Ge_{1-x}Si_X$ solid solutions (x = 0.85). The energy of the optical transition $E_1(\Lambda_1^c - \Lambda_3^v)$ of $Ge_{1-x}Si_x$ (x=0.85) solid solutions is 3.254 eV. The experimental spectra of optical transmittance in the spectral region 2 - 25µm of $Ge_{1-x}Si_X$ (x = 0.85) solid solutions showed that, with this laser treatment, the optical transmittance decreases with increasing of laser irradiation energy density. The minimum optical transmittance is located at 16.36µm wavelength.

Electronic Properties of the Near-Surface Layer of n-GaAs Single Crystals (100)

Demchyna L.A., Mynaylo A.M., Pekur D.V., Gentsar P.O.,
Stronski A.V., Vlasenko O.I.

V.E. Lashkaryov Institute of Semiconductor Physics NAS of Ukraine, 03028, Nauky av. 41, Kyiv, Ukraine, rastneg@isp.kiev.ua

In this work, the electronic properties of the near-surface layer of n-GaAs (100) single crystals were investigated to establish a quantitative correlation between the phenomenological broadening parameter Γ and the electron concentration N in n-GaAs (100) single crystals by means of modulation electron reflection spectroscopy. Electroreflectance spectra of the surface of single crystals n-GaAs (100) with an electron concentration N = 10^{21} - 10^{24} m^{-3} were obtained by the electrolytic technique at room temperature in the energy range 1.3 eV - 1.65 eV. The relation between the Franz-Keldysh oscillations and electronic parameters in the strong-field mode of measurements of the reflectance spectra, in particular between the Franz-Keldysh oscillation periods ΔE_m and the electro-optical energy $\hbar\theta$, is analysed. The correlation between the energy position of the reflectance peaks in the strong-field mode of measurements of reflectance spectra and the electro-optical energy ($E_m = f(\hbar\theta)$, where m = 1,2,3....)

$$E_m = E_0 + \Delta E = E_0 + \left(\frac{3}{4}(m\pi - \psi)\right)^{2/3} \cdot \hbar\theta = E_0 + \left(\frac{3}{4}(m\pi - \psi)\right)^{2/3} \cdot \left(\frac{e^2F^2\hbar^2}{2\mu}\right)^{1/3},$$

$$E_m = E_0 + \left(\frac{3}{4}\left(m - \frac{1}{2}\right)\right)^{2/3} \cdot \left(\frac{e^2F^2\hbar^2}{2\mu}\right)^{1/3}$$

where E_0 is the energy of the fundamental optical transition of the semiconductor, $\hbar\theta$ is the electro-optical energy, and ψ is the relative phase factor.

The physical parameters and parameters of the spatial charge region of the near-surface layer of the studied material were obtained: electronic transition energy E_0 (optical transition $\Gamma_{8v} - \Gamma_{6c}$); electro-optical energy $\hbar\theta$; phenomenological broadening parameter Γ; surface electric field F_s; relative phase factor ψ; energy distance from the electronic transition energy E_0 to the extremum of the last Franz-Keldysh oscillation; the oscillation length of the wave function of a quantum mechanical particle λ_{FK} with a reduced effective mass μ at a given surface electric field F_s; the thickness of the enrichment layer L (L = 2kT/eFs); the light penetration depth d (d =$\lambda/4\pi|\tilde{N}|$); the electric field penetration depth L_D ($L_D = \left(\frac{\varepsilon\varepsilon_0\kappa T}{e^2N}\right)$). The empirical dependence of the phenomenological broadening parameter Γ on the electron concentration N is obtained.

Electronic Structure and Optical Properties of Ag_8SnTe_6 Crystal Calculated by DFT

Semkiv I.V., Kashuba N.Y., Ilchuk H.A., Kashuba A.I.

Lviv Polytechnic National University, S. Bandera Str. 12, 79013 Lviv, Ukraine

Argyrodite family [1], which has a great variety of compounds and is characterized by the general formula $(A^+)_{12-n}B^{n+}(X^{2-})_6$ (with A^+= Li^+, Cu^+, Ag^+; B^{n+}= Ga^{3+}, Si^{4+}, Ge^{4+}, Sn^{4+}, P^{5+}, As^{5+}; X^{2-}= S^{2-}, Se^{2-}, Te^{2-}), are actively studied for potential use in photovoltaics, thermoelectricity, nonlinear optic, solid-state batteries, hydrogen generation, etc. [2].

The theoretical calculations were performed within the framework of the density functional theory (DFT). To calculate the properties of Ag_8SnTe_6 crystal, a crystalline lattice with the basal parameters of a= 15.298 Å, b= 7.552 Å, c= 10.699 Å, V= 1236.06 Å^3 ($Pna2_1$ space group (No. 33)) was used. The generalized gradient approximation (GGA) functional and Perdew-Burke-Ernzerhof (PBE) parameterization was used to describe the exchange-correlation energy of the electronic subsystem. Ultrasoft Vanderbilt's pseudopotentials served as ionic potentials. In our calculations, the value $E_{\text{cut-off}}$= 330 eV was taken for the cutting-off energy of the plane waves (this energy corresponded to the minimum value of the total energy). The convergence of the total energy was about 5 10^{-6} eV/atom. Integration over the Brillouin zone (BZ) was performed on a 2×2×1 grid of **k** points, using a Monkhorst-Pack scheme. The atomic coordinates and the unit-cell parameters were optimized following a Broyden-Fletcher-Goldfarb-Shanno technique. Optimization was continued until the forces acting on atoms became less than 0.01 eV/Å , the maximum displacement was less than 5.0 10^{-4} Å, and the mechanical stresses in the cell were less than 0.02 GPa.

Based on the electron energy structure has been established that the smallest optical band gap is localized at the Γ-point of the Brillouin zone and corresponds to direct optical transitions. The effective mass of the electrons and holes was calculated based on the electronic band structure. Dispersion behaviors of electron energy level are discuses based on results of effective mass. Based on electron energy structure calculation, the optical properties (optical dielectric functions, refractive index, absorption coefficient, et al.) are estimated using the Kramers-Kronig relation.

[1]. Kuhs W.F., Nitsche R., Scheunemann K. The argyrodites — A new family of tetrahedrally close-packed structures. *Mater. Res. Bull.* 1979. V. 14, No 2. P. 241–248.

[2]. Semkiv I.V., Kashuba N.Y., Ilchuk H.A., Kashuba A.I. Photoluminescence and electronic structure of α'-Ag_8GeS_6 crystals. *Fizyka Nyzkykh Temperatur*. 2023. V. 49, No 9. P. 1163–1171.

Experimental observation of light holes in CdTe

Uhryn Y.O.[1], Brytan V.B.[1], Peleshchak R.M.[2]

[1]*Drohobych Ivan Franko State Pedagogical University, 82100, Ukraine, Drohobych,*
24 Franko str. vbrytan2@gmail.com
[2]*Lviv Polytechnic National University*

Semiconductors A2B6 are a promising material for the manufacture of radiation photo detectors, solar energy converters [1], elements of telecommunication networks and a number of other solid-state electronic devices. Among the materials that are already used as uncooled semiconductor detectors of ionizing radiation, CdTe occupies a leading position [2]. The main requirements for materials for gamma and X-ray detectors are their high conductivity and high mobility of charge carriers [2,3]. In this case, electrically active intrinsic point defects must be in equilibrium, i.e. compensation must occur.

The aim of this work is to establish a theoretical method for calculating the basic parameters of light holes in cadmium telluride and their experimental detection, which would make it possible to take into account the influence of these current carriers on the transport phenomena in the presence of two types of current carriers.

The concentration and mobility of light and heavy holes in CdTe at room temperature were calculated based on the analysis of the experiment on the magnetic field dependence of the Hall voltage. The calculation was carried out within the framework of the semi-classical phenomenological two-band model. The presence of holes of two types in this semiconductor is confirmed by the law of dispersion, from the graphic representation of which it is clearly visible that in the valence band there are two branches of the dispersion curve with different curvatures [3].

[1]. D.M. Freik, V.M. Chobanyuk, O.S Krunutcky, I.V. Gorichok Photovoltaic Solar Energy Converters Based on Cadmium Telluride II. The Main Achievements and Current Status (Review) // *Physics and chemistry of solid state.* 2012. V. 13 No 3. P. 744-758.

[2]. Korbutyak D.V., Melnychuk S.V., Korbut E.V., Borysyuk M.M. Cadmium telluride: impurity-defect states and detector properties // *K.: Ivan Fedoriv,* 2000. P. 198.

[3]. V. D. Popovych, F. F. Sizov, O. A. Parfenjuk, Z. F. Tsybrii (Ivasiv) The effect of inhomogeneous dopant distribution on the electrical transport properties and thermal stability of CdTe:Cl single crystals // *Semicond. Sci. Technol.* 2010. 25. P. 035001.

High-Entropy Alloys in the $Cu_8B^{IV}S_6$+$Ag_8B^{IV}Se_6$↔$Cu_8B^{IV}Se_6$+$Ag_8B^{IV}S_6$ (B^{IV}-Si, Ge) Systems

Poladova A.N.[1], Namazov J.S.[2], Yusibov Yu.A.[2], Babanly M.B.[1]

[1]Institute of Catalysis and Inorganic Chemistry, Baku, Azerbaijan,
[2]Ganja State University, Ganja, Azerbaijan
babanlymb@gmail.com

Argyrodite family compounds attract the attention of researchers as environmentally friendly polyfunctional materials with mixed ion-electronic conductivity, as well as thermoelectric, photovoltaic, optical, and other properties [1,2]. One of the ways to optimize the properties, especially thermoelectric properties, of these materials is the entropy design, i.e. production of high-entropy alloys (HEA) with high thermodynamic stability. According to the definition, high-entropy alloys are considered alloys, which include at least five elements, the content of each of which should be from 5 to 35 at. % [3].

In this work, in order to obtain HEAs based on argyrodite compounds, phase equilibria in the $Cu_8B^{IV}S_6$+$Ag_8B^{IV}Se_6$↔$Cu_8B^{IV}Se_6$+$Ag_8B^{IV}S_6$ (A) reciprocal systems were studied.

Alloys of system A were prepared by melting of preliminarily synthesized and identified initial compounds in the required ratios under vacuum. After fusion, the samples were annealed at 900 K for 500 h, followed by slow cooling.

The studies were carried out by DTA (NETZSCH 404 F1 Pegasus system instrument), XRD (Bruker D8 ADVANCE powder diffractometer) and SEM (PhilipsXL-30 FEG).

Projections of the liquidus and solidus surfaces, as well as a number of vertical sections and an isothermal section at 300 K of the phase diagrams of systems A were constructed.

It has been established that in both systems the formation of solid solutions leads to stabilization at room temperature and below high-temperature ion-conducting phases. They are more favorable for the development of high-performance thermoelectric materials

[1]. Lin S., Li W., Pei Y. Thermally insulative thermoelectric argyrodites // *Materialstoday*. 2021. V. 48. P.198

[2]. Sardarly R.M., Ashirov G.M., Mashadiyeva L.F., Aliyeva N.A., Salmanov F.T., Agayeva R.Sh., Mamedov R.A., Babanly M.B. Ionic conductivity of the Ag_8GeSe_6 compound. *Mod. Phys. Lett. B.*, 2023. V. 36. P. 2250171

[3]. George E.P., Raabe D., Ritchie R.O. High-entropy alloys. *Nature Reviews Materials*, 2019. V.4. P.515

Influence of Ge Doping on the Optical Properties of n-CdTe Single Crystals in the Region of the Fundamental Optical Transition E_0

Gentsar P.O., Mynaylo M.A., Pekur D.V., Demchyna L.A., Vuichyk M.V., Strilchyk O.M. , Stronskyi O.V., Zayats N.S., Trishchuk L.I.

V.E. Lashkaryov Institute of Semiconductor Physics NAS of Ukraine,
03028, Nauky av. 41, Kyiv, Ukraine, rastneg@isp.kiev.ua

CdTe is used to manufacture uncooled gamma-ray detectors. One of the main problems when using A^2B^6 semiconductor compounds as a base material for optoelectronics is obtaining a bulk homogeneous material. The doping of cadmium telluride single crystals with germanium atoms leads to stability and reproducibility of the electrophysical properties of electronic devices based on cadmium telluride. In connection with the above mentioned, the study of the effect of doping on the physical properties of semiconductors is relevant.

In this work, optical (reflection spectra, transmission spectra) studies of n-CdTe single crystals doped with germanium with a concentration of $N_{Ge} = (2 - 10) \cdot 10^{24}$ m^{-3} with a resistivity of 10^4 Ohm·cm^{-} $5 \cdot 10^6$ Ohm·cm were carried out in the 800 nm – 1100 nm spectral range and in the 2 μm – 25 μm spectral range and measurements of photoluminescence spectra of n-CdTe single crystals doped with germanium with a concentration of $N_{Ge} = (2\text{-}10) \cdot 10^{24}$ m^{-3} at 77 K under excitation by laser radiation with an electromagnetic wavelength of 660 nm in the 1.3 eV - 1.65 eV energy range. The following results were obtained: the energy relaxation time τ and the effective "optical" mobility of free charge carriers for germanium-doped n-CdTe single crystals were estimated; the energy of the fundamental optical transition E_0 - 1.459 eV for germanium-doped n-CdTe single crystals at T = 300 K was determined; it was determined that the fundamental optical transition E_0 for germanium-doped n-CdTe single crystals at T = 77 K is equal to 1.580 eV; the temperature coefficient of the band gap change of n-CdTe single crystals doped with germanium with a concentration of $N_{Ge} = (2\text{-}10)\ 10^{24}$ m^{-3} with a resistivity of 10^4 Ohm·cm - $5 \cdot 10^6$ Ohm·cm, which is equal to $-5.426 \cdot 10^{-4}$ eV/K; the correlation between the energy of the fundamental optical transition E_0 for germanium-doped n-CdTe single crystals and the temperature T in the temperature range $77\ K \leq T \leq 300$ K is established: E_0(CdTe: Ge) = 1.580 eV - $5.426 \cdot 10^{-4}$ eV/K (T-77K); optical absorption spectra of the studied materials ($\ln(I_0/I) = f(\lambda)$) were obtained; it was shown that the studied crystals have high detector quality, which is crucial for the manufacture of highly sensitive and high-resolution ionizing radiation sensors; the practical value of the obtained results is in determination of the electronic and physical parameters of the technically important germanium-doped CdTe semiconductor.

Kinetic Parameters of Nanostructure of Amorphous Metal Alloys based on Aluminium

Khrushchyk K.[1,2], Chava M.[1], Pihel V.[1], Zubko M.[2], Karolus M.[2], Boichyshyn L.[1]

[1]*Ivan Franko National University of Lviv, Faculty of Chemistry, Department of Physical and Colloid Chemistry, 6 Kyryla i Mefodiya Str., Lviv, 79005, Ukraine*
[2]*University of Silesia in Katowice, Institute of Materials Engineering, Faculty of Science and Technology, 75 Pulku Piechoty 1A, Chorzow, 41-500, Poland*
khrystyna.khrushchyk@us.edu.pl

Amorphous metal alloys (AMA) based on Aluminium have high strength, plasticity at T=2-4 K they have magnetic properties. The main requirement for use as structural materials is structural stability at high temperatures. It is known that AMAs based on aluminum mainly crystallizes in three stages when heated. Doping with p-, d- and f-elements changes the temperature and number of crystallization stages. The temperature of nanocrystallization depends on the quantitative ratio and the nature of the alloy components.

In the paper, there is presented determination of the kinetic parameters of crystallization of amorphous metallic alloys based on aluminum doped with rare-earth metals (REM) by the method of differential scanning calorimetry (DSC). It is shown that the amorphous metallic alloys based on aluminum crystallize in three stages. By using the Kissinger, Avrami and Ozawa models, we compute the energies of activation for the second stage of crystallization on the basis of the results of differential scanning calorimetry.

The complex of properties of AMAs during the transition from the amorphous to the nanocrystalline (crystalline) state changes noticeably [1–2], although the chemical composition, in general, remains unchanged.

[1]. Jiaojiao Yi, Liqiao Yue, Rongjie Xue at al. Mechanism underlying two-step separated fcc-Al crystallization in Al-based metallic glasses. Materials Letters. 2021. 303(15). pp. 130488. https://doi.org/10.1016/j.matlet.2021.130488

[2]. Inoue A. Amorphous, nanoquasicrystalline and nanocrystalline alloys in Al–based systems .Progr. Mat. Sci. 1998. 43. pp. 365–520. https://doi.org/10.1016/S00796425%2898%2900005-X

Light Sources based on CdTe/CdS/ZnS Heterostructures

Slyotov M.M.[1,*], Slyotov O.M.[1,**], Kinzerska O.V.[1], Mazur T.M.[2,+]

[1] *Yuriy Fedkovych Chernivtsi National University, Kotsyubynsky Str., 2, Chernivtsi, 58002, Ukraine, email: *m.slyotov@chnu.edu.ua, **o.slyotov@chnu.edu.ua*

[2] *Ivano-Frankivsk National Technical University of Oil and Gas, 15, Karpatska Str, Ivano-Frankivsk, 76019, Ukraine, email: +tetiana.mazur@nung.edu.ua*

Heterostructures based on CdTe and ZnS are widely used in solid-state electronics. In addition, the corresponding devices manufactured according to modern technologies are of great importance in fiber optics in the formation of photosensitive devices and radiation sources [1]. For them, the high efficiency of the corresponding generation-recombination processes is important, which causes significant attention to the heterosystems produced on them.

This paper presents the results of the obtained and conducted studies of the radiation properties of CdTe/CdS/ZnS heterostructures (HS) carried out for the first time. They were grown by the method of isovalent substitution (IVS). For this purpose, CdS heterolayers (HL) were formed under appropriate conditions on a specially prepared CdTe substrate, on which wide-band ZnS was obtained under the invented substitution conditions. This process made it possible to obtain a complex combined heterostructure for the first time. Comprehensive studies of electrical, optical (absorption T_ω, reflection R_ω) and luminescence parameters were carried out. Based on the used λ-modulation technique, the basic parameters E_g, Δ_{CR}, Δ_{SO} of the energy structure were determined, which correlate with the known literature data of the components of CdTe/CdS/ZnS HS. The obtained high quantum efficiency η of radiation is fundamentally important for possible practical use. For surface HS of ZnS, the value of η is 12-14%. The luminescence spectrum covers a wide range of photon energies $\Delta\hbar\omega \approx 2.2$-$3.5$ eV with a maximum at $\hbar\omega_m = 3.05$ eV. Under the same experimental conditions, the properties of typical ZnS crystals give $\Delta\hbar\omega \approx 2.2$-$3.2$ eV with $\hbar\omega_m = 2.75$ eV at $\eta = 2$-3%. For the first time, the growing conditions of CdTe/CdS/ZnS HS components and their basic parameters and properties were determined. It is shown that under the identified conditions of production, a variation of the nature of the total radiation spectrum becomes possible due to generation-recombination processes in the components of CdS, CdTe and transition films of $Zn_xCd_{1-x}S$ and $CdTe_xS_{1-x}$ solid solutions. The efficiency of the corresponding bands forming the total radiation was determined. Under certain conditions, it is complex in terms of the spectral distribution of radiation, as well as in efficiency, which reaches $\eta = 7$-9%. The selection of appropriate growing conditions provides the ability to control the spectral information signal of the CdTe/CdS/ZnS heterostructure.

[1]. Kosyachenko L. A. Fundamentals of integral and fiber optics. Chernivtsi: Ruta, 2004. 348 p. (Ukrainian)

Microstructure and Temperature-Frequency Dispersion of Conductivity of Lithium-Iron Spinel Synthesized by Sol-Gel Autocombustion Technology

Vakalyuk A.V.[1], Gasiuk I.M.[1], Vakalyuk V.M.[2]

[1]Vasyl Stefanyk Precarpathian University, Ivano-Frankivsk, Ukraine,
andrii.vakaliuk.19@pnu.edu.ua
[2]Ivano-Frankivsk National Technical University of Oil and Gas, Ivano-Frankivsk, Ukraine

Spinel ferrites are widely used in radio engineering, radar, communication systems, and also as a promising material for the manufacture of the cathode matrix of portable lithium current sources. The electrical properties of ferrites strongly depend on the method of synthesis, preparation conditions, chemical composition, cation distribution and microstructure of the material.

In this work, samples of lithium-iron spinels were synthesized using the sol-gel autocombustion technology. Dielectric and conductive properties have been determined by complex impedance parameters. Measurements were carried out using an Autolab PGSTAT 12/FRA-2 spectrometer in the frequency range of 10^{-2}-10^{5} Hz and in the temperature range of 293-473 K with a step of 20 K.

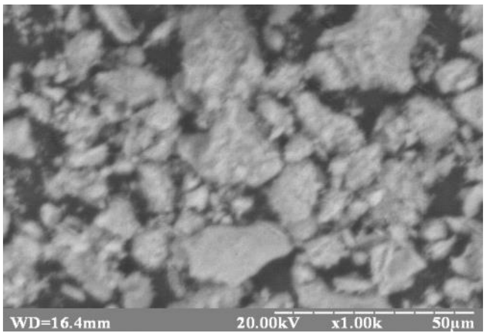

Fig. 1. SEM image of the structure of $Li0_5Fe_{2,5}O_4$.

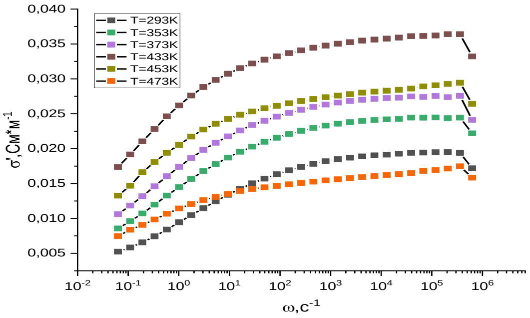

Fig. 1. Frequency dependences of the real part of the specific conductivity σ'(ω) at different temperature values.

The analysis of the σ′(ω) curves presented in Fig. 2 shows that, as in the case of the samples synthesized by the ceramic method [1], the electronic hopping mechanism of conductivity dominates, which is realized through chain percolation processes $Fe^{+2} - e^{-} \leftrightarrow Fe^{+3}$ in the octapositions of lithium oxoferrite spinel.

[1]. Gasiuk I.M., Chervinko D.M., Gasiuk M.I., Lozinska L.Y. Phenomenology of the Temperature-Frequency Dispersion of Electrical Properties of Aluminium-Substituted Lithium-Iron Spinel. *Physics and Chemistry of Solid State*. 2019. V. 20, No 4. P. 423-431.

Nano-Morphology, Local Structural and Electrical Features of Dislocation Etch Pits on Boron-Doped HPHT-Diamond

Danylenko I.M.[1], Lytvyn P.M.[1], Nikolenko A.S.[1], Strelchuk V.V.[1],
Malyuta S.V.[1], Kovalenko T.V.[2], Suprun O.M.[2], Lysakovskyi V.V.[2],
Ivakhnenko S.O.[2]

[1] *V.E. Lashkaryov Institute of Semiconductor Physics of NASU, pr. Nauky 41, 03028 Kyiv, Ukraine*

[2] *V. Bakul Institute for Superhard Materials of NASU, Avtozavodska str. 2, 04074 Kyiv, Ukraine*

igor.tesV@gmail.com

Boron doped-diamond (BDD) is a promising material for power and high-frequency electronics applications. Defects and their spatial distribution significantly affect the characteristics of diamond-based devices. This report employs an innovative approach, combining micro-Raman and frequency-modulated Kelvin probe force microscopy (KPFM) mapping, to investigate the nano-morphology, local structure, and electrical features of dislocation etch pits (EPs) in BDD grown under high-pressure and high-temperature conditions (HPHT). This approach enabled precise measurements of non-uniform distributions of crystallinity, internal strains, boron doping level, and local surface potential near the dislocation EPs formed during the initial stages of selective etching. Furthermore, micro-Raman mapping reveals a distinct pattern of elastic strain distribution induced by dislocations, encompassing compressive and tensile stress regions ranging from +18 MPa to -24 MPa.

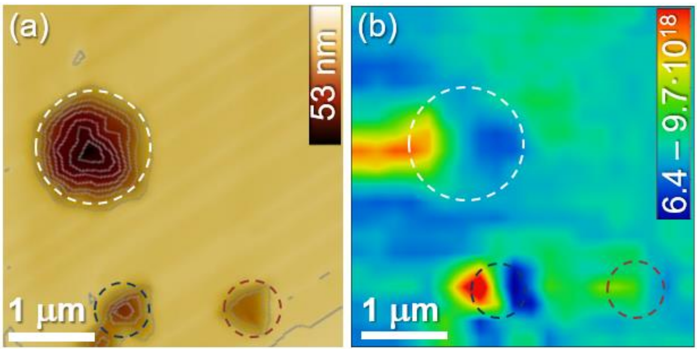

Fig. 1. (a) AFM height map near the EPs, (b) Raman map of the uncompensated boron impurity concentration [N_a-N_d].

Additionally, the relative intensity of boron-induced Raman bands was analyzed as a function of uncompensated boron impurity concentration [N_a-N_d] estimated by micro-FTIR mapping that allowed for evaluating the spatial distribution of boron content (Fig. 1.) near individual dislocation EPs ranging 6.4-9.7×10^{18} cm^{-3}. The distribution was highly heterogeneous and correlated with the compressive and tensile stress regions. The KPFM analysis demonstrated significant surface potential localization at the EPs varying around 30 mV and 50 mV. The study discusses the correlation between micro-Raman maps of deformation fields and boron content distribution as the origins of related surface potential fluctuations at the EPs. The report emphasizes defects' influence on BDD properties, which may be crucial for the development of diamond-based devices.

New Solution for Cd(Mn)Te Surface Passivation

Ivanitska V.G., Fochuk P.M.

Yurii Fed'kovych Chernivtsi National University, Chernivtsi, Ukraine,
v.ivanitska@chnu.edu.ua

In the fabrication of detectors, based on CdTe, Cd(Zn)Te and Cd(Mn)Te, semiconductor materials are subjected to various types of mechanical and chemical treatment. Each processing step can cause surface damage. Surface imperfections have a significant impact on the operation of devices. To eliminate surface defects, polishing, chemical etching and chemical passivation are used. The purpose of our study was to select the composition of the passivating solution and the conditions for the passivation process to obtain a high resistance film on the surface of Cd(Mn)Te crystals. Pretreatment of the crystals included mechanical grinding and polishing with abrasive powders.

To obtain a high-resistance surface film of the sample, we used an acidic solution of potassium perchlorate as an oxidizing agent. K^+ ions do not form poorly soluble compounds, which is a significant advantage of such a solution. The reaction products are easily removed during washing and do not contaminate the semiconductor surface.

Samples were prepared according to the standard procedure from $Cd_{0.85}Mn_{0.15}Te$ ingots, grown by the Bridgman method. The effect of passivation on the electrical properties of semiconductor was evaluated by the current-voltage characteristics.

The samples were treated by different methods: etching in $K_2Cr_2O_7$ aqueous solution; exposure in a concentrated KOH solution to eliminate local deviations from stoichiometry, passivation with a saturated solution of $KClO_4$ in concentrated HCl. The value of $Cd_{0.85}Mn_{0.15}Te$ samples resistivity, calculated from the obtained current-voltage dependences, after each stage of treatment is shown in the Table.

Table

Resistivity of the $Cd_{0,85}Mn_{0,15}Te$ sample after step-by-step chemical surface treatment

	Surface treatment	ρ, Ω*cm
1.	$K_2Cr_2O_7$	1,1 E+09
2.	$K_2Cr_2O_7$+KOH	2,2 E+09
3.	$K_2Cr_2O_7$+KOH+($KClO_4$+HCl)	4,4 E+09

It is shown that the treatment of $Cd_{0.85}Mn_{0.15}Te$ crystals in the indicated sequence leads to a decrease in surface leakage currents, since an increase in the resistivity of the sample is observed.

Percolation Effects in the Bi_2Se_3 Crystals at Se → Te Substitution

Rogacheva E.I., Martynova K.V., Vodoriz O.S., Nashchekina O.N.,
Men’shov Yu.V.

National Technical University "Kharkiv Polytechnic Institute",
Kharkiv, Ukraine, rogachova.olena@gmail.com

In a large number of semiconductor solid solutions that we have studied, in the region of low impurity concentrations, we have discovered a sharp change in properties, indicating the presence of a phase transition. We interpreted this as a manifestation of a percolation-type phase transition, which is characteristic of all solid solutions and corresponds to the reaching of the percolation threshold, when the so-called infinite cluster is formed, and the interaction of impurity atoms becomes cooperative. It is important that the existence and properties of such a transition be taken into account when doping crystals and thin films, and this determines the need for a detailed study of the properties of solid solutions in regions of low concentrations of the impurity component. The objects of this study are $Bi_2(Te_{1-x}Se_x)$ alloys, which are among the best thermoelectric (TE) materials for use in refrigerating devices. In [1,2], we observed the manifestation of percolation phenomena in this system in the concentration region in the vicinity of Bi_2Te_3. The goal of this work was to provide evidence for the presence of a similar phase transition in the same system, but from the Bi_2Se_3 side. We measured the dependences of microhardness H, the Seebeck coefficient S and electrical conductivity σ on composition x in the composition range $x = 1$–0.93 and found that near $x = 0.99$, there is a sharp change in properties (a decrease in H and S, and increase in σ), indicating the presence of the phase transition. The obtained results are important for studying percolation phenomena in thin $Bi_2(Te_{1-x}Se_x)_3$ films, whose application is increasingly expanding.

[1]. Rogacheva E.I., Martynova E.V., Shelest T.N., Doroshenko A.N., Nashchekina O.N. Percolation effects and self-organization processes in cold-pressed $Bi_2(Te_{1-x}Se_x)_3$ solid solutions *Materials Today: Proceedings.*2019. V.44, N 4, 3506 - 3510.

[2]. Rogacheva E.I., Shelest T.N., Martynova E.V., Doroshenko A.N., Nashchekina O.N., Men’shov Yu.V. Percolation effects and self-organization processes in $Bi_2(Te_{1-x}Se_x)_3$ solid solutions. *Functional Materials*. 2019. V. 26. №2. 254-261.

Quantum Cutting Effect in Doped $CsPbCl_3$:Yb Single Crystals

Muzyka T.M.[1], Chornodolskyy Ya.M.[1], Malynych S.Z.[2], Demkiv T.M.[1], Gamernyk R.V.[1]

[1]*Department of Physics, Ivan Franko National University of Lviv*
[2]*Hetman Petro Sahaidachnyi National Army Academy*
chornodolsky@gmail.com

Alkali metal lead halide perovskites possess a number of interesting properties from the application point of view, such as high luminescence quantum yield, narrow exciton emission band, long carrier diffusion length, and extended carrier lifetime [1], which make these materials attractive for numerous potential applications. Importantly, completely inorganic lead-halide perovskites exhibit high environmental resistance, radiation resistance against high-power ultraviolet radiation without photobleaching, and an extended operating temperature range. Doping with rare-earth elements RE^{3+} in perovskite materials enables them to exhibit luminescence across a wide spectral range, including the visible spectrum. In the case of Yb doping, quantum cutting is observed, resulting in a quantum yield of luminescence greater than one.

This work is devoted to the optical and photoelectric studies of doped $CsPbCl_3$:Yb single crystals grown by the Bridgman method. Using photoelectric techniques, the positions of energy levels of dopant ions Yb^{2+} and Yb^{3+} in the forbidden band of the $CsPbCl_3$:Yb crystal have been determined. Two mechanisms of exciting electrons into the conduction band of the $CsPbCl_3$:Yb crystal have been identified: via band-to-band transitions and from the Yb^{3+} ion into the conduction band. The role of Yb^{2+} ions in the energy transfer mechanism from the $CsPbCl_3$ crystal to the Yb^{3+} ions has been demonstrated, facilitating efficient quantum cutting.

The key role of the Yb^{2+} ions in the quantum cutting effect is clearly demonstrated. This effect results in the enhancement in the luminescence efficiency of $CsPbCl_3$:Yb single crystals and has significant implications for the development of advanced optoelectronic devices. Furthermore, a non-uniform distribution of ytterbium dopants within the volume of $CsPbCl^3$:Yb single crystals is revealed. In particular, isolated clusters of $CsPbCl_3$:Yb coexist with the pristine $CsPbCl_3$ matrix, indicating a complex interactions between the dopant ions and the host lattice. These results allow for a deeper understanding of the processes of inclusion of dopants and their diffusion in the crystal structure.

[1]. Khatoon S., Yadav S. K., Chakravorty V., Singh J., Singh R. B., Hasnain M. S., Hasnain S. M. Perovskite solar cell's efficiency, stability and scalability: A review. *Materials Science for Energy Technologies.* 2023. V.6. P.437-459. https://doi.org/10.1016/j.mset.2023.04.007

Reinvestigation of the Pseudo-Binary System GeTe-Sb_2Te_3

Izzatli S.B.[1], Orujlu E.N.[2], Jafarov Y.I.[1], Babanly M.B.[1,3]

[1]*Baku State University, Baku, Azerbaijan,* sahile.izzetli@bk.ru
[2]*Azerbaijan State Oil and Industry University, Baku, Azerbaijan,* elnur.oruclu@yahoo.com
[3]*Institute of Catalysis and Inorganic Chemistry, Baku, Azerbaijan,* babanlymb@gmail.com

Thermodynamically stable homologous series compounds of the pseudo-binary $A^{IV}Te$-$B^{V}{}_2Te_3$ (A^{IV} = Ge, Sn; B^{V} = Sb, Bi) systems which have long-periodically ordered tetradymite-derivative structures exhibit thermoelectric, superconductivity, topological insulating, etc. properties [1,2]. An analysis of literature data shows that there is a lack of phase diagram information which is often incomplete and contradictory for these systems and remains to be clarified.

The need for precise materials data, such as phase diagrams and thermodynamic parameters is considered a key factor in the success of materials synthesis, crystal growth, or design [3].

Here, we report the results of an experimental reinvestigation of the GeTe-Sb_2Te_3 pseudo-system which is valuable for the chemical design of its intermediate phases with predictable composition and structure.

Alloys of the studied system were prepared by co-melting of pre-synthesized binary compounds in the vacuum-sealed quartz ampoules at 700-900°C depending on the composition and annealed at 500°C for 1000 h to form equilibrium phases. All synthesized alloys were examined using the PXRD (powder X-ray diffraction), DTA (differential thermal analysis), and SEM (scanning electron microscope) methods.

The combined results of PXRD, DTA, and SEM were used to construct a self-consistent phase diagram of the system. The exitence of series of ternary compounds with general formula $n\mathrm{GeTe}\cdot m\mathrm{Sb_2Te_3}$ (n and m are integers) were confirmed in the sysrem and melting character of some of these compounds were studied for first time. Besides, solid solubility of starting binary compounds, GeTe and Sb_2Te_3 were determined as well. The improved T-x phase diagram can be usefull for the designing of the Ge–Sb–Te-based high-performance materials.

[1]. Wang L.-L. Highly tunable band inversion in AB_2X_4 (A=Ge, Sn, Pb; B=As, Sb, Bi; X=Se, Te) compounds. *Physical Review Materials V.* 2022, 6, Iss. 9, P. 094201.
[2]. Nurmamat M., Okamoto K., Zhu S., Menshchikova T.V., et al., Topologically non-trivial phase-change compound $GeSb_2Te_4$. *ACS Nano*, 2020, V. 14, Iss. 7, P. 9059-9065.
[3]. Babanly M.B., Chulkov E.V., Aliev Z.S., Shevelkov A.V., Amiraslanov I.R. Phase Diagrams in materials science of topological insulators based on metal chalcogenides. *Russian Journal of Inorganic Chemistry*. 2017, V. 62, P. 1703-1729.

Research of a New Thermoelectric Material $TiCo_{1-x}Cr_xSb$

Romaka L.[1], Stadnyk Yu.[1], Romaka V.A.[2], Horyn A.[1], Romaka V.V.[3]

[1]Ivan Franko National University of Lviv, Kyryla and Mefodiya Str. 6, Lviv, 79005, Ukraine;
[2]National University "Lvivska Politechnika", 12, S. Bandera Str., Lviv, 79013, Ukraine;
[3]Leibniz Institute for Solid State and Materials Research, IFW-Dresden, Helmholtzstr. 20, 01069 Dresden, Germany

The structural, kinetic, and energy properties of the new semiconductor thermoelectric material $TiCo_{1-x}Cr_xSb$, obtained by replacing Co atoms with Cr atoms in the 4*a* crystallographic position of the TiCoSb half-Heusler phase, were studied. Structural studies of samples $TiCo_{1-x}Cr_xSb$, x=0–0.1, established the complex nature of the inclusion of Cr atoms (r_{Cr}=0.128 nm) in the matrix of the TiCoSb half-Heusler phase (Fig. 1*a*). At concentrations x=0–0.02, an increase in the lattice parameter $a(x)$ is predicted, since the atomic radius of Co (r_{Co}=0.125 nm) is smaller than that of Cr. However, the decrease in the values of $a(x)$ for x>0.02 indicates the simultaneous partial occupation of Cr atoms as well as positions 4*a* of Ti atoms (r_{Ti}=0.146 nm).

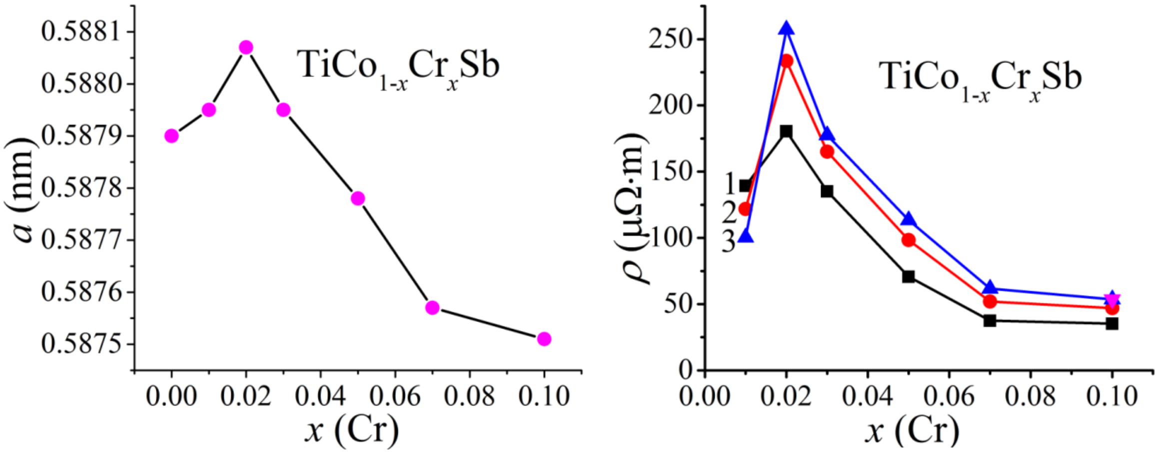

a ***b***

*Fig. 1. Variation of lattice parameter a(x) (**a**) and specific electrical resistivity ρ(x,T) (1 – 80 K, 2 – 250 K, 3 – 380 K) (**b**) of* $TiCo_{1-x}Cr_xSb$

An increase in the values of the specific electrical resistivity $\rho(x,T)$ of $TiCo_{1-x}Cr_xSb$ (Fig. 1*b*) in the concentration range x=0–0.01 at all temperatures indicates a decrease in the concentration of electrons. The reason is the generation of acceptor states in $TiCo_{1-x}Cr_xSb$ when Co atoms ($3d^74s^2$) are replaced by Cr atoms ($3d^64s^1$), which is consistent with the behavior of the unit cell parameter $a(x)$. However, at concentrations x=0–0.03, the main carriers are still electrons. At higher concentrations of Cr atoms, the holes determine the conductivity of the semiconductor, which is evidenced by the positive values of the thermopower coefficient $\alpha(x,T)$. The studied semiconductor solid solution $TiCo_{1-x}Cr_xSb$ is a promising thermoelectric material.

Structure and Phase Changes in Fe-Ti System under the Influence of Thermocycling

Yaremiy I.P., Makohin M.P., Umantsiv I.M.

Vasyl Stefanyk Precarpathian University, Ivano-Frankivsk, Ukraine,
yaremiyip@pnu.edu.ua

Alloys of the Fe-Ti system are widely used in the field of structural materials, primarily due to their ability to produce materials with enhanced mechanical properties. Titanium, when forming solid solutions with iron, acts as a more effective strengthening element than the commonly used nickel, molybdenum, and chromium. Methods of powder metallurgy have been successfully developed and applied to obtain iron-titanium alloys. The presence of two intermetallic compounds, FeTi and Fe_2Ti, in the Fe-Ti system, which participate in eutectic reactions with titanium and iron, allows for sintering in the presence of a liquid phase. This intensifies the sintering process and achieves increased density in the final product. The ability to form intermetallic compounds within the plastic matrix based on iron makes it promising to create new anti-friction and wear-resistant materials, for which a heterogeneous structure is often optimal.

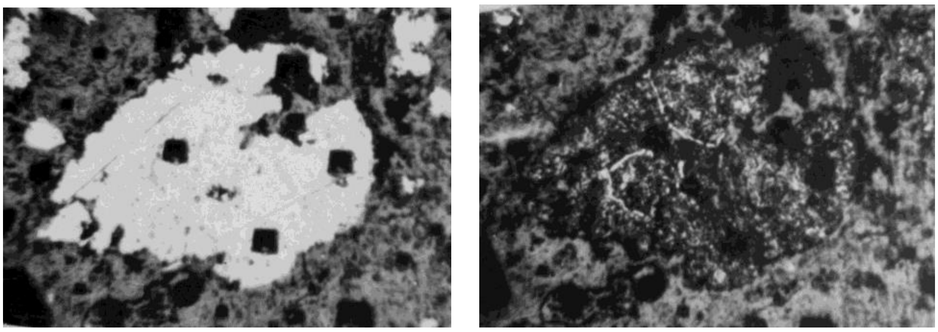

a) б)

Fig. 3. Intermetallics at the grain boundary between iron and titanium.
a) Unetched grain of iron.
b) The same, etched grain.

A study on the formation of the structure of a composite iron-titanium material obtained by sintering in a thermal cycling regime within the temperature range of phase transformations of iron and titanium (850-950°C) was conducted. According to X-ray structural and metallographic analyses, the sintered material contains phases of the original components and intermetallic compounds. Figure 1 shows that intermetallic phases form at the grain boundaries of Fe. These phases act as limiting factors for diffusion between the grains of iron and titanium.

Temperature Dependencies of Fermi Level in CdSb Crystals with Deep Energy Levels

Koval Yu., Fedosov S., Zakharchuk D., Yashchynskyy L., Panasyuk L., Shymchuk S.

Lutsk National Technical University, Lutsk, Ukraine,
dima.zakharchuk@gmail.com

The presence of various defects which develop in semiconductor volume in consequence of doping with certain impurities in the process of crystal growing or on account of irradiation leads to the formation of deep energy levels in the forbidden band. Determination of Fermi level in dependence on temperature is of interest when studying the band structure of semiconductors with deep levels so long as it gives useful information concerning the distribution of charge carriers in energy bands.

We have investigated dependencies of Fermi level for temperature interval 77 – 300 К in CdSb crystals with deep energy levels which are brought about, correspondingly: in the first case – by doping with tellurium, in the second case – by γ-irradiation of doped with tellurium crystals by a dose $\Phi \sim 10^{18}$ Q/cm^2 and in the third case – by γ-irradiation of crystals doped with indium by a dose $\Phi \sim 4 \cdot 10^{18}$ Q/cm^2.

At temperature rise the concentration of charge carriers increases in the conduction band and decreases on the deep levels. i.e., they are being exhausted. At full exhaustion of impurity the concentration of charge carriers in the conduction band becomes practically equal to donor impurity concentration. At further rise of temperature more intensive excitation of proper carriers begins and Fermi level moves in the direction to the middle of forbidden band. It should also be noted that after irradiation the lowering velocity of Fermi level for crystals with deeper radiation level is greater than that for crystals with shallower level.

The obtained results are of practical value, in particular, for various calculations with the use of Fermi level value in dependence on temperature.

The Induced Blue Phase of Cholesteric-Nematic Mixtures Under the Action of Acetone Vapors

Mykytyuk Z.M.[1], Kachurak Y.M.[1], Vistak M.V.[2], Kohut I.T.[3], Politansky R.L.[4], Shymchyshyn O.Y.[1], Diskovskyi I.S.[2], Vashchenko R.V.[5]

[1]*Department of Electronic Engineering, Lviv Polytechnic Nationa University. Mytropolyta Andreya str., 1, Lviv-79000, Ukraine. yurii.m.kachurak@lpnu.ua*

[2]*Danylo Halytsky Lviv National Medical University, Pekarska str, 69, Lviv-79010, Ukraine.*

[3]*Vasyl Stefanyk Precarpathian National University, Shevchenko str, 57, Ivano-Frankivsk-76018, Ukraine.*

[4]*Yuriy Fedkovych Chernivtsi National University, Kotsyubinsky str, 2, Chernivtsi-58012, Ukraine.*

[5]*Institute for Scintillation Materials, National Academy of Sciences of Ukraine, Nauky ave. 60, Kharkiv-61072, Ukraine.*

Blue phases of liquid crystal mixtures can be used to detect some harmful substances. [1] We conducted research on the detection of the blue phase under the influence of harmful organic substances, in particular acetone at room temperature.

To detect acetone vapors, a cholesteric-nematic mixture of nematic E7 and cholesteric impurity CB15 with concentrations in the range of 38-44 wt.% was used. And our previous work showed the possibility of creating an acetone sensor based on liquid crystalline substances. [2]

As a result of the experiment, manifestations of the blue phase were revealed for this liquid crystal mixture under the action of acetone. The obtained dependence of the half-width of the existence of the blue phase on the concentration of acetone vapors. It was established that the existence interval of the blue phase depends on the concentration of acetone vapors. Thus, changing the interval of existence of the blue phase makes it possible to use this effect when creating an acetone sensor.

[1]. Gurboga, Berfin, and Emine Kemiklioglu. "Optical sensing of organic vapor using blue phase liquid crystals." Liquid Crystals 49.11 (2022): 1428-1435.

[2]. Mykytiuk, Zynovii, et al. "Features of the transition to the isotropic state of the liquid crystal sensitive element of the gas sensor under the action of acetone vapor." Physics and Chemistry of Solid State 23.3 (2022): 473-477.

Thermodynamic Analysis of the Equilibrium Vapor Phase Composition of the Cd-I$_2$ System

Rybak O.V.

Lviv Polytechnic National University, Lviv, Ukraine,
oksana.v.rybak@lpnu.ua

Layered crystals of cadmium iodide attract the attention of researchers due to the possibility of their use as scintillation materials, as well as in photography and lithography.

A promising method for obtaining cadmium iodide crystals is crystallization from the vapor phase in a closed system. The mechanism of mass transport in the system and the optimal conditions for single crystals growing are determined by the temperature dependence of the equilibrium composition of the vapor and condensed phases.

A thermodynamic analysis of the composition of the vapor phase of the Cd-I$_2$ system in the temperature range of 300-2000 K at the values of the total pressure in the system from 0.1 kPa to 100 kPa was carried out.

Taking into account the results of experimental studies, the calculations assumed that the Cd-I$_2$ system in the vapor phase contains the following components: I, I$_2$, Cd, CdI, CdI$_2$. The chemical interaction was described by three independent reactions:

$$CdI_2 = Cd + I_2 \ (1),\quad CdI_2 = CdI + I \ (2),\quad I_2 = 2I \ (3).$$

Using the standard thermodynamic data of the vapor phase components, the equilibrium constants of independent reactions K_1, K_2, K_3 in the temperature range of 300-2000 K were calculated.

Chemical equilibrium in the vapor phase was described by the equations:

$$K_1=p_1^2/p_2 \ (4),\quad K_2=(p_1 \cdot p_4)/p_5 \ (5),\quad K_3=(p_2 \cdot p_3)/p_5 \ (6),$$

$$p_1+2p_2+p_4+2p_5=2(p_3+p_4+p_5) \ (7),\quad p= p_1+p_2+p_3+p_4+p_5 \ (8),$$

where $p_1 = p(\mathrm{I})$, $p_2 = p(\mathrm{I_2})$, $p_3 = p(\mathrm{Cd})$, $p_4 = p(\mathrm{CdI})$, $p_5 = p(\mathrm{CdI_2})$, p is the total pressure.

As a result of solving the system of equations (4)-(8), the temperature dependences of partial pressures in the system Cd-I$_2$ are obtained.

On the basis of thermodynamic analysis and calculation of the temperature dependence of partial pressures, the equilibrium composition of the vapor phase of the Cd-I$_2$ system in the temperature range of 300-2000 K was determined. As the temperature and total pressure in the system increase, the pressure CdI increases, but at a temperature of 1500 K, its pressure is 1–2 orders of magnitude lower than the pressure CdI$_2$. The dissociation of CdI$_2$ into individual components is significant at temperatures of 1500–2000 K. Among the products of dissociation, Cd and I$_2$ predominate. As a first approximation, the equilibrium in the vapor phase of the Cd-I$_2$ system in the temperature range of 300–1500 K is described by a reaction (1).

Thermodynamic Properties of the $FeIn_2X_4$ (X-S, Se) Compounds

Mammadov F.M.[1], Shukurova G.M.[2], Imamaliyeva S.Z.[1], Babanly M.B.[1,2]

[1]Institute of Catalysis and Inorganic Chemistry, Baku, Azerbaijan,
[2]Baku State University Baku, Azerbaijan, babanlymb@gmail.com

Compounds of the MB_2X_4 type (M – Mn, Fe; B – Ga, In,; X – S, Se, Te) exhibiting electrophysical, magnetic and optical properties are promising for creating lasers, light modulators, photodetectors and other functional devices based on them, controlled by magnetic field [1, 2]. The development of methods for directed synthesis of these phases is based on data on phase equilibria and thermodynamic properties of the corresponding systems [3].

This paper presents the results of a study of solid-phase equilibria and thermodynamic properties of Fe-In-X (X-S, Se) systems by the electromotive forces (EMF) measuruments of the the following concentration cells

(–) Fe (s.) | glycerol + KCl + $FeCl_3$ | (Fe in alloys) (s.) (+) (1)
(–) FeX (s.) | glycerol + KCl + $FeCl_3$ | (Fe in alloys) (s.) (+) (2)

and their EMF were measured in the 300-390 K (sulfide system) or 300-430 K (selenide system) temperature range.

Cells of type (1) were used to determine the partial molar functions of Fe in monochalcogenides, and cells of type (2) were used to determine the partial properties of FeX in alloys richer in chalcogen. FeX and alloys – anodes of the cells of type (1) and (2) were synthesized by direct interaction of high purity elementary components in evacuated (10^{-2}Pa) silica ampoules at 1000-1100 K. The achievement of equilibrium and the phase compositions of the alloys were controlled by powder X-ray diffraction analysis.

By combining the experimental data of the obtained concentration chains of types (1) and (2), the partial thermodynamic functions of Fe in the alloys are determined, based on which the standard thermodynamic formation functions and the standard entropies of the $FeIn_2S_4$ and $FeIn_2Se_4$ intermediate compounds are calculated.

[1]. Wyzga P., Veremchuk I., Bobnar M. et.al. Ternary MIn_2S_4 (M = Mn, Fe, Co, Ni) Thiospinels – Crystal Structure and Thermoelectric Properties. *Z. Anorg. Allg. Chem.* 2020. V. 646. P.1–9.

[2]. Zhang, B., Liu, Y., Zhu, H. et al. Enhanced visible light photocatalytic performance of a novel FeIn2S4 microsphere/BiOBr nanoplate heterojunction with a Z-scheme configuration. *Environ Sci Pollut Res.* 2023. V.30. P.13438–13448.

[3]. Babanly M.B., Mashadiyeva L.F., Babanly D.M. et al. Some issues of complex investigation of the phase equilibria and thermodynamic properties of the ternary chalcogenide systems by the EMF method. *Russian J. Inorg. Chem.* 2019. V.64. No13. P.1649-1671

XRD and ND Study and Structural Changes in Ge-S-Ag Glasses

Lishchynskyy I.M.[1], Kaban I.G.[2], Voitkiv H.V.[1], Stronski A.V.[3], Boychuk O.V.[1]

[1]*Vasyl Stefanyk Precarpathian National University, Ivano-Frankivsk, Ukraine*
[2]*Leibniz Institute for Solid State and Materials Research Dresden*
[3]*V.Lashkaryov Institute of semiconductor physics NAS Ukraine, Kyiv, Ukraine*

Nowadays are increasing amount of digital information, and the demand on memory devices being able to store, communicate, and compute this information is also increasing. Currently, flash memory based on charge storage is widely used in cell phones and music players and continuously replace hard disc drives in PCs and even in data centers. However, flash memory is challenged by a down-scaling problem because of the charge leakage from the storage layer. In this view, alternative memory technologies such as, for example, phase-change memory (PCM) and conductive-bridge memory (CBM) have been suggested.

Work of PCM is based on a non-volatile reversible switching of an active material, e.g. Ge-Sb-Te chalcogenide, from amorphous to crystalline state characterized by remarkably different electrical resistivity. The amorphous-to-crystalline transformation is thermally controlled by the current passing through the material.

It has been known for a long time that chalcogenide glasses (ChG), which are basically semiconductors, become superionic conductors upon doping with metal species. Ge-S-Ag glasses are very attractive, first of all, due to significantly higher glass transition temperature and consequently better thermal stability compared to the other based glasses. Also, Ge-S-Ag glasses are free of toxic elements.

In this work, we perform a microstructural study of GeS_2-Ag, $Ge_{42}S_{58}$-Ag and GeS_3-Ag chalcogenide glasses, extending the accessed composition range. Investigations along ChG-Ag lines are also of interest in a view of the CBM applications, in which a chalcogenide glass acts as a matrix and Ag atoms diffuse into the matrix from a silver electrode.

We have been analized the maxima of the intensity of the main three XRD and ND peaks and compared with the corresponding SEM images. The intensity of the XRD first sharp diffraction peak (FSDP) of $(GeS_3)_{100-x}Ag_x$ and $(Ge_{42}S_{58})_{100-x}Ag_x$ glasses decreases, while its position at about 1.06 $Å^{-1}$ remains constant.

The second maximum shifts to smaller values of the diffraction vector Q and its intensity increases. The next maxima also shift to lower Q-values but the intensity of oscillations decreases with increasing Ag concentration.

The more detailed analysis reveals that for homogeneous $(Ge_{42}S_{58})_{100-x}Ag_x$ glasses position Q_{FSDP} increases practically linearly, whereas that for the phase separated glasses $(GeS_3)_{100-x}Ag_x$ and $(GeS_2)_{100-x}Ag_x$ deviates from the linearity.

Session 6

Thin films technology for energy saving

Surface-Barrier CdTe Diodes for Photovoltaics

Mazur T.M., Mazur M.P.

Ivano-Frankivsk National Technical University of Oil and Gas., Ivano-Frankivsk, Ukraine
tetiana.mazur@nung.edu.ua

An urgent problem of our time and the near future, including Ukraine, is the energy crisis and the need to use renewable energy sources. Photovoltaics, especially thin-film CdTe solar panels [1], are a promising way to generate electricity directly from solar energy.

To prepare the samples, substrates with a size of 5×5 mm² and a thickness of 1 mm made of a CdTe crystal with a resistivity of about 20 Ohm cm were used. The crystals were produced by the Bridgman method and did not contain alloying additives, possessing electronic conductivity due to their own defects. The substrates were subjected to mechanical and chemical treatment, including polishing in a $K_2Cr_2O_7$:H_2O:HNO_3 solution (4:20:10 ratio), washing with deionized water, and drying. The resulting samples had a mirror surface and demonstrated moderate edge luminescence when irradiated with a He-Ne laser.

When annealing under special conditions, a nanostructure was formed on the surfaces of the samples used, which was visible in the topogram obtained using a Nanoscope-III atomic force microscope. According to the topogram, the surface is characterized by a granular structure with lateral grain sizes of 10-50 nm, which are combined into larger (100-500 nm) subgrains. The value of the short circuit current density was calculated taking into account the effective photosensitive area according to the formula $J_{sc} = I_{sc} / \mathrm{S}$ and for these test samples it had a value of ~$2 \cdot 10^{-1}$ cm^{-2}. It has been studied that modification of substrates entails an increase in the efficiency of solar cells η, and the maximum efficiency is observed for surface-barrier diodes with a quantum-sized surface [1].

With increasing temperature *T*, the short-circuit current increases I_{sc}, which is associated with an increase in the number of absorbed low-energy photons. The consequence of reducing the band gap is a decrease in the series resistance of the diode. In addition, with increasing temperature *T*, the open-circuit voltage V_{oc} decreases as a result of the greater temperature dependence of the dark current compared to the photocurrent. This effect is caused by the surface morphology itself, and not by the formation of any other chemical compound due to annealing. This is experimentally confirmed by the fact that the differential reflection spectra of the substrates are identical and correspond to the peak value of the CdTe band gap.

[1]. Makhniy V.P., Berezovskiy, M.M., Kinzerska O.V., Mazur M.P., Mazur T.M., Prokopiv V.V. Prospects of using surface and barrier CdTe-diodes in solar energy. *Sensor Electronics and Microsystem Technologies*. 2019. Vol.16, №2. P. 32-42.

The Influence Shading Effect on the Change Output Power of Photovoltaic Modules

Fedenko V.Y., Dzundza B.S.

Vasyl Stefanyk Precarpathian National University, Ivano-Frankivsk, Ukraine,
vitalii.fedenkoj@gmail.com

Considering the energy crisis, interest in renewable energy sources is growing sharply. In particular, the use of both monocrystalline and thin-film solar cells with a large area is actively developing. The advantage of thin-film elements is their significantly lower cost and the ability to generate energy in scattered sunlight and in cloudy weather. Research on the issue of partial shading shows that the reduction in the efficiency of classic solar panels can reach significant values[1]. The efficiency of the photocell is determined by the equation:

$$\eta = V_{oc} I_{sc} F_F / P_{in}$$

where V_{oc} – open-circuit voltage; I_{sc} – short-circuit current; FF – fill factor.

In this research using the method of computer simulation, a model is developed in the Simulink environment, which consists of several PV modules connected to each other. Parallel to the panels are connected bypass diodes. Each photovoltaic panel contains a parameter; the temperature value is 25°C. Insolation value is a variable for each individual experiment. When a different amount of insolation is set, it stimulates the shading process. Based on the results, the "I-V" and "P-V" dependence curves are constructed.

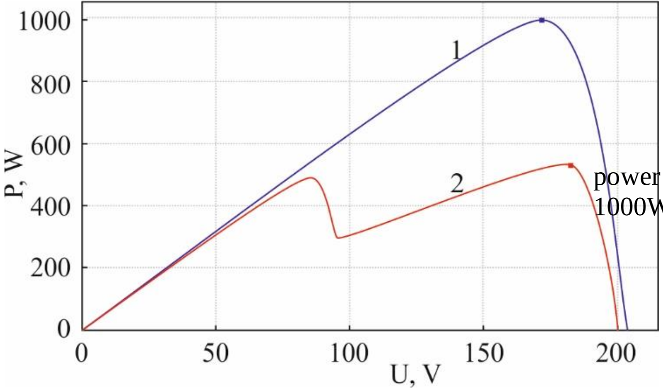

Fig. 1 – Dependencies of the maximum power point for different degrees of shading: 1 – 1000W/m^2, 2 –500W/m^2

From the obtained parameters, the values of the maximum output power and, accordingly, its loss in the case of modeling shaded elements are determined by a graphical method.

Based on the built model can be concluded that the shading of PV modules has a significant effect on the output power, so the choice of the location panels should be chosen carefully avoiding shading objects.

1. Abdelaziz G. Hichem H. Gharbi R. Shading effect on the performance of a photovoltaic panel. *2nd IEEE International Conference on Signal*. 2022.

Thermoelectric Properties of Thin Film Microgenerators Based on Lead Telluride

Holovata O.B., Dzundza B.S.

Vasyl Stefanyk Precarpathian National University, Ivano-Frankivsk, Ukraine,
oksanakostuk@gmail.com

In recent times, alternative energy resources have captured increasing attention. Thin film thermoelectric generators have wide-ranging applications, especially in wearable and implantable biomedical devices, due to their high reliability and miniature size.

Thin film thermoelectric generator samples were obtained through physical vapor deposition from the vapor phase of a previously synthesized material based on four-component compounds PbSnAgTe and doped PbTe:Sb on flexible mica substrates. The thermoelectric properties were investigated using both classical methods, which provided a temperature difference ΔT between the hot and cold junctions, and impedance spectroscopy methods.

Research on the thickness-dependent thermoelectric parameters showed that the maximum power is achieved at thicknesses of approximately 5 μm. With further increases in thickness, microcracks form in the films, leading to increased internal resistance and a deterioration in characteristics.

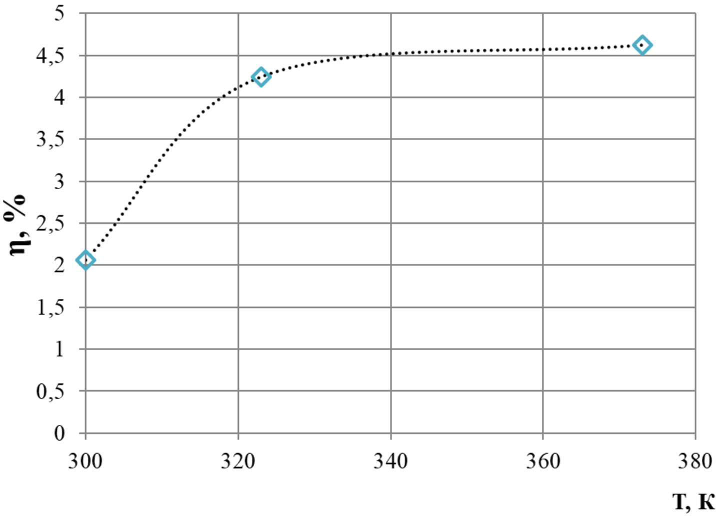

Fig. 1. The thermoelectric efficiency of a thin-film module based on compounds of PbSnAgTe (p-leg) and doped PbTe:Sb (n-leg).

Based on the results of impedance measurements, the temperature dependence of the thermoelectric efficiency η has been calculated for the investigated thin film modules at a temperature difference of 100 K (Figure 1). The obtained efficiency values are comparable to, if not superior to, similar modules based on IV-VI compounds [1].

[1]. Karthikeyan V., Surjadi J.U., Wong J.C., Kannan V., Lam K.H., Chen X., Lu Y., Roy V.A. Wearable and flexible thin film thermoelectric module for multi-scale energy harvesting. *Journal of Power Sources*. 2020. Vol. 455. P. 227983.

Using the Thermoelectric Properties of Sb and Bi Doped Lead Telluride to Convert Solar Thermal Energy into Electrical Energy

Halushchak M.O., Mazur T.M.

Ivano-Frankivsk National Technical University of Oil and Gas., Ivano-Frankivsk, Ukraine
galushchak@nung.edu.ua; tetiana.mazur@nung.edu.ua

One of the promising types of renewable energy sources is solar radiation. Using the classical approach to solving energy saving problems using solar panels is the simplest and most well-known, but ineffective in conditions of low solar insolation. It is also known that solar cells are able to perceive only 18% of the radiation falling on them, and most of the sun's energy, and this is approximately 70%, is dissipated in the form of thermal energy, which cannot be used using photoelectric conversion. Therefore, solar energy in combination with thermoelectric energy today has all the prerequisites to partially solve Ukraine’s energy problems.

We have developed a new method and technology for producing thermoelectric materials based on PbTe with a high dimensionless thermoelectric figure of merit ZT [1]. The work also investigated the structural and thermoelectric properties of samples obtained by pressing powdered PbTe:Sb and PbTe:Bi with an impurity concentration in the range (0.0-1.0) at. % Sb(Bi). The powder pressing method ensures the formation of a significant number of grain boundaries in the sample, which helps to reduce its thermal conductivity coefficient, and by controlling the pressure and size of the fractions, you can effectively influence the electrical conductivity of the samples and, in the case of a grain size commensurate with the mean free path of electrons, but less than its wavelength , on the thermo-EMF coefficient. In this way, can control the main parameters when obtaining samples. There is also no need to grow single crystals, which is a complex technological process.

Research has shown that alloying also leads to an increase in the basic thermoelectric characteristics of the material [1]. In particular, for PbTe:Sb with an impurity content of 0.3 at.% specific electrical conductivity is ≈ 700 $(\text{Ohm cm})^{-1}$, and the thermo-EMF coefficient is ≈ 300 μV/K. For PbTe:Bi, the optimal impurity concentration is 0.1 at.% Vi, at which $\sigma \approx 600$ $(\text{Ohm cm})^{-1}$ and $S \approx 150$ μV/K. The non-monotonic change in the lattice parameter with increasing content of Sb(Bi) atoms was also established, explained by the excellent mechanisms of impurity entry into the PbTe crystal lattice: up to a concentration of 0.3 at.% Sb (0.1 at.% Bi), filling with stibium (bismuth) atoms occurs.) tellurium vacancies, and at higher concentrations – simultaneous completion of the anion and cation substructures.

[1]. Galushchak M.O., Horichok I.V., Krynytskyi O.S., Freik D.M. Thermoelectricity of lead telluride doped with Sb and Bi. *Thermoelectricity*. 2014. No. 2, P. 23-30.

Session 7

Nanomaterials for biomedical application

Copper Single-Phase Ferrite Nanoparticles as Promise Materials for Magnetic Hyperthermia Application

Mazurenko J.[1], Kaykan L.[2], Moiseienko M.[1], Kuzyshyn M.[1], Vytvytskyi A.[1]

[1] *Ivano-Frankivsk National Medical University, Ivano-Frankivsk, Ukraine,*
yumazurenko@ifnmu.edu.ua
[2] *G.V. Kurdyumov Institute for Metal Physics, N.A.S. of Ukraine, Kyiv, Ukraine,*
larysa.kaykan@gmail.com

Magnetic hyperthermia plays a crucial role in cancer treatment strategies [1]. This technique operates on the principle that cancerous cells are more vulnerable to increases in temperature compared to healthy cells. As such, a localized increase in heat within a specified range can selectively eliminate the cancerous cells while preserving healthy ones. Specific magnetic nanoparticles have the unique capability to transform energy derived from high-frequency electromagnetic fields into heat.

Using the sol-gel self-combustion technique, we synthesized ferrite nanoparticles of $CuFe_2O_4$ composition. Two types of fuels were used in this process: citric acid, resulting in CCF copper ferrite, and polyethylene glycol (specifically PEG-2000), resulting in CPF copper ferrite. X-ray analysis confirmed the single-phase nature of the systems produced. As determined by the Debye-Scherrer and Williamson Hall methods, particle sizes were 28 nm for the CCF ferrites and 8 nm for the CPF ferrites.

The created samples underwent mechanical milling, followed by an ultrasonic treatment operating at 80W for one hour. We evaluated the proficiency of the particle's magnetic heating using an alternating current generator. The results of this evaluation are displayed in the corresponding figure.

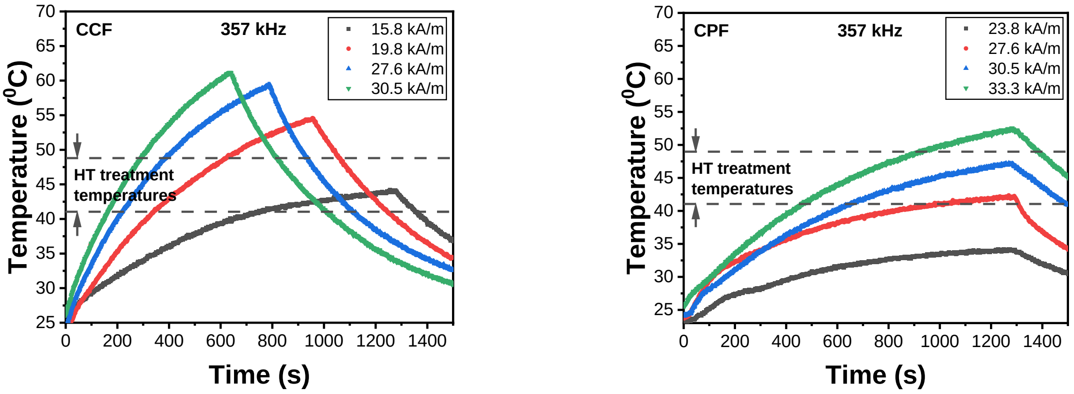

Fig. 1. Heating response curve of the synthesized nanoparticles in relation to field and frequency.

[1]. Santana-Otero, A., Gómez-Cerezo, D., Lozano-Pedraza, & Ortega, D. Ferrite nanoparticles for hyperthermia. *Ferrite Nanostructured Magnetic Materials.* 2023. P. 775–803.

Development of Optical Immunosensors based on TiO_2 Thin Films

Tereshchenko A.V.

Odesa National I.I. Mechnikov University, Odesa, Ukraine, alla_teresc@onu.edu.ua

Immunosensors based on nanostructured TiO_2 thin films are broadly applied in different areas of human life – from medical diagnostics up to national security and defense [1,2]. Immunosensors are the class of biosensors that is based on the interaction between antibodies and antigens by formation of an immune complex that is known as highly specific and selective form of interaction. Optical immunosensors are increasingly studied class of biosensors since they allow the evaluation of some inter-molecular interactions contactless, without the damage of biological samples and without the use of the additional chemical or physical labels [3]. The photoluminescence-based sensors seem to be very promising for the improvement in the diagnosis of virus induced diseases. In photoluminescence-based immunosensors, the nanostructured metal oxide thin film based on TiO_2 (or some other metal oxide, e.g. ZnO) is used as an efficient photoluminescence transducer [1-3]. However, the interaction mechanism of immune complex based proteins with TiO_2 and the origin of the changes in the photoluminescence spectra are poorly discussed, although the mechanism of the interaction between semiconductor nanomaterial and proteins is the key in solving many of problems, which are still arising during the development of TiO_2-based immunosensors, such as an improvement of sensitivity and selectivity [4]. Therefore, development of biosensors based on the optical detection methods that can be applied for the determination of large variety of analytes is of great interest. This work is aiming to highlight the origin of the changes in the photoluminescence spectra of TiO_2 resulted after the protein adsorption on its surface during the formation of biosensitive layer and after its interaction with target analyte.

[1]. A. Tereshchenko, M. Bechelany, R. Viter, et.al. Optical biosensors based on ZnO nanostructures: advantages andperspectives. A review. *Sensors and Actuators B, Chemical*, 229, 2016, 664-677.
[2]. R. Viter, A. Tereshchenko, V. Smyntyna, et.al. Toward development of optical biosensors based on photoluminescence of TiO_2 nanoparticles for the detection of Salmonella. *Sensors and Actuators B: Chemical*, 252, 2017, 95-102.
[3]. A. Tereshchenko, V. Fedorenko, V. Smyntyna, et.al. ZnO films formed by atomic layer deposition as an optical biosensor platform for the detection of Grapevine virus A-type proteins. *Biosensors and Bioelectronics*, 92, 2017, 763-769.
[4]. A. Tereshchenko, V. Smyntyna and A. Ramanavicius, Interaction mechanism between TiO_2 nanostructures and bovine leukemia virus proteins in photoluminescence-based immunosensors, *RSC Advances*, 8, 2018, 37740.

Influence of Shooting Factors on Electrical Impedance Spectra of Biological Tissues

Pryimak T.V.[1], Gasiuk I.M.[2], Chervinko D.M.[3]

Vasyl Stefanyk Precarpathian National University, Department of Materials Science and New Technology, 57 T. Shevchenko St., Ivano-Frankivsk, 76025, Ukraine,
pryjmak488taras1996@ukr.net

The method of impedance spectroscopy (IS) is one of the most popular ways to characterize biological tissues based on their passive electrical properties, allowing for active use in various fields, including medical [1] and food-oriented [2] applications.

The aim of the proposed study is to determine the reasons for changes in impedance spectra during the repeated registration of the electrical impedance spectrum.

It was shown that upon repeated measurement of a sample of the same size, differences in the obtained spectra are observed, which are manifested in a significant reduction of the real and imaginary part of the electrical resistance for all registered frequencies, for the second measurement and restoration of the order of the registered values in subsequent measurements to the values of the first experiment. Such a tendency is probably caused by the impact on the sample of a measuring electric potential of a sinusoidal form in the low-frequency range, which leads to the irreversible localization of the conductivity ions of the electrolyte subsystem at the boundaries of the structural elements of the biological sample.

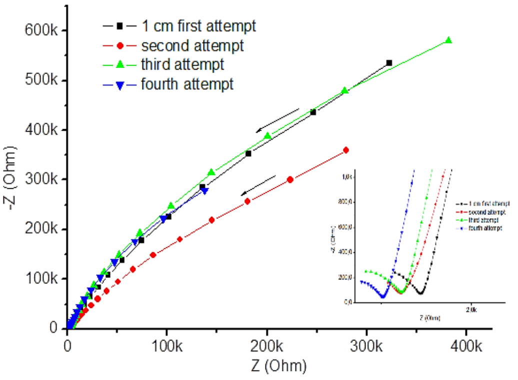

Figure 1. Impedance spectra of fresh liver tissue samples of 1 cm in the frequency range of 0.01 Hz – 100 kHz, -Z‘‘- imaginary part, Z‘ – real part of the electrical impedance, in the inset – high-frequency sections of the diagram, arrows indicate the direction of frequency increase.

[1]. Moqadam SM, Grewal PK, Haeri Z, Ingledew PA, Kohli K, Golnaraghi F. Cancer Detection Based on Electrical Impedance Spectroscopy: A Clinical Study. *J Electr Bioimpedance*. 2018;9(1):17-23. Published 2018 Aug 16. doi:10.2478/joeb-2018-0004.

[2]. Afonso J, Guedes C, Santos V, et al. Utilization of Bioelectrical Impedance to Predict Intramuscular Fat and Physicochemical Traits of the Beef *Longissimus Thoracis et Lumborum* Muscle. *Foods*. 2020;9(6):836. Published 2020 Jun 25. doi:10.3390/foods9060836.

Interactions of Human Serum Albumin with II-VI Based Semiconductor Quantum Dots Probed by Optical Spectroscopy Methods

Stolyarchuk I.D.[1], Kuzyk O.V.[1], Dan'kiv O.O.[1], Stolyarchuk A.I.[1],
Pryima Yu.A.[1], Wojnarowska-Nowak R.[2]

[1]*Drohobych Ivan Franko State Pedagogical University, Drohobych, Ukraine,*
i.stolyarchuk@dspu.edu.ua
[2]*University of Rzeszow, Rzeszow, Poland*

In the past decade, a variety of nanoscale structures have been used for a range biological and biomedical application. Major classes of biologically relevant nanostructures include semiconductor quantum dots (QDs), magnetic nanostructures and metallic nanoparticles. QDs are useful as a novel probe in biosensor and bioimaging due to their unique size dependent optical and electrical properties [1,2].

In this work, we report on comparative studies of interactions between II-VI:Me (Me: Mn, Co) QDs and model proteins type of human serum albumin (HSA). In addition to conventional UV-Vis absorption and luminescence spectroscopic methods we have included micro-Raman spectroscopy.

The obtained results show the changes of protein luminescence spectra after adding of semiconductor quantum dots (ZnO:Mn, CdS:Mn, CdS:Co) in appropriate solution. First of all the quenching of luminescence from HSA was observed after adding of semiconductor nanoparticles. The UV-vis absorption spectra of the proteins have also changed because of formation of QDs –HSA bioconjugates. The effect of temperature on the structural and spectroscopic properties of HSA and QDs –HSA bioconjugates was also been researched by optical spectroscopy. The results demonstrate that QDs –HSA bionanocomplex exhibites a more complex temperature-dependent fluorescence emission and suggests the possibility of employing QDs as probes to monitor the thermal denaturation of proteins. In conjunction with the energy transfer results it appears possible to apply the colloidal quantum dots for use as components of modern diagnostic systems including biosensors.

[1]. Wen-jing Liu, Li-juan Wang, Chun-yang Zhang. Progress in quantum dot-based biosensors for microRNA assay: A review. *Analytica Chimica Acta.* 2023, 341615 (In Press), https://doi.org/10.1016/j.aca.2023.341615.

[2]. Mohammad Ali Farzin, Hassan Abdoos. A critical review on quantum dots: From synthesis toward applications in electrochemical biosensors for determination of disease-related biomolecules, *Talanta*. 2021, 224,121828.

Nanoimaging in the Diagnosis of Malignant Tumours

Kindrativ E.[1], Chuiko N.[2], Hryshchuk M.[3]

[1]Ivano-Frankivsk National Medical University,
Ivano-Frankivsk, Ukraine, ekindrativ@ifnmu.edu.ua,
[2]Ivano-Frankivsk National Medical University,
Ivano-Frankivsk, Ukraine, nchuiko@ifnmu.edu.ua,
[3]Ivano-Frankivsk National Medical University,
Ivano-Frankivsk, Ukraine, mhryshchuk@ifnmu.edu.ua

Nanotechnology has a significant potential in the diagnosis and treatment of malignant tumours. Nanoparticles can be used to improve the quality of tumour imaging (nanoimaging) [4]. Nanoimaging can be performed using various methods including magnetically reactive nanoparticles. Typically, these are nanoparticles which have magnetic properties and can be directed to the tumour site by an external magnetic field. Nanoparticles that are introduced into the body can actively accumulate in the tumour due to a phenomenon known as passive accumulation based on microcirculatory disorders in tumour tissues. Once nanoparticles have accumulated in a tumour, magnetic resonance imaging can be used to image the tumour [1]. The nanoparticles increase the contrast of the images and allow to determine the size and location of the tumour more accurately. Some nanoparticles can emit light which can be used for fluorescent tumours imaging during surgical removal or for monitoring [2]. This technology is currently undergoing clinical trials and may be introduced in the nearest future [3]. The use of nanoparticles for imaging allows doctors to obtain more detailed and sensitive data on tumours, which helps in early detection and accurate determination of their condition, dynamics, etc. These innovations can significantly improve the efficiency of diagnosis and treatment of malignant tumours and contribute to early detection and more accurate monitoring of these diseases.

[1]. Faiz K, Lam FC, Chen J, Kasper EM, Salehi F. The Emerging Applications of Nanotechnology in Neuroimaging: A Comprehensive Review. Front Bioeng Biotechnol. 2022 Jul 6;10:855195. doi: 10.3389/fbioe.2022.855195

[2]. Quan YH, Oh CH, Jung D, Lim JY, Choi BH, Rho J, Choi Y, Han KN, Kim BM, Kim C, Park JH, Kim HK. Evaluation of Intraoperative Near-Infrared Fluorescence Visualization of the Lung Tumor Margin With Indocyanine Green Inhalation. JAMA Surg. 2020 Aug 1;155(8):732-740. doi: 10.1001/jamasurg.2020.1314.

[3]. Vahrmeijer AL, Hutteman M, van der Vorst JR, van de Velde CJ, Frangioni JV. Image-guided cancer surgery using near-infrared fluorescence. Nat Rev Clin Oncol. 2013 Sep;10(9):507-18. doi: 10.1038/nrclinonc.2013.123.

[4]. Lam FC. Editorial: Nano-Imaging in Translational Cancer Medicine. Front Bioeng Biotechnol. 2022 Jul 22;10:969430. doi: 10.3389/fbioe.2022.969430

Session 8

Innovative methods for teaching

Demonstrating the Magnetic Properties of the Matters for the High School Students'

Stolyarchuk I.D., Kuzyk O.V., Pan'kiv L.I., Dan'kiv O.O., Holskiy V.B.

Drohobych Ivan Franko State Pedagogical University, 24 I.Franko str., 82100 Drohobych, Ukraine, i.stolyarchuk@dspu.edu.ua

Magnetism is one of the few branches of physics for which a small number of demonstration experiments have been developed in its study in secondary schools. Important in the study of this section is also the generalization and systematization of students' knowledge using formulas, graphs, figures and tables. This allows you to comprehensively characterize the studied properties of different types of magnetics.

The physical experiment method is one of the main methods in teaching physics and is reflected in modern programs for institutions of general secondary education in Ukraine [1]. Scientific analysis of phenomena and processes, which is the result of the experiment, uses not only calculations but also visualization. With the help of visualization, information is generalized and systematized in the form of certain conclusions and investigated regularities [2].

In this paper, we propose of the simple experimental demonstrations of the magnetic properties of matter. For the first time we proposed a method for demonstrating the Curie temperature in ferromagnets with the help of which the attention of students is accented estoration of ferromagnetic properties of substances at a decrease of temperature, below the Curie point (temperature). The experiments can be reproduced in a school laboratory and can be recommended for students' project activity.

[1]. Fizyka i astronomiia. Navchalni prohramy dlia 10-11 klasiv zakladiv zahalnoi serednoi osvity (riven standartu, profilnyi riven). Zatverdzheno Ministerstvom osvity i nauky Ukrainy (nakaz № 1539 vid 24. 11. 2017 r.) Avtorskyi kolektyv pid kerivnytstvom Liashenka O. I.
[2]. Babych O., Semenikhina O. Do pytannia pro spivvidnoshennia poniat naochnist i vizualizatsiia // Fizyko-matematychna osvita. Naukovyi zhurnal. – Sumy :SumDPUim. A.S.Makarenka, 2014.– № 2(3). – p. 47-53.

Information and Communication Technologies in Teaching Physical and Colloidal Chemistry at the Faculty of Pharmacy

Dmytriv A.M.

Ivano-Frankivsk State Medical University, Ivano-Frankivsk, Ukraine,
admytriv@ifnmu.edu.ua

In the conditions of the modernization of the higher education system, new problems and tasks appear, the solutions of which should be worked on by the teachers of higher educational medical institutions. One of the problems is the drop in the success rate of students in studying chemical disciplines by future masters-pharmacists, as evidenced by the low results of passing the licensed exam Krok 1.

The use of information and communication technologies opens up new perspectives and opportunities for teaching chemistry, in particular, physical and colloidal chemistry. The use of computer programs and animation allows you to see what is impossible in a regular class. All the novelties of technological progress are met with special enthusiasm by students. Therefore, it is very important to use the curiosity and high cognitive activity of students for purposeful development of their personality.

The advantages of using computer technologies in chemistry classes are:

- ✓ individual and differentiated approach to education;
- ✓ carry out control with feedback, error diagnosis and evaluation of educational activity results;
- ✓ exercise self-control;
- ✓ carry out training in the process of assimilation of educational material and self-training of students;
- ✓ visualize educational information using visual material;
- ✓ display on the monitor screen of processes that are not available in the educational laboratory.

When using computer technologies in chemistry classes, the following results were achieved:

- ✓ perception of information simultaneously by several sense organs;
- ✓ activation of attention and increased interest in the discipline;
- ✓ visibility, curiosity and emotionality of learning;
- ✓ improving the quality of the taught material;
- ✓ effective use of class time;
- ✓ comprehensive development of students;
- ✓ increasing the effectiveness and quality of education.

Therefore, by applying innovative technologies during chemistry classes, we increase the competence of students, develop creative mental activity, activate abilities, and increase the effectiveness of learning in the discipline.

Innovative Technologies as a Means of Intensifying the Educational Process

Moiseienko M.I., Pysklynets U.M., Rachkevych I.O.

Department of medical informatics, medical and biological physics
Ivano-Frankivsk National Medical University, Ivano-Frankivsk, Ukraine
upysklynec@ifnmu.edu.ua

The integration of higher medical education of Ukraine into the European educational space during martial law, is encourages to higher medical educational institutions to intensively search for effective scientific and pedagogical approaches to train highly qualified specialists, that are competitive on both the domestic and foreign job markets. Improving the quality of education becomes especially relevant. Therefore the introduction of implementation of innovative training technologies into the educational medical field makes it possible to improve it. This raises the important question of combining traditional forms of organization of the educational process with the latest teaching technologies, aimed to providing students with much more independently in studying academic disciplines.

The effective introduction of innovative technologies and teaching methods in the study of medical and biological physics improves the quality of students learning and the activation of their educational and cognitive activities. During of interactive training, students learn to proficiently analyze of this information, to think critically, to make thoughtful decisions, to transfer the acquired knowledge to non-standard situations, which is the most characteristic of doctor practical activity. There are most effective among the interactive learning methods, are next: cooperative learning (work in pairs, work in groups, idea circles, aquarium); methods of collective and group training (brainstorming, microphone, openwork saw, decision tree); situational modeling technologies (imitation games, role-playing games); technologies for processing debatable issues (take a position, scale of opinions, discussion, debate).

Also creative tasks are considered in the medical and biological physics classes: prediction, optimization, review, research, logical, management, communicative and creative, problem tasks. The main task of interactive training is the preparation of competitive specialist. The introduction of innovative teaching methods into the educational process of higher medical educational institutions contributes to a deeper understanding and assimilation of theoretical knowledge, practical skills, forms professional thinking, the ability to make reasonable and rational conclusions.

Thus, the modern interactive technologies play an important role in the study of natural sciences, in particular medical and biological physics, in the system of training doctors. They allow to doing future specialists to a higher level of competence and professionalism, which meets the requirements of the European educational space. And, it is a priority direction for the development of medical education in Ukraine nowadays.

Innovative Technologies for Enhanced Physical and Mathematical Learning in the Central Europe: Contemporary Issues and Trends of Fractal Approach

Yurkovych N.[1], Mar’yan M.[1], Seben V.[2]

[1]*Uzhhorod National University, Ukraine,*
nataliya.yurkovych@uzhnu.edu.ua, mykhaylo.maryan@uzhnu.edu.ua
[2]*V. Seben, University of Preshov, Slovakia, vladimir.seben@unipo.sk*

The features of the presented fractal approach reflect the specifics of modern information and communication systems, including physical and mathematical education. Main aspects of modern information and communication systems development are that scientific areas and directions, namely – information systems and education, programming and information technology, self-organization and artificial intelligence, are naturally compatible, integrated, synchronized, combined through fractality and information environment. We have developed and published the Educational and Training manuals “*Computer Modeling and Innovative Approaches in Physics” (2017), «Innovative Technologies of Computer Modeling for Physical and Information Processes. Synergetics of Information and Communication Systems” (2019), “Endless World of Fractality: a World with Endless Possibilities” (2022)*. These materials contain practical tasks in the physical and mathematical field of education with the use computer modeling, the involvement of information technologies, test tasks and familiarization with the fractal approach to the presentation of the material.

The implementation of the fractal approach to the teaching of physical and mathematical disciplines using computer modeling is substantiated [1,2]. The formation of a fractal structure is established and iterations are defined that reflect the integrity and spontaneity of information presentation. The involvement of students of related specialties from two universities – Uzhhorod Natonal University (Faculty of Physics) and University of Presov (Faculty of Humanities and Natural Sciences) – demonstrates the feasibility of using the fractal approach in training future teachers and scientists of natural sciences in higher educational institutions. Studies of the behavior of self-organized fractal structures in the context of physical and mathematical education are effective and will be continued in the future. The possibility of introducing tried-and-tested aspects of the fractal approach to science teaching in higher education institutions of Central Europe will also be developed and promoted [2].

[1]. 1.Yurkovych, N., Seben, V. & Mar’yan, M. (2017). Fractal approach to teaching physics and computer modeling. *Journal of Science Education*, 18(2), 117-120.

[2]. 2. Yurkovych, N., Mar’yan, M., Opachko, M., & Seben, V. (2023). Methods of the fractal approach in science education: innovative technology and concepts of computer modeling. *Physical and Mathematical Education*, 38(3), 73-78.

Methodical support of the course "Physical foundations of information technologies"

Klanichka V.M., Klanichka Yu.V.

Vasyl Stefanyk Precarpathian National University, Ivano - Frankivsk, Ukraine, v.klanichka@gmail.com

The study of physical phenomena underlying modern computers and information technologies is important for students at the bachelor's level of education at Vasyl Stefanyk Prykarpatsky National University, majors - Secondary Education (Physics), Secondary Education (Physics and Mathematics), Secondary Education (Informatics) , "Secondary education (informatics, English language)", and "Secondary education (mathematics)" and included in the curriculum of the elective subject - "Physical foundations of information technologies".

Magnetic phenomena and the physics of semiconductors and their role in the processes of recording, reproduction and storage of information are considered here. Elements of wave theory, optics and optical methods used in the field of information systems are also studied. Special attention is paid to advanced technologies in the field of computing, such as fluorescent, holographic and quantum technologies.

The discipline defines information technology as a system of means and methods for storing, processing and transmitting information. The purpose of this training course is the formation of scientific and research competence in students and the study of theoretical and practical aspects of the use of physical phenomena in modern computer technologies.

We also carry out research aimed at developing methodological foundations for teaching this discipline.

After completing the course, students gain knowledge about the structure and content of the course, as well as the possibility of applying new physical methods, such as magnetic, semiconductor, optical, and others, in computer technologies. The development of these methods can significantly increase the amount of memory and the performance of computers in future stages. Nowadays, optical systems are used for mathematical calculations, holographic methods for processing and storing information, and there are already significant achievements in the creation of quantum computers and the use of optoelectronic converters that combine optical and electronic components of computers.

The introduction of the discipline "Physical foundations of information technologies" to the educational process in various specialties indicates the importance of this subject and serves as the basis for the development of a teaching methodology that includes several stages.

Lecture classes, during which visual materials, different teaching methods and additional explanations are used. The lectures cover basic concepts such as computer structure, data formats, computer components, processor characteristics, memory types, and more.

Hands-on classes where students learn the practical aspects of computing, including rectifiers, decoders, registers, and more. They also become familiar with the structure and instructions of the microprocessor and conduct research on logic operations.

Students' independent work includes the study of the contribution of Ukrainian scientists to the development of computer technology, familiarization with the elements of computers, such as cache memory and flash memory, as well as the characteristics of monitors, sound cards and acoustic systems.

Assessment of students' knowledge is carried out through the final and current examination, as well as through the performance of control and coursework using the point-rating system. Knowledge is tested during a test or exam.

Accordingly, it can be noted that the method used in teaching the discipline "Physical foundations of information technologies" is effective and helps students successfully cope with applied tasks and adapt to new programs and technologies.

[1]. Lyashenko O.V. Physical foundations of electronic computers. Education manual for students Faculty of Natural Sciences. / Lyashenko O.V. Zhabinchenko M.K. - K.: Kyiv University Editorial and Publishing Center, 2000.

[2]. Kravchuk S.O. Basics of computer technology: components, systems, networks: education. manual for students higher education institutions / S.O. Kravchuk, V.O. Shonin - K.: Polytechnic Publishing House: Karavela Publishing House, 2005.

[3]. Fundamentals of technical electronics; in 2 books, Book 2. Schemotechnics: a textbook [V.I. Boyko, A.M. Gurzhii, V.Ya. Zhuykov et al.] – K.: Vyshcha shk.., 2007 – 510p.

[4]. Sysoev V.M. Basics of radio electronics: Textbook for pedagogic universities/ V.M. Sysoev. - K.: Vyshcha shk.., 2004. - 279p.

[5]. Sysoev V. M. Radio technology with elements of computer technology: teaching. manual Workshop / Sysoev V. M., Chernyavskyi V. P. - K.: Vyshcha shkola, 1986. - 184p.

PMT-2 Thermocouple Vacuum Gauge Embedded Measurement Module Development

Maksymchuk D.M., Penyukh B.R., Bihun R.I.

Ivan Franko National University of Lviv, Lviv, Ukraine, danylo.maksymchuk@lnu.edu.ua

Various types of thermal and ionization manometers are used to measure low pressures in the range of rough and high vacuum in PVD and CVD systems. The most common are the PMT-2 and PMI-2 gauges, connected with cables to measuring units. However, as the vacuum system becomes more complicated there is a need to simultaneously measure the pressure in different parts of the system. It's controlled by a single automation system. We designed a prototype of vacuum gauge for the PMT-2 sensor in the form of compact module using built-in solutions within the framework of the IOT concept. The advantage of this approach is the relatively low cost of the module, ease implementing and the possibility of scaling the solution in complex vacuum systems and remote monitoring of their operation.

The PMT-2 transmitter is a thermocouple manometer [1], which belongs to thermal class manometers and its operation is based on the dependence of gas thermal conductivity on pressure. In the direct current mode, the overheating of the filament is registered with a thermocouple as the pressure in the sensor chamber decreases. In general, the prototype consists of blocks: current stabilization, EMF registration, control, output and storage of information and a power supply unit. The device is controlled by the ESP32 controller. The MAX6675 module was used as the EMF measurement system of the PMT-2 sensor thermocouple. The SPI interface is used to connect the MAX6675 module to the microcontroller. The advantage of this module is high accuracy (12-bit ADC) and the presence of a thermal stabilization unit for the cold ends of the thermocouple. For the correct operation of the sensor, it is necessary to ensure the stabilization of the current through the filament. Typical values vary from 100 to 150 mA, and depend on the manufacturing conditions of specific sensor. The value of stabilization current is determined during the sensor calibration based on the fact that the filament current should provide a thermocouple EMF value of 10 mV, in the case when the sensor is connected to a vacuum chamber where the gas pressure is less than 10^{-4} torr. Data output and device control is carried out through the web interface, and the microcontroller itself is connected to the network via WI-FI in client mode or can be configured in AP (access point) mode. It is also implemented data output and control via Modbus, and additionally install a small OLED screen 128x64.

[1]. Fundamentals of Vacuum Technology. 2007. Kat.-Nr. 199 90. P. 87-88,82

Research on the Effectiveness of Interdisciplinary Competence Formation in Integrated Physics and Geography Lessons

Lishchynskyy I.M., Voitkiv H.V., Madar N.I., Boychuk O.V.

Vasyl Stefanyk Precarpathian University, Ivano-Frankivsk, Ukraine,
igor.lishchynskyy@pnu.edu.ua

One of the tasks of modern education is to prepare graduates who can address a wide range of problems and possess the ability for self-improvement. The State Standard of Basic and Complete Secondary Education emphasizes a competency-based approach to education in general, focusing on the development of interdisciplinary competence, which is the ability of students to apply skills, knowledge, and methods of activity across a range of school subjects.

The formation of interdisciplinary competence can only be achieved through the active use of interdisciplinary connections during the study of individual subjects, as well as through the implementation of integrated lessons.

We conducted research and experiments to investigate the effectiveness of forming interdisciplinary competencies during the study of physics and geography. The study involved 30 students from 9th grade, divided equally into control and experimental groups.

At the initial stage of the research, we offered students a series of interdisciplinary tasks to assess the level of cognitive activity. The analysis of the diagnostic results showed that 18.7% of students had a high level of cognitive activity, 61.5% had an average level, and 19.8% had a low level. For the majority of students, an average level of cognitive activity was typical.

In the second stage of the experiment, we conducted activities with students to enhance their cognitive activity by using interdisciplinary connections between physics and geography. After an integrated physics and geography lesson, students were given tasks to solve as part of the control stage of the experiment. The criteria for assessing the quality of task completion were correctness and completeness of answers.

Comparing the answers of students from the experimental and control groups revealed significant differences in the levels of cognitive activity. None of the students in the experimental group were found to have a low level of cognitive activity, whereas 10.2% of students in the control group had a low level.

The analysis of the experiment's results confirms that the use of integrated lessons and interdisciplinary connections activates cognitive activity, resulting in the formation of interdisciplinary competencies and more effective assimilation of educational material.

AUTHORS INDEX

Наукове видання
ФІЗИКА І ТЕХНОЛОГІЯ ТОНКИХ ПЛІВОК ТА НАНОСИСТЕМ
Матеріали XIX Міжнародної Фреїківської конференції

МКФТТПН-XIX

PHYSICS AND TECHNOLOGY OF THIN FILMS AND NANOSYSTEMS
Materials of XIX International Freik Conference

ICPTTFN-XIX

Технічний редактор *Роман Дзумедзей*
Відповідальний за випуск *Любомир Никируй*

Усі матеріали подано у авторський редакції

Підписано до друку 06.10.2023.
Гарнітура «Times New Roman».

Видавець
Прикарпатський національний університет
імені Василя Стефаника,
вул. С. Бандери, 1, м. Івано-Франківськ, 76000.
Тел. (0342) 71-56-22.

Свідоцтво суб'єкта видавничої справи
ДК №2718 від12.12.2006.